Challenging the concepts related to leptin, the hypothalamus, and energy balance

Kathy C.G. de Git

Challenging the concepts related to leptin, the hypothalamus, and energy balance

Uitdaging van de concepten gerelateerd aan
leptine, de hypothalamus en energiebalans

(met een samenvatting in het Nederlands)

Proefschrift

ter verkrijging van de graad van doctor aan de Universiteit Utrecht
op gezag van de rector magnificus, prof.dr. H.R.B.M. Kummeling,
ingevolge het besluit van het college voor promoties in het openbaar te
verdedigen op **dinsdag 30 oktober 2018 des middags te 12.45 uur**

door
Catharina Geertje de Git
geboren op 16 april 1990
te Utrecht

Colophon

Cover design: Kathy de Git and proefschrift-aio.nl
Layout and printing: proefschrift-aio.nl

ISBN: 978-90-393-7051-3

Copyright © Kathy de Git

The research described in this thesis was performed at Brain Center Rudolf Magnus, Department of Translational Neuroscience, University Medical Center Utrecht, The Netherlands.

Research in this thesis was financially supported by the Dutch Technology Foundation STW (grant 12264), which is part of the Netherlands Organisation for Scientific Research (NWO), and which is partly funded by the Ministry of Economic Affairs.

Promotoren:
Prof. dr. R.A.H. Adan
Prof. dr. S.E. la Fleur

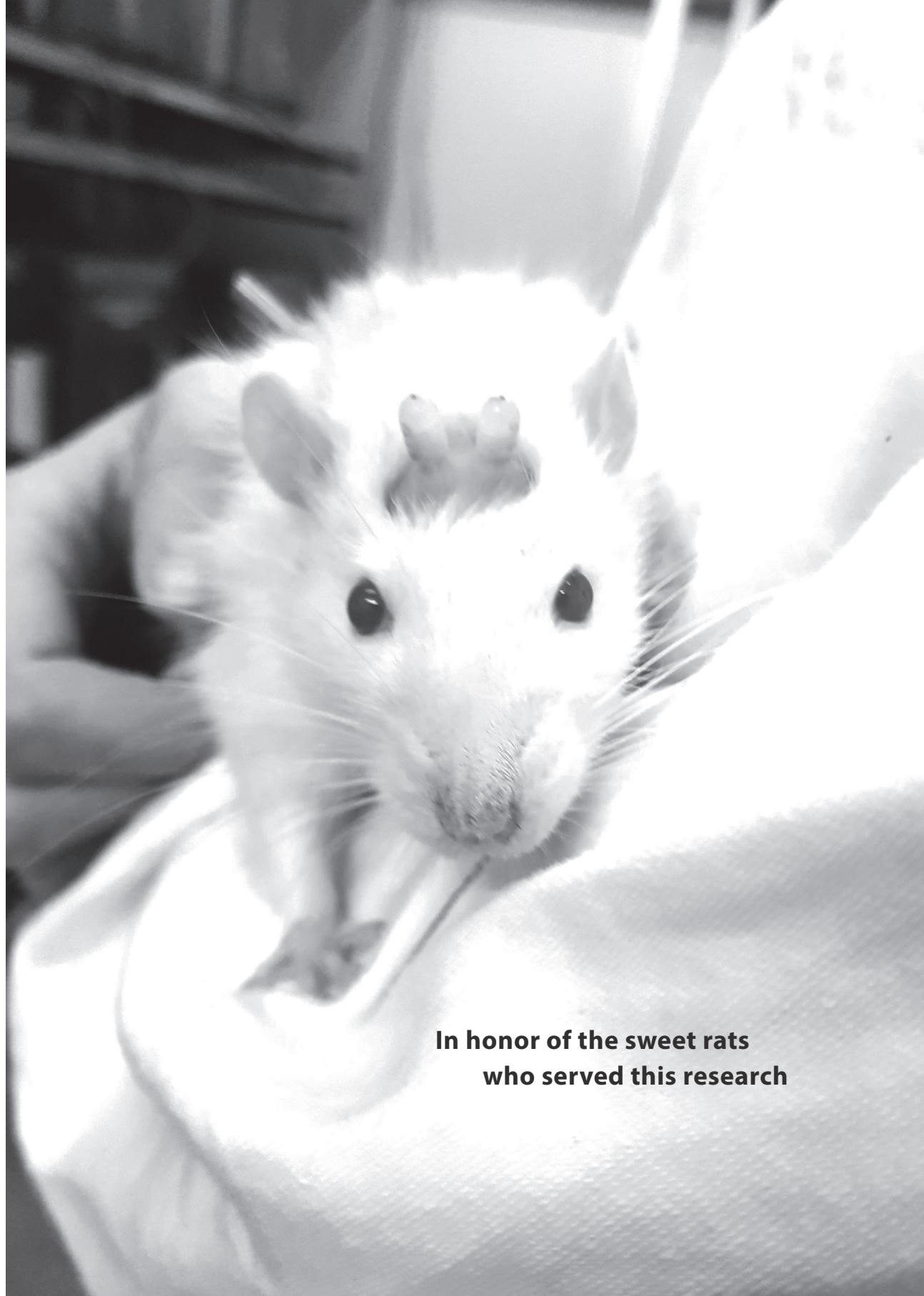

In honor of the sweet rats
who served this research

Table of contents

General introduction 9

Chapter 1
Leptin, the hypothalamus, and energy balance 11

Leptin and hypothalamic control of energy balance 49

Chapter 2
Leptin resistance in diet-induced obesity: the role of hypothalamic inflammation 51

Chapter 3
Is leptin resistance the cause or consequence of diet-induced obesity? 85

Chapter 4
Rats that are predisposed to excessive obesity show reduced (leptin-induced) thermoregulation before becoming obese 115

Regulation of energy balance beyond the hypothalamus 145

Chapter 5
Anatomical projections of the dorsomedial hypothalamus to the periaqueductal grey and their role in thermoregulation: a cautionary note 147

Chapter 6
Zona incerta neurons projecting to the ventral tegmental area promote action initiation towards feeding 175

Summary and general discussion 205

Chapter 7
Summary and general discussion: novel insights into concepts related to leptin, the hypothalamus, and energy balance 207

Addendum 247

Appendix:
- I. Inflammatory signaling after free-choice high-fat high-sucrose diet exposure 248
- II. Meal patterns in two types of leptin responders 254
- III. Technical challenges of viral vector mediated blockade of leptin receptor signaling in the DMH 260
- IV. Input from leptin receptor positive neurons in the hypothalamus to the periaqueductal grey 270
- V. Difficulties in targeting the DMH with dual viral vector technology 276

Dutch summary / Nederlandse samenvatting 286
Acknowledgements / dankwoord 292
List of publications 298
Curriculum vitae 300

General introduction

Chapter 1

General introduction:
Leptin, the hypothalamus, and energy balance

Kathy C.G. de Git

Brain Center Rudolf Magnus, Dept. of Translational Neuroscience, University Medical Center Utrecht, Utrecht University, Utrecht 3584 CG, The Netherlands

1.Obesity and energy balance 13
1.1 (Im)balance between energy intake and energy expenditure 13
1.1.1 Specification of energy intake and energy expenditure 13
1.1.2 Central regulation of energy intake and energy expenditure 15

2. Leptin and hypothalamic control of energy balance 16
2.1 Leptin production 16
2.2 Leptin receptor signaling 17
2.3 Leptin and central control of energy homeostasis 17
2.3.1 Neural control of energy intake 18
2.3.2 Neural control of energy expenditure 19
2.4 Leptin resistance 21
2.4.1 Molecular mechanisms of leptin resistance 22
2.4.2 Selective leptin resistance 23
2.4.3 Pre-existing leptin resistance 24

3. Regulation of energy balance beyond the hypothalamus 25
3.1 The periaqueductal grey and thermoregulation 25
3.2 The ventral tegmental area and feeding 26

4. Studying the neural circuitry of energy balance 28
4.1 Modeling human obesity 28
4.2 Monitoring feeding behavior and energy expenditure 29
4.3 Retrograde viral tracing 31
4.4 Modulation of the activity of specific neuronal projections 31

5. Thesis outline 35

1. Obesity and energy balance

The prevalence of obesity has increased dramatically over the last few decades, affecting men, women, and children [1]. In 2016, more than 1.9 billion adults worldwide were overweight (body mass index ≥ 25), and at least 650 million of them were obese (body mass index ≥ 30) [1]. The obesity epidemic provides a major public health problem, as obesity is associated with the development of chronic disorders, such as cardiovascular disease, type 2 diabetes, hypertension, and some forms of cancer [2-5]. The majority of obesity is thought to result from a combination of a genetic susceptibility and the modern human lifestyle, such as sedentary behavior, and the overconsumption of energy-dense diets, high in saturated fat and sugar [4-8]. Living in our modern society, some individuals become heavily obese, whereas others appear obesity resistant [9]. This high variability in the susceptibility for the development of obesity remains largely unexplained, illustrating the importance of a precise understanding of the physiological processes that balance energy intake and expenditure, as well as of susceptibility factors that increase the risk for the development of obesity.

1.1 (Im)balance between energy intake and energy expenditure

Body weight is normally maintained within a narrow range by a balance between energy intake and energy expenditure [10]. Individuals do not seek to maintain constant levels of either process, but rather adapt their energy expenditure to changes in energy intake and *vice versa* [6, 7]. Accordingly, obesity does not result from the overconsumption of energy-dense diets *per se*; instead, obesity primarily results from a failure of the regulatory systems to compensate for excess energy intake by either commensurately increasing energy expenditure or by reducing food intake at subsequent meals [6, 7, 11]. Chronic periods of positive energy balance result in an overload of triglycerides stored in white adipose tissues, leading to body weight gain, and eventually obesity [2, 3, 10].

1.1.1 Specification of energy intake and energy expenditure

Energy intake is influenced by factors such as appetite, satiety, motivational drive, and palatability of food (Figure 1A). Energy expenditure is the counterpart of energy intake, and total energy expenditure comprises four main components: 1) basal metabolic rate (BMR), which is defined as the energy expended on cellular metabolism at complete rest in the post-absorptive state [12-14]; 2) the thermic effect of food, or diet-induced thermogenesis, which is the energy cost of converting ingested food into components for use or storage [12, 13]; 3) physical activity, whereby energy expenditure results from muscular activity; 4) (cold-induced) thermogenesis,

which is the energy expended to maintain core body temperature [12]. Although all these processes generate heat, thermogenesis is a specific heat producing process that is induced at temperatures below thermo-neutrality, and is classified into shivering and non-shivering thermogenesis. Shivering thermogenesis results from the contraction of antagonistic groups of skeletal muscles [12], whereas non-shivering or adaptive thermogenesis is a tightly regulated heat producing process that is primarily executed by brown adipose tissue (BAT) [5, 15-17].

Figure 1.

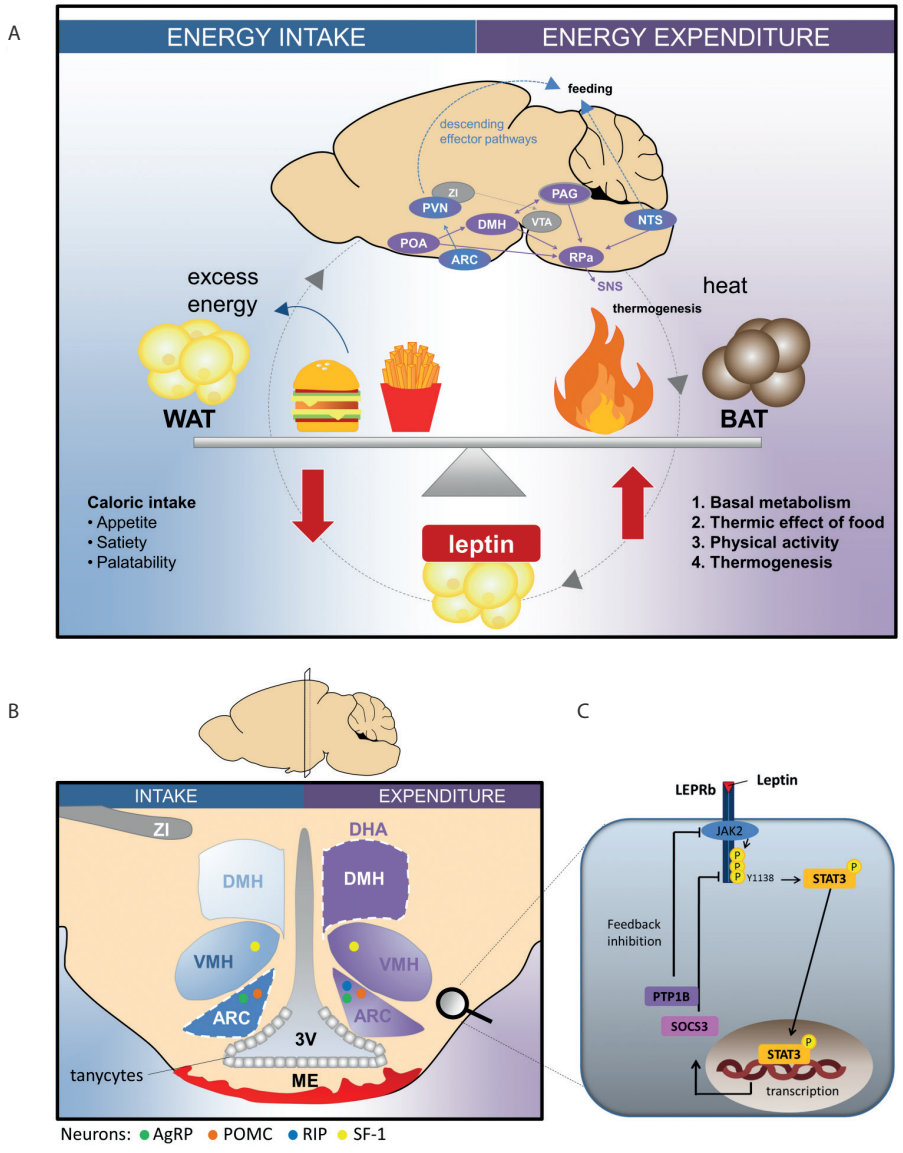

< Figure 1. Leptin regulation of energy balance. (A) Energy homeostasis is maintained via a fine balance between energy intake (blue) and energy expenditure (purple). Energy intake comes from food intake and excess energy is stored in white adipose tissue (WAT), whereas energy expenditure is mediated via several processes, including heat production by brown adipose tissue (BAT) (*i.e.* thermogenesis). The regulation of energy balance involves interactions between adipose tissue and the brain. Leptin is secreted by adipose tissue, in proportion to the amount of adiposity, and informs the brain about peripheral energy storage and availability. Leptin suppresses appetite and promotes energy expenditure by acting on the long form of the leptin receptor (LEPRb) in several hypothalamic nuclei in the brain, including the arcuate nucleus (ARC), ventromedial hypothalamus (VMH), dorsomedial hypothalamus (DMH), and paraventricular nucleus (PVN). These neurons form interconnected neural circuits, and also project to other regions of the brain, such as the periaqueductal grey (PAG) and raphe pallidus (RPa), to control energy balance. Neural circuits mediating leptin's effect on energy intake and energy expenditure are shown in blue and purple (or both colors), respectively. This thesis shows that the projection from the zona incerta (ZI) to ventral tegmental area (VTA) (shown in grey) is also involved in energy homeostasis, but the role of leptin signaling was not investigated. (B) Relative contribution of the ARC, VMH and DMH to energy intake (blue) and energy expenditure (purple). The intensity of the color indicates the relative importance of the nucleus in mediating energy intake/expenditure. The ARC is known as a critical site for energy intake, whereas the DMH is known as a critical site for energy expenditure. The ZI is also involved in energy intake. The border between the ARC and median eminence (ME) is lined by tanycytes. (C) Leptin signaling through the Janus kinase 2 / signal transducer and activator of transcript 3 (JAK2/STAT3) pathway. SOCS3, suppressor of cytokine signaling 3 and PTP1B, phosphotyrosine phosphatase-1B are negative regulators of leptin signaling. P = tyrosine phosphorylation. POA, preoptic area; NTS, nucleus of the solitary tract; SNS, sympathetic nervous system; DHA, dorsohypothalamic area; 3V, third ventricle; AgRP, agouti-related protein: POMC, pro-opiomelanocortin; RIP, rat insulin promotor ; SF-1, steroidogenic factor-1.

1.1.2 Central regulation of energy intake and energy expenditure

The complex regulatory system that maintains energy balance involves interactions between adipose tissue and the brain [3, 8] (Figure 1A). Adipose tissue acts as energy storage, and has a central role in the secretion of several hormones into the circulation, including leptin and adiponectin, which act as adiposity signals to inform the brain about energy storage and availability [2, 3, 18]. The brain, particularly the hypothalamus, senses and integrates these adiposity signals with various other metabolic signals, and responds by adapting energy intake and energy expenditure accordingly [3].

A key role for the hypothalamus in the control of energy balance was established in the mid-1900s by classical studies showing that crude hypothalamic lesions elicit profound changes in eating and body weight [6, 19]. Lesions of the ventromedial hypothalamus (VMH) resulted in voracious appetite and bodyweight gain, whereas lesions of the lateral hypothalamus (LH) resulted in loss of appetite and even death by starvation [6, 19]. Since then, further research has both refined and expanded the

understanding of the neural systems that regulate energy homeostasis, showing for example that the hypothalamus does not act in isolation, but regulates energy balance via functional connections with other major brain areas, such as the midbrain and corticolimbic system [6, 7]. Thus, the maintenance of energy balance is controlled by sophisticated brain circuits.

2. Leptin and hypothalamic control of energy balance

The discovery of leptin in 1994 by Friedman et al. was a major breakthrough in obesity research [20]. Decades before leptin's discovery, its presence was already predicted based on parabiosis studies by Coleman et al. [20, 21], in which the vascular systems of obese *ob/ob* mice and diabetic *db/db* mice were connected, to allow for the exchange of circulating factors. From these studies, it was concluded that *ob/ob* mice were missing a satiety factor in the circulation that was overproduced in *db/db* mice. This satiety factor cured obesity in *ob/ob* mice, while *db/db* mice failed to respond to it. Later, the circulating satiety factor became known as leptin, based on the Greek word "leptos", meaning thin [20, 22, 23]. The severe obesity that was observed in both *ob/ob* mice and *db/db* mice was caused by a mutation in the *ob/ob* gene and *db/db* gene, respectively, resulting in leptin deficiency in the former and leptin receptor deficiency in the latter mouse strain [8, 20, 22, 24, 25]. Similarly, congenital leptin deficiency in humans leads to morbid obesity [26-28], and leptin replacement therapy reverses obesity and associated metabolic disorders in leptin-deficient patients [28-31]. The importance of leptin signaling in the control of energy homeostasis and bodyweight has been confirmed by numerous studies in both rodents and humans [3].

2.1 Leptin production

Leptin is a 16-kDa polypeptide that is primarily secreted from visceral adipose tissue in rodents, and from subcutaneous adipose tissue in humans [18]. Plasma leptin levels are directly proportional to the amount of adiposity in both rodents and humans [18]. Leptin expression and circulating levels are pulsatile and follow a circadian rhythm [18, 25]. In rats, plasma leptin levels peak during the active late dark phase (zeitgeber time 11), and gradually drop during the inactive light phase, reaching their nadir during the late light phase (zeitgeber time 9) [32]. The circadian fluctuations in leptin expression are very modest (~1.5-fold) compared to the rapid, profound changes in response to metabolic challenges, such as fasting and cold exposure [18]. Fasting reduces leptin expression and circulating levels by about 60-75% in both rodents and humans [33, 34], whereas 4h of cold exposure leads to undetectable leptin mRNA levels in mice [35]. These decreases in leptin levels are independent of changes in adiposity, and have been proposed to be mediated by the central nervous system (CNS) (for review see [18]). Together, these findings suggest that leptin levels reflect energy demand rather than adiposity.

2.2 Leptin receptor signaling

Leptin exerts its biological actions by acting on leptin receptors (LEPRs) [36]. At least six isoforms of the LEPR have been identified [2, 36]. The long leptin receptor isoform (LEPRb) is primarily responsible for leptin receptor signaling, and is highly expressed in the CNS, particularly in the hypothalamus [36]. Leptin binding to the LEPRb activates several different signaling cascades that act coordinately to regulate energy balance (for an overview see [3, 36]). The most studied leptin signaling pathway is the Janus kinase 2 / signal transducer and activator of transcript 3 (JAK2/STAT3) pathway [7, 36] (Figure 1C). Leptin binding to the LEPRb activates JAK2, which phosphorylates LEPRb on three tyrosine residues. Phospho-Tyr^{1138} recruits STAT3, which becomes phosphorylated by JAK2 [3, 7]. Phosphorylated STAT3 (pSTAT3) then homodimerizes and translocates to the nucleus, where it acts as a transcription factor to regulate expression of its target genes, including neuropeptides and two negative regulators of leptin signaling: suppressor of cytokine signaling 3 (SOCS3) and phosphotyrosine phosphatase-1B (PTP1B) [3, 7, 25]. SOCS3 and PTP1B provide negative feedback regulation on JAK2/STAT3 signaling by binding to a specific tyrosine residue on the LEPRb or dephosphorylating JAK2, respectively, which functions to limit the magnitude and duration of leptin signaling [3, 25, 37, 38].

The JAK2/STAT3 signaling pathway is critically involved in leptin regulation of energy balance, and mediates both energy intake and energy expenditure, including leptin-induced BAT thermogenesis [36, 39-43]. Since transduction of leptin signaling is marked by increased STAT3 phosphorylation, pSTAT3 activation is often used as a marker for cellular leptin sensitivity [39, 42, 44-47].

2.3 Leptin and central control of energy homeostasis

Within the CNS, the hypothalamus shows the highest expression of leptin receptors, and is generally accepted to be the main target for central leptin action [14, 25]. Leptin action in the hypothalamus mediates both the appetite-suppressing and energy expenditure-promoting effects of leptin [14]. The distinct hypothalamic nuclei, including the arcuate nucleus (ARC), ventromedial hypothalamus (VMH), and dorsomedial hypothalamus (DMH), form interconnected neural circuits that collectively contribute to leptin's overall effect on energy homeostasis [7, 25]. These neurons also project to other regions of the brain, such as the midbrain and brainstem, to control energy balance [7] (Figure 1A,B).

2.3.1 Neural control of energy intake

The ARC has become recognized as a critical center in the control of energy intake, and is uniquely positioned to detect changes in circulating leptin [7, 25, 36]. Leptin reaches most central neurons via a regulated, saturable transport system across the BBB or through the CSF. The ARC lies adjacent to the third ventricle and immediately above the median eminence (ME), a circumventricular organ with an incomplete blood-brain barrier (BBB) [7, 25, 36]. Although the ARC is protected from the general circulation by a border between the ARC and ME, which is composed of tanycytes, specialized glial cells that line the base of the third ventricle, the unique character of the ARC-ME border allows ARC neurons, particularly those in close proximity to the ME, to easily detect changes in circulating signals such as leptin and nutrients (for overview see [25]) (Figure 1B).

Within the ARC, the LEPRb is expressed in (subsets of) at least two populations of neurons that have opposing actions on energy balance: the orexigenic (appetite-stimulating) agouti-related protein (AgRP) neurons and the anorexigenic (appetite-suppressing) pro-opiomelanocortin (POMC) neurons [3, 7, 10, 25, 36]. POMC neurons express the anorexigenic neuropeptides POMC and cocaine- and amphetamine-regulated transcript (CART). Leptin acts via the LEPRb to stimulate the secretion of POMC, a precursor protein that is proteolytically cleaved into α-melanocyte-stimulating hormone (α-MSH). α-MSH is an anorexigenic neuropeptide that decreases food intake by activating melanocortin-3 and melanocortin-4 receptors (MC3R and MC4R), which are expressed in second-order neurons in other hypothalamic nuclei, especially the paraventricular nucleus (PVN). While stimulating POMC neurons, leptin inhibits AgRP neurons, which co-express the orexigenic neuropeptides AgRP and neuropeptide Y (NPY). AgRP exerts it's orexigenic effects by acting both as an α-MSH/MC4R antagonist and an MC4R inverse agonist. In addition, AgRP neurons have been reported to provide inhibitory GABAergic input to POMC neurons. Leptin inhibits the orexigenic effects of AgRP neurons by both inhibiting AgRP neuronal activity and the secretion of AgRP/NPY. Thus, leptin suppresses food intake by simultaneously promoting the expression of POMC/CART and inhibiting the expression of AgRP/NPY. Conversely, states of negative energy balance, such as fasting, result in low leptin levels and produce the opposite effects [3, 7, 10, 25, 36].

The initial idea that the ARC is the critical center nucleus mediating leptin's effects on energy intake has been refined by studies showing that selective deletion of LEPRs in either POMC or AgRP neurons, or both, results in mild obesity [48, 49]. The obesity phenotypes were far less severe than the obesity and hyperphagia observed in systemic LEPR-deficient *db/db* mice. These findings indicate that, in addition to POMC and AgRP neurons in the ARC, other LEPRb-expressing neurons also mediate leptin's action. Indeed, ARC neurons account for only 15-20% of the total number of LEPR-expressing neurons in the brain [36, 50]. The LEPR is expressed in multiple other hypothalamic and extra-hypothalamic brain areas [10], including the VMH, DMH, LH, ventral tegmental area (VTA), hippocampus, and the brainstem [10].

Two hypothalamic nuclei that are of particular interest to this thesis are the VMH and DMH. There is limited evidence that the VMH might also mediate leptin's anorexigenic effects. Leptin stimulates the secretion of two anorexigenic neuropeptides expressed in the VMH: steroidogenic factor-1 (SF-1) and brain-derived neurotrophic factor (BDNF) [51, 52]. Further, selective deletion of LEPRs in VMH SF-1 neurons was shown to result in marked hyperphagia and obesity by Dhillon et al. [51], but this result was not replicated by Bingham et al [53]. They showed the development of mild obesity without severe hyperphagia [53]. The DMH is another key site of leptin action. However, leptin signaling in the DMH has contradictory effects on food intake, but is instead particularly known to regulate energy balance by increasing energy expenditure, as discussed below [46, 54, 55].

Taken together, no single LEPRb population fully mediates leptin's control of energy intake. The distinct LEPRb populations vary in the level to which they are responsible for certain aspects of energy homeostasis, and the sum and interaction of LEPRb signaling in distinct nuclei account for leptin's full control of energy homeostasis.

2.3.2 Neural control of energy expenditure

With regard to leptin regulation of energy expenditure, much of the recent research has focused on BAT thermogenesis. BAT has the specific metabolic function to dissipate energy in the form of heat [13, 16, 17, 55-57]. Heat production in BAT is mediated via uncoupling protein 1 (UCP1), which is a proton channel of the inner mitochondrial membrane that dissipates mitochondrial proton motive force as heat [56-58]. BAT energy expenditure requires the uptake and oxidation of metabolic fuel substrates, including glucose and free fatty acids [16, 18]. The availability of these substrates is signaled by hormones like leptin, that influence BAT thermogenesis in a permissive manner [16]. BAT is an important thermoregulatory effector organ in rodents in various physiological conditions [17, 57], and recent evidence acknowledged metabolically active BAT in adult humans [59-62].

BAT thermogenesis is governed by central pathways that control sympathetic innervation of BAT [13, 15-17, 56, 57]. The DMH is now recognized as one of the key players in the thermoregulatory circuit [13, 55-57, 63], as disinhibition of DMH neurons was shown to elicit a marked and rapid increase in BAT sympathetic nerve activity (SNA) and BAT

temperature [64, 65] that preceded the increase in core body temperature [64, 66]. Several lines of evidence demonstrate a critical role for leptin signaling in the DMH in mediating BAT-dependent thermogenesis: 1) Injection of leptin directly into the DMH increased BAT temperature [56-58]; 2) Leptin-induced increases in BAT temperature were blocked by pre-injection of a leptin receptor antagonist directly into the DMH [56-58]; 3) Selective activation of leptin receptor (LEPRb) expressing neurons within the DMH increased BAT and core body temperature [55]; 4) Knock-out of the LEPRb in a specific population of DMH neurons, expressing prolactin-releasing peptide, blocked leptin-induced increases in UCP1 and core body temperature [54]. Together, these studies indicate that leptin receptor signaling in DMH neurons is sufficient and necessary to control BAT thermogenesis.

The activity of DMH neurons depends on inhibitory and excitatory inputs from other central sites, including the preoptic area (POA) [15, 18, 56]. Thermosensing neurons in the POA integrate temperature information from the CNS, periphery and deep-body via thermoreceptors [15], and relay this information to neurons in the DMH. Activation of DMH neurons is known to stimulate sympathetic premotor neurons in the raphe pallidus (RPa) to control sympathetic input to BAT. There is evidence that the periaqueductal grey (PAG) is also an important relay in the descending pathways mediating thermogenesis [57, 63, 66, 67]. The DMH and POA are both direct leptin targets within this thermoregulatory circuit. LEPRb expressing DMH and POA neurons are both labeled by pseudorabies virus injections into the BAT, and directly innervate the RPa. In addition, LEPRb expressing POA neurons directly innervate the DMH, while LEPRb expressing DMH neurons directly innervate the PAG [15, 18, 56]. Also the RPa and PAG contain neurons that express considerable levels of leptin receptors [68-70].

Besides leptin action in the above mentioned LEPRb expressing neurons, leptin signaling in the VMH and ARC also contributes to energy expenditure. Especially the role of leptin signaling in the ARC has been investigated. Deletion of leptin receptors in the ARC prevents leptin-stimulated BAT sympathetic nerve activity [71]. Leptin receptor signaling in AgRP and/or POMC neurons seems to only partially mediate leptin's thermoregulatory action [48, 49]. Leptin also acts through GABAergic neurons that can be targeted by the rat insulin promotor (RIP) [72]. Deletion of GABA signaling from these neurons suppresses energy expenditure and BAT thermogenesis, and attenuates leptin-induced BAT thermogenesis [72]. Although limited, evidence also supports a role for leptin signaling in the VMH in the regulation of BAT thermogenesis. Leptin infusion into the VMH increases glucose uptake in BAT, which is blocked by sympathetic denervation [73]. Further, mice with selective deletion of LEPRs in VMH SF-1 neurons show defective adaptive thermogenesis in response to a high-fat diet (HFD), suggesting that leptin signaling in VMH SF-1 neurons is especially required for the promotion of energy expenditure in response to HFD exposure (51, 53). Interestingly, some leptin thermoregulatory functions are mediated independent of the hypothalamus, via leptin signaling in the brainstem [15, 25].

BAT thermogenesis is influenced by locomotor activity, ambient temperature, and nutritional state [25]. The effects of leptin on BAT and core body temperature are most robust in states of low leptin levels, like fasting and leptin deficiency [16, 55, 56]. An explanation for this phenomenon is that leptin is thought to influence BAT thermogenesis in a permissive manner rather than being actively thermogenic, *i.e.* it probably signals the availability of lipid and glucose fuel supplies for oxidation in BAT, and acts through LepRb to enhance the excitability of neurons controlling BAT activity, thereby facilitating BAT activation [15, 16, 56]. Leptin regulation of core body temperature appears not to arise exclusively from BAT thermogenesis, as BAT temperature did not always precede and exceed the increase in core body temperature evoked by leptin [55]. More recently, it has been reported that, at least in *ob/ob* mice, systemic leptin injection leads to a pyrexic increase in core body temperature by reducing heat loss via the tail, without affecting BAT thermogenesis [74]. Accordingly, regulation of blood flow in the tail has been recognized as another major sympathetic thermoregulatory mechanism in rats and mice [15, 17, 57]. Further research is needed to compare the contribution of BAT thermogenesis and heat loss via the tail to leptin regulation of core body temperature, and to study whether these thermoregulatory mechanisms are controlled by identical thermoregulatory circuits.

2.4 Leptin resistance

Both in humans and rodents, the development and/or maintenance of obesity has been assumed to result from leptin resistance [44, 75-84]. As discussed above, normal weight individuals respond to increased plasma leptin levels by reducing food intake and increasing energy expenditure [45, 46, 85, 86]. Most obese individuals show high circulating leptin levels (hyperleptinemia) [45, 47, 80, 81, 83, 84]. After exogenous administration of leptin, obese individuals do not respond with a decrease in food intake that is normally observed in lean individuals, and are hence considered leptin resistant [44, 47, 77, 79-83, 87, 88]. Overconsumption is thought to be both a cause and a consequence of leptin resistance. That is, overconsumption, particularly of energy-dense diets, may induce leptin resistance in the absence of obesity by acting on leptin-responsive neurons, and leptin resistance in obesity may maintain overconsumption [89]. To study the role of overconsumption in the development and/or maintenance of leptin resistance and obesity, rodent models have been developed in which obesity is induced by dietary manipulation, *i.e.* diet-induced obesity (DIO).

2.4.1 Molecular mechanisms of leptin resistance

In general, two distinct forms of leptin resistance are distinguished in DIO models: resistance to peripherally and centrally administered leptin, representing impaired access of leptin to the CNS and impaired responsiveness of LEPRb-expressing neurons to available leptin, respectively [87, 89].

Peripheral leptin resistance is characterized by high peripheral leptin levels but relatively low cerebrospinal fluid (CSF) concentrations, and is thought to result from defective serum leptin transport across the BBB [2, 87]. This form of leptin resistance is strongly associated with DIO, and occurs relatively soon after the initiation of high-fat diet feeding, before the onset of central leptin resistance [87]. The underlying mechanism may involve saturation of active leptin transport across the BBB by hyperleptinemia, as well as the interference of elevated triglycerides with leptin BBB transport [36, 87].

Central leptin resistance, often referred to as cellular leptin resistance, may be mediated by various mechanisms, including reduced cell surface LEPRb levels and impaired LEPRb signaling within specific brain regions [2, 3]. Only a small portion of the LEPRb's is present at the plasma membrane. The majority of LEPRb's are localized in the Golgi apparatus and endosomes, and cell surface LEPRb's are constitutively internalized via endocytosis. Downregulation of cell surface LEPRb levels, either due to decreased forward trafficking to the plasma membrane and/or increased endocytosis, results in impaired leptin sensitivity [3]. Molecular mechanisms contributing to impaired LEPRb signaling include the upregulation of two negative regulators of LEPRb signaling: SOCS3 and PTP1B [2, 3, 36, 87]. SOCS3 and PTP1B provide negative feedback regulation on JAK2/STAT3 signaling by binding to a specific tyrosine residue on the LEPRb or dephosphorylating JAK2, respectively [3, 25, 37, 38] (Figure 1C). This negative feedback mechanism prevents over-activation of LEPRb signaling pathways and explains how hyperleptinemia in obese individuals may actually result in impaired leptin receptor signaling.

The overconsumption of high-fat diets in DIO models has been shown to result in the induction of an inflammatory response in the hypothalamus, which contributes to the development of central leptin resistance and obesity [90-92]. This inflammatory response is mediated by the innate immune system and is, in contrast to the classical inflammatory response, not pathogen-induced and relatively low-grade [93, 94]. It involves dynamic changes in the expression and activity of several mediators of the innate immune system, including toll-like receptor 4, IκB kinase-β/nuclear factor-κB (IKKβ/NF-κB), c-Jun N-terminal kinase, suppressor of cytokine signaling 3 and pro-inflammatory cytokines, as well as the induction of endoplasmic reticulum stress and autophagy defect [2, 3, 95]. Further, this response is mediated by interactions between neurons and non-neuronal cells such as microglia and astrocytes. Although the exact cellular mechanisms by which hypothalamic inflammation promotes central leptin resistance have not been resolved yet, current understandings propose that this inflammatory signaling might be induced by the accumulation of saturated fatty acids (SFAs) in the hypothalamus (for overview see Ch2, [95]). In short, SFAs may act on glial cells, that act as drivers of inflammatory signaling by releasing pro-inflammatory cytokines. The upregulated cytokine-induced IKKβ/NF-κB signaling converges with classical STAT3 signaling (that is also upregulated due to hyperleptinemia) in hypothalamic neurons to upregulate SOCS3 expression, which subsequently mediates leptin resistance by providing negative feedback on the LEPRb [95]. The evidence for a role of inflammatory signaling in mediating central leptin resistance has mostly been obtained by studies in which rodents were offered a high-fat diet [95].

2.4.2 Selective leptin resistance

In DIO models, the development of cellular leptin resistance is often demonstrated by an attenuation in the incremental increase or maximal level of leptin-induced pSTAT3 activation in the ARC, while the DMH and other hypothalamic nuclei remain leptin sensitive [44-47]. In line with selective leptin resistance in the ARC, mice fed a high-fat diet were shown to develop resistance to leptin's anorexigenic effects [47], but remained sensitive to leptin's thermoregulatory effects, which are critically mediated by the DMH [46]. The upregulation of SOCS3 in the ARC, but not in the VMH or DMH, upon high-fat diet feeding may explain the development of selective leptin resistance in the ARC in DIO [47], as SOCS3 acts to limit the magnitude and duration of leptin signaling [3, 25, 37, 38]. The site selective SOCS3 upregulation has been proposed to result from the unique character of the ARC-ME border, which makes ARC neurons easily accessible for circulating signals such as leptin and nutrients [25]. Both elevated leptin signaling and the accumulation of nutrients, like SFAs, in the ARC result in the upregulation of SOCS3 via upregulated leptin receptor signaling and inflammatory signaling [95, 96]. Interestingly, AgRP neurons, which lie partially outside the BBB and are the predominant responders to subtle fluctuations in leptin levels, develop leptin resistance more quickly than POMC neurons [97].

Importantly, the failure of exogenously injected leptin to suppress food intake or induce an incremental increase in pSTAT3 activation does not necessarily indicate leptin resistance; instead, it may reflect maximal endogenous leptin signaling that cannot be further increased by exogenously administered leptin. To measure endogenous leptin action in hyperleptinemic DIO mice, high-fat diet fed mice were previously treated with a leptin antagonist that acts as a competitive agonist of the leptin receptor [81]. The antagonist increased food intake and BW comparably in lean and DIO mice, and accordingly blocked pSTAT3/SOCS3 signaling [81]. These findings show ongoing endogenous leptin signaling in DIO mice, which contributes to the control of BW and food intake suppression, despite resistance to exogenously injected leptin.

2.4.3 Pre-existing leptin resistance

It is generally believed that leptin resistance results from the overconsumption of high-energy diets (HED), and that this diet-induced leptin resistance contributes to the development of obesity. However, there is some evidence that reduced leptin sensitivity does not necessarily result from HED feeding, but may already be present before HED exposure and predispose rats to exacerbated DIO. Both Levin et al. and Ruffin et al. showed that reduced sensitivity to leptin's food intake suppressing effects on a control diet is related to exacerbated body weight gain during subsequent HED exposure [9, 98], but they did not test whether leptin sensitivity is a stable parameter in a rat. Therefore, it remains unclear to what extent a pre-existing reduction in leptin sensitivity is a predictor for DIO. Furthermore, as leptin sensitivity was only tested before HED exposure, it is currently unknown whether exposure to a HED further reduces the pre-existing reduction in leptin sensitivity in DIO prone rats and thereby aggravates DIO. Importantly, the molecular mechanisms underlying diet-induced leptin resistance might differ from those underlying a pre-existing leptin resistance. Diet-induced leptin resistance is initially characterized by peripheral leptin resistance, but prolonged high-fat diet feeding eventually also induces central leptin resistance, especially in the ARC [44-47, 87]. In contrast, studies in selectively bred DIO and diet-resistant (DR) rats by Levin et al. indicate that a pre-existing leptin resistance does not result from impaired leptin transport across the BBB, but from reduced central leptin resistance, as reflected in reduced LEPRb expression, leptin receptor binding, and pSTAT3 activation, in the ARC, VMH, and DMH [99-102].

3. Regulation of energy balance beyond the hypothalamus

Energy balance is controlled by specific but distributed neural networks [6]. In addition to metabolic centers located in the hypothalamus that control energy homeostasis, other brain areas, such as the midbrain and the corticolimbic system, are also implicated in the regulation of energy balance [6, 7]. Two midbrain regions that are of particular interest to this thesis are the VTA and the PAG, which are both innervated by the hypothalamus, and were previously shown to regulate energy intake [122-128] and energy expenditure [66, 67, 103, 104], respectively.

3.1 The periaqueductal grey and thermoregulation

The neural circuitry that has been proposed to control BAT thermogenesis involves the activation of DMH neurons, which stimulate sympathetic premotor neurons in the RPa to control sympathetic input to BAT [15, 18, 56] (see section 2.3.2). Although the PAG is generally not included in this thermoregulatory circuit, there is evidence that the PAG is also an important relay in the descending pathways mediating thermogenesis [57, 63, 66, 67]. Tracing studies have shown that the projections from the DMH to the PAG are much more abundant than those to the RPa [105-107], underlining the potential importance of the PAG in the regulation of DMH evoked thermogenesis.

The PAG is a relatively long midbrain region that can be divided into dorsomedial (dmPAG), dorsolateral (dlPAG), lateral (lPAG) and ventrolateral (vlPAG) subdivisions, which differ with respect to their functional properties and anatomical projections [108] (Figure 2). At least some of these subdivisions may have an opposite function in rostral versus caudal PAG extensions [66]. In regard to thermogenesis, it seems that neuronal activity in the rostral vPAG functions to inhibit BAT SNA and BAT temperature [67], whereas neuronal activity in the caudal (v)lPAG functions to increase BAT temperature [104]. Neuronal activity in the caudal l/dlPAG [66, 103] but not caudal (v) lPAG was shown to increase core body temperature [104] (Figure 2).

Previously, the projections from the DMH to the PAG and their role in thermoregulation were only studied at a limited number of anterior-posterior levels from bregma [66, 67, 106, 109]. Further, the distinct PAG subdivisions were often investigated in separate studies with different experimental settings, making it difficult to directly compare the distinct PAG subdivisions. In these studies, the functional connection between the DMH and the PAG was investigated by chemically (dis) inhibiting the DMH and PAG via local injection of drugs [66, 67]. The findings of these pharmacological studies suggest that the DMH increases thermogenesis through

a combination of an inhibition of BAT sympathoinhibitory neurons in the rostral vPAG [67], and a facilitation of BAT sympathoexcitatory neurons in the caudal l/dlPAG [66] (Figure 2). One important limitation of drug delivery through local cannulas is that it is difficult to precisely track intra-parenchymal drug diffusion, which may result in misinterpretation of the targeted PAG subdivision and the targeted subregion of the hypothalamus. In this thesis, dual viral vector technology was employed to target the projections from the DMH to the distinct PAG subdivisions, which allows visible confirmation of the viral spread.

Interestingly, the caudal PAG (cPAG) and RPa are innervated by neurons in the same subregion of the DMH [110]. Since the cPAG is transsynaptically labeled from BAT [111, 112], and retrogradely labeled from the RPa [113, 114], it has been hypothesized that the cPAG forms a neuronal relay in the projection from the DMH to the RPa [57]. This indirect pathway may function in parallel to a direct pathway from the DMH to the RPa [57, 63]. Further, it has been shown that increases in thermogenesis evoked from the caudal l/dlPAG depend on neuronal activity in the DMH [103], indicating that the DMH and caudal l/dlPAG may communicate bi-directionally to regulate thermogenesis. Thus, the PAG appears to play a central role in the neural circuitry that controls thermogenesis (Figure 1A).

The connection between the DMH and PAG might be a direct leptin target. As discussed in section 2.3.2, leptin signaling in the DMH plays a critical role in the regulation of BAT-dependent thermogenesis. LEPRb expressing DMH neurons directly innervate the PAG [115, 116], and the PAG also contains a substantial number of LEPRb expressing neurons, supporting that the connection between the DMH and PAG is leptin sensitive [68-70]. However, further research is needed to determine whether leptin action in the DMH regulates thermogenesis via projections to the PAG. Since previous studies did not specify the anterior-posterior level(s) and specific PAG subdivisions that are innervated by LEPRb-expressing DMH neurons [115, 116], this should be investigated first.

3.2 The ventral tegmental area and feeding

Among neural circuits regulating feeding, the mesolimbic dopamine (mesDA) system has been implicated in food motivation [117-121]. The mesDA system consists of dopaminergic neurons in the ventral tegmental area (VTA) that project to cortico-limbic structures such as the ventral striatum [120, 121]. DA is an important modulator of feeding behavior. DA-deficient mice starve to death without additional treatment with the dopamine precursor L-DOPA [122]. Conversely, alterations in the mesDA system, such as reduced DA D2 receptor expression in the striatum, have been

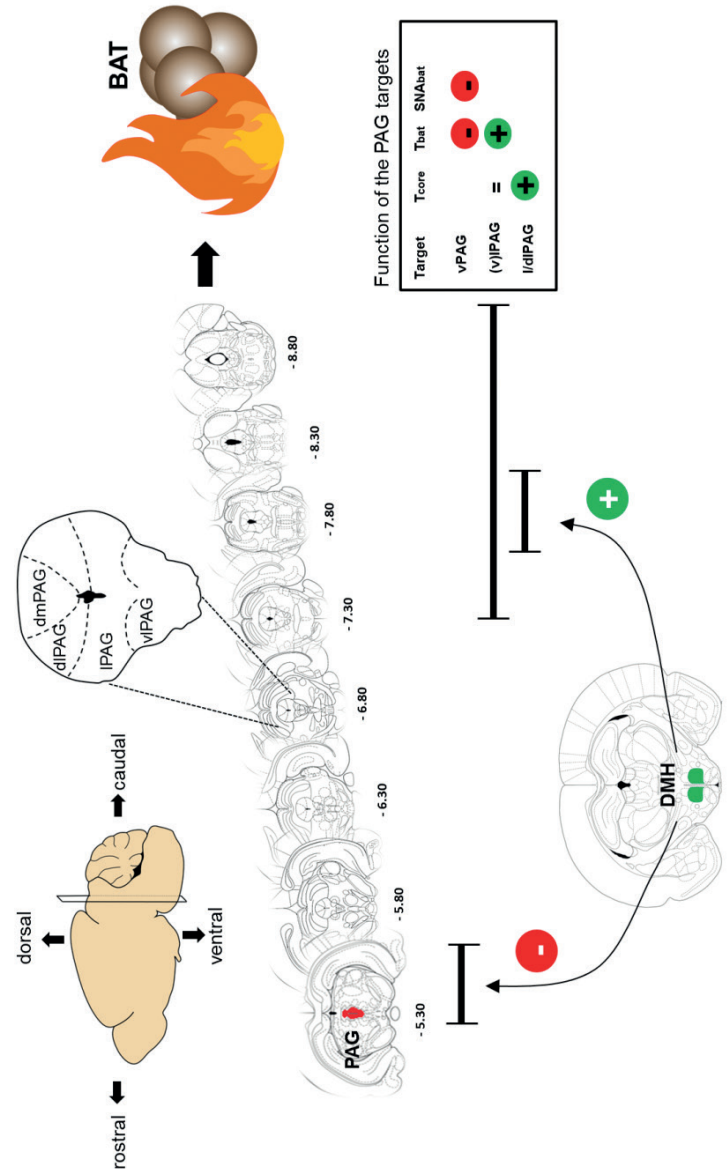

Figure 2. Regulation of thermogenesis via projections from the DMH to distinct PAG subdivisions. The periaqueductal gray (PAG) is a relatively long midbrain region that can be divided into dorsomedial (dmPAG), dorsolateral (dlPAG), lateral (lPAG) and ventrolateral (vlPAG) subdivisions. The PAG is shown along the entire anterior-posterior axis, and the effect of distinct PAG subdivisions on core body temperature (Tcore), BAT temperature (TBAT), and BAT sympathetic nerve activity (SNABAT) are shown for the indicated anterior-posterior levels. The dorsomedial hypothalamus (DMH) promotes BAT-dependent thermogenesis by inhibiting BAT sympathoinhibitory neurons in the rostral vPAG, and facilitating BAT sympathoexcitatory neurons in the caudal l/dlPAG. +, facilitation; -, inhibition; =, no effect.

associated with overconsumption and obesity in both animals and humans [123-128]. The precise role of VTA DA signaling in the control of food intake is incompletely understood, but VTA DA signaling is at least crucially involved in the motivation to work for food [117-119, 129, 130], and was shown to facilitate both the initiation and cessation of feeding [129]. Of note, although the majority of VTA neurons are dopaminergic, the VTA also contains GABAergic (~30%) and glutamatergic (~2-10%) neurons. VTA GABA neurons interact locally to regulate DA neurons [128].

The VTA receives input from metabolic centers in the hypothalamus that sense and regulate energy homeostasis [119, 120, 131]. Within the hypothalamus, the LH, and zona incerta (ZI) provide the major direct innervation to the VTA, but the neighboring DMH and anterior hypothalamus also provide prominent input to the VTA [132, 133]. While the LH to VTA projection has been extensively studied [5], the role of the input from the other hypothalamic subregions to the VTA remains largely elusive.

4. Studying the neural circuitry of energy balance

4.1 Modeling human obesity

The majority of human obesity is thought to result from a combination of a genetic susceptibility and the modern human lifestyle, such as sedentary behavior, and the overconsumption of energy-dense diets, high in saturated fat and sugar [5-8]. Many rodent models have been developed to study the effect of fat and sugar overconsumption on obesity development. Diet interventions in these models mainly consist of energy-dense pellets, in which all nutrients are combined [134-137]. Although these pellets are usually high in saturated fat and often contain a considerable amount of sugar, they do not represent a Western-style diet, which is characterized by a free choice between several healthy and unhealthy food items. To mimic the human diet more closely, we offer rats a free-choice high-fat high-sucrose (fcHFHS) diet. This diet consists of a choice between a 30% sucrose solution and saturated fat, in addition to regular chow and tap water (Figure 3A).

Rats offered the fcHFHS diet have previously been shown to persistently overconsume calories, resulting from an increase in meal frequency due to sugar drinking that is not compensated for by reducing meal size [138]. Persistent hyperphagia and snacking behavior are important features of human obesity that are mimicked by the fcHFHS diet [138], but not by most other (pelleted) diet interventions, which usually provoke an initial period of hyerphagia followed by compensation over time [136, 139]. Rats offered the fcHFHS diet are also willing to work hard for a food reward during a motivation task, even when sated [4], which mimics increased food motivation in human obesity [140, 141]. Because of the persistent hyperphagia, rats that are subjected to a fcHFHS diet rapidly increase their body weight gain, (abdominal) fat stores, and plasma leptin concentrations [4, 79, 85, 138, 142]. Moreover, they develop peripheral and central leptin resistance, as well as glucose intolerance characterized by beta cell unresponsiveness and insulin resistance, within 8-21 days of fcHFHS diet feeding [79, 85, 86, 142]. Thus, exposure of rats to the fcHFHS diet is a DIO model that mimics important features of human obesity, including human eating behavior and its metabolic consequences.

Like humans, several rats strains show individual differences in the susceptibility for the development of DIO, which provides opportunities to study the interaction between a genetic propensity for obesity development and eating behavior [9, 98, 99, 143]. Outbred Wistar rats offer such a unique model, as they show high individual variability in the feeding response to leptin before the onset of obesity. The response to leptin before exposure to an obesogenic diet was previously related to the susceptibility for obesity development [9].

4.2 Monitoring feeding behavior and energy expenditure

To continuously monitor feeding behavior in rats, without disturbing them, various automated monitoring systems have been developed. In the home cage, the automated food-monitoring system (Scales, Department Biomedical Engineering, UMC Utrecht, The Netherlands) records the weight of the food hoppers automatically every 12 s (Figure 3A). This system also measures drinking behavior by monitoring contact with the nipple of the drinking bottle, which is detected by a lickometer. Based on changes in the weight of the food hoppers, cumulative food intake and meal patterns can be calculated. As previously [138, 144], in this thesis, a meal is defined as an episode of food intake with a minimal consumption of 1 kcal (0.3 gr chow), and a minimal inter-meal interval of 5 min. Next to the automated measurement of feeding behavior in the home cage, operant methods in skinner boxes allow for the measurement of certain aspects of feeding behavior. For example, the motivation to work for food rewards can be tested under a progressive ratio schedule, where the response requirement to obtain a sucrose pellet is progressively increased after each obtained reward [4].

The implantation of intra-abdominal transmitters allows for the continuous measurement of body temperature and locomotor activity in the home cage (Figure 3B). In this thesis, two different types of transmitters are used: 1) Transmitters (TA10TA-F40, Data Science International (DSI), USA) that lie loosely in the abdomen and allow measurement of core body temperature; 2) Dual transmitters (TL11M3F40-TT, DSI, USA) with temperature-sensing leads to the portal vein in

the liver and to interscapular BAT, which measure core body temperature and BAT thermogenesis, respectively. Each home cage is placed on a receiver plate (DSI, USA) that receives radiofrequency signals from the abdominal transmitter. All plates are connected to software (DSI) that continuously records body temperature and locomotor activity. Telemetric measurements do not enable measurement of the temperature of the tail, which is an important thermoregulatory organ in rodents [15, 17, 57]. Tail temperature can be measured by an infrared/thermosensitive camera, which is difficult to employ without human interference.

A

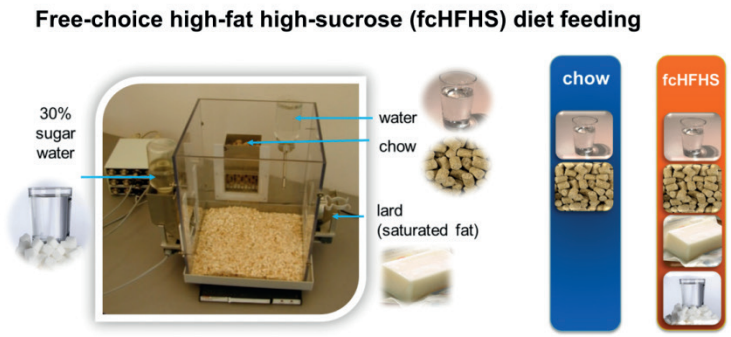

B

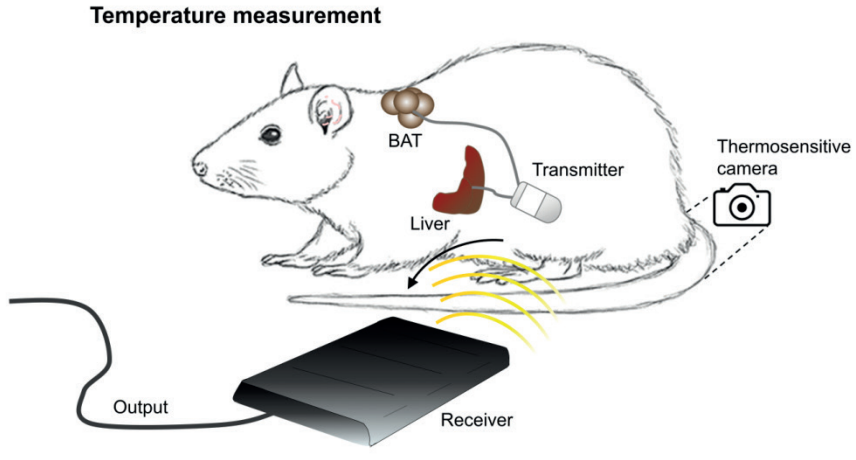

Figure 3. Monitoring system for feeding behavior and body temperature. (A) Home cage in which the free-choice high-fat high-sucrose (fcHFHS) diet is offered. Feeding behavior is monitored by the automatic weighing system. (B) Measurement of body temperature and locomotor activity. Telemetry is used to measure core body (liver) and brown adipose tissue (BAT) temperature, while an infrared/thermosensitive camera is used for tail temperature measurements.

4.3 Retrograde viral tracing

Retrograde viral tracers can be used to visualize neuronal connections, and to reveal the exact location of the projection neurons. Unlike most conventional chemical retrograde tracers, viral retrograde tracers abundantly express their products in infected neurons, resulting in a strong labeling [145, 146]. In this thesis, two different retrograde viral tracers are used, rabies virus (RABV) and herpes simplex virus type 1, which both retrogradely infect neurons [146-149] (Figure 4). To visualize all direct presynaptic inputs to the injection site (in the PAG), a G gene deletion mutant RABV, deficient in the expression of the RABV G coat, was employed [145, 150]. A fluorescent protein (mCherry) was inserted in place of the deleted G, permitting the visualization of infected neurons [145]. Note that the injected rabies virus carries a rabies G coat (since is was generated in a packaging cell line constitutively expressing rabies G), so that it infects all axon terminals near the injection site. From here, it is retrogradely transported to the cell body, where it initiates an infectious cycle, resulting in the expression of the fluorescent protein from RABV (mCherry). RABV is unable to spread to second order neurons because of the G gene deletion (since viral particles only contain the G protein but not the G gene). Thus, the G gene deletion mutant RABV is a retrograde viral tracer that can be used to identify the direct presynaptic inputs (neurons sending axon terminals) to the area where the virus was injected [145, 150]. Since this tracer does not cross synapses, it is unable to establish direct synaptic connectivity between presynaptic inputs and neurons in the injected area [145].

To restrict retrograde viral tracing to a specific cell-type, viral tracers can be designed to be Cre-dependent [147]. When the coding sequence for the fluorescent protein is inserted into a viral vector using a double-floxed inverted open reading frame (DIO), the Cre recombinase enzyme is required to recombine (reorient) the sequence, allowing expression of the fluorescent protein (mCherry). Cre is not endogenously expressed in animals, but can be introduced using transgenic animals. In this thesis, the LEPR-Cre mouse line is used, which expresses Cre in LEPR expressing neurons [55]. A Cre-dependent HSV virus was infused into (the PAG of) these mice, which allows the determination of the direct LEPR-positive presynaptic inputs to the injection site [147-149] (Figure 4).

4.4 Modulation of the activity of specific neuronal projections

Over the last few years, several tools have been developed to investigate the effects of altered neuronal activity on behavior, including optogenetics, chemogenetics, and technology to silence neurons permanently. The latter two techniques are employed in this thesis.

4.4.1 Reversible modulation of neuronal activity by DREADD

Designer receptors exclusively activated by designer drugs (DREADD), or chemogenetics, is a technology that allows reversible manipulation of the activity of selected neuronal populations and pathways [151-153]. DREADDs are human muscarinic receptors that have been mutated as such that they are no longer activated by their endogenous ligand, acetylcholine, but exclusively by the pharmacologically inert "designer drug" clozapine N-oxide (CNO). Two major classes of DREADDs have been developed: the excitatory hM3Dq and the inhibitory hM4Di, which are both G-protein coupled receptors that couple to Gq and Gi proteins, respectively. The (peripheral) administration of CNO leads to the activation of DREADDs, resulting in the initiation of several intracellular signaling cascades, which either enhance (Gq) or reduce (Gi) neuronal excitability [151-153].

A

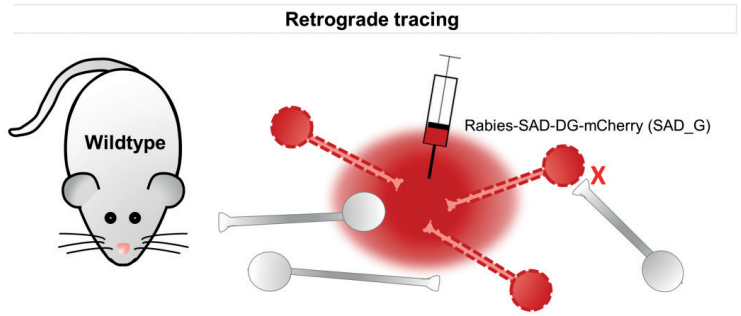

B

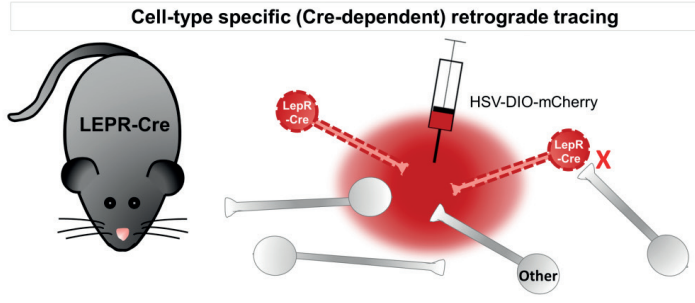

Figure 4. Retrograde viral tracing. (A) The retrograde viral tracer RABV ΔG (Rabies-SAD-DG-mCherry (SAD_G)), coated with its native G coat, is taken up by all axon terminals near the injection site, and can be used for retrograde labeling of direct presynaptic inputs. (B) Cre-dependent retrograde tracing (HSV-DIO-mCherry) allows cell-type specific retrograde tracing. The viral tracer is only expressed in Cre-expressing neurons, which are LEPR positive in this example.

The combination of DREADD technology with Cre-mediated homologous recombination enables specific manipulation of selected neuronal populations and pathways [153]. The infusion of Cre-dependent DREADD in mouse Cre-lines allows for the targeting of specific neuronal populations, such as LEPR positive neurons in LepR-Cre mice, while the combination of Cre-dependent DREADD technology with Cre-expressing viral vectors enables manipulation of specific neural pathways. The latter technique can be applied in wildtype animals and involves the infusion of two viral vectors: DREADD and canine adenovirus 2 expressing Cre recombinase (CAV2Cre) into two sites that are connected through a direct synaptic connection, representing a neuronal pathway (Figure 5). The DREADD virus is infused in "region A" that contains the cell bodies, while CAV2Cre is infused in "region B", which contains axon terminals originating from the cell bodies in "region A". CAV2Cre is taken up by the axon terminals in "region B", and retrogradely transported towards the cell bodies of neurons that project to "region B", including those in "region A". The expression of the Cre enzyme in "region A", in which the Cre-dependent DREADD virus with a double-floxed inverted open reading frame (DIO) was infused, is necessary for the reorientation of the inverted sequence of DREADD, thereby prompting the expression of DREADD receptors. This technique ensures that DREADD receptors are not expressed in all infected neurons, but exclusively in those neurons that are also infected with CAV2Cre. Therefore, CNO administration will selectively (and reversibly) modulate the activity of neurons that project from "region A" to "region B" [153].

4.4.2 Permanent inactivation of neuronal activity by TetTox

The combination of Cre-dependent tetanus toxin (TetTox) light chain technology with Cre-mediated homologous recombination can be used to permanently silence selected neuronal populations and pathways (Figure 5). This combinational approach is similar as described above for DREADD technology. Expression of TetTox in projection neurons prevents neurotransmitter release from infected neurons [154, 155]. The underlying mechanism involves TetTox light chain mediated proteolytical cleavage of VAMP2 (also termed synaptobrevin), a synaptic vesicle-associated membrane protein [156]. In the absence of VAMP2, the assembly of the SNARE protein complex, which is required for the fusion of synaptic vesicles with the presynaptic terminal, is inhibited. This leads to blockade of synaptic transmission, without resulting in neuronal cell death [156]. The combined use of Cre-dependent TetTox in "region A" and CAV2Cre in "region B" allows for selective and permanent inactivation of neurons that project from "region A" to "region B".

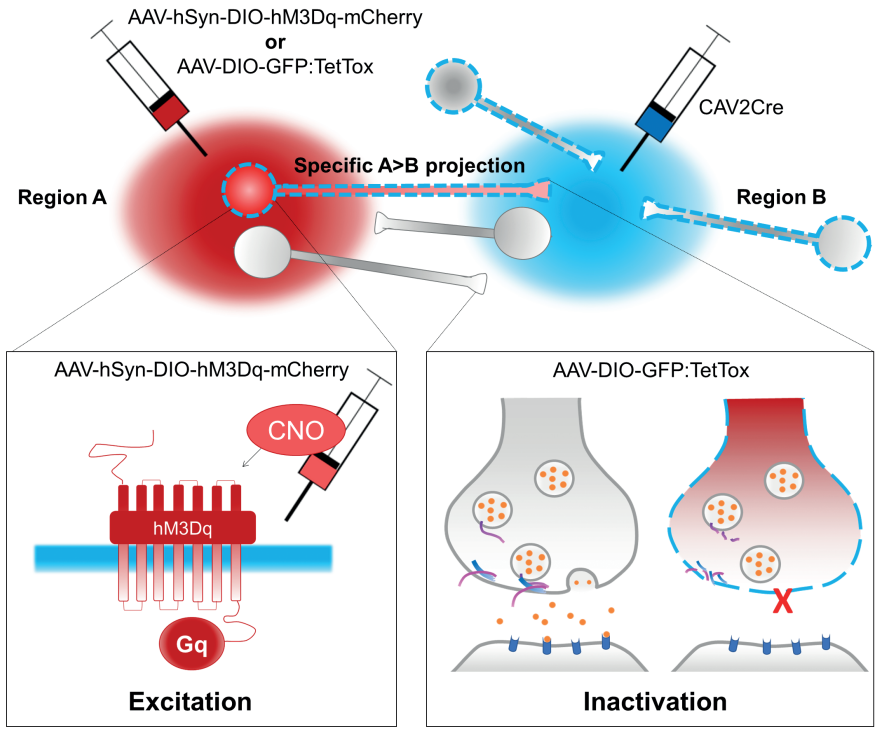

Figure 5. DREADD and TetTox technology combined with Cre-mediated homologous recombination. Infusion of a Cre-dependent DREADD virus (AAV-hSyn-DIO-hM3Dq-mCherry) or a Cre-dependent TetTox virus (AAV-DIO-GFP:TetTox) into region A, and CAV2Cre into region B for the specific manipulation of the A>B projection. Left panel: binding of CNO to hM3Dq receptors initiates signaling through the Gq signaling pathway, which results in the release of intracellular calcium stores and enhances neuronal excitation. Right panel: expression of TetTox light chain in infected projection neurons results in cleavage of the synaptic vesicle protein VAMP2, which prevents exocytosis of synaptic vesicles, resulting in a blockade in synaptic transmission.

5. Thesis outline

Living in our modern society, some individuals become heavily obese, whereas others appear obesity resistant [9]. This high variability in the susceptibility for the development of obesity remains largely unexplained. The overall aim of this thesis is to improve the understanding of the neural control of physiological processes that balance energy intake and expenditure, as well as of certain susceptibility factors that increase the risk for the development of obesity. These findings may eventually improve the prevention and/or treatment of obesity. Further, in this thesis, several technical challenges in studying the role of neural circuits in the control of energy balance are discussed, and several generally accepted concepts related to leptin, the hypothalamus, and energy balance are challenged.

Section I: Leptin and hypothalamic control of energy balance

The maintenance of a positive energy balance in obesity is regulated by multiple neural circuits that control energy intake and energy expenditure. Among these circuits, the hypothalamus is particularly known for its critical role in the control of energy balance [3, 6, 19]. It senses and integrates information from adiposity hormones like leptin, which inform the brain about energy storage and availability, with other metabolic signals, and responds by adapting energy intake and energy expenditure accordingly [3]. Therefore, the first section of this thesis focusses on leptin and hypothalamic control of energy balance.

Chapter 2. This chapter provides a detailed overview of the currently known cellular mechanisms by which hypothalamic inflammation is mediated in DIO, and how it promotes central leptin resistance and obesity. In the reviewed studies, DIO is usually modelled by exposing rodents to pelleted high-fat diets, which may confound the interpretation of the importance of inflammatory signaling in the development of central leptin resistance and obesity in the human situation. The fcHFHS diet mimics the human diet more closely than pelleted diets [4, 79, 85, 86, 138, 142]. Therefore, in ***appendix I***, the development of inflammatory signaling was studied in the mediobasal hypothalamus of rats that have been exposed to the fcHFHS diet for 8 weeks.

Chapter 3. It is generally believed that leptin resistance results from the overconsumption of energy-dense diets, high in saturated fat and sugar, via processes like inflammatory signaling, and that this diet-induced leptin resistance contributes to the development of obesity. However, there is some evidence that reduced leptin sensitivity does not necessarily result from energy-dense diet feeding, but may already be present before energy-dense diet exposure and

predispose rats to exacerbated DIO [9, 98]. Especially Wistar rats were previously reported to show high variability in the feeding response to leptin, which was related to the susceptibility to obesity development [9]. However, it was not tested whether leptin sensitivity is a stable parameter in a rat. Therefore, it was unclear to what extent a pre-existing reduction in leptin sensitivity is a predictor for DIO. In chapter 3, we first tested in Wistar rats whether leptin sensitivity is a stable parameter in a rat over time. Then, we investigated whether individual leptin sensitivity on a chow diet predicts the development of obesity on a fcHFHS diet, and how this is related to the development of diet-induced leptin resistance. Finally, we studied how the sensitivity to leptin's food intake suppressing effects is related to cellular leptin sensitivity in the ARC, VMH, and DMH of the hypothalamus.

Previously, hyperphagia in DIO prone rats was caused by an increase in meal size, but not meal number, compared with both DR rats and chow diet fed rats [157]. However, it was not studied whether DIO prone rats already consume larger meals before high-fat diet exposure, which may predispose them to exacerbated DIO. Therefore, we studied in ***appendix II*** whether individual leptin sensitivity on a chow diet and the susceptibility for the development of DIO are related to the consumption of larger meal sizes on chow diet.

Chapter 4. Two key findings of chapter 3 are that we confirmed that reduced sensitivity to leptin's anorexigenic effects is a pre-existing vulnerability factor for DIO, and that reduced pSTAT3 activation in the DMH (and VMH), but not the ARC, on a chow diet likely explains the difference in developing excessive obesity or not on a fcHFHS diet. From this study, it was still unclear how the pre-existing reduction in pSTAT3 activation in the DMH predisposes rats to exacerbated DIO. Leptin is particularly known to activate brown adipose tissue (BAT) thermogenesis via neurons in the DMH [15, 46, 54, 55, 158]. Therefore, the aim of chapter 4 was to unravel whether rats that are less sensitive to the anorexigenic effects of peripherally injected leptin also show a reduced thermogenic response to peripheral leptin. Further, to explore whether a reduced thermogenic response to peripheral leptin could be due to reduced cellular leptin signaling in the DMH (as opposed to, for example, impaired leptin transport across the blood-brain barrier), we compared leptin regulation of thermogenesis after peripheral versus intra-DMH leptin injection. More recently, it has been reported that, at least in ob/ob mice, systemic leptin injection leads to a pyrexic increase in core body temperature by reducing heat loss via the tail, without affecting BAT thermogenesis [74]. Therefore, we also compared the contribution of BAT thermogenesis and heat loss via the tail to leptin's effect on core body temperature.

In ***appendix III***, we aimed to study whether viral vector mediated blockade of leptin receptor signaling within DMH neurons, or inactivation of LEPR-expressing DMH neurons, reduces core body temperature, and thereby results in increased body adiposity. The appendix describes the challenges in using viral vector technology to downregulate leptin receptor signaling specifically in DMH neurons.

Section II: Regulation of energy balance beyond the hypothalamus

The hypothalamus does not act in isolation, but regulates energy balance via functional connections with other major brain areas, such as the midbrain [6, 7]. Therefore, the second section of this thesis focusses on the regulation of energy balance by projections from the hypothalamus to two other brain areas that are implicated in the control of energy balance: the PAG and the VTA.

Chapter 5. The DMH is generally accepted to exert its sympathetic control of BAT thermogenesis via projections to sympathetic premotor neurons in the RPa [13, 56, 57, 63, 65, 67, 104], but there is evidence that the PAG is also an important relay in the descending pathways mediating thermogenesis [57, 63, 66, 67]. The PAG is a relatively long midbrain region that can be divided into distinct subdivisions [108]. The anatomical projections from the DMH to the distinct PAG subdivisions and their function are largely elusive, and may differ per anterior-posterior level from bregma [66, 106, 108, 109]. In chapter 5, we aimed to investigate the anatomical projections from the DMH to the PAG along the entire anterior-posterior axis of the PAG by using anterograde and retrograde viral tracers, and to study the role of these projections in thermogenesis by using DREADD technology. In this chapter, we also describe the technical challenges of (dual) viral vector technology that hampered precise determination of anatomical and functional projections from the DMH to specific subregions of the PAG.

In ***appendix IV,*** we studied whether the projections from the DMH to the PAG are leptin sensitive. Leptin signaling in the DMH is known to critically mediate thermogenesis [46, 54, 55], and at least some subdivisions of the PAG, at unknown anterior-posterior levels, were previously shown to receive input from LEPR-positive neurons in the DMH [115, 116]. We extended the results of previous studies by investigating which subdivisions and anterior-posterior levels of the PAG receive input from LEPR-positive neurons in the DMH, and whether LEPR-positive neurons in the DMH form a major hypothalamic input area to the PAG.

Chapter 6. As also discussed in chapter 5, we experienced several technical challenges in targeting the DMH and its projections with dual viral vector technology. ***Appendix V*** gives an overview of the difficulties in targeting the DMH with (dual) viral vector technology. In chapter 6, we aimed to target the DMH to VTA projection, but the histology analysis revealed that the DMH was not the main target; instead, the zona incerta (ZI) appeared to be the main target. In accordance, the ZI was previously shown to provide the major direct hypothalamic innervation of the VTA, together with the LH [132, 133]. Both the ZI and the VTA have been implicated in feeding behavior, but it has not been studied before whether the ZI to VTA projection regulates feeding. In chapter 6, we investigated the role of the ZI to VTA projection in the regulation of several aspects of feeding behavior, including the motivation to work for food and feeding microstructure. Locomotor activity and body temperature were also tested in order to determine whether the ZI to VTA projection specifically mediates feeding behavior, or also has a role in energy metabolism.

Summary and general discussion

Chapter 7. In the final chapter, it is discussed how the findings from the experimental studies may be combined to provide a comprehensive overview of how a pre-existing reduction in leptin sensitivity may predispose rats to exacerbated obesity. In this discussion, several generally accepted concepts related to leptin, the hypothalamus, and energy balance are challenged. Further, this chapter discusses the unanticipated results regarding the neural projections that control energy intake and energy expenditure. Also the technical challenges and limitations in performing these studies are described. Finally, it is proposed how the findings of this thesis translate to the human situation, and how they may contribute to the prevention and/or treatment of obesity.

References

1. World Health Organization, 2016. Overweight and obesity.
2. Pan H, Guo J, Su Z. Advances in understanding the interrelations between leptin resistance and obesity. *Physiol Behav* 2014; **130**: 157-169.
3. Zhou Y, Rui L. Leptin signaling and leptin resistance. *Front Med* 2013; **7**: 207-222.
4. la Fleur SE, Vanderschuren LJ, Luijendijk MC, Kloeze BM, Tiesjema B, Adan RA. A reciprocal interaction between food-motivated behavior and diet-induced obesity. *Int J Obes (Lond)* 2007; **31**: 1286-1294.
5. Ferrario CR, Labouebe G, Liu S, Nieh EH, Routh VH, Xu S, et al. Homeostasis Meets Motivation in the Battle to Control Food Intake. *J Neurosci* 2016; **36**: 11469-11481.
6. Berthoud HR, Munzberg H, Morrison CD. Blaming the Brain for Obesity: Integration of Hedonic and Homeostatic Mechanisms. *Gastroenterology* 2017; **152**: 1728-1738.
7. Wilson JL, Enriori PJ. A talk between fat tissue, gut, pancreas and brain to control body weight. *Mol Cell Endocrinol* 2015; **418 Pt 2**: 108-119.
8. Pandit R, de Jong JW, Vanderschuren LJ, Adan RA. Neurobiology of overeating and obesity: the role of melanocortins and beyond. *Eur J Pharmacol* 2011; **660**: 28-42.
9. Ruffin MP, Adage T, Kuipers F, Strubbe JH, Scheurink AJ, van Dijk G. Feeding and temperature responses to intravenous leptin infusion are differential predictors of obesity in rats. *Am J Physiol Regul Integr Comp Physiol* 2004; **286**: R756-63.
10. Morris DL, Rui L. Recent advances in understanding leptin signaling and leptin resistance. *Am J Physiol Endocrinol Metab* 2009; **297**: E1247-59.
11. Seale P, Lazar MA. Brown fat in humans: turning up the heat on obesity. *Diabetes* 2009; **58**: 1482-1484.
12. Abreu-Vieira G, Xiao C, Gavrilova O, Reitman ML. Integration of body temperature into the analysis of energy expenditure in the mouse. *Mol Metab* 2015; **4**: 461-470.
13. Clapham JC. Central control of thermogenesis. *Neuropharmacology* 2012; **63**: 111-123.
14. Pandit R, Beerens S, Adan RAH. Role of leptin in energy expenditure: the hypothalamic perspective. *Am J Physiol Regul Integr Comp Physiol* 2017; **312**: R938-R947.
15. Rezai-Zadeh K, Munzberg H. Integration of sensory information via central thermoregulatory leptin targets. *Physiol Behav* 2013; **121**: 49-55.
16. Morrison SF, Madden CJ, Tupone D. Central neural regulation of brown adipose tissue thermogenesis and energy expenditure. *Cell Metab* 2014; **19**: 741-756.
17. Morrison SF. Central neural control of thermoregulation and brown adipose tissue. *Auton Neurosci* 2016; **196**: 14-24.
18. Caron A, Lee S, Elmquist JK, Gautron L. Leptin and brain-adipose crosstalks. *Nat Rev Neurosci* 2018; **19**: 153-165.
19. Elmquist JK, Elias CF, Saper CB. From lesions to leptin: hypothalamic control of food intake and body weight. *Neuron* 1999; **22**: 221-232.
20. Zhang Y, Proenca R, Maffei M, Barone M, Leopold L, Friedman JM. Positional cloning of the mouse obese gene and its human homologue. *Nature* 1994; **372**: 425-432.
21. Coleman DL. A historical perspective on leptin. *Nat Med* 2010; **16**: 1097-1099.
22. Halaas JL, Gajiwala KS, Maffei M, Cohen SL, Chait BT, Rabinowitz D, et al. Weight-reducing effects of the plasma protein encoded by the obese gene. *Science* 1995; **269**: 543-546.
23. St-Pierre J, Tremblay ML. Modulation of leptin resistance by protein tyrosine phosphatases. *Cell Metab* 2012; **15**: 292-297.
24. Lee GH, Proenca R, Montez JM, Carroll KM, Darvishzadeh JG, Lee JI, et al. Abnormal splicing of the leptin receptor in diabetic mice. *Nature* 1996; **379**: 632-635.

25. Munzberg H, Morrison CD. Structure, production and signaling of leptin. *Metabolism* 2015; **64**: 13-23.
26. Montague CT, Farooqi IS, Whitehead JP, Soos MA, Rau H, Wareham NJ, et al. Congenital leptin deficiency is associated with severe early-onset obesity in humans. *Nature* 1997; **387**: 903-908.
27. Strobel A, Issad T, Camoin L, Ozata M, Strosberg AD. A leptin missense mutation associated with hypogonadism and morbid obesity. *Nat Genet* 1998; **18**: 213-215.
28. Farooqi IS, Jebb SA, Langmack G, Lawrence E, Cheetham CH, Prentice AM, et al. Effects of recombinant leptin therapy in a child with congenital leptin deficiency. *N Engl J Med* 1999; **341**: 879-884.
29. Farooqi IS, Matarese G, Lord GM, Keogh JM, Lawrence E, Agwu C, et al. Beneficial effects of leptin on obesity, T cell hyporesponsiveness, and neuroendocrine/metabolic dysfunction of human congenital leptin deficiency. *J Clin Invest* 2002; **110**: 1093-1103.
30. Gibson WT, Farooqi IS, Moreau M, DePaoli AM, Lawrence E, O'Rahilly S, et al. Congenital leptin deficiency due to homozygosity for the Delta133G mutation: report of another case and evaluation of response to four years of leptin therapy. *J Clin Endocrinol Metab* 2004; **89**: 4821-4826.
31. Licinio J, Caglayan S, Ozata M, Yildiz BO, de Miranda PB, O'Kirwan F, et al. Phenotypic effects of leptin replacement on morbid obesity, diabetes mellitus, hypogonadism, and behavior in leptin-deficient adults. *Proc Natl Acad Sci U S A* 2004; **101**: 4531-4536.
32. Sukumaran S, Xue B, Jusko WJ, Dubois DC, Almon RR. Circadian variations in gene expression in rat abdominal adipose tissue and relationship to physiology. *Physiol Genomics* 2010; **42A**: 141-152.
33. Trayhurn P, Thomas ME, Duncan JS, Rayner DV. Effects of fasting and refeeding on ob gene expression in white adipose tissue of lean and obese (oblob) mice. *FEBS Lett* 1995; **368**: 488-490.
34. Boden G, Chen X, Mozzoli M, Ryan I. Effect of fasting on serum leptin in normal human subjects. *J Clin Endocrinol Metab* 1996; **81**: 3419-3423.
35. Trayhurn P, Duncan JS, Rayner DV. Acute cold-induced suppression of ob (obese) gene expression in white adipose tissue of mice: mediation by the sympathetic system. *Biochem J* 1995; **311 (Pt 3)**: 729-733.
36. Dardeno TA, Chou SH, Moon HS, Chamberland JP, Fiorenza CG, Mantzoros CS. Leptin in human physiology and therapeutics. *Front Neuroendocrinol* 2010; **31**: 377-393.
37. Velloso LA, Schwartz MW. Altered hypothalamic function in diet-induced obesity. *Int J Obes (Lond)* 2011; **35**: 1455-1465.
38. Ryan KK, Woods SC, Seeley RJ. Central nervous system mechanisms linking the consumption of palatable high-fat diets to the defense of greater adiposity. *Cell Metab* 2012; **15**: 137-149.
39. Bates SH, Stearns WH, Dundon TA, Schubert M, Tso AW, Wang Y, et al. STAT3 signalling is required for leptin regulation of energy balance but not reproduction. *Nature* 2003; **421**: 856.
40. Jiang L, You J, Yu X, Gonzalez L, Yu Y, Wang Q, et al. Tyrosine-dependent and -independent actions of leptin receptor in control of energy balance and glucose homeostasis. *Proc Natl Acad Sci U S A* 2008; **105**: 18619-18624.
41. Piper ML, Unger EK, Myers MG,Jr, Xu AW. Specific physiological roles for signal transducer and activator of transcription 3 in leptin receptor-expressing neurons. *Mol Endocrinol* 2008; **22**: 751-759.
42. Gao Q, Wolfgang MJ, Neschen S, Morino K, Horvath TL, Shulman GI, et al. Disruption of neural signal transducer and activator of transcription 3 causes obesity, diabetes, infertility, and thermal dysregulation. *Proc Natl Acad Sci U S A* 2004; **101**: 4661-4666.
43. Mark AL. Selective leptin resistance revisited. *Am J Physiol Regul Integr Comp Physiol* 2013; **305**: R566-81.
44. Haring SJ, Harris RB. The relation between dietary fructose, dietary fat and leptin responsiveness in rats. *Physiol Behav* 2011; **104**: 914-922.

45. Enriori PJ, Evans AE, Sinnayah P, Jobst EE, Tonelli-Lemos L, Billes SK, et al. Diet-induced obesity causes severe but reversible leptin resistance in arcuate melanocortin neurons. *Cell Metab* 2007; **5**: 181-194.
46. Enriori PJ, Sinnayah P, Simonds SE, Garcia Rudaz C, Cowley MA. Leptin action in the dorsomedial hypothalamus increases sympathetic tone to brown adipose tissue in spite of systemic leptin resistance. *J Neurosci* 2011; **31**: 12189-12197.
47. Munzberg H, Flier JS, Bjorbaek C. Region-specific leptin resistance within the hypothalamus of diet-induced obese mice. *Endocrinology* 2004; **145**: 4880-4889.
48. Balthasar N, Coppari R, McMinn J, Liu SM, Lee CE, Tang V, et al. Leptin receptor signaling in POMC neurons is required for normal body weight homeostasis. *Neuron* 2004; **42**: 983-991.
49. van de Wall E, Leshan R, Xu AW, Balthasar N, Coppari R, Liu SM, et al. Collective and individual functions of leptin receptor modulated neurons controlling metabolism and ingestion. *Endocrinology* 2008; **149**: 1773-1785.
50. Myers MG, Cowley MA, Munzberg H. Mechanisms of leptin action and leptin resistance. *Annu Rev Physiol* 2008; **70**: 537-556.
51. Dhillon H, Zigman JM, Ye C, Lee CE, McGovern RA, Tang V, et al. Leptin directly activates SF1 neurons in the VMH, and this action by leptin is required for normal body-weight homeostasis. *Neuron* 2006; **49**: 191-203.
52. Gao Q, Horvath TL. Neuronal control of energy homeostasis. *FEBS Lett* 2008; **582**: 132-141.
53. Bingham NC, Anderson KK, Reuter AL, Stallings NR, Parker KL. Selective loss of leptin receptors in the ventromedial hypothalamic nucleus results in increased adiposity and a metabolic syndrome. *Endocrinology* 2008; **149**: 2138-2148.
54. Dodd GT, Worth AA, Nunn N, Korpal AK, Bechtold DA, Allison MB, et al. The thermogenic effect of leptin is dependent on a distinct population of prolactin-releasing peptide neurons in the dorsomedial hypothalamus. *Cell Metab* 2014; **20**: 639-649.
55. Rezai-Zadeh K, Yu S, Jiang Y, Laque A, Schwartzenburg C, Morrison CD, et al. Leptin receptor neurons in the dorsomedial hypothalamus are key regulators of energy expenditure and body weight, but not food intake. *Mol Metab* 2014; **3**: 681-693.
56. Heeren J, Munzberg H. Novel aspects of brown adipose tissue biology. *Endocrinol Metab Clin North Am* 2013; **42**: 89-107.
57. Dimicco JA, Zaretsky DV. The dorsomedial hypothalamus: a new player in thermoregulation. *Am J Physiol Regul Integr Comp Physiol* 2007; **292**: R47-63.
58. Cote I, Sakarya Y, Green SM, Morgan D, Carter CS, Tumer N, et al. iBAT sympathetic innervation is not required for body weight loss induced by central leptin delivery. *Am J Physiol Endocrinol Metab* 2017;: ajpendo.00219.2017.
59. van Marken Lichtenbelt WD, Vanhommerig JW, Smulders NM, Drossaerts JM, Kemerink GJ, Bouvy ND, et al. Cold-activated brown adipose tissue in healthy men. *N Engl J Med* 2009; **360**: 1500-1508.
60. Nedergaard J, Bengtsson T, Cannon B. Unexpected evidence for active brown adipose tissue in adult humans. *Am J Physiol Endocrinol Metab* 2007; **293**: E444-52.
61. Cypess AM, Lehman S, Williams G, Tal I, Rodman D, Goldfine AB, et al. Identification and importance of brown adipose tissue in adult humans. *N Engl J Med* 2009; **360**: 1509-1517.
62. Virtanen KA, Lidell ME, Orava J, Heglind M, Westergren R, Niemi T, et al. Functional brown adipose tissue in healthy adults. *N Engl J Med* 2009; **360**: 1518-1525.
63. Morrison SF, Nakamura K, Madden CJ. Central control of thermogenesis in mammals. *Exp Physiol* 2008; **93**: 773-797.
64. Zaretskaia MV, Zaretsky DV, Shekhar A, DiMicco JA. Chemical stimulation of the dorsomedial hypothalamus evokes non-shivering thermogenesis in anesthetized rats. *Brain Res* 2002; **928**: 113-125.

65. Cao WH, Fan W, Morrison SF. Medullary pathways mediating specific sympathetic responses to activation of dorsomedial hypothalamus. *Neuroscience* 2004; **126**: 229-240.
66. de Menezes RC, Zaretsky DV, Fontes MA, DiMicco JA. Microinjection of muscimol into caudal periaqueductal gray lowers body temperature and attenuates increases in temperature and activity evoked from the dorsomedial hypothalamus. *Brain Res* 2006; **1092**: 129-137.
67. Rathner JA, Morrison SF. Rostral ventromedial periaqueductal gray: a source of inhibition of the sympathetic outflow to brown adipose tissue. *Brain Res* 2006; **1077**: 99-107.
68. Mercer JG, Hoggard N, Williams LM, Lawrence CB, Hannah LT, Trayhurn P. Localization of leptin receptor mRNA and the long form splice variant (Ob-Rb) in mouse hypothalamus and adjacent brain regions by in situ hybridization. *FEBS Lett* 1996; **387**: 113-116.
69. Elmquist JK, Bjorbaek C, Ahima RS, Flier JS, Saper CB. Distributions of leptin receptor mRNA isoforms in the rat brain. *J Comp Neurol* 1998; **395**: 535-547.
70. Laque A, Zhang Y, Gettys S, Nguyen TA, Bui K, Morrison CD, et al. Leptin receptor neurons in the mouse hypothalamus are colocalized with the neuropeptide galanin and mediate anorexigenic leptin action. *Am J Physiol Endocrinol Metab* 2013; **304**: E999-1011.
71. Harlan SM, Morgan DA, Agassandian K, Guo DF, Cassell MD, Sigmund CD, et al. Ablation of the leptin receptor in the hypothalamic arcuate nucleus abrogates leptin-induced sympathetic activation. *Circ Res* 2011; **108**: 808-812.
72. Kong D, Tong Q, Ye C, Koda S, Fuller PM, Krashes MJ, et al. GABAergic RIP-Cre neurons in the arcuate nucleus selectively regulate energy expenditure. *Cell* 2012; **151**: 645-657.
73. Minokoshi Y, Haque MS, Shimazu T. Microinjection of leptin into the ventromedial hypothalamus increases glucose uptake in peripheral tissues in rats. *Diabetes* 1999; **48**: 287-291.
74. Fischer AW, Cannon B, Nedergaard J. Leptin-deficient mice are not hypothermic, they are anapyrexic. *Mol Metab* 2016; **6**: 173.
75. Schwartz MW, Peskind E, Raskind M, Boyko EJ, Porte D,Jr. Cerebrospinal fluid leptin levels: relationship to plasma levels and to adiposity in humans. *Nat Med* 1996; **2**: 589-593.
76. Considine RV, Stephens TW, Nyce M, Ohannesian JP, Marco CC, McKee LJ, et al. Serum immunoreactive-leptin concentrations in normal-weight and obese humans. *The New England Journal of Medicine* 1996; **334**: 292.
77. Heymsfield SB, Greenberg AS, Fujioka K, Dixon RM, Kushner R, Hunt T, et al. Recombinant leptin for weight loss in obese and lean adults: a randomized, controlled, dose-escalation trial. *JAMA* 1999; **282**: 1568-1575.
78. Caro JF, Kolaczynski JW, Nyce MR, Ohannesian JP, Opentanova I, Goldman WH, et al. Decreased cerebrospinal-fluid/serum leptin ratio in obesity: a possible mechanism for leptin resistance. *Lancet* 1996; **348**: 159-161.
79. Apolzan JW, Harris RBS. Rapid onset and reversal of peripheral and central leptin resistance in rats offered chow, sucrose solution, and lard. *Appetite* 2013; **60**: 65-73.
80. Myers MG,Jr. Leptin keeps working, even in obesity. *Cell Metab* 2015; **21**: 791-792.
81. Ottaway N, Mahbod P, Rivero B, Norman LA, Gertler A, D'Alessio DA, et al. Diet-induced obese mice retain endogenous leptin action. *Cell Metab* 2015; **21**: 877-882.
82. Shapiro A, Tumer N, Gao Y, Cheng KY, Scarpace PJ. Prevention and reversal of diet-induced leptin resistance with a sugar-free diet despite high fat content. *Br J Nutr* 2011; **106**: 390-397.
83. Scarpace PJ, Matheny M, Tumer N, Cheng KY, Zhang Y. Leptin resistance exacerbates diet-induced obesity and is associated with diminished maximal leptin signalling capacity in rats. *Diabetologia* 2005; **48**: 1075-1083.
84. Frederich RC, Hamann A, Anderson S, Lollmann B, Lowell BB, Flier JS. Leptin levels reflect body lipid content in mice: evidence for diet-induced resistance to leptin action. *Nat Med* 1995; **1**: 1311-1314.
85. Harris RB, Apolzan JW. Changes in glucose tolerance and leptin responsiveness of rats offered a choice of lard, sucrose, and chow. *Am J Physiol Regul Integr Comp Physiol* 2012; **302**: R1327-39.
86. van den Heuvel JK, Eggels L, van Rozen AJ, Luijendijk MC, Fliers E, Kalsbeek A, et al. Neuropeptide Y and leptin sensitivity is dependent on diet composition. *J Neuroendocrinol* 2014; **26**: 377-385.
87. Scarpace PJ, Zhang Y. Leptin resistance: a prediposing factor for diet-induced obesity. *Am J Physiol Regul Integr Comp Physiol* 2009; **296**: R493-500.
88. Desai BN, Harris RB. An acute method to test leptin responsiveness in rats. *Am J Physiol Regul Integr Comp Physiol* 2014; **306**: R852-60.
89. Pandit R, Mercer JG, Overduin J, la Fleur SE, Adan RA. Dietary factors affect food reward and motivation to eat. *Obes Facts* 2012; **5**: 221-242.
90. Wang X, Ge A, Cheng M, Guo F, Zhao M, Zhou X, et al. Increased hypothalamic inflammation associated with the susceptibility to obesity in rats exposed to high-fat diet. *Exp Diabetes Res* 2012; **2012**: 847246.
91. Milanski M, Degasperi G, Coope A, Morari J, Denis R, Cintra DE, et al. Saturated fatty acids produce an inflammatory response predominantly through the activation of TLR4 signaling in hypothalamus: implications for the pathogenesis of obesity. *J Neurosci* 2009; **29**: 359-370.
92. Thaler JP, Yi CX, Schur EA, Guyenet SJ, Hwang BH, Dietrich MO, et al. Obesity is associated with hypothalamic injury in rodents and humans. *J Clin Invest* 2012; **122**: 153-162.
93. Williams LM. Hypothalamic dysfunction in obesity. *Proc Nutr Soc* 2012; **71**: 521-533.
94. Purkayastha S, Cai D. Neuroinflammatory basis of metabolic syndrome. *Mol Metab* 2013; **2**: 356-363.
95. de Git KC, Adan RA. Leptin resistance in diet-induced obesity: the role of hypothalamic inflammation. *Obes Rev* 2015; **16**: 207-224.
96. Konner AC, Bruning JC. Selective insulin and leptin resistance in metabolic disorders. *Cell Metab* 2012; **16**: 144-152.
97. Olofsson LE, Unger EK, Cheung CC, Xu AW. Modulation of AgRP-neuronal function by SOCS3 as an initiating event in diet-induced hypothalamic leptin resistance. *Proc Natl Acad Sci U S A* 2013; **110**: E697-706.
98. Levin BE, Dunn-Meynell AA. Reduced central leptin sensitivity in rats with diet-induced obesity. *Am J Physiol Regul Integr Comp Physiol* 2002; **283**: R941-8.
99. Levin BE, Dunn-Meynell AA, Banks WA. Obesity-prone rats have normal blood-brain barrier transport but defective central leptin signaling before obesity onset. *Am J Physiol Regul Integr Comp Physiol* 2004; **286**: R143-50.
100. Irani BG, Dunn-Meynell AA, Levin BE. Altered hypothalamic leptin, insulin, and melanocortin binding associated with moderate-fat diet and predisposition to obesity. *Endocrinology* 2007; **148**: 310-316.
101. Bouret SG, Gorski JN, Patterson CM, Chen S, Levin BE, Simerly RB. Hypothalamic neural projections are permanently disrupted in diet-induced obese rats. *Cell Metab* 2008; **7**: 179-185.
102. Levin BE, Dunn-Meynell AA, Ricci MR, Cummings DE. Abnormalities of leptin and ghrelin regulation in obesity-prone juvenile rats. *Am J Physiol Endocrinol Metab* 2003; **285**: E949-57.
103. de Menezes RC, Zaretsky DV, Fontes MA, DiMicco JA. Cardiovascular and thermal responses evoked from the periaqueductal grey require neuronal activity in the hypothalamus. *J Physiol* 2009; **587**: 1201-1215.
104. Chen XM, Nishi M, Taniguchi A, Nagashima K, Shibata M, Kanosue K. The caudal periaqueductal gray participates in the activation of brown adipose tissue in rats. *Neurosci Lett* 2002; **331**: 17-20.
105. Lee SJ, Kirigiti M, Lindsley SR, Loche A, Madden CJ, Morrison SF, et al. Efferent projections of neuropeptide Y-expressing neurons of the dorsomedial hypothalamus in chronic hyperphagic models. *J Comp Neurol* 2013; **521**: 1891-1914.
106. ter Horst GJ, Luiten PG. The projections of the dorsomedial hypothalamic nucleus in the rat. *Brain Res Bull* 1986; **16**: 231-248.
107. Papp RS, Palkovits M. Brainstem projections of neurons located in various subdivisions of the dorsolateral hypothalamic area-an anterograde tract-tracing study. *Front Neuroanat* 2014; **8**: 34.

108. Dampney RA, Furlong TM, Horiuchi J, Iigaya K. Role of dorsolateral periaqueductal grey in the coordinated regulation of cardiovascular and respiratory function. *Auton Neurosci* 2013; **175**: 17-25.
109. Thompson RH, Canteras NS, Swanson LW. Organization of projections from the dorsomedial nucleus of the hypothalamus: a PHA-L study in the rat. *J Comp Neurol* 1996; **376**: 143-173.
110. Yoshida K, Konishi M, Nagashima K, Saper CB, Kanosue K. Fos activation in hypothalamic neurons during cold or warm exposure: projections to periaqueductal gray matter. *Neuroscience* 2005; **133**: 1039-1046.
111. Bamshad M, Song CK, Bartness TJ. CNS origins of the sympathetic nervous system outflow to brown adipose tissue. *Am J Physiol* 1999; **276**: R1569-78.
112. Cano G, Passerin AM, Schiltz JC, Card JP, Morrison SF, Sved AF. Anatomical substrates for the central control of sympathetic outflow to interscapular adipose tissue during cold exposure. *J Comp Neurol* 2003; **460**: 303-326.
113. Hermann DM, Luppi PH, Peyron C, Hinckel P, Jouvet M. Afferent projections to the rat nuclei raphe magnus, raphe pallidus and reticularis gigantocellularis pars alpha demonstrated by iontophoretic application of choleratoxin (subunit b). *J Chem Neuroanat* 1997; **13**: 1-21.
114. Nogueira MI, de Rezende BD, do Vale LE, Bittencourt JC. Afferent connections of the caudal raphe pallidus nucleus in rats: a study using the fluorescent retrograde tracers fluorogold and true-blue. *Ann Anat* 2000; **182**: 35-45.
115. Gautron L, Lazarus M, Scott MM, Saper CB, Elmquist JK. Identifying the efferent projections of leptin-responsive neurons in the dorsomedial hypothalamus using a novel conditional tracing approach. *J Comp Neurol* 2010; **518**: 2090-2108.
116. Zhang Y, Kerman IA, Laque A, Nguyen P, Faouzi M, Louis GW, et al. Leptin-receptor-expressing neurons in the dorsomedial hypothalamus and median preoptic area regulate sympathetic brown adipose tissue circuits. *J Neurosci* 2011; **31**: 1873-1884.
117. Wise RA. Dopamine, learning and motivation. *Nat Rev Neurosci* 2004; **5**: 483-494.
118. Berridge KC. The debate over dopamine's role in reward: the case for incentive salience. *Psychopharmacology (Berl)* 2007; **191**: 391-431.
119. Meye FJ, Adan RA. Feelings about food: the ventral tegmental area in food reward and emotional eating. *Trends Pharmacol Sci* 2014; **35**: 31-40.
120. van Zessen R, van der Plasse G, Adan RA. Contribution of the mesolimbic dopamine system in mediating the effects of leptin and ghrelin on feeding. *Proc Nutr Soc* 2012; **71**: 435-445.
121. Boekhoudt L, Roelofs TJM, de Jong JW, de Leeuw AE, Luijendijk MCM, Wolterink-Donselaar IG, et al. Does activation of midbrain dopamine neurons promote or reduce feeding? *Int J Obes (Lond)* 2017; **41**: 1131-1140.
122. Zhou QY, Palmiter RD. Dopamine-deficient mice are severely hypoactive, adipsic, and aphagic. *Cell* 1995; **83**: 1197-1209.
123. Wang GJ, Volkow ND, Logan J, Pappas NR, Wong CT, Zhu W, et al. Brain dopamine and obesity. *Lancet* 2001; **357**: 354-357.
124. Volkow ND, Wang GJ, Fowler JS, Telang F. Overlapping neuronal circuits in addiction and obesity: evidence of systems pathology. *Philos Trans R Soc Lond B Biol Sci* 2008; **363**: 3191-3200.
125. Johnson PM, Kenny PJ. Dopamine D2 receptors in addiction-like reward dysfunction and compulsive eating in obese rats. *Nat Neurosci* 2010; **13**: 635-641.
126. Cone JJ, Chartoff EH, Potter DN, Ebner SR, Roitman MF. Prolonged high fat diet reduces dopamine reuptake without altering DAT gene expression. *PLoS One* 2013; **8**: e58251.
127. Stice E, Yokum S, Blum K, Bohon C. Weight gain is associated with reduced striatal response to palatable food. *J Neurosci* 2010; **30**: 13105-13109.
128. McCutcheon JE. The role of dopamine in the pursuit of nutritional value. *Physiol Behav* 2015; **152**: 408-415.

129. Boekhoudt L, Wijbrans EC, Man JHK, Luijendijk MCM, de Jong JW, van der Plasse G, et al. Enhancing excitability of dopamine neurons promotes motivational behaviour through increased action initiation. *Eur Neuropsychopharmacol* 2018; **28**: 171-184.
130. Salamone JD, Correa M. The mysterious motivational functions of mesolimbic dopamine. *Neuron* 2012; **76**: 470-485.
131. van der Plasse G, van Zessen R, Luijendijk MC, Erkan H, Stuber GD, Ramakers GM, et al. Modulation of cue-induced firing of ventral tegmental area dopamine neurons by leptin and ghrelin. *Int J Obes (Lond)* 2015; **39**: 1742-1749.
132. Ogawa SK, Cohen JY, Hwang D, Uchida N, Watabe-Uchida M. Organization of monosynaptic inputs to the serotonin and dopamine neuromodulatory systems. *Cell Rep* 2014; **8**: 1105-1118.
133. Gonzalez JA, Jensen LT, Fugger L, Burdakov D. Convergent inputs from electrically and topographically distinct orexin cells to locus coeruleus and ventral tegmental area. *Eur J Neurosci* 2012; **35**: 1426-1432.
134. Huang X, Charbeneau RA, Fu Y, Kaur K, Gerin I, MacDougald OA, et al. Resistance to diet-induced obesity and improved insulin sensitivity in mice with a regulator of G protein signaling-insensitive G184S Gnai2 allele. *Diabetes* 2008; **57**: 77-85.
135. Bruckbauer A, Zemel MB, Thorpe T, Akula MR, Stuckey AC, Osborne D, et al. Synergistic effects of leucine and resveratrol on insulin sensitivity and fat metabolism in adipocytes and mice. *Nutr Metab (Lond)* 2012; **9**: 77-7075-9-77.
136. Woods SC, Seeley RJ, Rushing PA, D'Alessio D, Tso P. A controlled high-fat diet induces an obese syndrome in rats. *J Nutr* 2003; **133**: 1081-1087.
137. Thibault L, Woods SC, Westerterp-Plantenga MS. The utility of animal models of human energy homeostasis. *Br J Nutr* 2004; **92 Suppl 1**: S41-5.
138. la Fleur SE, Luijendijk MC, van der Zwaal EM, Brans MA, Adan RA. The snacking rat as model of human obesity: effects of a free-choice high-fat high-sugar diet on meal patterns. *Int J Obes (Lond)* 2014; **38**: 643-649.
139. Mercer JG, Archer ZA. Putting the diet back into diet-induced obesity: diet-induced hypothalamic gene expression. *Eur J Pharmacol* 2008; **585**: 31-37.
140. Giesen JC, Havermans RC, Douven A, Tekelenburg M, Jansen A. Will work for snack food: the association of BMI and snack reinforcement. *Obesity (Silver Spring)* 2010; **18**: 966-970.
141. Rollins BY, Dearing KK, Epstein LH. Delay discounting moderates the effect of food reinforcement on energy intake among non-obese women. *Appetite* 2010; **55**: 420-425.
142. la Fleur SE, Luijendijk MC, van Rozen AJ, Kalsbeek A, Adan RA. A free-choice high-fat high-sugar diet induces glucose intolerance and insulin unresponsiveness to a glucose load not explained by obesity. *Int J Obes (Lond)* 2011; **35**: 595-604.
143. Tulipano G, Vergoni AV, Soldi D, Muller EE, Cocchi D. Characterization of the resistance to the anorectic and endocrine effects of leptin in obesity-prone and obesity-resistant rats fed a high-fat diet. *J Endocrinol* 2004; **183**: 289-298.
144. van der Zwaal EM, Luijendijk MC, Evers SS, la Fleur SE, Adan RA. Olanzapine affects locomotor activity and meal size in male rats. *Pharmacol Biochem Behav* 2010; **97**: 130-137.
145. Ginger M, Haberl M, Conzelmann KK, Schwarz MK, Frick A. Revealing the secrets of neuronal circuits with recombinant rabies virus technology. *Front Neural Circuits* 2013; **7**: 2.
146. Ohara S, Inoue K, Witter MP, Iijima T. Untangling neural networks with dual retrograde transsynaptic viral infection. *Front Neurosci* 2009; **3**: 344-349.
147. Zhu H, Yan H, Tang N, Li X, Pang P, Li H, et al. Impairments of spatial memory in an Alzheimer's disease model via degeneration of hippocampal cholinergic synapses. *Nat Commun* 2017; **8**: 1676-017-01943-0.
148. Neve RL, Lim F. Generation of high-titer defective HSV-1 vectors. *Curr Protoc Neurosci* 2013; **Chapter 4**: Unit 4.13.

149. Neve RL. Overview of gene delivery into cells using HSV-1-based vectors. *Curr Protoc Neurosci* 2012; **Chapter 4**: Unit 4.12.
150. Ghanem A, Conzelmann KK. G gene-deficient single-round rabies viruses for neuronal circuit analysis. *Virus Res* 2016; **216**: 41-54.
151. Gomez JL, Bonaventura J, Lesniak W, Mathews WB, Sysa-Shah P, Rodriguez LA, et al. Chemogenetics revealed: DREADD occupancy and activation via converted clozapine. *Science* 2017; **357**: 503-507.
152. Mahler SV, Aston-Jones G. CNO Evil? Considerations for the Use of DREADDs in Behavioral Neuroscience. *Neuropsychopharmacology* 2018; **43**:934-936.
153. Boender AJ, de Jong JW, Boekhoudt L, Luijendijk MC, van der Plasse G, Adan RA. Combined use of the canine adenovirus-2 and DREADD-technology to activate specific neural pathways in vivo. *PLoS One* 2014; **9**: e95392.
154. Carter ME, Han S, Palmiter RD. Parabrachial calcitonin gene-related peptide neurons mediate conditioned taste aversion. *J Neurosci* 2015; **35**: 4582-4586.
155. Campos CA, Bowen AJ, Han S, Wisse BE, Palmiter RD, Schwartz MW. Cancer-induced anorexia and malaise are mediated by CGRP neurons in the parabrachial nucleus. *Nat Neurosci* 2017; **20**: 934-942.
156. Yamamoto M, Wada N, Kitabatake Y, Watanabe D, Anzai M, Yokoyama M, et al. Reversible suppression of glutamatergic neurotransmission of cerebellar granule cells in vivo by genetically manipulated expression of tetanus neurotoxin light chain. *J Neurosci* 2003; **23**: 6759-6767.
157. Farley C, Cook JA, Spar BD, Austin TM, Kowalski TJ. Meal pattern analysis of diet-induced obesity in susceptible and resistant rats. *Obes Res* 2003; **11**: 845-851.
158. Jo YH, Buettner C. Why leptin keeps you warm. *Mol Metab* 2014; **3**: 779-780.

Section I

Leptin and hypothalamic control of energy balance

Chapter 2:

Leptin resistance in diet-induced obesity: the role of hypothalamic inflammation

K.C.G. de Git, R.A.H. Adan

Department of Translational Neuroscience, Brain Center Rudolf Magnus, University Medical Center Utrecht, Utrecht, The Netherlands

Published in Obesity Reviews (2015) Mar;16(3):207-24. doi: 10.1038/s41366-018-0111-4.

Summary

The consumption of Western diets, high in sugar and saturated fat, is a crucial contributor to the alarming incidence of obesity and its associated morbidities. These diets have been reported to induce an inflammatory response in the hypothalamus that promotes the development of central leptin resistance and obesity. This inflammatory signaling involves dynamic changes in the expression and activity of several mediators of the innate immune system, including toll-like receptor 4, IκB kinase-β/nuclear κB (IKKβ/NF-κB), c-Jun N-terminal kinase, suppressor of cytokine signaling 3, and pro-inflammatory cytokines, as well as the induction of endoplasmic reticulum stress and autophagy defect. Although the exact cellular mechanisms remain incompletely understood, recent evidence suggests that the inflammatory response is at least mediated by interactions between neurons and non-neuronal cells like microglia and astrocytes. Current evidence of the contribution of each inflammatory mediator to leptin resistance and DIO, including their reciprocal interactions and cell type specific effects, is reviewed and integrated in a conceptual model. Based on this model and pharmacological intervention studies, several inflammatory mediators are proposed to be promising therapeutic targets for the treatment of diet-induced obesity.

Introduction

The increasing incidence of obesity provides a major public health problem, as it is associated with the development of morbidities such as Type 2 Diabetes Mellitus and cardiovascular disease [1-3]. The increased availability of a variety of energy-dense diets, high in saturated fat and sugar, and a sedentary life style are crucial environmental factors in the obesity epidemic [4,5]. In order to study the pathophysiological mechanisms underlying obesity, rodent models have been developed where obesity is induced by dietary manipulation, i.e. diet-induced obesity (DIO), as a model of the human situation [6].

It has been widely accepted that obesity is associated with a state of chronic low-grade inflammation, characterized by the expression of pro-inflammatory markers in metabolic tissues and the circulation [1,3,7]. This inflammatory response is mediated by the innate immune system and is, in contrast to the classical inflammatory response, not pathogen-induced and relatively low-grade [1,7]. Studies in DIO rodent models have not only indicated peripheral inflammation, but also increased inflammatory signaling in the hypothalamus, which was linked to the development of central leptin resistance and obesity [8-10]. Although the understanding of the mechanisms by which hypothalamic inflammation promotes central leptin resistance has been improved over the past few years, the exact cellular mechanisms remain to be elucidated. This review provides a detailed overview of the currently known cellular mechanisms by which hypothalamic inflammation is mediated in DIO, and how this leads to central leptin resistance. In addition, the potential of pharmacological intervention to revert leptin resistance in DIO will be discussed.

Hypothalamic control of food intake

Leptin, a 16-kDa circulating polypeptide that is primarily secreted from adipose tissue, is recognized as one of the critical hormones controlling energy balance [11]. It signals to brain areas involved in energy homeostasis. The brain responds to high plasma leptin levels by reducing food intake and increasing energy expenditure, as well as by improving glucose metabolism by reducing glucose production in the liver [12, 83]. Leptin's biological action is mediated by the long form of the leptin receptor (LEPRb), which is expressed in many brain areas including the hypothalamus, the main leptin target [11]. Leptin binding to the LEPRb activates Janus kinase 2 (JAK2), thereby initiating several signal transduction pathways that act coordinately to regulate energy balance and body weight [for an overview see 11,12]. Transduction

of leptin signaling is marked by increased phosphorylation of signal transducer and activator of transcript 3 (STAT3) [13], a critical transcription factor for leptin's anti-obesity actions [14].

The hypothalamus contains several sub-nuclei, of which the arcuate nucleus (ARC) is a major site of leptin action. The ARC lies within the mediobasal hypothalamus (MBH), adjacent to the third ventricle and immediately above the median eminence (ME), a circumventricular organ with an incomplete blood brain barrier (BBB) [1,12,14] (Fig. 1). Consequently, the ARC lies partially outside the BBB and is perfectly accessible to hormones and nutrients from the circulation and the cerebrospinal fluid (CSF) [1]. The ARC contains at least two principal populations of neurons that have opposing actions on energy balance: the orexigenic (appetite-stimulating) agouti-related protein (AgRP) neurons and the anorexigenic (appetite suppressing) proopiomelanocortin (POMC) neurons [1,11,12]. Both neuronal populations contain LEPRb-expressing cells and cells that project to second order neurons in other hypothalamic nuclei, such as the paraventricular nucleus (PVN) and ventromedial hypothalamus (VMH), to regulate energy balance [11,15]. Leptin exerts its anorexigenic effects by inhibiting AgRP neurons while activating POMC neurons [1,11].

Leptin resistance

Most obese individuals show increased food intake despite high circulating leptin levels [16], implying a state of leptin resistance, i.e. reduced responsiveness to leptin's appetite and weight gain suppressing effects [11]. Indeed, after exogenous administration of leptin, obese individuals do not respond with a decrease in food intake that is normally observed in lean individuals [17,18]. Overnutrition is thought to be both a cause and a consequence of leptin resistance in DIO. That is, overnutrition, particularly a high-fat diet (HFD), may induce leptin resistance in the absence of obesity by acting on leptin-responsive neurons, and leptin resistance in obesity may maintain overnutrition [5]. Various mechanisms have been proposed to mediate leptin resistance in DIO, including impairment in leptin transport over the BBB, LEPRb trafficking, and leptin signaling (for review see [11,14]). In this review, however, we focus on the mechanisms by which hypothalamic inflammation mediates leptin resistance.

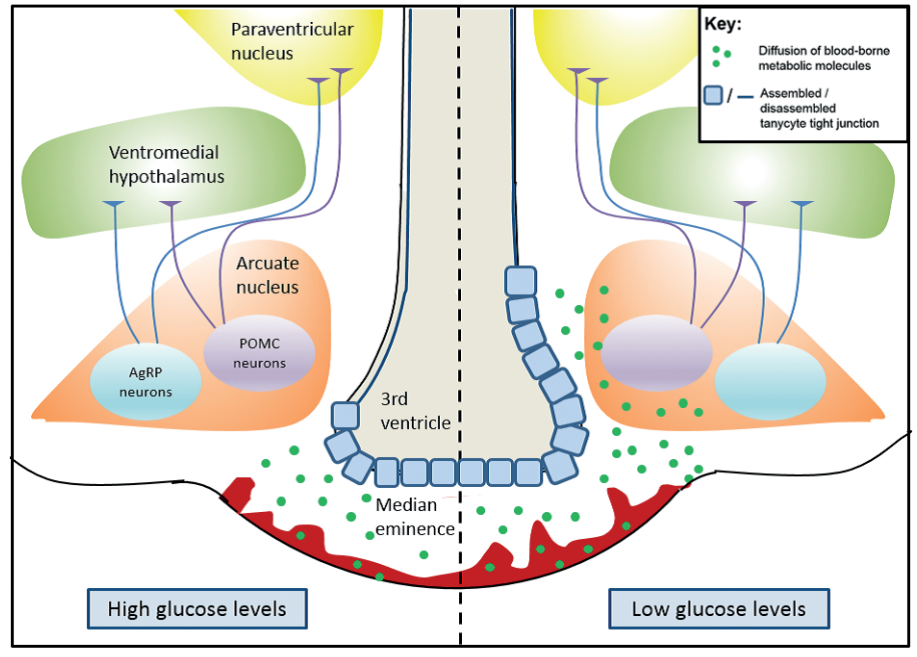

Figure 1. Control of energy balance by hypothalamic neurons and the blood-CSF barrier. The arcuate nucleus with proopiomelanocortin (POMC) and agouti-related peptide (AgRP) neurons, which receive direct input from circulating hormones such as leptin. They then signal second order neurons located in areas such as the paraventricular nucleus and ventromedial hypothalamus to control energy balance. The blood-CSF barrier is controlled by tanycytes. Under low glucose levels, tanycyte tight junctions are assembled, which allows diffusion of blood-borne metabolic signals to the ARC. Conversely, under high glucose levels the diffusion is blocked due to disassembled tanycyte tight junctions.

Inflammatory pathways mediating leptin resistance in DIO

Several components of the innate immune system have been proposed to mediate leptin resistance under conditions of overnutrition, showing a dynamic signaling pattern in DIO rodents (Table 1). Since most studies have used whole hypothalamus extracts to determine the expression of inflammatory mediators by means of Western blotting or RT-PCR, it remains largely elusive which specific cell types mediate HFD-induced inflammation. The relative importance of each signaling component in mediating leptin resistance and DIO, as well as current understanding of their reciprocal interactions and cell type specific effects, will be discussed below.

Table 1. Dynamics of inflammatory signaling in diet-induced obesity

Length dietary manipulation	Diet or nutrient	Rodent type/strain	Brain region/cell type	Effect on expression or activity	Ref
IKKβ/ NF-κB					
4 hr	Palmitate*	Long Evans rats	Hypothalamus	↑ P-IKKβ; ↓IκBα protein	21
6 hr	Glucose/OA*	C57BL/6 mice	Hypothalamus	↑ NF-κB activity	20
1,3/7/14,28 d	HFDα	Long Evans rats	Hypothalamus	=/=/=IκBα mRNA; ↑/=/↑IKKβ mRNA	10
3/7 d	HFDα	C57BL/6 mice	Hypothalamus	↑/= IκBα mRNA; ↑/= IKKβ mRNA	10
4 wk	HFD	Long Evans rats	MBH	↑P-IKKβ; ↓IκBα protein	21
8 wk	HFDβ	Swiss mice	Hypothalamus	↑ P-IκBα protein	27
12 wk	HFDβ	Wistar rats	Hypothalamus	↑P-IKK; ↓ IκBα protein	28
13/16 wk	HFD	Wistar rats	Hypothalamus	=/↑ NF-κB activation	29
16 wk	HFDγ	C57BL/6 mice	MBH	↑P-IKK	24, 81
18 wk	HFD-DIO	Sprague-Dawley rats	Hypothalamus	↑ NF-κB mRNA	8
20 wk	HFDα	Long Evans rats	Hypothalamus	↑ IκBα mRNA; = IKKβ mRNA	10
N.A.	HFDα	C57BL/6 mice	Hypothalamus/ MBH neurons	↑/↑ NF-κB activity; ↑/N.A. IKKβ and IκBα mRNA	20
JNK					
1,2,3 d	AA*	Wistar rats	Hypothalamus	↑ P-JNK	9
10, 30 d	WD	Wistar rats	Hypothalamus	↑ P-JNK	31
8 wk	HFDα	C57BL/6 mice	Hypothalamus	↑ P-JNK	32,33
8 wk	HFDβ	Swiss mice	Hypothalamus	↑ P-JNK	27
13, 16 wk	HFD	Wistar rats	Hypothalamus, ARC, LH	↑ P-JNK	29
TLR4					
3 d	AA*	Wistar rats	Hypothalamus	↑TLR4/MyD88 associations	9
8 wk	HFDδ	Wistar rats	Hypothalamus	↑TLR4/MyD88 associations	9
12 wk	HFDβ	Wistar rats	Hypothalamus	↑TLR4 protein	28
18 wk	HFD-DIO	Sprague-Dawley rats	Hypothalamus	↑TLR4 mRNA	8
ER stress					
1,2,3 d	AA*	Wistar rats	Hypothalamus	↑P-PERK, ↑P-eIF2α; ↑GRP78 protein	9
2 d/10 wk	HFDα	C57BL/6 mice	AgRP, ARC	= nr. P-eIF2α-positive neurons	44
8 wk	HFDα	C57BL/6 mice	Hypothalamus	↑P-IRE1; ↑CHOP protein; ↑GRP78 protein, ↑XBP-1s	32
12 wk	HFD	Sprague-Dawley rats	ARC / PVN	↑/= P-PERK; ↑/= P-eIF2α	43
12 wk	HFDβ	Wistar rats	Hypothalamus	↑ P-PERK; ↑ CHOP protein	28
16 wk	HFDα	C57BL/6 mice	Hypothalamus	↑ P-PERK; ↑ P-IRE1	45
25 wk	HFD	C57BL/6 mice	Hypothalamus	↑ P-PERK; ↑ P-IRE1	46
N.A.	HFDα	C57BL/6 mice	Hypothalamus	↑P-PERK	20
Autophagy defect					
16-20 wk	HFDα	C57BL/6 mice	Hypothalamus/ ARC neurons	↓/↓Atg7 protein; ↓/N.A. Atg5 protein; =/N.A. Atg7 and Atg5 mRNA	22
20 wk	HFDα	C57BL/6 mice	POMC	↑ nr. autophagosome-positive neurons	10
SOCS3					
1/3/7,14/28 d	HFDα	Long Evans rats	Hypothalamus	=/↑/=/↑ SOCS3 mRNA	10
2 d	HFDα	C57BL/6 mice (m/f)	AgRP/POMC	=/= nr. SOCS3-positive neurons; ↑/= SOCS3 protein	44
2 wk	HFDα	C57BL/6 mice	AgRP/POMC/extra-ARC	=/↑/↑ nr. SOCS3-positive neurons	44
8 wk	HFDβ	Swiss mice	Hypothalamus	↑ SOCS3 protein	27
12 wk	HFDα	Sprague-Dawley rats	ARC	↑ SOCS3 protein	43
13, 16 wk	HFD	Wistar rats	Hypothalamus	↑ SOCS3 protein	29
16 wk	HFDγ	C57/BL6	MBH	↑ SOCS3 protein	24
N.A.	HFDα	C57BL/6	Hypothalamus, MBH	↑ SOCS3 mRNA	20
PTP1B					
28 d	HFDα	Long Evans rats	MBH	↑ PTP1B protein	59
12 wk	HFDα	Sprague-Dawley rats	ARC	↑ PTP1B protein	43
16 wk	HFDγ	C57BL/6	MBH	↑ PTP1B	81
20 wk	HFD	FVB mice (f)	ARC/VMH/ DMH/LH	↑/↑/↑/= PTP1B protein	58
Cytokines					
1/3/7/14/28 d	HFDα	Long Evans rats	Hypothalamus	↑/↑/=/=/↑ IL-6 mRNA; ↑/=/=/=/↑ TNFα mRNA; =/=/↓/=/= IL-1β mRNA	10
1d/3d/8 wk	HFDδ	Balb-c mice	Hypothalamus	↑/=/= TNFα; =/↑/↓ IL-1β	64
1d/ 3d, 8wk	HFDδ	Swiss mice	Hypothalamus	↑/↑ TNFα mRNA; =/↑ IL-1β mRNA	64
3 d	AA*	Wistar rats	Hypothalamus	↑TNFα, IL-1β, IL-6 and IL-10 mRNA	9
3 d	OA*	Wistar rats	Hypothalamus	↑IL-6 and IL-10 mRNA	9
3 d	VM*	Wistar rats	Hypothalamus	↑TNFα and IL-1β protein; ↑IL-6 and IL-10 mRNA	9
3 d	SM*	Wistar rats	Hypothalamus	↑ TNFα, IL-1β and IL-6 protein; ↑IL-6 mRNA	9
3/7 d	HFDα	C57BL/6 mice	Hypothalamus	↑/= IL-1β mRNA	10
7 d	HFDα	Wistar rats	MBH	↑ IL-1β mRNA; =IL-6 and TNFα mRNA	30
2/4,8 wk	HFDβ	Swiss mice	Hypothalamus	↑/↑ IL-1β mRNA; =/↑ TNFα mRNA; ↑/↑ TNFα and IL-10 protein	27
8 wk	HFDδ	Wistar rats	Hypothalamus	↑TNFα, IL-1β, IL-6, and IL-10 mRNA	9
12 wk	HFDβ	Wistar rats	Hypothalamus	↑ IL-6 protein and mRNA; ↑IL-10 protein	28
13/ 16 wk	HFD	Wistar rats	Hypothalamus (ARC, LH)	↑/↑IL-6 protein; ↑/N.A. IL-1β mRNA; N.A./↑ IL-1β protein; (↑/↑TNFα protein and mRNA)	29
16 wk	HFDγ	C57BL/6 mice	MBH	↑TNFα and IL-6 protein; = IL-1β protein	24,81
16 wk	HFDδ	Wistar rats	Hypothalamus	↑ TNFα, IL-1β and IL-6 protein; = IL-10 protein	9
18 wk	HFD-DIO	Sprague-Dawley rats	Hypothalamus	↑ TNFα, IL-1β, and IL-6 mRNA; ↓ IL-10 mRNA	8
20 wk	HFDα	Long Evans rats	Hypothalamus	↑ IL-6 mRNA	10
Glial cells					
1,3/7/ 14,28 d	HFDα	Long Evans rats	Hypothalamus	↑/=/↑mRNA encoding F4/80 antigen; ↑/=/↑ GFAP mRNA	10
1/ 3 ,7, 14 d	HFDα	Long Evans rats	ARC (LH, VMH)	=/↑ Iba1 protein; (=/= Iba1 protein)	10
1d/3d/ 2, 8 wk	HFDδ	Balb-c mice	Hypothalamus	=/↑/= CD11b mRNA	64
1, 3d / 2, 8 wk	HFDδ	Swiss mice	Hypothalamus	↑/= CD11b mRNA	64
1, 2/ 3/32 wk	HFDα	C57BL/6 mice	ARC; ME	↑/=/↑ GFAP protein	10
6 wk	HFD	C57BL/6 mice	ARC	↑(Iba1 protein positive) microglia	80
~8 wk	HFD	C57BL/6 mice	ARC	↑ GFAP mRNA	75
12 wk	HFD-DIO	Sprague-Dawley rats	POMC	↑ astrocyte coverage	75

Table 1: Continued

16 wk	HFDδ	Wistar rats	ARC; ME	↑F4/F80 antigen	9
20 wk	HFD-DIO	Sprague-Dawley rats	POMC, NPY	↑ glial ensheatment	75

The data are grouped by inflammatory component and then by length of dietary manipulation. Energy percentage derived from total amounts of fat ranges from 36-60% for high-fat diets compared with 4-21.6% for chow or control diets. Identical diets are marked by the same symbol (α, β, γ or δ). All results were obtained in male animals, except for results indicated by (f), only in females or (f/m), both in males and females. *Intracerebroventricular administration; ↑increased; ↓decreased; =no change compared with control animals; P-, indicates phosphorylated state; N.A., not available. IKKβ, IkappaB kinase beta; NF-κB, nuclear factor kappaB; IκBα, inhibitor of nuclear factor kappa B; JNK, c-Jun N-terminal kinase; TLR4, toll-like receptor 4; MyD88, myeloid differentiation primary response gene; ER, endoplasmic reticulum; CHOP, C/EBP homologous protein; eIF2α, eukaryotic translation initiation factor 2α; GRP78, 78 kDa glucose-regulated protein; IRE1, inositol requiring enzyme-1; PERK, PKR-like endoplasmic reticulum kinase; XBP-1s, spliced form of X-box binding protein-1; Atg7, autophagy-related protein 7; SOCS3, suppressor of cytokine signaling-3; PTP1B, protein tyrosine phosphatase 1B; IL, interleukin; F4/F80 antigen, microglia marker; CD11b, cluster of differentiation molecule 11B, microglia marker; GFAP, glial fibrillary acidic protein (astrocyte marker); Iba1, microglia marker; HFD, high fat diet; HFD-DIO, only the results of animals that have been selected as prone to develop diet-induced obesity are shown (as opposed to DIO resistant animals); AA, arachidic acid; OA, oleic acid; SM, mixture of animal fat; VM, vegetable mixture of fatty acids; WD, Western diet; AgRP, agouti-related protein; ARC, arcuate nucleus; DMH; dorsomedial hypothalamus; LH, lateral hypothalamus; MBH, mediobasal hypothalamus; ME, median eminence; POMC, proopiomelanocortin; VMH, ventromedial hypothalamus.

IKKβ/NF-κB signaling

IkB kinase-β/nuclear κB (IKKβ/NF-κB) signaling is a key intracellular pro-inflammatory pathway, often described as "the master switch" of the innate immune system [19] (Fig. 2). IKKβ is predominantly expressed in neurons of the MBH, but its signaling remains suppressed under normal nutritional conditions [20]. Various studies have demonstrated increased IKKβ/NF-κB signaling in the hypothalamus of HFD-fed rodents (Table 1), which has already been observed after one day of HFD-feeding [10]. Also acute overnutrition in the absence of obesity by intracerebrovascular (ICV) infusion of glucose or fatty acids was shown to enhance IKKβ/NF-κB signaling in the hypothalamus [20,21]. Importantly, this separation of chronic overnutrition from obesity suggests that oversupply of certain nutrients acutely activates IKKβ/NF-κB signaling before the onset of obesity [20]. To specifically test the role of hypothalamic IKKβ/NF-κB signaling in DIO, IKKβ/NF-κB signaling has been manipulated in mice using viral vector-based or genetic approaches (Table 2). While introduction of constitutive active IKKβ in the MBH increased weight gain and food intake along with impaired leptin signaling, brain- and MBH-specific deletion of IKKβ protected against HFD-induced obesity [20,22]. Further, pharmacological inhibition of IKKβ/NF-κB improved leptin sensitivity in HFD-fed mice [24]. Interestingly, mice with AgRP neuron-specific

deletion of IKKβ were partially protected from HFD-induced obesity and showed preserved leptin signaling, whereas restoration of IKKβ in the MBH eliminated the protection against weight gain [20]. In contrast, POMC-specific IKKβ deletion was insufficient to protect against HFD-induced obesity [23,25]. Collectively, these findings suggest that IKKβ/NF-κB signaling in AgRP but not POMC neurons of the MBH plays a critical role in the pathogenesis of DIO.

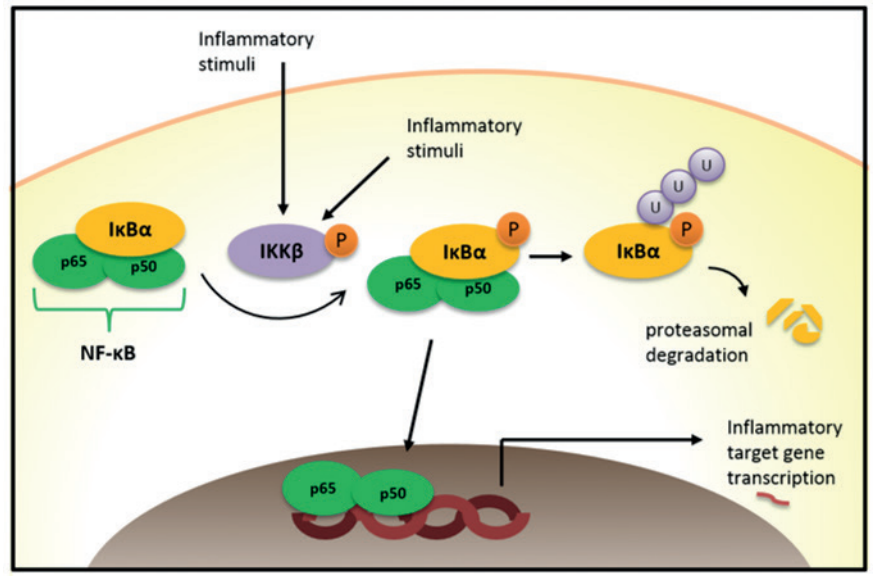

Figure 2. IKKβ/NF-κB signaling. In the quiescent state, NF-κB dimers, often consisting of a p50 and a p65 subunit, reside in an inactive form in the cytoplasm through binding to the inhibitor of NF-κB α (IκBα). Inflammatory stimuli activate the serine kinase IKKβ, which phosphorylates IκBα, leading to its ubiquitination and proteosomal degradation, and subsequent release of NF-κB. Activated NF-κB translocates to the nucleus, where it mediates transcription of its target genes, including a number of inflammatory genes.

NF-κB has also been implicated in POMC neurons during normal feeding regulation, as leptin-induced POMC expression depends on hypothalamic IKKβ/NF-κB signaling in chow-fed mice, probably via direct binding of NF-κB to its binding site on the POMC promotor [23]. However, NF-κB activation in mice chronically fed a HFD failed to promote POMC transcription, which was associated with hypermethylation of the binding site for p65 (a subunit of NF-κB) within the POMC promoter [26]. *In vitro* studies indicated impaired interaction between p65 and the POMC promotor when the promotor was hypermethylated [26]. Thus, even though IKKβ/NF-κB activation is enhanced during chronic overnutrition and NF-κB is translocated into the nucleus, it

fails to induce POMC transcription due to a hypermethylated POMC promotor. This suggest a differential role for IKKβ/NF-κB signaling in POMC neurons compared with AgRP neurons, whereby the pathology of DIO is mediated by impairment of NF-κB induced POMC expression and enhanced IKKβ/NF-κB (inflammatory) signaling in AgRP neurons. Studies with cultured cells showed that p65 also directly interacts with (P-)STAT3, which abolished leptin-induced P-STAT3 regulation of POMC transcription [26]. These findings provide a direct link between IKKβ/NF-κB and leptin resistance, presumably at a level downstream of STAT3 phosphorylation.

IKKβ/NF-κB is suggested to interact with up- and downstream inflammatory mediators. Overnutrition-induced IKKβ/NF-κB signaling was shown to upregulate the expression of suppressor of cytokine signaling 3 (SOCS3), a negative regulator of leptin signaling [20], and is associated with pro-inflammatory cytokine expression in the hypothalamus [8,10,27-29]. The upstream signaling events of hypothalamic IKKβ/NF-κB signaling remain to be fully understood, but include TLR4 signaling, ER stress, autophagy defect, and cytokine signaling, as will be discussed below.

Finally, it should be noted that, although HFD-induced IKKβ/NF-κB signaling has been reported in several rat and mouse strains (Table 1), the critical role of hypothalamic IKKβ/NF-κB signaling in DIO and leptin resistance has only been demonstrated in HFD-fed C57BL/6 mice [20,22,25]. Therefore, it will be important to validate the role of IKKβ/NF-κB signaling in DIO and leptin resistance in rats and other mouse strains, especially because ICV infusion of the IKK inhibitor PS-1145 could not protect Wistar rats from the development of DIO [30], and has only been reported to reduce food intake in Long Evans rats [21].

JNK signaling

Next to IKKβ/NF-κB signaling, c-Jun-*N*-terminal kinase (JNK) is a key pro-inflammatory signaling component [1,13], though its role in DIO is less evident. JNK is activated by multiple inflammatory and environmental stimuli and is thought to exert its pro-inflammatory effects by stabilizing mRNAs encoding pro-inflammatory cytokines and other inflammatory mediators [1,13].

In DIO rodent models, hypothalamic JNK activity was shown to be induced within a few days by direct intra-third ventricle exposure to saturated fatty acids (SFAs) [9] and within 10 days by Western diet feeding [31] (Table 1). JNK activity was permanently upregulated in the ARC during chronic HFD-feeding [27,29, 31, 32,33]. Several studies have used mice with a whole body or brain-specific deletion of JNK1 to study its role in DIO and leptin resistance, with controversial results (Table 2). Whole body and brain-specific JNK1 deletion, as well as ICV infusion of a JNK inhibitor, were shown to protect against HFD-induced obesity [33-35] [but see 36]. However, these manipulations may already reduce food intake and body weight in mice fed a control diet [33,35]. This indicates a body weight reducing effect of JNK1 deletion itself, which complicates interpretation of JNK1 as a specific mediator of DIO. Inhibition of JNK in the brain, either by genetic deletion or pharmacological inhibition, failed to rescue HFD-induced impairment of leptin's anorexigenic actions or STAT3 signaling [29,36], but improved leptin sensitivity by protecting against HFD-induced downregulation of hypothalamic LEPRb expression [34]. Taken together, there are indications but not solid evidence for a role of JNK in DIO and leptin resistance.

Overnutrition-induced upregulation of hypothalamic JNK activity was associated with increased NF-κB activation, TLR4 activity, and expression of ER stress markers, pro-inflammatory cytokines and SOCS3 [9,27,29,32]. Few studies have investigated the interaction between JNK and these inflammatory mediators. Studies in cultured hypothalamic neurons indicated that JNK at least may act as a upstream mediator of ER stress [37].

TLR4 signaling

Some inflammatory mediators have been proposed to act upstream from IKKβ/NF-κB and JNK, including TLR4, a membrane-bound pattern recognition receptor that is a key player of the innate immune system. In the classical immune response, it stimulates the synthesis of inflammatory mediators upon activation by lipopolysaccharide (LPS) and other microbial components [2,3,38]. In the hypothalamus, TLR4 is predominantly expressed by microglia, whereas AgRP and POMC neurons barely express the receptor [9].

During chronic HFD-feeding, hypothalamic TLR4 expression and activity was increased [8,28] (Table 1). Also ICV infusion of SFAs was demonstrated to promote the interaction between TLR4 and myeloid-differentiation primary-response gene 88 (MyD88) [9], an adaptor molecule that couples TLR4 to intracellular inflammatory signaling cascades like JNK and IKKβ/NF-κB [13,38]. SFAs may be able to directly bind and thereby activate TLR4, supposedly primarily on microglia [39,40] [but see 41]. To study the role of TLR4/MyD88 signaling in DIO and leptin resistance, mice with a whole body TLR4 loss-of-function mutation or brain-specific MyD88 deletion were generated (Table 2). Both whole body TLR4 loss-of-function and either central or peripheral administration of a pharmacological TLR4 inhibitor reduced HFD-induced weight gain and the latter also restored impairment of leptin signaling [9]. Similarly, brain-specific MyD88 deletion protected against the development of DIO and restored

leptin sensitivity, even before the appearance of a reduced body weight compared with HFD-fed control mice [36]. This suggests that overnutrition-induced MyD88 activation induces leptin resistance in the absence of obesity, rather than being a mediator of obesity-induced inflammation and consequent leptin resistance. Further, direct ICV infusion of SFAs inhibited leptin-induced STAT3 phosphorylation in the ARC, which was mediated through MyD88 signaling [36]. Thus, overnutrition-induced hypothalamic TLR4/MyD88 signaling may be an initiating signaling event in DIO and leptin resistance, which might be primarily mediated by microglia given the expression pattern of TLR4 [9].

Although TLR4/MyD88 inflammatory signaling acts both through JNK and IKKβ/NF-κB signaling in the classical immune response [38], brain-specific deletion of MyD88 abolished IKKβ/NF-κB signaling but not JNK activity in the ARC of HFD-fed obese mice [36]. This finding is consistent with the reported controversial role for JNK in DIO (Table 2) and points to TLR4/MyD88 as an upstream mediator of IKKβ/NF-κB signaling. Since TLR4 expression is predominantly shown on microglia [9] and IKKβ signaling in MBH neurons [20], microglia and neurons may interact in mediating hypothalamic inflammation.

Table 2. Metabolic phenotypes in rodents with (tissue-specific) deletion or activation of inflammatory mediators

Signaling component	Target	Targeted tissue/ cell type	Cre used	Diet	Leptin sensitivity	Body weight	Food intake	Reference
IKKβ/ NF-κB	IKKβ KO	Brain	Nestin	CD	N.A.c	=	=	20,22
				HFDα	N.A.	↓	↓	
	IKKβ CA	MBH	Synapsin1	HFDα	↓	↑	↑	20
	IKKβ KO	MBH	MBH	HFDα	N.A.	↓	↓	20
	IKKβ KO	AgRP	AgRP	CD	N.A.	=	=	20, 25
				HFDα	↑	↓	↓	
	IKKβ KO	POMC	POMC	CD	↓	=	=	23, 25
				HFDα	N.A.	=	=	
JNK	JNK1 KO	Whole body	-	CD	N.A.	= or↓	N.A.	35
				HFD	N.A.	↓	=	
	JNK1 KO	Brain	Nestin	CD	= or ↓a	= or ↓	=	33, 34, 36
				HFD	= or ↑a	= or ↓	= or ↓	
TLR4	TLR4 KO*	Whole body	-	HFDδ	N.A.	↓	=	9
	MyD88 KO	Brain	Nestin	CD	N.A.	= (m/f)	N.A.	36
				HFD	↑ (m/f)	↓ (m/f)	= or ↓ (m/f)	
ER stress	XBP1 KO	Brain	Nestin	CD	=	=	N.A.	46
				HFD	↓	↑	↑	
Autophagy defect	Atg7 KO	MBH (ARC)	2	CD	N.A.	↑	↑	22
				HFDα	N.A.	↑	↑	
	Atg7 KO	POMC	POMC	CD	↓/= (m/f)†	↑	↑	49
				HFDα	N.A.	↑	↑	
	Atg7 KO	AgRP	AgRP	CD	N.A.	↓	=	53
SOCS3	SOCS3 KO	Brain	Nestin, Synapsin	CD	↑ (m/f)	= (m/f)	N.A.	56
				HFD	N.A.	↓ (m/f)	↓ (m/f)	
	SOCS3 KO	MBH	2	HFHS	N.A.	↑	=	55
	SOCS3 OE	LEPRb neurons	LEPRb	CD	= or ↑	↓	↓	54
				HFDα	N.A.	=	N.A.	
	SOCS3 OE	AgRP	AgRP	CD	↓	=	↑	44
	SOCS3 OE	POMC	POMC	CD	↓	↑	=	54
PTP1B	PTP1B KO	Brain	Nestin	CD	↑	↓	↓	61
				HFD	N.A.	↓ (m/f)	↓	
		POMC	POMC	CD	↑	= (m/f)	N.A.	60
				HFD	N.A.	↓ (m/f)	=	
Cytokine	TNFα KO	Whole body	-	CD	N.A. (m/f)	= (m/f)	N.A. (m/f)	58
				HFD	N.A. (m/f)	= (m/f)	N.A. (m/f)	
	TNF-R1/ R2 KO	Whole body	-	CD	N.A.	= or ↑	=	65
				HFHS	N.A.	↑	=	
	TNF-R1 KO	Whole body	-	CD	↑	=	↑	64, 68
				HFDδ	↑	↓	↑	
	IL-6 KO	Whole body	-	CD	↓	↑ (f)	= or ↑	66
	IL-10 KO	Whole body	-	CD	N.A.	↓	N.A.	64
				HFDδ	N.A.	↓	N.A.	
	IL-6 OE	Astrocytes	GFAP3	CD	N.A.	↓ (m/f)	= (m/f)	77
				HFD	N.A.	↓ (m/f)	= (m/f)	

↑ increased, ↓ decreased, = no change compared with control mice; N.A., not available. All results were obtained in male animals, except for results indicated by (f), only in females or (f/m), both in males and females. † Result is shown for male and female animals, respectively. All studies were performed in mice with a C57BL/6 background, except for *C3H/HeJ mice. [1]Lentiviral vector-targeted delivery, [2]lentiviral small hairpin RNA, and [3]IL-6-GFAP transgenic mice were used, respectively. [a]Leptin sensitivity was determined by LEPRb expression. IKKβ, IkappaB kinase beta; JNK, c-Jun N-terminal kinase; TLR4, toll-like receptor 4; MyD88, myeloid differentiation primary response gene; XBP1, X-box binding protein 1; Atg7, autophagy-related protein 7; SOCS3, suppressor of cytokine signaling 3; PTP1B; protein tyrosine phosphatase 1B; TNF-R1/R2, tumor necrosis factor receptor 1/2; IL-6, interleukin 6; GFAP; glial fibrillary acidic protein; KO, knockout; CA, constitutive active; OE, overexpression; MBH, mediobasal hypothalamus; AgRP, agouti-related protein; POMC, proopiomelanocortin; ARC, arcuate nucleus; LEPRb, long form of leptin receptor; CD, control or chow diet; HFD, high-fat diet; HFHS, free-choice high-fat high-sugar diet. Identical diets are marked by the same symbol (α, δ).

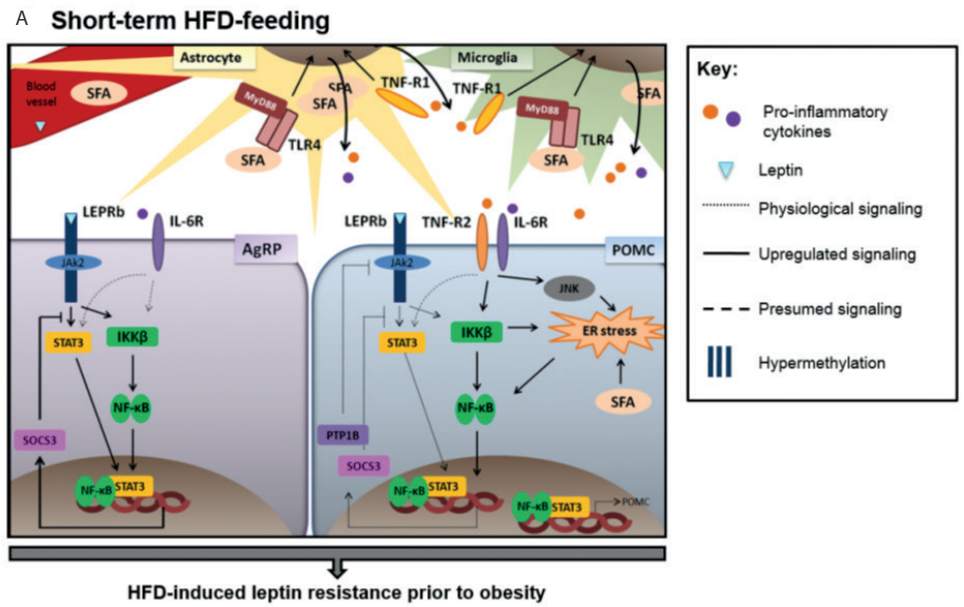

< Figure 3. Overview of inflammatory signaling in the ARC during HFD-feeding. Overnutrition-induced inflammatory signaling, evoked by either short-term (several days; **A**) or long-term (several weeks to months; **B**) high-fat diet (HFD) feeding is shown. Activation of toll-like receptor 4 (TLR4) on microglia and astrocytes, upon direct detection of saturated fatty acids (SFAs), may initiate hypothalamic inflammation via the release of pro-inflammatory cytokines. These cytokines differentially induce inflammatory signaling in proopiomelanocortin (POMC) and agouti-related protein neuron (AgRP) neurons, mainly through upregulation of central IkB kinase-β/nuclear κB (IKKβ/NF-κB) signaling, which converges with stimulated leptin signaling to induce suppressor of cytokine signaling 3 (SOCS3) and protein tyrosine phosphatase 1B (PTP1B) expression, resulting in leptin resistance. (**C**) Endoplasmic reticulum (ER) stress induces the unfolded protein response (UPR) to relieve ER stress. The UPR generally consists of three pathways, of which only induction of the PKR-like ER kinase (PERK) and inositol-requiring enzyme 1 (IRE1) pathway were demonstrated after HFD-feeding. PERK phosphorylates eukaryotic initiation factor 2 (eIF2α), leading to general inhibition of protein translation and allowing eIF2α-independent translation of activating transcription factor 4 (ATF4). IRE1 catalyzes the alternative splicing of X-box binding protein 1 (XBP1) mRNA, leading to the expression of the active transcription factor XBP1. Together, the pathways of the UPR increase the expression of chaperones like 78 kDa glucose-related protein (GRP78) to enhance protein folding capacity, and enhance ER-associated protein degradation of misfolded proteins. Apoptosis is triggered when the UPR fails to relieve ER stress. AgRP, agouti-related protein neuron; CHOP, C/EBP homologous protein, a pro-apoptotic protein; ER, endoplasmic reticulum; IKKβ, IkappaB kinase beta; JAK2, Janus kinase 2; JNK, c-Jun N-terminal kinase; LEPRb, long form of leptin receptor; IL-6R, interleukin 6 receptor; MyD88, myeloid differentiation primary response gene (adaptor protein TLR4); NF-κB, nuclear factor of kappaB; SFA, saturated fatty acid; POMC; proopiomelanocortin neuron; SOCS3, suppressor of cytokine signaling 3; STAT3, signal transducer and activator of transcript 3; TLR4, toll-like receptor 4; TNF-R1/R2, tumor necrosis factor receptor 1/2.

ER stress

Both TLR4, IKKβ/NF-κB, and JNK have been proposed to interact with ER stress in mediating the metabolic phenotype of DIO. The ER is an organelle for the synthesis, folding, and maturation of proteins. Increased demand on the ER disturbs the balance between protein loading and folding, causing accumulation of unfolded and misfolded proteins in the ER lumen, a condition known as ER stress [42]. ER stress activates the unfolded protein response (UPR), which includes the inositol-requiring-1 (IRE1), PKR-like ER kinase (PERK), and activating transcription factor 6 (ATF6) pathway (Fig. 3C). The UPR relieves ER stress by reducing protein synthesis, increasing protein folding capacity by upregulating the expression of chaperones, and enhancing proteasomal degradation of unfolded or misfolded proteins. When the UPR fails to alleviate ER stress, the cell undergoes apoptosis [42].

ER stress was induced in the hypothalamus of DIO rodents upon 8 weeks of HFD-feeding [32], but also within a few days by a direct oversupply of SFAs in the third ventricle [9] (Table 1). The hypothalamic ARC but not PVN showed induction of ER stress [43], which may, at least during the first days of HFD-feeding, not be mediated by AgRP neurons in the ARC [44]. Activation of both the PERK and IRE1 pathway of

the UPR has been demonstrated in the hypothalamus of DIO but not DIO-resistant rodents [9,20,28,43,45,46] (Fig. 3C). Pharmacological induction of ER stress in chow-fed rodents caused a similar activation of the UPR response along with impaired leptin-induced STAT3 phosphorylation [20,28,32,43,46], whereas pharmacological inhibition of ER stress in HFD-rodents decreased body weight and improved leptin sensitivity [20,28,32,43,46]. Together, these findings suggest that overnutrition-induced hypothalamic ER stress may contribute to the development of leptin resistance and DIO. This is further supported by the metabolic phenotype of mice with deletion of X-box protein 1 (XBP1), an important regulator of ER folding capacity (see Table 2) [46].

Remarkably, LEPRb folding and translocation to the cell membrane remained preserved in cultured cells after pharmacological induction of ER stress [46], suggesting that ER stress induced leptin resistance might not be mediated by reduced LEPRb processing. Rather, ER stress induced by HFD-feeding resulted in accumulation of POMC protein and lower alpha-melanocyte stimulating hormone (α-MSH) peptide levels in the ARC [43]. HFD-induced ER stress blocks posttranslational modification of POMC by reducing the protein expression of proconverting enzyme 2, an enzyme that acts in the processing cascade of POMC, thereby decreasing the production of anorexigenic α-MSH [43]. Thus, inhibition of posttranslational POMC processing provides a role for ER stress in POMC neurons in mediating DIO.

IKKβ/NF-κB signaling may act both upstream and downstream from ER stress in DIO [20]. ICV infusion of a pharmacological ER stress inhibitor suppressed the activation of hypothalamic NF-κB in HFD-fed mice, demonstrating that NF-κB acts downstream from ER stress [20]. Conversely, since HFD-feeding failed to induce hypothalamic ER stress in mice with a brain-specific IKKβ deletion, IKKβ seems to be an upstream mediator of ER stress [20]. Chow-fed mice with ARC-specific NF-κB inhibition developed pharmacologically-induced ER stress to a similar extent as control mice [47], suggesting that ER stress induction depends on IKKβ but not NF-κB signaling. This is consistent with a study reporting that IKK may act independently of NF-κB, such as via the mammalian target of rapamycin (mTOR) complex [48]. Regardless of the mechanisms, the above findings indicate that hypothalamic IKKβ/NF-κB signaling and ER stress enhance each other under conditions of overnutrition.

Although TLR4/MyD88 signaling was shown to act upstream from IKKβ/NF-κB signaling, it is suggested that MyD88-independent TLR4 signaling acts as an upstream mediator of ER stress and pro-inflammatory cytokine expression in DIO. Brain-specific MyD88 deletion did not affect HFD-induced expression of ER stress markers and pro-inflammatory cytokines in the hypothalamus [36], whereas TLR4 inhibition completely inhibited SFA-induced expression of cytokines and ER stress markers in the hypothalamus [9]. The suggestion of a MyD88-independent TLR4 signaling pathway is in accordance with the involvement of a similar (late phase) pathway in classical inflammation [38]. ER stress acts as a downstream mediator of TLR4, as ICV infusion of a chemical chaperone inhibited SFA-induced ER stress without affecting TLR4 signaling [9]. Pharmacological inhibition of TLR4 but not ER stress completely abolished HFD-induced obesity and leptin resistance [36]. ICV infusion of an ER stress inhibitor only partially inhibited SFA-induced cytokine expression [36]. Together, these findings suggest that overnutrition activates TLR4 to induce expression of pro-inflammatory cytokines, which is partially mediated through ER stress (and its reciprocal interaction with IKKβ/NF-κB signaling) in at least POMC neurons and results in obesity and leptin resistance.

Autophagy defect

A next inflammatory pathway induced by overnutrition is defective autophagy. Autophagy is a catabolic process essential for the maintenance of cellular homeostasis [1,2,22,49]. In response to nutrient deficiency or stress, such as defective organelles or misfolded proteins, autophagy is employed to supply energy or digest the defective intracellular components, respectively [50,51]. Autophagy has been reported to critically depend on a set of autophagy-related proteins (Atg), including Atg7, which functions to form the autophagosome [50,51], a double-membrane vesicle that sequesters defective intracellular components and delivers them to lysosomes for degradation [52]. Prolonged cellular stress may result in a failure of the autophagy machinery to remove defective proteins and organelles from the cytosol, which is known as the autophagy defect [1,49].

Reduced autophagy activity was shown in neurons of the ARC during chronic HFD-feeding [22], though an increased number of autophagosome-positive POMC neurons was demonstrated [10] (Table 1). These findings could be interpreted as a compromised autophagic response that was initially induced as protection to ongoing cell injury during HFD-feeding. Moreover, defective autophagy has only been observed after long-term (4-5 months) HFD-feeding [22], which is indicative for a role in the maintenance rather than the initiation of DIO. Inhibition of autophagy by knockdown of the key gene *Atg7*, either in the MBH or specifically in POMC neurons, was shown to potentiate HFD-induced obesity along with increased food intake [22,49] (Table 2). Under chow feeding, however, similar (though milder) effects were observed together with leptin resistance in mice with POMC neuron-specific Atg7 deletion [22,49]. In contrast, AgRP neuron-specific deletion of Atg7 reduced body weight [53]. Together, these findings suggest that regulation of energy homeostasis

requires functional autophagy in both AgRP and POMC neurons of the MBH. However, these experiments do not provide convincing evidence for a critical role of defective autophagy in DIO, as it seems obvious that full genetic deletion of a crucial component of autophagosomes such as Atg7 in POMC or AgRP neurons results in cellular defects, which may ultimately lead to disruption of energy homeostasis.

MBH-specific knockdown of Atg7 has been shown to enhance IKKβ/NF-κB signaling along with increased expression of SOCS3, TLR4, and pro-inflammatory cytokines in the hypothalamus of chow-fed mice [22]. Brain-specific deletion of IKKβ was demonstrated to abolish the food intake and body weight promoting effects of MBH-specific Atg7 knockdown, both under chow- and HFD-feeding conditions [22]. Taken together, these findings indicate that defective autophagy promotes IKKβ signaling in the hypothalamus during chronic overnutrition. Further, it seems logical to speculate that, at least in POMC neurons, prolonged ER stress (and its reciprocal interaction with IKKβ/NF-κB signaling) promotes defective autophagy under chronic HFD-feeding conditions.

Negative regulators: SOCS3 and PTP1B

SOCS3 and PTP1B are negative regulators of leptin signaling, inhibiting JAK2-STAT3 signaling through binding to a specific tyrosine-residue on LEPRb or dephosphorylating JAK2, respectively [11,13,38]. Both SOCS3 and PTP1B are induced by leptin-mediated STAT3 transcriptional activity and their negative feedback regulation functions to limit the magnitude and duration of leptin signaling [13]. Originally, however, SOCS3 was identified as an anti-inflammatory mediator, as it was shown to provide negative feedback on JAK-STAT signaling of pro-inflammatory cytokine receptors, thereby limiting inflammatory responses [38].

Hypothalamic SOCS3 expression appears to be limited to neurons in DIO [20] and follows a complex "on-off" pattern during the first days of HFD-feeding [10,44], to become permanently upregulated upon chronic HFD-feeding [24,27,29,43] (Table 1). SOCS3 upregulation in AgRP neurons seems to precede that in POMC neurons, as it was first observed in AgRP neurons after two days and in POMC neurons after two weeks of HFD-feeding [20,44]. SOCS3 expression was primarily upregulated in AgRP neurons located outside the BBB along with diminished leptin-induced P-STAT3 expression [44], implying SOCS3 mediated inhibition of leptin signaling. To investigate the cell-type specific role of SOCS3, mice with AgRP and POMC neuron-specific overexpression of SOCS3 have been generated (Table 2), though Reed and colleagues failed to confirm POMC neuron-specific overexpression of SOCS3 [54]. While SOCS3 overexpression in AgRP neurons impaired leptin sensitivity without affecting body weight [44], in POMC neurons it induced leptin resistance prior to a significant increase in body weight [54].

Together, these findings indicate that SOCS3 may directly induce leptin resistance in the absence of obesity and point to a differential role for SOCS3 in AgRP and POMC neurons. It has been proposed that SOCS3 upregulation signals short-term changes in nutritional status in AgRP neurons, but signals long-term energy oversupply in POMC and other hypothalamic neurons, resulting in weight gain [44]. A cell-type specific role for SOCS3 might explain the controversial metabolic phenotypes found in mice with LEPRb neuron-specific overexpression of SOCS3 and MBH- or brain-specific SOCS3 deletion [54-56] (Table 2). Though, at least some contradictions may also be explained by the strengths and weaknesses of the genetic *versus* viral vector-based manipulations that were employed (Table 3).

Table 3. Interpretation of limitations in approach

Approach of manipulation	Limitations and advantages of approach
1. Full genetic deletion, either in the whole body, the brain, or a specific cell type.	Limitation: Potential compensation of the missing gene by redundant genes; effects of the background strain; developmental defects; the manipulation may have such an impact on the physiology of the targeted cells that the interpretation of the role of the deleted gene in DIO might be skewed, irrespectively of the exact site of the deletion; Cre expression during the development, in cells in which it is not expressed during adulthood, may result in unintended deletion of the gene in other tissues and thereby compromise interpretation of the cell-type specific role of the deleted gene. [55,82] Advantage: Allows "clean" tissue- and cell type-specific deletion of a gene by means of Cre-Lox recombination.
2. Viral vector-mediated knockdown or introduction of a (constitutive active) inflammatory mediator.	Limitation: Difficulties to transduce all targeted cells; toxicity of viral particles. [20,55] Advantage: It might reveal a more representative (patho)physiological role of the manipulated gene, as it has a more modest effect on the expression levels of targeted genes, which are not affected yet during the development of the animal. [20,55]
3. Pharmacological inhibition	Limitation: Does not allow the study of the cell type- or hypothalamic-specific role of an inflammatory mediator; interpretation of its effects may be skewed by possible side effects of drugs. [82] Advantage: Identical to approach 2.
4. Pharmacological introduction of an inflammatory mediator	Limitation: The dose of administered signaling molecules, in particular in case of supraphysiological doses of cytokines, may determine whether a (patho) physiological effect or rather a manipulation-induced disruption of the (patho) physiology is studied.

HFD-induced PTP1B expression has been observed in several hypothalamic areas, but most abundantly in the ARC [57-59] (Table 1). Both brain- and POMC neuron-specific PTP1B deletion protected against HFD-induced obesity and improved leptin sensitivity in chow-fed mice [60,61] (Table 2). Also ICV infusion of a PTP1B antisense oligonucleotide (ASO) improved leptin sensitivity in chow-fed rats [62]. These findings

suggest that PTP1B induction in POMC neurons mediates leptin resistance and HFD-induced obesity, but its role in AgRP neurons and other hypothalamic cell types remains to be elucidated.

HFD-induced PTP1B expression is not necessarily mediated by elevated leptin levels [59], suggesting that other mechanisms, such as inflammation, may also regulate PTP1B levels. Indeed, upregulated expression of the negative regulators PTP1B and SOCS3 was reported in the ARC of DIO rodents and chow-fed rodents after pharmacological induction of ER stress [43]. In accordance, *in vitro* studies demonstrated that ER stress causes leptin resistance via the induction of PTP1B, but the role of SOCS3 is more controversial [43,57].

Cytokine signaling

Several inflammatory mediators, including TLR4, ER stress and defective autophagy, were shown to induce cytokine expression, as discussed above. Cytokines can elicit both pro- and anti-inflammatory effects. Tumor necrosis factor α (TNFα), interleukin (IL)-6, and IL-1β are considered to be pro-inflammatory cytokines, whereas IL-4 and IL-10 are anti-inflammatory cytokines [63]. Cytokines exert their biological actions by activating cytokine receptors on target cells, for instance resulting in JAK-STAT signaling [38]. Within the hypothalamus, TNF-receptor 1 (TNF-R1) is mostly expressed in non-neuronal cells, whereas TNF-R2 is expressed in POMC neurons of the ARC [25]. Also IL-6R and IL-10R are abundantly expressed in POMC and AgRP neurons [28], implying a role for both neuronal and non-neuronal hypothalamic cells in cytokine signaling.

Various studies have reported induction of pro-inflammatory TNFα, IL-1β and IL-6 mRNA and protein expression in the hypothalamus during HFD-feeding as well as after ICV infusion of SFAs [8,28,29,36] (Table 1). However, other studies have observed unaltered or reduced pro-inflammatory cytokine expression, resulting in a complex "on-off" expression pattern especially during short-term HFD-feeding [10,24,27,30]. Remarkably, anti-inflammatory IL-10 expression was demonstrated to be upregulated by overnutrition [27,28,36] (but see 8), which may represent a neuroprotective response as ICV infusion of IL-10 was demonstrated to protect against the metabolic phenotype of DIO [28] (but see 64). Surprisingly, whole body deletion of pro-inflammatory IL-6 or TNF-R1 and –R2 was shown to impair leptin sensitivity and to promote DIO, respectively [65,66], whereas specific TNF-R1 deletion improved these metabolic parameters in HFD-fed mice [64, 68] (Table 2). ICV infusion of IL-6 reduced food intake and restored leptin sensitivity in DIO rats [28], whereas ICV infusion of anti-inflammatory IL-4 promoted HFD-induced obesity [30]. Conversely, ICV infusion of a low dose of

TNFα impaired leptin sensitivity in chow-fed rats [28,62]. The interpretation of the role of typically low-grade cytokine signaling in DIO is complicated by the manipulations that were employed, i.e. infusion of supraphysiological doses of cytokines and whole body rather than hypothalamic- or cell type-specific cytokine (receptor) deletion. The degree of change in cytokine (receptor) availability by the employed manipulations may have skewed the interpretation of the role of cytokines in DIO, especially because the biological actions of some cytokines are determined by the extent of signaling and their interactions [2,28,63]. Therefore, studies using proper dose-response curves and more specific manipulations are required to assess hypothalamic cytokine signaling as a critical mediator of DIO and leptin resistance.

TLR4, ER stress, and autophagy defect were shown to induce pro-inflammatory cytokine expression, at least partially through IKKβ/NF-κB signaling (as discussed above). Conversely, peripheral or central administration of TNFα induced JNK activity, ER stress, and mRNA and/or protein expression of SOCS3, PTP1B, IL-1β and IL-6 in the hypothalamus of chow-fed rodents, which resulted in leptin resistance [58,62,69]. TNFα-induced ER stress was shown to be mediated through TNF-R1 [70], which, given the expression pattern of TNF-R1, may point to a role for non-neuronal cells [25]. ICV infusion of TNFα induced IKKβ activity in the majority of POMC (but few AgRP) neurons in the ARC of chow-fed mice [25], and both TNFα and IL-1β were shown to activate NF-κB in cultured hypothalamic neurons [23]. Moreover, TNFα-induced NF-kB directly regulated the activity of the PTP1B promotor *in vivo* [58], and was suggested to directly regulate transcriptional activity of the SOCS3 promotor [20]. Together, these findings suggest that pro-inflammatory cytokines differentially activate IKKβ in POMC and AgRP neurons, resulting in NF-κB regulated transcription of inflammatory mediators, such as SOCS3. In addition, it was reported that both HFD- and leptin-induced SOCS3 expression depend on IKKβ/NF-κB signaling [20], suggesting a direct link between inflammatory and (elevated) leptin signaling in mediating the pathology of DIO.

Involvement of non-neuronal cells

More than 70% of the cell population of the CNS consists of glial cells, including microglia and astrocytes, that support neuronal metabolism, maintain the BBB, provide structural support, and initiate a local innate immune response in reaction to injury [71,72]. Several lines of evidence suggest critical involvement of glial cells in the initiation of HFD-induced hypothalamic inflammation: [1] TLR4 is primarily expressed by microglia [9]; [2] cultured hypothalamic neurons do not directly respond to SFAs with the induction of IKKβ/NF-κB and cytokine signaling [73]; [3] some cytokine receptors of pro-inflammatory cytokines are mainly expressed by non-neuronal cells [25,74]; [4] both

microglia and astrocytes become rapidly activated during HFD-feeding [10].

Both astrocyte and microglial markers were shown to be induced in the ARC and ME within several days of HFD-feeding, initially showing an alternating expression pattern, followed by permanent upregulation upon chronic HFD-feeding [9,10,75] (Table 1). An increase in both the number and size of microglia was observed during the first two weeks of HFD-feeding, as well as thickening of astrocyte processes that ultimately coalesced into a dense fibrous network to form a syncytium, which is all indicative of reactive gliosis [10]. After several months of HFD-feeding, astrocyte gliosis was also shown to form an astroglial coverage over the plasma membrane of POMC and NPY neurons, and to affect the structure of the BBB such that ARC neurons became less accessible to blood-borne metabolic signals [10,75]. Reactive gliosis may, therefore, contribute to leptin resistance upon chronic HFD-feeding by impairing the penetration of leptin to the brain. Recently, blood glucose levels were shown to regulate the structural organization of the blood-CSF barrier, which is composed of tanycytes, specialized glial cells that line the base of the third ventricle [76] (Fig. 1). Low glucose levels promoted the organization of tanycyte tight junctions such that the diffusion of blood-borne metabolic signals from the CSF to the ARC was improved. In contrast, tanycyte tight junctions were disassembled under high glucose levels, thereby forming a physical diffusion barrier, which impaired the sensitivity to peripherally administered leptin [76]. Therefore, regulation of the structural organization of the tanycytic blood-CSF barrier may provide an additional mechanism by which overnutrition mediates leptin resistance. Moreover, tanycytes might also contribute to inflammatory signaling in DIO, as TNFα activated IKKβ in these cells [25].

Although it is likely that microglia, the immune cells of the brain, as well as astrocytes participate in hypothalamic inflammatory signaling, only few studies have investigated their role. Recently, the recruitment of bone marrow cell-derived microglia to the hypothalamus was shown to play an important role in the progression of hypothalamic inflammation and the promotion of DIO during HFD-feeding [64]. In addition, TNFα induction was shown in microglia in the ARC of HFD-fed mice [79]. Similar to the unexpected results of whole body IL-6 deletion [10,66], transgenic mice with astrocyte-specific overproduction of IL-6 were protected from HFD-induced obesity [77] (Table 2). Both SFAs and pro-inflammatory cytokines were shown to activate cultured astrocytes, thereby triggering the release of pro-inflammatory cytokines, also after depletion of co-cultured microglia [74,74,78]. The response to SFAs was prevented by pharmacological inhibition of TLR4, suggesting that SFAs directly activate TLR4, either on astrocytes or microglia, to induce pro-inflammatory cytokine expression, which was surprisingly reported to occur independently from JNK and NF-κB signaling [78]. The latter finding

is in accordance with a study showing that IKKβ signaling occurs predominantly in neurons of the MBH [20]. Collectively, these findings argue for a model where SFAs induce pro-inflammatory cytokine release by microglia and astrocytes through TLR4 signaling, which subsequently activates cytokine receptors on POMC and AgRP neurons resulting in the induction of IKKβ/NF-κB signaling. Recently, also leptin itself was shown to stimulate TNFα and IL-1β mRNA expression in cultured hypothalamic microglia [80]. Obviously, further *in vivo* studies are needed to elucidate the contribution of astrocytes and microglia to hypothalamic inflammatory signaling in DIO, as well as to determine the signaling mechanisms by which SFAs, cytokines and leptin promote the release of cytokines from these cells.

Integrated model of hypothalamic inflammation in DIO

The dynamic expression pattern of inflammatory mediators has mostly been studied in whole hypothalamic extracts through Western blotting or RT-PCR, instead of in specific cell types via techniques like immunohistochemistry. Therefore, the cell type specific role of inflammatory mediators in DIO is unresolved, but based upon current understandings of cell-type specific effects an integrated model is presented here.

AgRP neurons, especially those located outside the BBB, are the predominant responders to subtle changes in leptin signaling upon short-term HFD-feeding (<3 days) [44]. Leptin-activated LEPRb signals through both classical STAT3 and IKKβ/NF-κB to upregulate SOCS3 expression, which provides negative feedback on LEPRb to rapidly induce leptin resistance in AgRP neurons [20,44] (Fig. 3A). Further, HFD-feeding results in accumulation of SFAs in the hypothalamus that may promote ER stress in neurons [37,73], supposedly in POMC but not AgRP neurons, as ER stress was not observed in AgRP neurons upon short-term HFD-feeding [44]. ER stress may result from an increased protein folding demand, which is hypothesized to be evoked by upregulated lipid metabolism as well as by increased hormone and inflammatory signaling in response to nutrient excess. Also astrocytes and microglia become activated in the hypothalamus [10], presumably by direct binding of accumulated SFAs to TLR4 [26,78], resulting in their proliferation and enlargement and the release of pro-inflammatory cytokines. These cytokines may subsequently act on cytokine receptors expressed on AgRP and POMC neurons, thereby enhancing IKKβ/NF-κB signaling and JNK signaling, which further promotes ER stress and the induction of the negative regulators SOCS3 and PTP1B. In addition, the released pro-inflammatory cytokines may also act on cytokine receptors expressed by microglia and astrocytes to stimulate further release of cytokines, resulting in an autocrine

positive feedback loop. Thus, upon short-term HFD-feeding, inflammatory signaling may predominantly function to limit and cope with excessive nutrient-related signaling in neurons.

Under prolonged HFD-feeding conditions, however, long-term nutrient oversupply may further enhance inflammatory and leptin signaling, with deleterious effects on neuronal functioning as a consequence (Fig. 3B). Leptin signaling becomes strongly stimulated in POMC neurons and converges with upregulated cytokine-induced IKKβ/NF-κB signaling to stimulate a considerable induction of both PTP1B and SOCS3, which subsequently mediate leptin resistance by providing negative feedback on LEPRb. Further, leptin resistance also seems to be mediated beyond the level of STAT3 and NF-κB activation in POMC neurons, as NF-κB cannot induce POMC transcription under conditions of overnutrition because its binding site on the POMC promotor has become hypermethylated [26]. Moreover, ER stress blocks the post-translational processing of POMC proteins that have been produced despite inhibited POMC transcription, thereby lowering the production of the anorexigenic peptide α-MSH [43]. Collectively, these processes in POMC neurons result in hyperphagia, weight gain, and ultimately obesity. In addition, autophagy activity may first become increased in POMC neurons during long-term HFD-feeding (10), supposedly to digest the increasing number of defective cellular components (such as misfolded proteins overflowing from the ER) and to increase lipid metabolism. However, autophagy eventually becomes compromised in both AgRP and POMC neurons and defective autophagy may contribute to inflammatory signaling by stimulating IKKβ/NF-κB [22]. Taken together, several lines of evidence indicate that prolonged HFD-feeding compromises the functioning of POMC neurons, resulting in leptin resistance and DIO. AgRP neurons might be more protected from the deleterious effects of excessive overnutrition-related signaling, as they rapidly upregulate SOCS3 upon short-term HFD-feeding. Glial cells may be the primary responders to excess nutrients like SFAs and act as drivers of an inflammatory response by means of cytokine signaling, which initially protects neurons, but may ultimately and unintentionally promotes neuronal injury.

It should be noted that this model is based upon findings of studies using variable high-fat diet compositions, including the type (e.g. palmitate or oleic acid) and source (e.g. vegetable or animal fat, pork/cow) of fat, the energy percentage derived from fat (36-60%), and the presence of other components like sugar. The effect of individual food components on (the intervention of) inflammatory signaling could confound overall interpretation of the mechanisms of HFD-induced inflammatory signaling, though this might play a limited role as the majority of studies employing the palatable high-fat diet have used an identical diet (Table 1, 2, 4).

Targeting leptin resistance and DIO

Leptin resistance may both initiate and maintain DIO, and the discovery that HFD-induced inflammatory signaling seems to critically mediate leptin resistance suggests that targeting key inflammatory mediators might be a promising addition to lifestyle interventions for the treatment of DIO. This might especially be successful as switching from HFD to chow diet failed to reduce hypothalamic inflammation in DIO rodents [8], suggesting that inflammatory signaling is maintained upon caloric food restriction, complicating successful weight-loss by lifestyle interventions.

Table 4. Pharmacological inhibition of inflammatory signaling

Target	Pharmacological inhibitor	Administration	Rodent type/ strain	Diet	↓ Food intake	↓Body weight	Rescue leptin sensitivity	Reference
ER stress	PBA	Oral (7d; 10-16d)	C57BL/6 mice	CD	N.A.	N.A.	-	46, 32
				HFDα	-	-	+	
		IP (8 wk)	Wistar rats	HFDδ	-	-	-	9
	TUDCA	IP (5d) /ICV (10d)	C57BL/6 mice	CD	-	-	-	20, 46
				HFDα	N.A./+	-/+	N.A.	
		IP (2d)	Sprague-Dawley rats	CD	N.A.	-	-	43
				HFD	+	+	-	
	CO	Inhalation (10 wk)	C57BL/6 mice	CD	-	-	N.A.	45
				HFDα	+	+	+	
IKKβ/ NF-κB	IKK inhibitory peptide	ICV (single)	C57BL/6 mice	CD	-	-	-	23
	PS-1145	ICV (9d)	Wistar rats	HFDα	-	-	N.A.	30
		ICV (single)	Long Evans rats	LFD	-	N.A.	N.A.	21
				HFDα	+	N.A.	N.A.	
	Teasaponin	IP (2; 21d)	C57BL/6 mice	HFDγ	+	+	+	24
JNK	SP600125	ICV (1 wk)	Wistar rats	CD	+	+	N.A.	29
				HFD	+	+	-	
PTP1B	PTP1B-ASO	ICV (4d)	Wisar rats	CD	+	N.A.	+	62
TLR4	TLR4 inhibiting antibody	IP (8 wk)/ICV (7d)	Wistar rats	HFDδ	N.A.	+/+	+/N.A.	9
Non-specific (IL-6, IL-1β, P-IKK, SOCS3, PTP1B)	Rb1	IP (2d/ 21 d)	C57/BL6	HFDγ	-/+	-	+/-	81

ER, endoplasmic reticulum; IKKβ, IkappaB kinase beta; JNK, c-Jun N-terminal kinase; PTP1B, protein tyrosine phosphatase 1; TLR4, toll-like receptor 4; PBA, 4-phenyl butyrate acid; TUDCA, tauroursodeoxycholic acid; CO, carbon monoxide; ASO, anti-sense oligonucleotide; Rb1, tetracyclic triterpenoid ginsenoside Rb1; IP, intraperitoneal, ICV, intracerebrovascular; HFD, high-fat diet; CD, control or chow diet. Identical diets are marked by the same symbol (α, γ, δ). N.A. not available.

Since TLR4 activation, upon the detection of SFAs, may act as an initiator of an inflammatory signaling cascade in the hypothalamus during HFD-feeding, targeting TLR4 could be a promising approach to control inflammation in DIO. This suggestion is supported by the finding that pharmacological inhibition of TLR4 reduced hypothalamic inflammation, and resulted in a marked inhibition of body weight gain and improvement of leptin sensitivity in DIO rats [36] (Table 4). Considering the presumed role of pro-inflammatory cytokines as messengers of astrocytes and microglia to drive an inflammatory response in ARC neurons, targeting pro-inflammatory cytokines like TNFα might also be a feasible approach to combat DIO, although it remains to be demonstrated that cytokine signaling is indeed a critical mediator of DIO. Further, IKKβ/NF-κB signaling could be a promising therapeutic target because it is a central mediator of inflammatory signaling in both AgRP and POMC neurons. Although NF-κB signaling also seems to have a physiological role in maintaining energy homeostasis [23], IKKβ/NF-κB signaling is relatively suppressed under normal nutritional conditions [20] suggesting that targeting HFD-induced upregulation of IKKβ/NF-κB might be a safe therapy for DIO. However, it remains uncertain whether pharmacological inhibition of IKKβ will be an effective approach, as specific IKKβ inhibitors have only been reported to reduce food intake in HFD-fed Long Evans but not Wistar rats [21,23,30] (Table 4). Conversely, treatment with teasaponin, a naturally derived inhibitor of NF-κB, has been shown to reduce body weight and to improve leptin sensitivity in DIO mice [24], suggesting that inhibition of NF-κB might be a successful approach. Although SOCS3 and PTP1B are the cellular mediators of leptin resistance and several studies showed that pharmacological inhibition of ER stress (partially) rescues the metabolic phenotype of DIO [20,32,43,46] (Table 4), these inflammatory mediators might not be the most successful therapeutic targets for DIO. Since the induction of ER stress and the negative regulators SOCS3 and PTP1B seems to largely result from excessive inflammatory and leptin signaling in response to excess nutrients, pharmacological inhibition of their upstream inflammatory signaling events might be a more successful approach to control hypothalamic inflammation and thereby DIO. Thus, especially TLR4, pro-inflammatory cytokines, and IKKβ/NF-κB signaling could be promising therapeutic targets for DIO that require further investigation.

Conclusions and future directions

Although exciting progress was made in the understanding of hypothalamic inflammation in DIO, many compelling questions remain. Firstly, further studies should identify the specific (non-)neuronal cell types in the hypothalamus that critically mediate inflammation in DIO rodents. In addition, *in vivo* studies are needed to determine whether microglia are indeed the primary responders to SFAs and trigger an inflammatory response upon HFD-feeding. The MyD88 (in) dependent intracellular signaling mechanisms through which activation of TLR4 on microglia and astrocytes leads to the release of pro-inflammatory cytokines also remain unknown. Further, it remains to be elucidated whether ER stress is also induced in other cell types than POMC neurons and if activation of NF-κB in POMC and AgRP neurons also induces the expression of pro- or anti-inflammatory cytokines under HFD-feeding conditions. Since the induction of cytokine expression critically depends on TLR4 signaling, and is partially mediated through ER stress and its reciprocal interaction with IKKβ/NF-κB [9,36], ER stress and IKKβ/NF-κB signaling may also be induced in microglia and astrocytes upon HFD-feeding. Alternatively, MBH neurons may express sufficient amounts of TLR4 and induce cytokine expression via signaling through ER stress and IKKβ/NF-κB. Although cytokines are presumed to play an important role in hypothalamic inflammation by acting as messengers between glial cells and neurons, their precise role in DIO remains to be elucidated. Despite the classical distinction between pro- and anti-inflammatory cytokines, understanding their individual roles in DIO is far more complex, as their interactions may influence their individual effects and many of them have pleiotropic effects [63]. Especially the role of IL-6 in HFD-induced inflammation is confusing, as this cytokine is generally considered to be pro-inflammatory, but can also exert anti-inflammatory effects, for instance by inducing IL-10 expression [28,63], and was proposed to exert a similar biological action as leptin [77]. Moreover, modest IL-6 overexpression specifically in astrocytes protected mice from HFD-induced obesity [77], suggesting that IL-6 signaling has a neuroprotective rather than a pro-inflammatory role in DIO. A neuroprotective role for IL-6 might explain why AgRP neurons, where the IL-6R is the predominantly expressed cytokine receptor [28], are less affected by inflammatory signaling than POMC neurons during HFD-feeding.

Since the majority of studies investigating the dynamics and pharmacological intervention of inflammatory signaling were performed in male animals, it remains unknown whether the inflammatory signaling mechanisms presented in this review are similar for female animals. Genetic intervention studies, however, were often also performed in female animals (Table 2). Here, similar effects were found in male

and female animals, albeit with different effect sizes, indicating that at least similar inflammatory mediators might be involved.

Thus, despite limits in current understandings, recent research on the dynamic changes in the expression and activity of inflammatory mediators during HFD-feeding, and their manipulation, provided essential insights into the mechanisms by which overnutrition may result in leptin resistance and obesity. Based on current understandings, several inflammatory mediators are proposed to be promising therapeutic targets for the treatment of DIO.

References

1. Williams LM. Hypothalamic dysfunction in obesity. *Proc Nutr Soc* 2012; **71**: 521.
2. Cai D and Liu T. Inflammatory cause of metabolic syndrome via brain stress and NF-κB. *Aging (Albany NY)* 2012; **4:** 98.
3. Fresno M, Alvarez R and Cuesta N. Toll-like receptors, inflammation, metabolism and obesity. *Arch Physiol Biochem* 2011; **117:** 151-164.
4. Nguyen DM and El-Serag HB. The epidemiology of obesity. *Gastroenterol Clin North Am* 2010; **39:** 1.
5. Pandit R, Mercer JG, Overduin J, la Fleur SE and Adan RA. Dietary factors affect food reward and motivation to eat. *Obes Facts* 2012; **5:** 221-242.
6. van den Heuvel, José K, van Rozen AJ, Adan RA and la Fleur SE. An overview on how components of the melanocortin system respond to different high energy diets. *Eur J Pharmacol* 2011; **660:** 207-212.
7. Purkayastha S and Cai D. Neuroinflammatory basis of metabolic syndrome. *Molecular Metabolism* 2013; **2**: 356-363.
8. Wang X, Ge A, Cheng M *et al.* Increased hypothalamic inflammation associated with the susceptibility to obesity in rats exposed to high-fat diet. *Exp Diabetes Res* 2012; **2012:** 847246.
9. Milanski M, Degasperi G, Coope A *et al.* Saturated fatty acids produce an inflammatory response predominantly through the activation of TLR4 signaling in hypothalamus: implications for the pathogenesis of obesity. *J Neurosci* 2009; **29:** 359-370.
10. Thaler JP, Yi C, Schur EA *et al.* Obesity is associated with hypothalamic injury in rodents and humans. *J Clin Invest* 2012; **122:** 153.
11. Zhou Y and Rui L. Leptin signaling and leptin resistance. *Front Med* 2013; **7:** 1-16.
12. Dardeno TA, Chou SH, Moon H, Chamberland JP, Fiorenza CG and Mantzoros CS. Leptin in human physiology and therapeutics. *Front Neuroendocrinol* 2010; **31:** 377-393.
13. Velloso L and Schwartz M. Altered hypothalamic function in diet-induced obesity. *Int J Obes* 2011; **35:** 1455-1465.
14. Morris DL and Rui L. Recent advances in understanding leptin signaling and leptin resistance. *Am J Physiol Endocrinol Metab* 2009; **297:** E1247-E1259.
15. Pandit R, de Jong JW, Vanderschuren LJ and Adan RA. Neurobiology of overeating and obesity: the role of melanocortins and beyond. *Eur J Pharmacol* 2011; **660:** 28-42.
16. Frederich RC, Hamann A, Anderson S, Löllmann B, Lowell BB and Flier JS. Leptin levels reflect body lipid content in mice: evidence for diet-induced resistance to leptin action. *Nat Med* 1995; **1:** 1311-1314.
17. Seeley R, Van Dijk G, Campfield L *et al.* Intraventricular leptin reduces food intake and body weight of lean rats but not obese Zucker rats. *Horm Metab Res* 1996; **28:** 664-668.
18. Halaas JL, Boozer C, Blair-West J, Fidahusein N, Denton DA and Friedman JM. Physiological response to long-term peripheral and central leptin infusion in lean and obese mice. *Proc Natl Acad Sci* 1997; **94:** 8878-8883.
19. Hayden MS and Ghosh S. Shared principles in NF-κB signaling. *Cell* 2008; **132:** 344-362.
20. Zhang X, Zhang G, Zhang H, Karin M, Bai H and Cai D. Hypothalamic IKKbeta/NF-kappaB and ER stress link overnutrition to energy imbalance and obesity. *Cell* 2008; **135:** 61-73.
21. Posey KA, Clegg DJ, Printz RL *et al.* Hypothalamic proinflammatory lipid accumulation, inflammation, and insulin resistance in rats fed a high-fat diet. *Am J Physiol Endocrinol Metab* 2009; **296:** E1003-E1012.
22. Meng Q and Cai D. Defective hypothalamic autophagy directs the central pathogenesis of obesity via the IκB kinase β (IKKβ)/NF-κB pathway. *J Biol Chem* 2011; **286:** 32324-32332.
23. Jang P, Namkoong C, Kang GM *et al.* NF-κB activation in hypothalamic pro-opiomelanocortin neurons is essential in illness-and leptin-induced anorexia. *J Biol Chem* 2010; **285:** 9706-9715.

24. Yu Y, Wu Y, Szabo A, *et al.* Teasaponin reduces inflammation and central leptin resistance in diet-induced obese male mice. *Endocrinology* 2013; **154:** 3130-3140.
25. Purkayastha S, Zhang G and Cai D. Uncoupling the mechanisms of obesity and hypertension by targeting hypothalamic IKK-[beta] and NF-[kappa] B. *Nat Med* 2011; **17:** 883-887.
26. Shi X, Wang X, Li Q *et al.* Nuclear factor kappaB (NF-kappaB) suppresses food intake and energy expenditure in mice by directly activating the Pomc promoter. *Diabetologia* 2013; **56:** 925-936.
27. Cintra DE, Ropelle ER, Moraes JC *et al.* Unsaturated fatty acids revert diet-induced hypothalamic inflammation in obesity. *PloS one* 2012; **7:** e30571.
28. Ropelle ER, Flores MB, Cintra DE *et al.* IL-6 and IL-10 anti-inflammatory activity links exercise to hypothalamic insulin and leptin sensitivity through IKKβ and ER stress inhibition. *PLoS biology* 2010; **8:** e1000465.
29. De Souza CT, Araujo EP, Bordin S *et al.* Consumption of a fat-rich diet activates a proinflammatory response and induces insulin resistance in the hypothalamus. *Endocrinology* 2005; **146:** 4192-4199.
30. Oh S, Thaler JP, Ogimoto K, Wisse BE, Morton GJ and Schwartz MW. Central administration of interleukin-4 exacerbates hypothalamic inflammation and weight gain during high-fat feeding. *Am J Physiol Endocrinol Metab* 2010; **299:** E47-E53.
31. Prada PO, Zecchin HG, Gasparetti AL *et al.* Western diet modulates insulin signaling, c-Jun N-terminal kinase activity, and insulin receptor substrate-1ser307 phosphorylation in a tissue-specific fashion. *Endocrinology* 2005; **146:** 1576-1587.
32. Won JC, Jang P, Namkoong C *et al.* Central administration of an endoplasmic reticulum stress inducer inhibits the anorexigenic effects of leptin and insulin. *Obesity* 2009; **17:** 1861-1865.
33. Belgardt BF, Mauer J, Wunderlich FT *et al.* Hypothalamic and pituitary c-Jun N-terminal kinase 1 signaling coordinately regulates glucose metabolism. *Proc Natl Acad Sci* 2010; **107:** 6028-6033.
34. Sabio G, Cavanagh-Kyros J, Barrett T *et al.* Role of the hypothalamic–pituitary–thyroid axis in metabolic regulation by JNK1. *Genes Dev* 2010; **24:** 256-264.
35. Hirosumi J, Tuncman G, Chang L *et al.* A central role for JNK in obesity and insulin resistance. *Nature* 2002; **420:** 333-336.
36. Kleinridders A, Schenten D, Könner AC *et al.* MyD88 signaling in the CNS is required for development of fatty acid-induced leptin resistance and diet-induced obesity. *Cell Metab* 2009; **10:** 249-259.
37. Mayer CM and Belsham DD. Palmitate attenuates insulin signaling and induces endoplasmic reticulum stress and apoptosis in hypothalamic neurons: rescue of resistance and apoptosis through adenosine 5′ monophosphate-activated protein kinase activation. *Endocrinology* 2010; **151:** 576-585.
38. Ryan KK, Woods SC and Seeley RJ. Central nervous system mechanisms linking the consumption of palatable high-fat diets to the defense of greater adiposity. *Cell Metab* 2012; **15:** 137-149.
39. Shi H, Kokoeva MV, Inouye K, Tzameli I, Yin H and Flier JS. TLR4 links innate immunity and fatty acid–induced insulin resistance. *J Clin Invest* 2006; **116:** 3015-3025.
40. Lee JY, Sohn KH, Rhee SH and Hwang D. Saturated fatty acids, but not unsaturated fatty acids, induce the expression of cyclooxygenase-2 mediated through Toll-like receptor 4. *J Biol Chem* 2001; **276:** 16683-16689.
41. Erridge C and Samani NJ. Saturated fatty acids do not directly stimulate Toll-like receptor signaling. *Arterioscler Thromb Vasc Biol* 2009; **29:** 1944-1949.
42. Ron D and Walter P. Signal integration in the endoplasmic reticulum unfolded protein response. *Nat Rev Mol Cell Biol* 2007; **8:** 519-529.
43. Çakir I, Cyr NE, Perello M *et al.* Obesity Induces Hypothalamic Endoplasmic Reticulum Stress and Impairs Proopiomelanocortin (POMC) Post-translational Processing. *J Biol Chem* 2013; **288:** 17675-17688.

44. Olofsson LE, Unger EK, Cheung CC and Xu AW. Modulation of AgRP-neuronal function by SOCS3 as an initiating event in diet-induced hypothalamic leptin resistance. *Proc Nat Acad Sci* 2013; **110:** E697-E706.
45. Zheng M, Zhang Q, Joe Y *et al.* Carbon monoxide-releasing molecules reverse leptin resistance induced by endoplasmic reticulum stress. *Am J Physiol Endocrinol Metab* 2013; **304:** E780-E788.
46. Ozcan L, Ergin AS, Lu A *et al.* Endoplasmic reticulum stress plays a central role in development of leptin resistance. *Cell Metab* 2009; **9:** 35-51.
47. Purkayastha S, Zhang H, Zhang G, Ahmed Z, Wang Y and Cai D. Neural dysregulation of peripheral insulin action and blood pressure by brain endoplasmic reticulum stress. *Proc Nat Acad Sci* 2011; **108:** 2939-2944.
48. Yang L and Hotamisligil GS. Stressing the brain, fattening the body. *Cell* 2008; **135:** 20-22.
49. Quan W, Kim H, Moon E *et al.* Role of hypothalamic proopiomelanocortin neuron autophagy in the control of appetite and leptin response. *Endocrinology* 2012; **153:** 1817-1826.
50. Yorimitsu T and Klionsky DJ. Autophagy: molecular machinery for self-eating. *Cell Death Differ* 2005; **12:** 1542-1552.
51. Levine B and Kroemer G. Autophagy in the pathogenesis of disease. *Cell* 2008; **132:** 27-42.
52. Klionsky DJ and Emr SD. Autophagy as a regulated pathway of cellular degradation. *Science* 2000; **290:** 1717-1721.
53. Kaushik S, Rodriguez-Navarro JA, Arias E *et al.* Autophagy in hypothalamic AgRP neurons regulates food intake and energy balance. *Cell metabolism* 2011; **14:** 173-183.
54. Reed AS, Unger EK, Olofsson LE, Piper ML, Myers MG and Xu AW. Functional role of suppressor of cytokine signaling 3 upregulation in hypothalamic leptin resistance and long-term energy homeostasis. *Diabetes* 2010; **59:** 894-906.
55. de Backer MW, Brans MA, van Rozen A *et al.* Suppressor of cytokine signaling 3 knockdown in the mediobasal hypothalamus: counterintuitive effects on energy balance. *J Mol Endocrinol* 2010; **45:** 341-353.
56. Mori H, Hanada R, Hanada T *et al.* Socs3 deficiency in the brain elevates leptin sensitivity and confers resistance to diet-induced obesity. *Nat Med* 2004; **10:** 739-743.
57. Hosoi T, Sasaki M, Miyahara T *et al.* Endoplasmic reticulum stress induces leptin resistance. *Mol Pharmacol* 2008; **74:** 1610-1619.
58. Zabolotny JM, Kim Y, Welsh LA, Kershaw EE, Neel BG and Kahn BB. Protein-tyrosine phosphatase 1B expression is induced by inflammation in vivo. *J Biol Chem* 2008; **283:** 14230-14241.
59. White CL, Whittington A, Barnes MJ, Wang Z, Bray GA and Morrison CD. HF diets increase hypothalamic PTP1B and induce leptin resistance through both leptin-dependent and-independent mechanisms. *Am J Physiol Endocrinol Metab* 2009; **296:** E291-E299.
60. Banno R, Zimmer D, De Jonghe BC *et al.* PTP1B and SHP2 in POMC neurons reciprocally regulate energy balance in mice. *J Clin Invest* 2010; **120:** 720.
61. Bence KK, Delibegovic M, Xue B *et al.* Neuronal PTP1B regulates body weight, adiposity and leptin action. *Nat Med* 2006; **12:** 917-924.
62. Picardi PK, Caricilli AM, Abreu, Lélia Lelis Ferreira de, Carvalheira JBC, Velloso LA and Saad MJA. Modulation of hypothalamic PTP1B in the TNF-α-induced insulin and leptin resistance. *FEBS Lett* 2010; **584:** 3179-3184.
63. John GR, Lee SC and Brosnan CF. Cytokines: powerful regulators of glial cell activation. *Neuroscientist* 2003; **9:** 10-22.
64. Morari J, Anhe GF, Nascimento LF *et al.* Fractalkine (CX3CL1) is involved in the early activation of hypothalamic inflammation in experimental obesity. *Diabetes* 2014; .
65. Pamir N, McMillen TS, Kaiyala KJ, Schwartz MW and LeBoeuf RC. Receptors for tumor necrosis factor-α play a protective role against obesity and alter adipose tissue macrophage status. *Endocrinology* 2009; **150:** 4124-4134.

66. Wallenius V, Wallenius K, Ahrén B *et al.* Interleukin-6-deficient mice develop mature-onset obesity. *Nat Med* 2002; **8:** 75-79.
67. Romanatto T, Cesquini M, Amaral ME *et al.* 67. *Peptides* 2007; **28:** 1050-1058.
68. Romanatto T, Roman EA, Arruda AP *et al.* Deletion of tumor necrosis factor-alpha receptor 1 (TNFR1) protects against diet-induced obesity by means of increased thermogenesis. *J Biol Chem* 2009; **284:** 36213-36222.
69. Dennis RG, Arruda AP, Romanatto T *et al.,* TNF-α transiently induces endoplasmic reticulum stress and an incomplete unfolded protein response in the hypothalamus. *Neuroscience* **170:** 1035-1044.
70. Denis R, Arruda A, Romanatto T *et al.* TNF-α transiently induces endoplasmic reticulum stress and an incomplete unfolded protein response in the hypothalamus. *Neuroscience* 2010; **170:** 1035-1044.
71. Thaler JP, Guyenet SJ, Dorfman MD, Wisse BE and Schwartz MW. Hypothalamic inflammation: marker or mechanism of obesity pathogenesis? *Diabetes* 2013; **62:** 2629-2634.
72. Sofroniew MV and Vinters HV. Astrocytes: biology and pathology. *Acta Neuropathol* 2010; **119:** 7-35.
73. Choi SJ, Kim F, Schwartz MW and Wisse BE. Cultured hypothalamic neurons are resistant to inflammation and insulin resistance induced by saturated fatty acids. *Am J Physiol Endocrinol Metab* 2010; **298:** E1122-E1130.
74. Bélanger M, Allaman I and Magistretti PJ. Differential effects of pro-and anti-inflammatory cytokines alone or in combinations on the metabolic profile of astrocytes. *J Neurochem* 2011; **116:** 564-576.
75. Horvath TL, Sarman B, García-Cáceres C *et al.* Synaptic input organization of the melanocortin system predicts diet-induced hypothalamic reactive gliosis and obesity. *Proc Natl Acad Sci* 2010; **107:** 14875-14880.
76. Langlet F, Levin BE, Luquet S *et al.* Tanycytic VEGF-A Boosts Blood-Hypothalamus Barrier Plasticity and Access of Metabolic Signals to the Arcuate Nucleus in Response to Fasting. *Cell Metab* 2013; **17:** 607-617.
77. Hidalgo J, Florit S, Giralt M, Ferrer B, Keller C and Pilegaard H. Transgenic mice with astrocyte-targeted production of interleukin-6 are resistant to high-fat diet-induced increases in body weight and body fat. *Brain Behav Immun* 2010; **24:** 119-126.
78. Gupta S, Knight AG, Gupta S, Keller JN and Bruce-Keller AJ. Saturated long-chain fatty acids activate inflammatory signaling in astrocytes. *J Neurochem* 2012; **120:** 1060-1071.
79. Li J, Tang Y and Cai D. IKKbeta/NF-kappaB disrupts adult hypothalamic neural stem cells to mediate a neurodegenerative mechanism of dietary obesity and pre-diabetes. *Nat Cell Biol* 2012; **14:** 999-1012.
80. Gao Y, Ottaway N, Schriever SC *et al.* Hormones and diet, but not body weight, control hypothalamic microglial activity. *Glia* 2014; **62:** 17-25.
81. Wu Y, Yu Y, Szabo A, Han M and Huang XF. Central inflammation and leptin resistance are attenuated by ginsenoside Rb1 treatment in obese mice fed a high-fat diet. *PLoS One* 2014; **9:** e92618.
82. Nelson RJ. The use of genetic "knockout" mice in behavioral endocrinology research. *Horm Behav* 1997; **31:** 188-196.
83. Berglund ED, Vianna CR, Donato J *et al.* Direct leptin action on POMC neurons regulates glucose homeostasis and hepatic insulin sensitivity. *J Clin Invest* 2012; **122:** 1000-1009

Chapter 3:

Is leptin resistance the cause or the consequence of diet-induced obesity?

Kathy C.G. de Git[1], Céline Peterse[1], Sanne Beerens[1], Mieneke C.M. Luijendijk[1], Geoffrey van der Plasse[1], Susanne E. la Fleur[2], Roger A.H. Adan[1,3]

1 Brain Center Rudolf Magnus, Dept. of Translational Neuroscience, University Medical Center Utrecht, Utrecht University, Utrecht 3584 CG, The Netherlands
2 Dept. of Endocrinology and Metabolism, Academic Medical Center, University of Amsterdam, Amsterdam, 1105 AZ, The Netherlands
3 Institute of Neuroscience and Physiology, Sahlgrenska Academy, University of Gothenburg, Sweden.

Published in International Journal of Obesity (2018)
doi: 10.1038/s41366-018-0111-4.

Abstract

Obesity is strongly associated with leptin resistance. It is unclear whether leptin resistance results from the (over)consumption of energy-dense diets or if reduced leptin sensitivity is also a pre-existing factor in rodent models of diet-induced obesity (DIO). We here tested whether leptin sensitivity on a chow diet predicts subsequent weight gain and leptin sensitivity on a free choice high-fat high-sucrose (fcHFHS) diet. Based upon individual leptin sensitivity on chow diet, rats were grouped in leptin sensitive (LS, n=22) and leptin resistant (LR, n=19) rats (P=0.000), and the development of DIO on a fcHFHS diet was compared. The time-course of leptin sensitivity was measured over weeks in individual rats. Both on a chow and a fcHFHS diet, high variability in leptin sensitivity was observed between rats, but not over time per individual rat. Exposure to the fcHFHS diet revealed that LR rats were more prone to develop DIO (P=0.013), which was independent of caloric intake (p≥0.320) and the development of diet-induced leptin resistance (P=0.769). Reduced leptin sensitivity in LR compared with LS rats before fcHFHS diet exposure, was associated with reduced leptin-induced phosphorylated signal transducer and activator of transcription 3 (pSTAT3) levels in the dorsomedial and ventromedial hypothalamus (P≤0.049), but not the arcuate nucleus (P=0.558). To conclude, a pre-existing reduction in leptin sensitivity determines the susceptibility to develop excessive DIO after fcHFHS diet exposure. Rats with a pre-existing reduction in leptin sensitivity develop excessive DIO without eating more calories or altering their leptin sensitivity.

Introduction

The prevalence of obesity has increased dramatically over the last few decades [1]. The majority of human obesity is thought to result from a combination of genetic susceptibility and environmental influences, such as the availability of a variety of energy-dense diets, high in saturated fat and sugar [1,2]. To model the human situation, rodent models have been developed in which obesity is induced by dietary manipulation, *i.e.* diet-induced obesity (DIO). Both in humans and rodents, the development and/or maintenance of obesity has been assumed to result from diet-induced leptin resistance [3-14].

In normal weight individuals, the brain responds to increased plasma leptin levels by reducing food intake and increasing energy expenditure [15-18]. Leptin exerts its effects by acting on leptin receptors, which are highly expressed in the arcuate nucleus (ARC) of the hypothalamus, but also in other (extra)hypothalamic brain regions, including the dorsomedial hypothalamus (DMH) [19-21]. Most obese individuals show high circulating leptin levels [8-10,13,14,17,22]. After exogenous administration of leptin, obese individuals do not respond with a decrease in food intake that is normally observed in lean individuals, and are hence considered leptin-resistant [5,7-9,11-13,22-24]. At the cellular level, the development of leptin resistance is often demonstrated by an attenuation in the incremental increase or maximal level of leptin-induced phosphorylation of signal transducer and activator of transcript 3 (pSTAT3), a critical transcription factor for leptin's action [25,26], in the ARC of rodents [12,17,18,22].

In DIO models, the resistance to leptin is often relative, i.e. a reduced but not complete absent sensitivity to the food intake suppressing effects of exogenous leptin, usually observed at one or a few time-points following leptin injection [7,12,15,16,23,24]. However, it is difficult to demonstrate the development of (absolute) leptin resistance, as there is no consensus with respect to the timing of leptin's food intake suppressing effects. Our systematic review of leptin sensitivity in control diet fed rats indicates that the anorectic effects of leptin range between 2-38h after leptin injection, and the effect sizes vary between 7-30% (Table S1). Even studies performed by the same research group showed variable results [7,11,12,15,23,27]. So, the well established food intake suppressing effect of leptin is not that straightforward. Interestingly, Ruffin et al. previously reported high variability in leptin sensitivity between rats, and the response to leptin at 2h food intake on a control diet was related to subsequent weight gain on a high-energy diet (HED) [28]. In addition, Levin et al. showed reduced central leptin sensitivity before HED exposure in rats that were retrospectively identified as DIO prone [29]. So, there is some evidence that reduced leptin sensitivity

does not necessarily result from HED feeding, but may already be present before HED exposure and predispose rats to exacerbated DIO. However, in previous studies it remains unclear whether leptin sensitivity is a stable parameter in a rat and therefore to what extent a pre-existing reduction in leptin sensitivity is a predictor for DIO. Furthermore, as leptin sensitivity was only tested before HED exposure, it is currently unknown whether exposure to a HED further reduces the pre-existing reduction in leptin sensitivity in DIO prone rats and thereby aggravates DIO.

Since the response to leptin is quite variable, we here aimed to carefully study leptin sensitivity of individual rats at 1-24h after leptin injection, and to make a trajectory of leptin sensitivity over weeks in rats that were offered a chow or a free-choice high-fat high-sucrose (fcHFHS) diet. Further, we also tested whether leptin sensitivity on a chow diet predicts subsequent body weight gain on a fcHFHS diet, and how this is related to the development of diet-induced leptin resistance. Leptin sensitivity was assessed by examining both the feeding response to leptin and the associated leptin receptor signal transduction, by using pSTAT3 activation as a marker for cellular leptin sensitivity.

Materials and Methods

Systematic review of leptin sensitivity

We searched PubMed for original articles concerning *the acute food intake suppressing effects of leptin in rats fed a control diet* until February 12th 2017. The full search strategy for PubMed was composed of four elements: leptin injection, diet, rats, and food intake/obesity (for complete search strategy see Table S2). No language restrictions were used. Studies were included in the systematic review if they fulfilled all of the following criteria: 1) the test subject was rat, 2) leptin was administered peripherally, 3) food intake after leptin injection was assessed, 4) a control diet group was included, 5) the study was an original full text paper (Figure S1). Studies were excluded if: 1) leptin was administered centrally or locally, 2) leptin was administered repeatedly, 3) the result or protocol was unclear, 4) no leptin sensitivity test was performed. Study selection was based on title and abstract. In case of doubt, the full text article was evaluated. After selection of all studies that assessed *the acute food intake suppressing effect of leptin in rats fed a control diet* in a relevant and clear way, a selection of the most common way to test leptin sensitivity was made. Intraperitoneal leptin injection after light phase food restriction was the most common way to test leptin sensitivity, and the timing of leptin's food intake suppressing effect was only compared between studies that used this protocol. If data were only presented graphically, effect sizes were estimated from the graphs. Only the effects of the control diet group were studied, and all different types of control diet were included.

Animals and dietary intervention

Male Wistar rats (7 weeks old; Charles River, Sulzfeld, Germany) were individually housed in Plexiglas cages in a temperature controlled (21-23 °C) and light controlled (lights on between 0700 and 1900 h) room. Upon arrival, all rats had ad libitum access to pelleted rat chow (3.31 kcal/g; Special Diet Service, UK) and tap water. When the rats had reached a body weight of >300 g, they were implanted with intra-arterial silicone catheters through the right jugular vein, according to the method of Steffens (30). Four weeks later, rats were equally divided into two diet groups based upon their average body weight, body weight gain, daily caloric intake, and leptin sensitivity in the week before the division. Sample sizes were calculated based on expected effect sizes and variance. One group of control rats remained on chow and tap water over the entire experimental period (n=21), whereas the other group was subjected to a fcHFHS diet for eight weeks (n=20). The fcHFHS diet consisted of a choice between lard (9.1 Kcal/g Ossewit/Blanc de Boeuf, Belgium) and 30% sucrose solution (1.0 M sucrose mixed from commercial grade sugar and tap water), in addition to regular chow and tap water. Subsequently, the chow and fcHFHS diet group were both divided into subgroups of LS and LR rats based upon their leptin sensitivity on chow diet, as described below. Body weight and 24-hour food intake were measured 5 days per week. All experiments were performed in accordance with Dutch laws (Wet op de Dierproeven, 1996) and European regulations (Guideline 86/609/EEC), and were approved by the Animal Ethics Committee of Utrecht University.

Leptin sensitivity

Leptin sensitivity was tested before fcHFHS diet exposure, and after 2, 4, and 8 weeks of fcHFHS diet exposure. To measure leptin sensitivity, animals were fasted overnight (10 gr chow at 1600h). The next morning at 0900 h, leptin (250 µg / 250 µl; recombinant murine leptin, NHPP, USA) or vehicle (250 µl, phosphate buffered saline, PBS) was injected via the jugular vein catheter, and 45 minutes later food was given back. A latin-square design was used, as such that half of the rats in each dietary group first received leptin, and 3-4 days later rats were tested a second time with treatments reversed. Food intake was measured 1-24h after food return by using data collected by Scales (Department Biomedical Engineering, UMC Utrecht, The Netherlands). This program records the weight of food hoppers in the home cage automatically every 12 s, as well as the amount of licks from water or sucrose bottles.

To divide the chow control group into two types of responders, leptin sensitivity of each individual rat was determined at four different time-points (before fcHFHS diet exposure, and at 2, 4, and 8 weeks of fcHFHS diet exposure), and subsequently the average response of all four tests was taken. Leptin sensitivity was measured by normalizing cumulative food intake after leptin injection to cumulative food intake after vehicle injection. Rats were divided into two subgroups based upon their feeding response at one hour after leptin injection, as the variability was the largest at this time-point. Rats showing a reduction in food intake (percentage suppression <100) were designated as LS (n=11), whereas rats showing no reduction or even an increase in food intake were designated as LR (percentage suppression ≥100, n=10). Rats offered the fcHFHS diet were selected as LS (n=11) or LR (n=7) based upon their leptin sensitivity test before fcHFHS diet exposure.

Immunohistochemistry

Rats were injected with leptin (250 µg / 250 µl) or vehicle via the jugular vein catheter, and subsequently all chow, lard, and the 30% sucrose solution were removed. Two hours later, rats were anesthetized with sodium pentobarbital (Nembutal, 100 mg/kg/ml) and perfused with ice cold 0.9% NaCl, followed by 4% paraformaldehyde (PFA). Brains were removed, incubated overnight in 4% PFA, and subsequently immersed in 30% sucrose solution in PBS. Brains were cut in 40 µm coronal free-floating slices, collected in six series, and pSTAT3 immunohistochemistry was performed as described previously [31]. In brief, one of the six series of free-floating slices was blocked in horse serum and then incubated overnight with rabbit anti-pSTAT3 (1:1000, rabbit monoclonal, Cell Signaling, #9145S). Slices were washed and incubated with biotinylated anti-rabbit antibody (1:250), followed by avidin-biotin-complex labeling. Pictures were taken using a bright-field microscope with a digital camera (Axiocam, Zeiss, Germany). Slices were matched to the stereotaxic brain atlas from Paxinos and Watson (1998; fourth edition), using the fornix, mammillothalamic tract, and optic tract as landmarks. For each animal, the number of pSTAT3 positive cells was counted blindly in both sides of the ARC and DMH, and the intensity of the bright field signal was quantified in the ventromedial hypothalamus (VMH) with background intensity subtracted, at one slice at Bregma -3.30.

Body composition

At the end of the experiment, rats were anesthetized and prior to perfusion, individual epididymal and subcutaneous (inguinal) white adipose tissues were dissected from the left side, cleaned and weighed.

Plasma leptin levels

Blood samples were taken shortly prior to leptin or vehicle injection during each leptin sensitivity test session and immediately chilled on ice. Blood was centrifuged (4 °C; 10.000 rpm; 20 min) and plasma was stored at -20°C until further analysis. Plasma leptin levels were measured in duplicate using a radioimmunoassay kit (Multi-Species Leptin RIA, XL-85K, Merck Millipore, USA). The amounts of sample, standards, label, antibody and precipitating reagent were divided by four.

Statistical analysis

Two rats could not be tested for their leptin sensitivity at week 4, three rats could not be tested at week 8, and two rats could not be tested during the entire experiment because of a blockade of their catheter. Blood collection was not successful at one or more time-points in 16 rats. These rats were excluded from the concerning analyses. Fat mass was only tested in a subgroup of 16 rats, and pSTAT3 levels were tested in a subgroup of 30 rats. Food intake data were computed automatically. Since the leptin sensitivity data of each rat was used to group them, and as rats were offered either a chow or fcHFHS diet, experimenters were not explicitly blinded for experimental treatments or group allocation.

For differences in body weight (gain), caloric intake, and plasma leptin levels, two-way repeated measures ANOVA's were performed with week as within-subject variable and diet (chow vs fcHFHS and/or responder) as between-subject variable. For fat mass analysis, a one-way ANOVA was performed with diet/responder as between-subject variable. Feeding responses to leptin were assessed using a three-way repeated measures ANOVA with time and treatment as within-subject variables and diet/responder as between subject-variable. Count data of leptin sensitivity was analyzed with a two-way repeated measures ANOVA with diet (before/after fcHFHS) as within subjects-variable and responder as between subject-variable. Analysis of pSTAT3 levels was performed with a MANOVA with treatment, diet, and group as between subject-variable.

Mauchly's test of sphericity was used to test whether variances of the differences between treatment levels were equal. If the assumption of sphericity was violated, degrees of freedom were corrected using Greenhouse-Geisser (GG) estimates of sphericity or Huynh-Feldt estimates of sphericity when the GG estimate was >0,75. When appropriate, post hoc analyses were conducted using Student's t-tests or pairwise Bonferroni comparisons. Each parameter was tested for normality with the Kolmogorov-Smirnov test. When data were not normally distributed, data were log transformed prior to statistical analyses.

The unbiased clustering analysis of leptin sensitivity on chow diet was carried out by means of a TwoStep cluster analysis. Individual leptin sensitivity at 1h after injection, as measured by cumulative food intake after leptin injection normalized to baseline vehicle, was introduced as input variable in the cluster analysis. The log-likelihood method was used to determine inter-subject distance. The number of clusters was determined automatically based on Schwarz's Bayesian criteria and log-likelihood method.

Statistical analyses were conducted using SPSS 20.3 for Windows. The threshold for statistical significance was set at $p<0.05$; all tests were two-sided. Data are presented as mean ± SEM.

Results

Exposure to the fcHFHS diet results in hyperphagia and obesity.

As reported previously [16,32], rats offered a fcHFHS diet (n=20) showed increased body weight, caloric intake, and adiposity compared with control rats on a chow diet (n=21) (Figure 1A,B,D). In addition, plasma leptin levels were higher from 4 weeks of fcHFHS diet exposure onwards compared with control rats (Figure 1C).

Both chow and fcHFHS fed rats show high variability in individual leptin sensitivity.

We next determined whether fcHFHS diet fed rats developed leptin resistance. Leptin sensitivity was tested before fcHFHS diet feeding, and after 2, 4, and 8 weeks of fcHFHS diet exposure. As leptin's food intake suppressing effects were previously reported at variable time-points after exogenous leptin injection (Table S1) [28,33], we here show leptin sensitivity at the four most common time-points reported by previous studies (Figure 2). Leptin sensitivity was tested via two common methods, *i.e.* by comparing absolute cumulative caloric intake after leptin or vehicle injection (Figure 2A-C) and by calculating the percentage suppression from baseline vehicle (Figure 2D-F). Before fcHFHS diet exposure, rats significantly reduced their food intake at 14h and 24h after leptin injection, and leptin sensitivity did not differ between prospective chow and fcHFHS diet fed rats (Figure 2A,D). At week 2, no differences in leptin sensitivity were observed between the chow and fcHFHS group (data not shown). However, from week 4 onwards leptin sensitivity was impaired in fcHFHS fed rats compared with chow controls (Figure 2B,C,E,F). The chow group was still leptin sensitive at both week 4 and week 8, whereas the fcHFHS group did no longer show a reduction in food intake after leptin injection. So, by testing leptin sensitivity at the group level, the fcHFHS group developed leptin resistance from week 4 onwards. However, individual data points show high variability in leptin sensitivity between rats in both the chow and fcHFHS group, especially at the first hours after injection (Figure 2D-F).

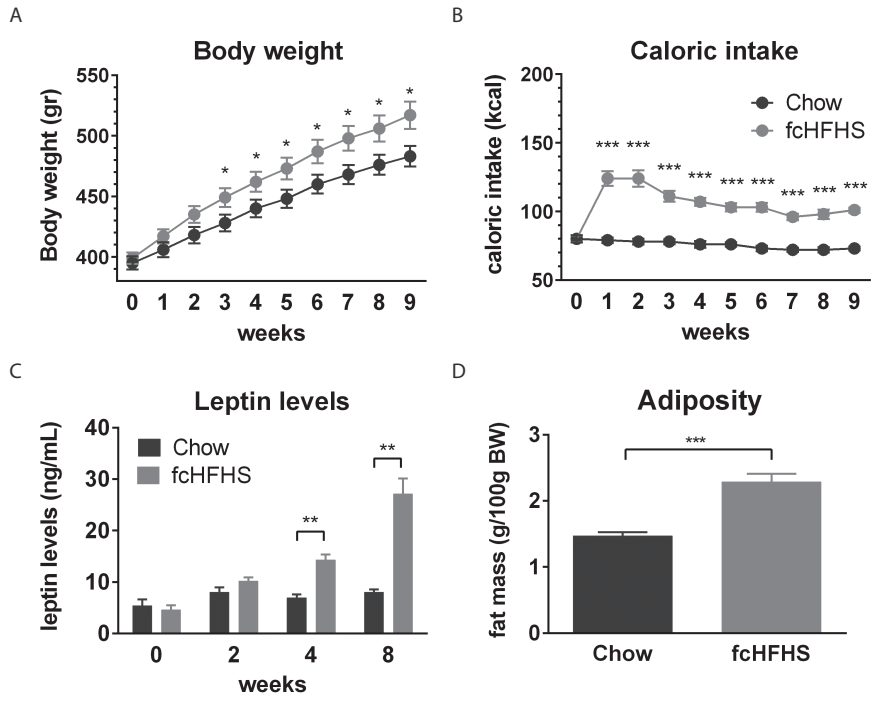

Figure 1. Obesity-related parameters in rats offered a chow or fcHFHS diet. (A) Body weight, (B) caloric intake, and (C) plasma leptin levels during the whole experimental period (n=20-21 per group). $F_{week*diet} \geq 6.402$, $p \leq 0.007$. (D) Epididymal and subcutaneous (inguinal) white adipose tissues at week 9 (n=8 per group), t=-6.042, p=0.000. Data is shown as mean ± SEM. *P<0.05, **P<0.01, ***P<0.001 compared with chow controls.

Based upon variability in individual leptin sensitivity on chow diet, rats were divided into two types of responders.

Since the chow group was kept on chow diet for 8 weeks and tested for leptin sensitivity every two weeks, we were able to determine whether leptin sensitivity is a stable parameter in a rat (Figure 3A). Leptin sensitivity was tested by normalizing 1-24h cumulative caloric intake after leptin injection to baseline vehicle. Individual rats showed a stable response pattern over weeks (Figure S2). Closer inspection of individual leptin sensitivity on chow diet revealed two types of responders. Rats were divided in those showing a reduction in food intake at the first hour after leptin

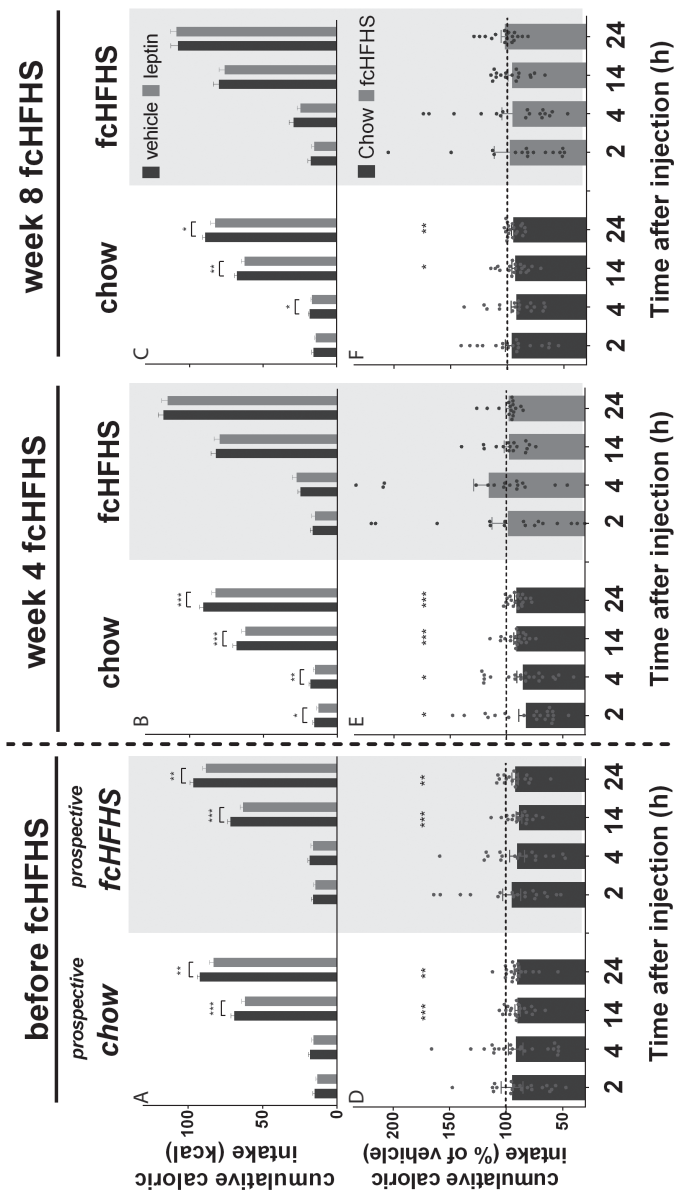

Figure 2. Feeding response to leptin in rats offered a chow or fcHFHS diet. (A-C) Leptin sensitivity, as measured by absolute cumulative caloric intake after vehicle or leptin injection, is shown (A) before, (B) after 4 weeks, and (C) after 8 weeks of fcHFHS diet exposure. (D-F) Leptin sensitivity, as measured by cumulative food intake after leptin injection normalized to vehicle cumulative food intake, was measured (D) before, (E) after 4 weeks, and (F) after 8 weeks of fcHFHS diet exposure. Before fcHFHS, $F_{diet*treatment} \geq 0.001$, $p \geq 0.951$, $F_{treatment} \geq 9.670$, $p \leq 0.004$; week 4 and 8, $F_{diet*treatment} \geq 4.397$, $p \leq 0.044$; chow week 4 and 8, $F_{treatment} \geq 6.529$, $p \leq 0.019$; fcHFHS week 4 and 8, $F_{treatment} \geq 0.118$, $p \geq 0.223$. Data is shown as mean ± SEM; n=17-21 per group. *P<0.05, **P<0.01, ***P<0.001 compared with vehicle.

injection (leptin sensitive, LS, n=11), and those that reduced their food intake at later time-points after leptin injection, showing no reduction or even an increase in food intake at the first hours after injection (relatively leptin resistant, LR, n=10) (Figure 3B,C). The selection of LS and LR rats was based on the average leptin sensitivity of four independent leptin sensitivity tests (Figure 3A,C and Figure S2). The response to leptin at 1h food intake ranged from -26,5% to -6,3% (-21,7±2,4) in LS rats and from +0,2 to +98,4% (+22,4±10,0) in LR rats. Statistical analyses confirmed that the selected LS and LR rats also responded differently to leptin at other time-points after injection, especially at 2-4h after injection (Figure 3). Only LS rats differed significantly from baseline vehicle at the first four hours after leptin injection. At 13-24h after leptin injection, LS and LR rats showed a similar reduction in food intake. In accordance with the general response patterns, LS rats showed their strongest reduction in food intake at an earlier time-point after leptin injection compared with LR rats (4,8±0,7 h vs. 7,6±0,6 h) (Figure 3D).

We confirmed our manual selection of LS and LR rats by carrying out an unbiased TwoStep clustering analysis based upon individual leptin sensitivity on chow diet. The number of clusters was determined automatically and yielded 2 clusters, in which rats were classified in exactly the same subgroups as in our manual classification (n=11, 52.4%; n=10, 47.6%). The cluster analysis resulted in an average Silhouette measure of cluster cohesion and separation of 0.70, indicating a good cluster quality.

A pre-existing reduction in leptin sensitivity on chow diet predicts the susceptibility to develop excessive DIO.

Like the chow diet group, the fcHFHS diet group was also divided into LS (n=12) and LR (n=9) rats based upon leptin sensitivity before fcHFHS diet exposure (Figure 4A). Obesity-related parameters were studied in both chow and fcHFHS diet fed LS and LR rats. Chow diet fed LS and LR rats did not differ in body weight gain, caloric intake, plasma leptin levels, and adiposity (Figure 4). However, LR rats offered a fcHFHS diet gained 10,6% more body weight compared with chow diet fed controls (Figure 4B). Body weight gain in fcHFHS diet fed LS rats did not differ from chow controls. Although both LS and LR rats fed a fcHFHS diet increased their plasma leptin levels and adiposity over the course of diet exposure, plasma leptin levels and adiposity were higher in LR rats compared with LS rats after 8 weeks of fcHFHS diet exposure (Figure 4C,D). Increased body weight gain on the fcHFHS diet in LR versus LS rats could not be explained by differences in average caloric intake or the average consumption of the different components of the fcHFHS diet (Figure 4E,F). So, these data show that leptin sensitivity on a chow diet predicts the susceptibility to develop excessive DIO, as LR rats were more prone to develop obesity on a fcHFHS diet compared with LS rats.

A

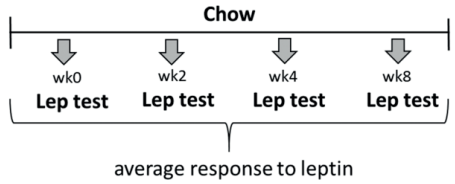

B

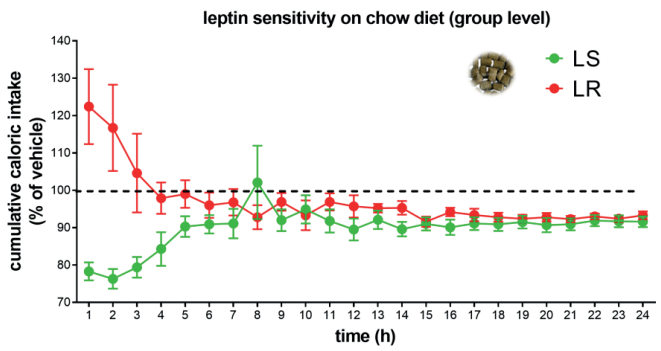

C

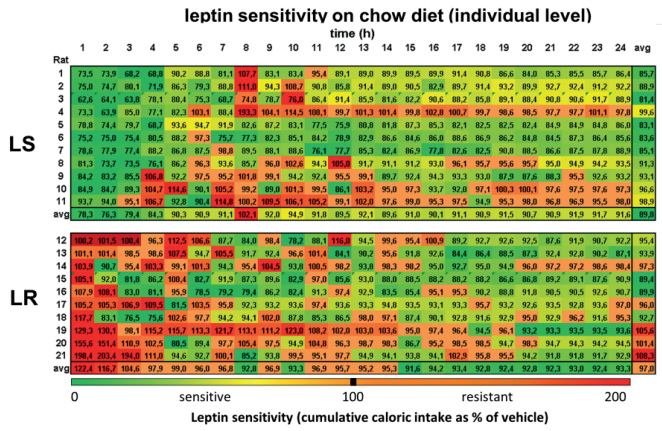

D

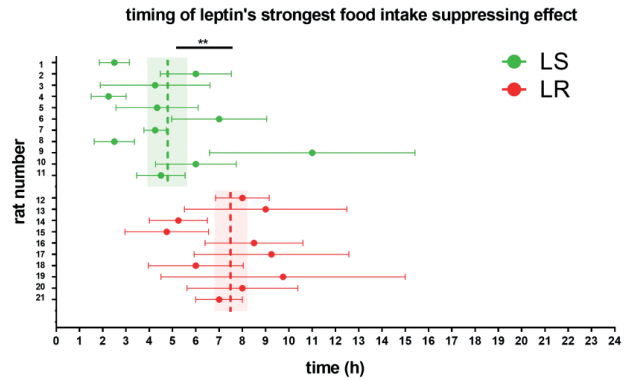

< Figure 3. Individual 1-24h leptin sensitivity in rats offered a chow diet. Based upon leptin sensitivity on chow diet, rats were divided in those showing a reduction in food intake at the first hour after leptin injection (LS) and those that did not change or increased their food intake with leptin at 1h food intake (LR). (A) Experimental design. Leptin sensitivity was measured by cumulative food intake after leptin injection normalized to vehicle food intake. Average leptin sensitivity of 4 tests is shown. Leptin sensitivity (B) at group level and (C) individual level; a heat plot of the relative level of sensitivity is shown at 1-24h food intake for each individual rat (i.e. each row). The heat plot indicates the relative degree of leptin sensitivity at a particular time point in comparison with the other time-points in the row. 1-24h: $F_{hour*treatment*group}$=8.239, p=0.000, post hoc p<0.05 at 1-4h. 1-4h: LS, $F_{treatment}$=48.561, p=0.000; LR, $F_{treatment}$=0.931, p=0.360. (D) The average time-point of the strongest food intake suppressing effect of leptin is shown for each individual rat (average of 4 tests is shown); t=-3.164, p=0.005. Data is shown as mean ± SEM; n=9-12 per group. **P<0.01 for LS vs. LR.

Exposure to the fcHFHS diet does not further reduce leptin sensitivity in rats with a pre-existing reduction in leptin sensitivity.

As diet-induced leptin resistance has been proposed to initiate and/or maintain DIO [5,7-9,11-13,22-24], the development of leptin resistance on the fcHFHS diet was compared between LS and LR rats. Leptin sensitivity was tested by normalizing 1-24h cumulative caloric intake after leptin injection to baseline vehicle (Figure S3), and by counting the number of time-points out of 24h time-points at which the rats did not reduce their food intake after leptin injection compared with vehicle (*i.e.* number of time-points with a percentage suppression of ≥100) (Figure 4G). The feeding response to leptin before fcHFHS diet exposure was compared with the average response at week 4 and 8 of the fcHFHS diet, as rats developed leptin resistance at the group level from 4 weeks of fcHFHS diet feeding onwards (Figure 2). Before fcHFHS diet exposure, LS rats were more leptin sensitive compared with LR rats (Figure 4G and Figure S3). LS rats became less leptin sensitive during fcHFHS diet exposure, whereas the fcHFHS diet did not further reduce leptin sensitivity in LR rats. As a result, leptin sensitivity did no longer differ between the subgroups after fcHFHS diet feeding. Thus, LR rats, which were more prone to develop DIO than LS rats (Figure 4), did not develop diet-induced leptin resistance. Conversely, LS rats, which were less prone to develop DIO, did develop leptin resistance after fcHFHS diet exposure (Figure 4). These findings indicate that a pre-existing reduction in leptin sensitivity rather than diet-induced leptin resistance is critical for the development of excessive DIO.

A pre-existing reduction in cellular leptin signaling in the DMH, but not the ARC, predicts the susceptibility to develop excessive DIO.

Finally, we studied whether the pre-existing reduction in leptin sensitivity in LR compared with LS rats could be explained by differences in cellular leptin sensitivity in the hypothalamus. The number of pSTAT3 positive neurons was counted in the ARC, VMH and DMH (Figure 5). Basal pSTAT3 levels did not differ between chow

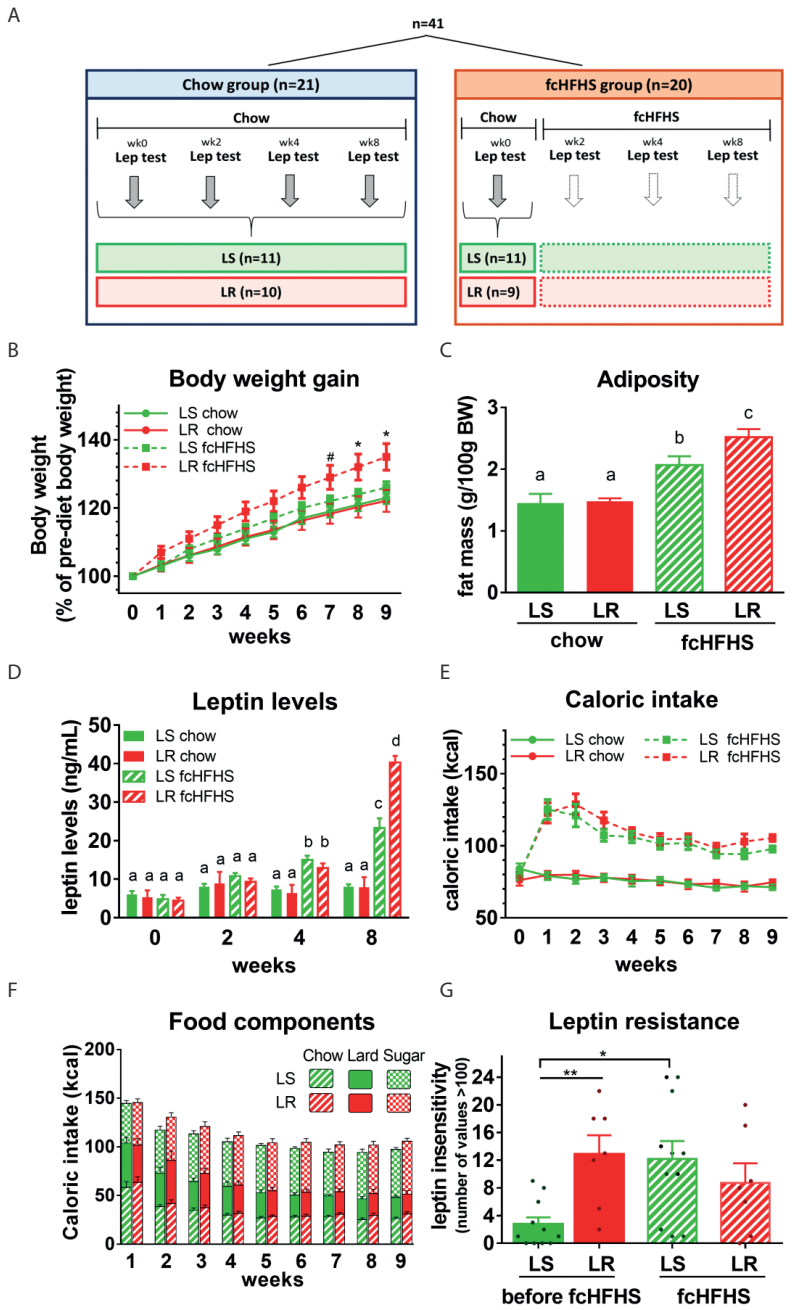

< Figure 4. Obesity-related parameters in LS and LR rats offered either a chow or fcHFHS diet. (A) Experimental design. Rats were first divided into a chow and fcHFHS group, and subsequently divided into LS and LR rats. The selection of LS and LR rats was based on the average leptin sensitivity of four independent leptin sensitivity tests in the chow diet group, and leptin sensitivity before fcHFHS diet exposure in the fcHFHS diet group. (B) Body weight gain, (C) Epididymal and subcutaneous (inguinal) white adipose tissues at week 9, and (D) Plasma leptin levels during the whole experimental period. $F_{week*diet/subgroup} \geq 3.390$, $p \leq 0.013$. (E) Caloric intake (week average of kcal per day), (F) consumption of the different components of the fcHFHS diet (week average of kcal per day). $F_{week*diet/subgroup}=8.340$, $p=0.000$; chow, $F_{subgroup}=0.008$, $p=0.931$; fcHFHS, $F_{subgroup} \geq 0.057$, $p \geq 0.320$. (G) Leptin resistance as measured by cumulative food intake after leptin injection normalized to vehicle food intake, followed by a count of the number of time-points with a value of ≥100. Data show the response to leptin before fcHFHS diet exposure (chow) and for the average of week 4 and 8 of the fcHFHS diet. $F_{diet*subgroup}=7.316$, $p=0.016$. Data is shown as mean ± SEM; n=4-12 per group. Different lowercase letters represent significant differences ($P<0.05$) between bars. #$P<0.07$; *$P<0.05$; **$P<0.01$ in comparison with the LS and/or LR rats on chow diet.

diet fed LS and LR rats. In the ARC, a leptin-induced increase in pSTAT3 levels was shown, but pSTAT3 levels did not differ between LS and LR rats (Figure 5A,B). In contrast, in the VMH and DMH, the leptin-induced pSTAT3 activation was lower in LR rats compared with LS rats (Figure 5A,C). So, the obesity-prone LR rats show a pre-existing reduction in cellular leptin sensitivity in the VMH and DMH but not the ARC.

We also studied the development of diet-induced leptin resistance at the cellular level. In the ARC, basal pSTAT3 levels were elevated in fcHFHS diet fed rats compared with chow controls (Figure 5A,B). Leptin injection did not further increase pSTAT3 levels in fcHFHS diet fed rats. Thus, fcHFHS diet fed rats showed increased endogenous leptin signaling in the ARC and could not further increase their signaling after leptin injection. fcHFHS diet fed LS and LR rats did not differ in either basal or leptin-induced pSTAT3 levels in the ARC. In the DMH, however, fcHFHS diet fed LS rats showed lower leptin-induced pSTAT3 levels compared with LR rats (Figure 5 A,C). In comparison with chow diet fed rats, leptin-induced pSTAT3 levels in the DMH and VMH were dramatically reduced (~70%) in fcHFHS diet fed LS rats, but not affected in fcHFHS diet fed LR rats. These findings show that exposure to the fcHFHS diet does not further reduce the pre-existing reduction in pSTAT3 activation in the VMH and DMH in the obesity-prone LR rats. Thus, a pre-existing, but not diet-induced, reduction in leptin signaling in the VMH and DMH is associated with the susceptibility to develop DIO.

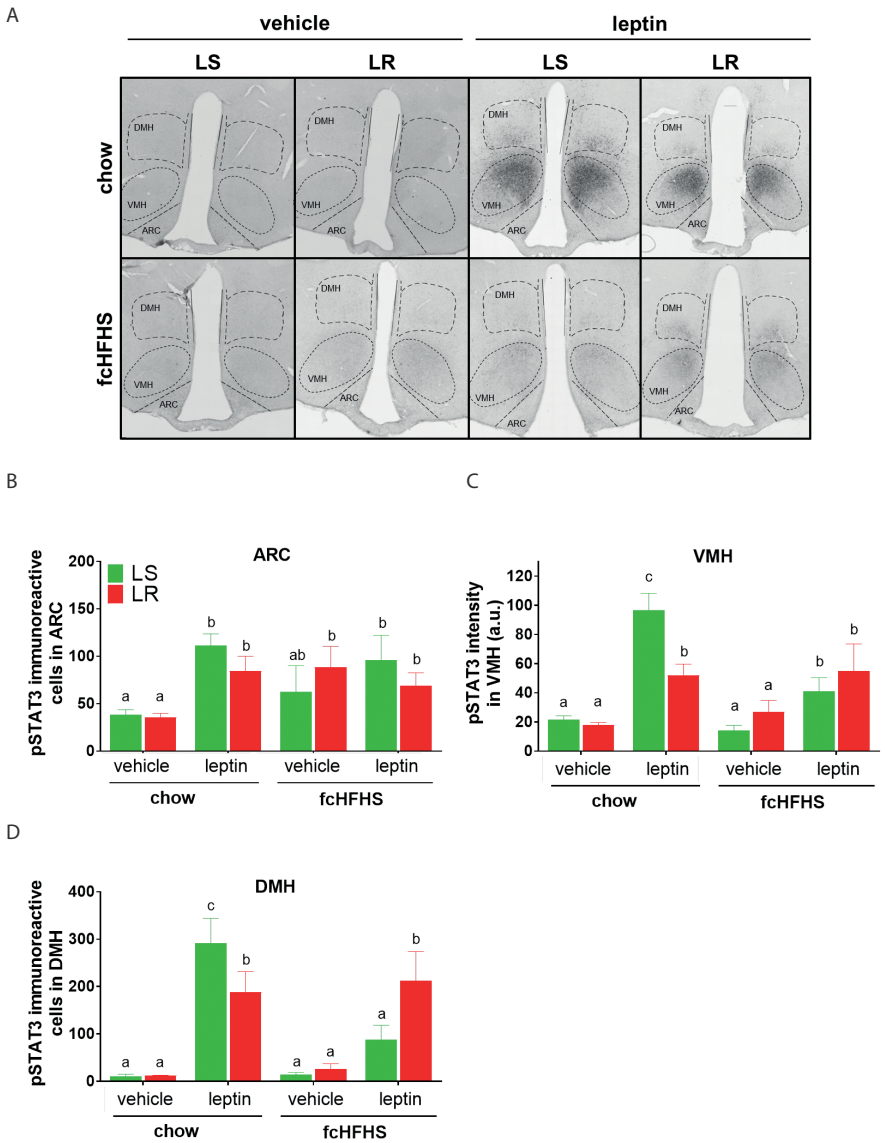

Figure 5. Hypothalamic leptin sensitivity in LS and LR rats. (A) Representative images of pSTAT3 immunoreactivity in the hypothalamic arcuate nucleus (ARC), ventromedial hypothalamus (VMH), and dorsomedial hypothalamus (DMH) of LS and LR rats fed a chow or fcHFHS diet. (B, C, D) Number of pSTAT3 immunoreactive cells in the ARC (B), VMH (C), and DMH (D). ARC, $F_{diet*treatment}$=4.348, p=0.049; $F_{subgroup}$=0.354, p=0.558. VMH, $F_{diet*treatment}$=4.490, p=0.046, $F_{diet*subgroup}$=8.530, p=0.008, $F_{treatment}$=40.151, p=0.000. DMH, $F_{diet*treatment*subgroup}$=4.338, p=0.049. Data is shown as mean ± SEM; n=3-5 per group. Different lowercase letters represent significant differences (P<0.05) between bars.

Discussion

Across species, there is a high and unexplained variability in the development of obesity upon exposure to energy-dense diets high in saturated fat and sugar. We here demonstrate that individual leptin sensitivity on a chow diet, prior to exposure to a diet high in saturated fat and sugar, predicts the susceptibility to develop DIO (Figure 6). We showed that leptin sensitivity is highly variable between chow-diet fed rats, but stable over time per individual rat, and is therefore a reliable predictor for DIO. Leptin resistant (LR) rats, which showed a pre-existing reduction in leptin sensitivity compared with leptin sensitive (LS) rats, gained more body weight and adiposity after 8 weeks of fcHFHS diet exposure, without eating more calories or altering leptin sensitivity. The pre-existing reduction in the anorectic response to leptin in LR compared with LS rats was associated with reduced leptin-induced pSTAT3 levels in the DMH and VMH but not the ARC, a brain area known to be a critical regulator of food intake [34-37]. These results challenge the generally accepted concept of diet-induced leptin resistance in the ARC as a causal factor for the initiation and/or maintenance of DIO.

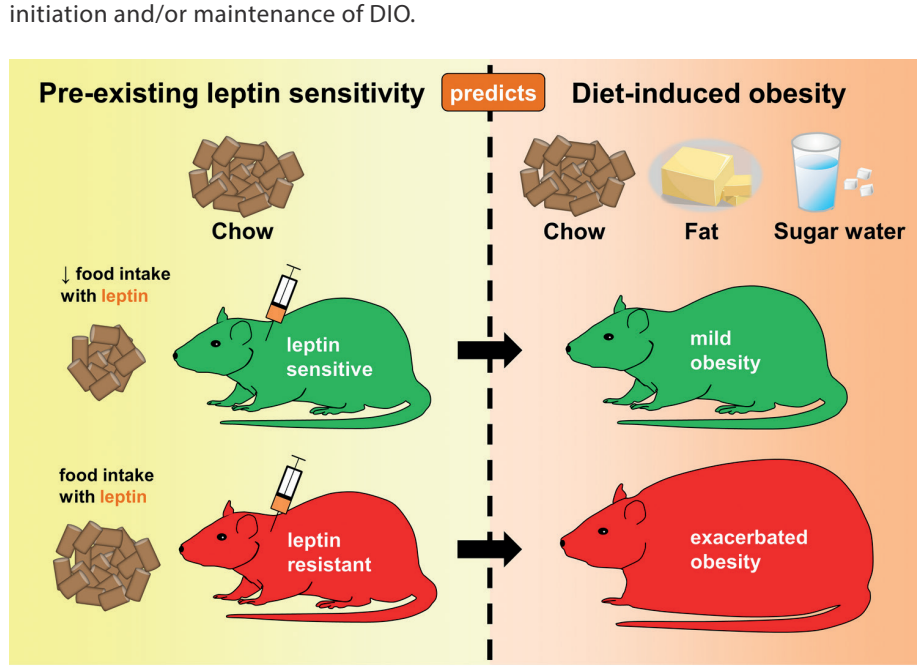

Figure 6. Summary of the main findings. Based on leptin sensitivity on a chow diet, rats were grouped in leptin sensitive and leptin resistant rats. After exposure to an obesogenic free-choice high-fat high-sugar diet, leptin resistant rats develop exacerbated obesity.

We first systematically reviewed literature to show that both the time-points and effect sizes of the anorectic response to leptin are very variable (Table S1) [28]. In addition, leptin sensitivity was often studied at the group level instead of by comparing the treatment effects within individual rats (Table S1). We next showed the importance of studying leptin sensitivity at the individual level and at multiple time-points after injection. At the group level, the fcHFHS diet group developed leptin resistance after 4 weeks of fcHFHS diet feeding, whereas the chow group was still leptin sensitive. However, both the chow and fcHFHS diet group showed high variability in individual leptin sensitivity. Closer inspection of individual leptin sensitivity on chow diet revealed two different types of leptin responders, LS and LR rats, which were hidden in the group average data. LS and LR rats especially differed in their leptin sensitivity at 1-4h after leptin injection, but did not differ at 13-24h food intake. Only since we monitored food intake continuously over 24h following leptin injection, we were able to discover the two types of leptin responders on a chow diet. This turned out to be crucial to predict which rats increase body weight after fcHFHS diet exposure.

Note that in contrast to earlier studies in which leptin was injected only once [28,29], in our study, we found that individual chow diet fed rats show a stable response pattern to leptin over weeks, as was tested with four independent leptin sensitivity tests. Thus, we show that leptin sensitivity is a stable parameter in a rat and is therefore a reliable predictor for DIO. The finding that LS and LR rats especially differed in their leptin sensitivity at 1-4h after leptin injection is in accordance with Ruffin et al. and Levin et al., who also reported the major differences in leptin sensitivity before HED exposure at 2h or 4h, but not 24h, food intake [28,29]. The predominant variability in leptin sensitivity at the first four hours after leptin injection might be due to the fasting prior to leptin sensitivity testing: rats might respond differently to fasting and/or the drive to eat was probably stronger at the first hours after food return. Interestingly, a highly variable effect of leptin (range -94% to +129%) on food intake was specifically reported by Ruffin et al. [28], who also administered leptin intravenously in male Wistar rats, as opposed to the more common intraperitoneal leptin administration in mostly Sprague-Dawley rats (Table S1) [29]. Therefore, the high variability in leptin sensitivity we observed, including the (non-significant) tendency of LR to increase their food intake after leptin injection, could be a strain effect or result from the intravenous instead of intraperitoneal route of administration.

Levin et al. reported that selectively bred DIO rats and DR rats, fed a chow diet, did not differ in leptin transport across the blood brain barrier [33]. However, DIO rats showed reduced Lepr-b expression [33,38], leptin receptor binding [39], and leptin-induced pSTAT3 levels in the ARC, VMH, and DMH compared with DR rats [33,40]. We here also studied whether the reduced anorectic response to leptin in chow diet fed LR compared with LS rats could be explained by differences in hypothalamic pSTAT3 activation, and found that LR rats showed lower leptin-induced pSTAT3 activation in the DMH and VMH but not the ARC. There is evidence that leptin's regulation of food intake is also mediated via leptin signaling in the DMH [18,41, but see 42]. So, lower leptin evoked pSTAT3 activation in the DMH could explain the reduced anorectic response to leptin in chow diet fed LR rats. The discrepancy with the above described results of Levin et al. [33] might result from their selective breeding of DR and DIO rats or differences in rat strain and/or supplier.

Despite that LS and LR rats were selected based on their acute feeding response to leptin, they displayed similar daily caloric intake on both a chow and fcHFHS diet. This is particularly fascinating as leptin is believed to be a physiological regulator of (long-term) energy intake [34,35,37]. Previous studies in rats with a pre-existing or experimentally induced impairment in leptin sensitivity showed a considerable increase in daily caloric intake on high-energy or high-fat diet, and sometimes even on chow diet [24,25,28,29]. In previous studies, obesity in (outbred or selectively bred) Wistar and Sprague-Dawley rats with a pre-existing reduction in leptin sensitivity largely resulted from hyperphagia. In contrast, we here show that daily caloric intake was similar in LS and LR rats. Thus, caloric intake cannot explain why LR rats gained more weight and adiposity on a fcHFHS diet compared with LS rats, which makes our model interesting to study food intake independent mechanisms by which a pre-existing reduction in leptin sensitivity predisposes rats to develop exacerbated DIO on a energy-dense diet. In the model of Levin et al., reduced cellular leptin sensitivity in the ARC may predispose DIO rats to hyperphagic obesity [33,40], while in our model the development of obesity may result from differences in pSTAT3 activation in the VMH/DMH between LS and LR rats. Leptin action in the DMH and VMH has been shown to regulate energy balance by increasing thermogenesis and energy expenditure [18,41,42-44]. Therefore, reduced thermogenesis and/or energy expenditure could explain the increased body weight gain and adiposity in fcHFHS diet fed LR rats. Alternatively, LR rats might have an increased capacity to absorb energy from the fcHFHS diet, as increased energy extraction has been associated with high-fat diet feeding, obesity, and reduced leptin sensitivity [45-47].

One major question we addressed in this study was whether DIO mostly results from diet-induced leptin resistance or if a pre-existing reduction in leptin sensitivity is more critical for the development of DIO. This issue was not resolved by previous studies, as leptin sensitivity was usually tested only before [28,29,33] or after [7,11,12,15,16,23] high-energy or high-fat diet exposure. LR rats showed a pre-existing reduction in leptin sensitivity on chow diet compared with LS rats. Exposure to the fcHFHS diet impaired leptin

sensitivity in LS rats, but did not further reduce leptin sensitivity in LR rats. Since LR rats showed exacerbated weight gain and adiposity compared with LS rats during fcHFHS diet feeding, our data indicate that the susceptibility to develop excessive DIO depends on a pre-existing reduction in leptin responsiveness rather than diet-induced leptin resistance. This conclusion is supported by the findings of leptin sensitivity at the cellular level, showing that LR rats showed a pre-existing reduction in leptin-induced pSTAT3 activation in the DMH and VMH compared with LS rats, which was not further reduced by fcHFHS diet exposure. Both LS and LR rats did not develop leptin resistance in the ARC after fcHFHS diet exposure. Leptin treatment did not induce pSTAT3 activation in the ARC, but this resulted from the elevated basal pSTAT3 levels upon exposure to the fcHFHS diet, indicating increased endogenous leptin signaling [9]. The finding of ongoing endogenous leptin signaling in the ARC of both LS and LR rats contradicts previous studies showing selective leptin resistance in the ARC after high-fat diet feeding [18,22]. Thus, our results challenge the generally accepted concept of diet-induced leptin resistance in the ARC as a causal factor for the initiation and/or maintenance of DIO. We show that a predisposing reduction in leptin sensitivity, as measured by both the early anorectic response to leptin and cellular leptin sensitivity in the VMH/DMH, is more critical for the development of excessive DIO than diet-induced leptin resistance.

To conclude, the results described in this study indicate that individual leptin sensitivity on chow diet, during the first hour following leptin injection, predicts the susceptibility to DIO. Those rats with a pre-existing reduction in leptin sensitivity escalated their weight gain merely during exposure to a diet high in saturated fat and sugar. Therefore, the overabundance of readily available energy-dense food in today's society might be especially a risk factor for individuals with a pre-existing susceptibility to develop obesity. It would be interesting to test whether the feeding response to leptin is suitable as a biomarker for humans with an increased susceptibility to develop excessive obesity, as such that those identified as susceptible know that they should be very cautious with their diet and lifestyle in order to prevent the development of obesity.

Acknowledgements

We thank Diana van Tuijl, Inge Wolterink-Donselaar, Jos Brits, Harrie van der Eerden, and Henk Spierenburg for their practical assistance.

Conflict of interest

The authors declare that no competing interests exist.

References

1. Nguyen DM, El-Serag HB. The epidemiology of obesity. *Gastroenterol Clin North Am* 2010; **39**: 1-7.
2. Pandit R, Mercer JG, Overduin J, la Fleur SE, Adan RA. Dietary factors affect food reward and motivation to eat. *Obes Facts* 2012; **5**: 221-242.
3. Schwartz MW, Peskind E, Raskind M, Boyko EJ, Porte D,Jr. Cerebrospinal fluid leptin levels: relationship to plasma levels and to adiposity in humans. *Nat Med* 1996; **2**: 589-593.
4. Considine RV, Stephens TW, Nyce M, Ohannesian JP, Marco CC, McKee LJ, et al. Serum immunoreactive-leptin concentrations in normal-weight and obese humans. *The New England Journal of Medicine* 1996; **334**: 292.
5. Heymsfield SB, Greenberg AS, Fujioka K, Dixon RM, Kushner R, Hunt T, et al. Recombinant leptin for weight loss in obese and lean adults: a randomized, controlled, dose-escalation trial. *JAMA* 1999; **282**: 1568-1575.
6. Caro JF, Kolaczynski JW, Nyce MR, Ohannesian JP, Opentanova I, Goldman WH, et al. Decreased cerebrospinal-fluid/serum leptin ratio in obesity: a possible mechanism for leptin resistance. *Lancet* 1996; **348**: 159-161.
7. Apolzan JW, Harris RB. Rapid onset and reversal of peripheral and central leptin resistance in rats offered chow, sucrose solution, and lard. *Appetite* 2013; **60**: 65-73.
8. Myers MG,Jr. Leptin keeps working, even in obesity. *Cell Metab* 2015; **21**: 791-792.
9. Ottaway N, Mahbod P, Rivero B, Norman LA, Gertler A, D'Alessio DA, et al. Diet-induced obese mice retain endogenous leptin action. *Cell Metab* 2015; **21**: 877-882.
10. Lin L, Martin R, Schaffhauser AO, York DA. Acute changes in the response to peripheral leptin with alteration in the diet composition. *Am J Physiol Regul Integr Comp Physiol* 2001; **280**: R504-9.
11. Shapiro A, Tumer N, Gao Y, Cheng KY, Scarpace PJ. Prevention and reversal of diet-induced leptin resistance with a sugar-free diet despite high fat content. *Br J Nutr* 2011; **106**: 390-397.
12. Haring SJ, Harris RB. The relation between dietary fructose, dietary fat and leptin responsiveness in rats. *Physiol Behav* 2011; **104**: 914-922.
13. Scarpace PJ, Matheny M, Tumer N, Cheng KY, Zhang Y. Leptin resistance exacerbates diet-induced obesity and is associated with diminished maximal leptin signalling capacity in rats. *Diabetologia* 2005; **48**: 1075-1083.
14. Frederich RC, Hamann A, Anderson S, Lollmann B, Lowell BB, Flier JS. Leptin levels reflect body lipid content in mice: evidence for diet-induced resistance to leptin action. *Nat Med* 1995; **1**: 1311-1314.
15. Harris RB, Apolzan JW. Changes in glucose tolerance and leptin responsiveness of rats offered a choice of lard, sucrose, and chow. *Am J Physiol Regul Integr Comp Physiol* 2012; **302**: R1327-39.
16. van den Heuvel JK, Eggels L, van Rozen AJ, Luijendijk MC, Fliers E, Kalsbeek A, et al. Neuropeptide Y and leptin sensitivity is dependent on diet composition. *J Neuroendocrinol* 2014; **26**: 377-385.
17. Enriori PJ, Evans AE, Sinnayah P, Jobst EE, Tonelli-Lemos L, Billes SK, et al. Diet-induced obesity causes severe but reversible leptin resistance in arcuate melanocortin neurons. *Cell Metab* 2007; **5**: 181-194.
18. Enriori PJ, Sinnayah P, Simonds SE, Garcia Rudaz C, Cowley MA. Leptin action in the dorsomedial hypothalamus increases sympathetic tone to brown adipose tissue in spite of systemic leptin resistance. *J Neurosci* 2011; **31**: 12189-12197.
19. Mercer JG, Hoggard N, Williams LM, Lawrence CB, Hannah LT, Trayhurn P. Localization of leptin receptor mRNA and the long form splice variant (Ob-Rb) in mouse hypothalamus and adjacent brain regions by in situ hybridization. *FEBS Lett* 1996; **387**: 113-116.
20. Elmquist JK, Bjorbaek C, Ahima RS, Flier JS, Saper CB. Distributions of leptin receptor mRNA isoforms in the rat brain. *J Comp Neurol* 1998; **395**: 535-547.

21. Hakansson ML, Brown H, Ghilardi N, Skoda RC, Meister B. Leptin receptor immunoreactivity in chemically defined target neurons of the hypothalamus. *J Neurosci* 1998; **18**: 559-572.
22. Munzberg H, Flier JS, Bjorbaek C. Region-specific leptin resistance within the hypothalamus of diet-induced obese mice. *Endocrinology* 2004; **145**: 4880-4889.
23. Desai BN, Harris RB. An acute method to test leptin responsiveness in rats. *Am J Physiol Regul Integr Comp Physiol* 2014; **306**: R852-60.
24. Scarpace PJ, Zhang Y. Leptin resistance: a prediposing factor for diet-induced obesity. *Am J Physiol Regul Integr Comp Physiol* 2009; **296**: R493-500.
25. Bates SH, Stearns WH, Dundon TA, Schubert M, Tso AW, Wang Y, et al. STAT3 signalling is required for leptin regulation of energy balance but not reproduction. *Nature* 2003; **421**: 856.
26. Gao Q, Wolfgang MJ, Neschen S, Morino K, Horvath TL, Shulman GI, et al. Disruption of neural signal transducer and activator of transcription 3 causes obesity, diabetes, infertility, and thermal dysregulation. *Proc Natl Acad Sci U S A* 2004; **101**: 4661-4666.
27. Shapiro A, Mu W, Roncal C, Cheng KY, Johnson RJ, Scarpace PJ. Fructose-induced leptin resistance exacerbates weight gain in response to subsequent high-fat feeding. *Am J Physiol Regul Integr Comp Physiol* 2008; **295**: R1370-5.
28. Ruffin MP, Adage T, Kuipers F, Strubbe JH, Scheurink AJ, van Dijk G. Feeding and temperature responses to intravenous leptin infusion are differential predictors of obesity in rats. *Am J Physiol Regul Integr Comp Physiol* 2004; **286**: R756-63.
29. Levin BE, Dunn-Meynell AA. Reduced central leptin sensitivity in rats with diet-induced obesity. *Am J Physiol Regul Integr Comp Physiol* 2002; **283**: R941-8.
30. Steffens AB. A method of frequent sampling blood and continuous infusion of fluids in the rat without disturbing the animal. *Physiol.Behav.* 1969; **4**: 836.
31. Munzberg H, Huo L, Nillni EA, Hollenberg AN, Bjorbaek C. Role of signal transducer and activator of transcription 3 in regulation of hypothalamic proopiomelanocortin gene expression by leptin. *Endocrinology* 2003; **144**: 2121-2131.
32. la Fleur SE, van Rozen AJ, Luijendijk MC, Groeneweg F, Adan RA. A free-choice high-fat high-sugar diet induces changes in arcuate neuropeptide expression that support hyperphagia. *Int J Obes (Lond)* 2010; **34**: 537-546.
33. Levin BE, Dunn-Meynell AA, Banks WA. Obesity-prone rats have normal blood-brain barrier transport but defective central leptin signaling before obesity onset. *Am J Physiol Regul Integr Comp Physiol* 2004; **286**: R143-50.
34. Wilson JL, Enriori PJ. A talk between fat tissue, gut, pancreas and brain to control body weight. *Mol Cell Endocrinol* 2015; **418**: 108-119.
35. Zhou Y, Rui L. Leptin signaling and leptin resistance. *Front Med* 2013; **7**: 207-222.
36. Satoh N, Ogawa Y, Katsuura G, Hayase M, Tsuji T, Imagawa K, et al. The arcuate nucleus as a primary site of satiety effect of leptin in rats. *Neurosci Lett* 1997; **224**: 149-152.
37. Morton GJ, Niswender KD, Rhodes CJ, Myers MG,Jr, Blevins JE, Baskin DG, et al. Arcuate nucleus-specific leptin receptor gene therapy attenuates the obesity phenotype of Koletsky (fa(k)/fa(k)) rats. *Endocrinology* 2003; **144**: 2016-2024.
38. Levin BE, Dunn-Meynell AA, Ricci M., Cummings DE. Abnormalities of leptin and ghrelin regulation in obesity-prone juvenile rats. *Am J Physiol Endocrinol Metab* 2003; **285**: E949–E957.
39. Irani BG, Dunn-Meynell AA, Levin BE, 2007. Altered hypothalamic leptin, insulin and melanocortin binding associated with moderate fat diet and predisposition to obesity. *Endocrinology* 2007; **148:** 310–316.
40. Bouret SG, Gorski JN, Patterson CM, Chen S, Levin BE, Simerly R.B., 2008. Hypothalamic neural projections are permanently disrupted in diet-induced obese rats. *Cell Metab* 2008; **7:** 179–185.
41. Dodd GT, Worth AA, Nunn N, Korpal AK, Bechtold DA, Allison MB, et al. The thermogenic effect of leptin is dependent on a distinct population of prolactin-releasing peptide neurons in the dorsomedial hypothalamus. *Cell Metab* 2014; **20**: 639-649.
42. Rezai-Zadeh K, Yu S, Jiang Y, Laque A, Schwartzenburg C, Morrison CD, et al. Leptin receptor neurons in the dorsomedial hypothalamus are key regulators of energy expenditure and body weight, but not food intake. *Mol Metab* 2014; **3**: 681-693.
43. Minokoshi Y, Haque MS, Shimazu T. Microinjection of leptin into the ventromedial hypothalamus increases glucose uptake in peripheral tissues in rats. *Diabetes* 1999; **48**: 287-291.
44. Pandit R, Beerens S, Adan RAH. Role of leptin in energy expenditure: the hypothalamic perspective. *Am J Physiol Regul Integr Comp Physiol* 2017; **312**: R938-R947.
45. Turnbaugh PJ, Ley RE, Mahowald MA, Magrini V, Mardis ER, Gordon JI. An obesity-associated gut microbiome with increased capacity for energy harvest. *Nature* 2006; **444**: 1027-1031.
46. Schele E, Grahnemo L, Anesten F, Hallen A, Backhed F, Jansson JO. The gut microbiota reduces leptin sensitivity and the expression of the obesity-suppressing neuropeptides proglucagon (Gcg) and brain-derived neurotrophic factor (Bdnf) in the central nervous system. *Endocrinology* 2013; **154**: 3643-3651.
47. Park DY, Ahn YT, Park SH, Huh CS, Yoo SR, Yu R, et al. Supplementation of Lactobacillus curvatus HY7601 and Lactobacillus plantarum KY1032 in diet-induced obese mice is associated with gut microbial changes and reduction in obesity. *PLoS One* 2013; **8**: e59470.
48. Qasem RJ, Li J, Tang HM, Pontiggia L & D'mello AP (2016) Maternal protein restriction during pregnancy and lactation alters central leptin signalling, increases food intake, and decreases bone mass in 1 year old rat offspring. *Clin Exp Pharmacol Physiol* 43(4): 494-502.
49. Imbernon M, et al (2014) Hypothalamic KLF4 mediates leptin's effects on food intake via AgRP. Mol Metab 3(4): 441-451.

Supplementary data

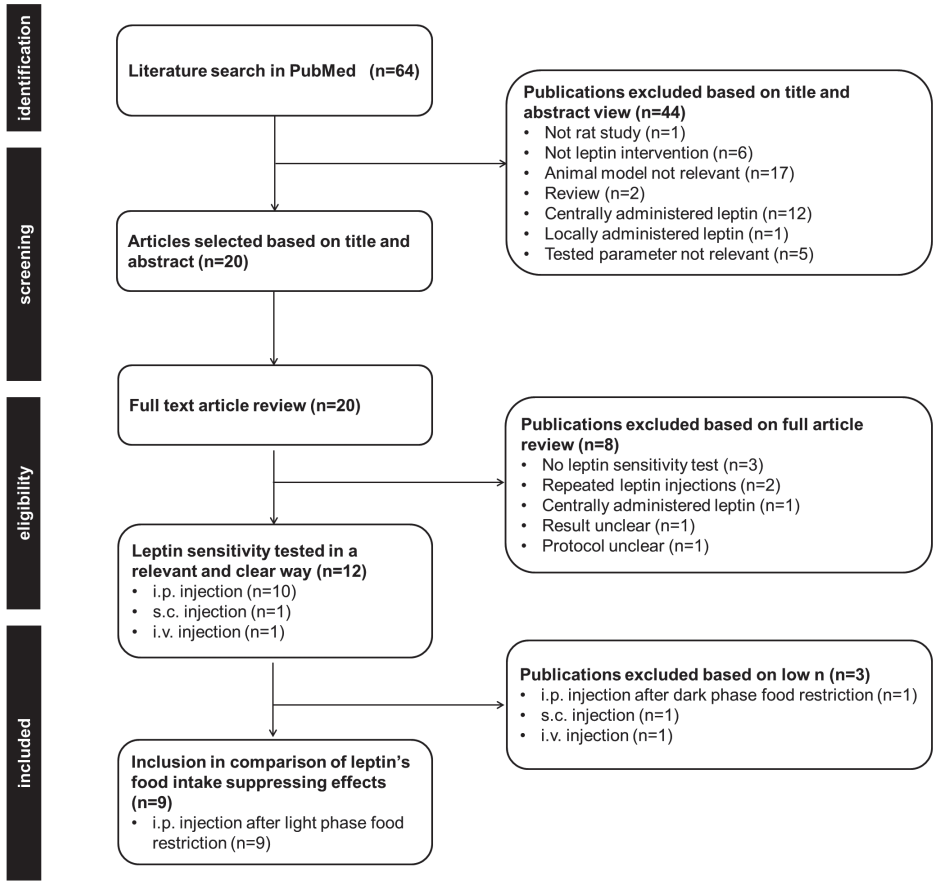

Figure S1. Flow chart of study selection in the systematic review of the timing of leptin's food intake suppressing effects.
i.p., intraperitoneal, s.c., subcutaneous, i.v., intravenous.

A

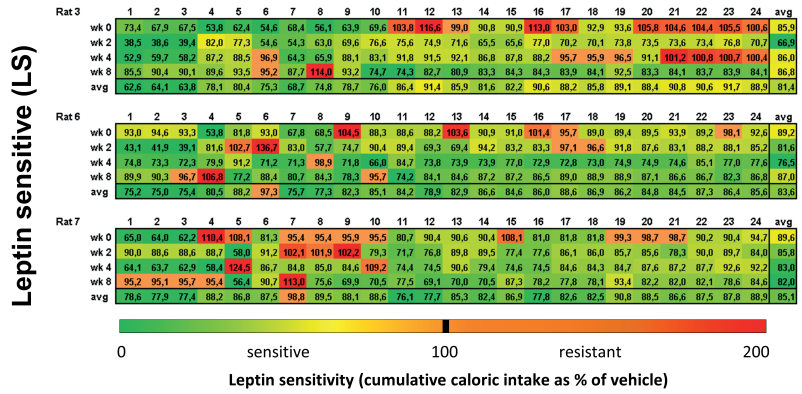

B

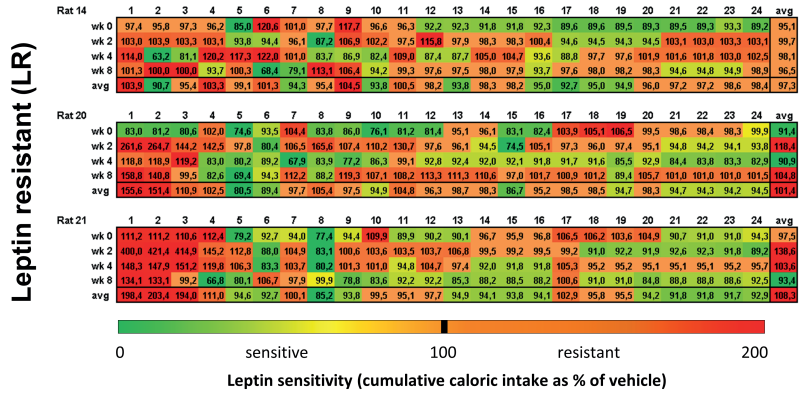

Figure S2. Heat plot examples of individual LS and LR rats on chow diet. For each subgroup of responders, three rats were randomly selected to show the stability of the response to leptin over weeks within a rat. Leptin sensitivity was measured by 1-24h cumulative food intake after leptin injection normalized to vehicle food intake. The response to leptin is shown for 4 independent tests (week 0, 2, 4, and 8 of the experiment), and for the average (avg) response. The heat plots indicate the relative degree of leptin sensitivity at a particular time point in comparison with the other time-points in the test (i.e. in a row).

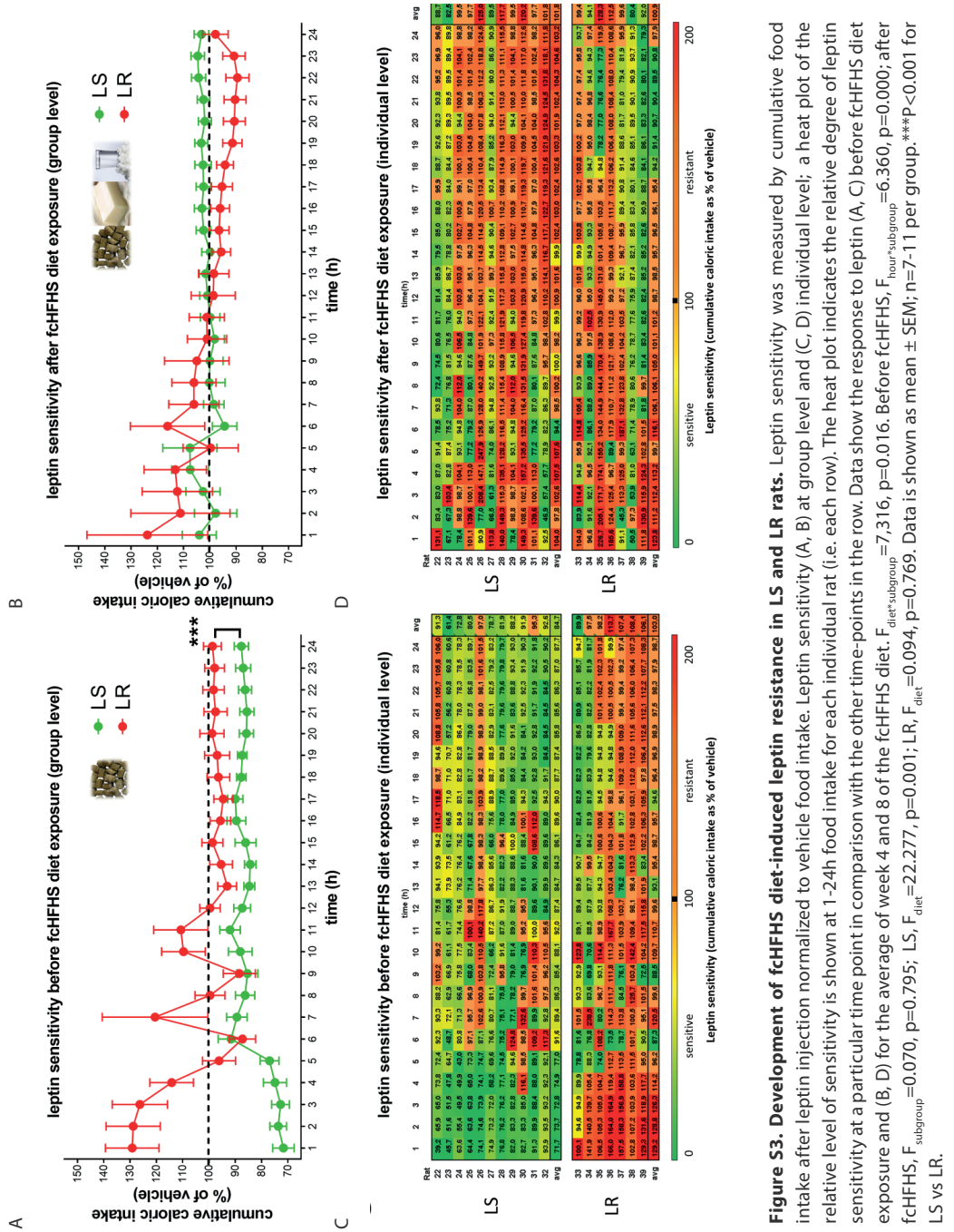

Figure S3. Development of fcHFHS diet-induced leptin resistance in LS and LR rats. Leptin sensitivity was measured by cumulative food intake after leptin injection normalized to vehicle food intake. Leptin sensitivity (A, B) at group level and (C, D) individual level; a heat plot of the relative level of sensitivity is shown at 1-24h food intake for each individual rat (i.e. each row). The heat plot indicates the relative degree of leptin sensitivity at a particular time point in comparison with the other time-points in the row. Data show the response to leptin (A, C) before fcHFHS diet exposure and (B, D) for the average of week 4 and 8 of the fcHFHS diet. $F_{diet*subgroup}$=6.360, p=0.000; after fcHFHS, $F_{subgroup}$=7,316, p=0.016. Before fcHFHS, $F_{diet*subgroup}$=0.070, p=0.795; LS, F_{diet}=22.277, p=0.001; LR, F_{diet}=0.094, p=0.769. Data is shown as mean ± SEM; n=7-11 per group.***P<0.001 for LS vs LR.

Table S1. Result of the systematic review of the timing of leptin's food intake suppressing effects.

Rat strain	Dose and type of leptin	Food restriction	Study design	Effect size per time-point (hour after food return)		Reference
Sprague-Dawley*	2 mg/kg (i.p.); source NA	8.00-18.00 h	Group (LS)	14h 24h	10.5-12.5% NA	7††
Sprague-Dawley*	2 mg/kg (i.p.); rat recombinant leptin	7.00-18.00 h (17.00h leptin injection)	Group (LS)	14h 24h 36h	22% NA 15%	15††
Sprague-Dawley*	2 mg/kg (i.p.); rat recombinant leptin	7.00-18.00 h (17.00h leptin injection)	Exp. 1) Group (LS) Exp. 2) Group#	Exp.1) 36h Exp. 2) 14h 24h 36h	7% 17,3% 14,6% 9,4%	23††
Sprague-Dawley†	2 mg/kg (i.p.); source NA	8.00-18.00 h (17.00 h leptin injection)	Group#	2h 14h 24h 38h	NA 12-30% NA 11,5%	12††
Sprague-Dawley‡	0.6 mg/kg (i.p.); source NA	9.00-16.30 h (16.30h leptin injection)	GroupII	24h	10,5-20%	11‡‡
Sprague-Dawley Exp. 1)* Exp. 2)§	0.6 mg/kg (i.p.) rat leptin (PeproTech)	9.00-16.30h (16.30h leptin injection)	Group**	Exp. 1) 2, 4, 15h 24h Exp. 2) 24h	 NA 18,9% 20.5%	27‡‡
Wistar*	1 mg/kg (i.p.); rat leptin	7.00-12.00 h (12.00h leptin injection)	Individual (LS)	2h 5, 24h	18-20% NA	16
Sprague-Dawley*	1 mg/kg (i.p.) leptin (PeproTech)	9.00-18.00h (17.45h leptin injection)	Group	2h 4h 6h 12h 24h	no effect 25% 25% 12,1% 15,2%	48
Sprague-Dawley*	1 mg/kg (i.p.) recombinant rat leptin	13.00-19:00h (16:00h leptin injection)	Group#	24h	17-21,7%	49

Overview of the feeding response to leptin in rats (study selection described in methods). Results are shown for the respective control diet groups (*chow; †low fructose; ‡sugar-free high-fat, §fructose free). In general, rats were tested at the group level (i.e. a comparison of the average cumulative food intake between the vehicle and leptin treated rats) or individual level (i.e. a group average of leptin-induced suppression from baseline vehicle for each individual rat). #Rats were injected with either leptin or vehicle; IIAll rats were injected with leptin on the day 1, and injected with vehicle on day 2; **All rats were injected with vehicle on day 1, and injected with leptin on day 2. Note the variability in the time-points at which the food intake response to leptin was measured, and the variability in the effect sizes. †† and ‡‡, studies were performed by the same research group, respectively. Exp., experiment; i.p., intraperitoneal administration; LS, latin-square design; NA, not available.

Table S2. Search strategy of the systematic review.

PubMed	
Component 1: leptin injection	leptin injection [Tiab] OR leptin injection [MeSH] OR leptin injections [Tiab] OR leptin injections [MeSH] OR leptin administration [Tiab] OR leptin administration [MeSH] OR leptin infusion [Tiab] OR leptin infusions [Tiab] OR leptin/kg [Tiab] OR peripheral* leptin [Tiab] OR peripheral leptin injection [Tiab] OR peripheral leptin injection [MeSH] OR exogenous administration of leptin [Tiab] OR exogenous administration of leptin [MeSH]
Component 2: diet	diet [Tiab]
Component 3: rat	rat [Tiab] or rats [Tiab]
Component 4: food intake/obesity	(Feeding response [Tiab] OR leptin responsiveness [Tiab] OR leptin responsive [Tiab] OR response to leptin [MeSH] OR leptin responses [Tiab] OR leptin inhibitory response [Tiab] OR food intake suppression [Tiab] OR appetite suppressing [Tiab] OR leptin's suppressive effects OR appetite depressants [Tiab] OR anorexic effect [Tiab] OR anorectic effect [Tiab] OR leptin sensitivity [Tiab] OR leptin sensitivity [MeSH] OR leptin sensitive [Tiab] OR leptin sensitive [Tiab] OR leptin resistance [Tiab] OR leptin insensitive [Tiab] OR leptin resistant [Tiab] OR leptin-resistant [Tiab]) AND (food intake [Tiab] OR food intake [MeSH] OR appetite [Tiab] OR appetite [MeSH] OR feeding [Tiab] OR eating behavior [Tiab] OR eating behavior [MeSH] OR eating behaviour [Tiab] OR eating behaviour [MeSH] OR energy intake [Tiab] or energy intake [MeSH]) AND (Obesity [Tiab] OR obesity [MeSh] OR metabolic syndrome [Tiab] or metabolic syndrome [Mesh] OR body weight [Tiab] OR body weight [MeSH])

Chapter 4:

Rats that are predisposed to excessive obesity show reduced (leptin-induced) thermoregulation before becoming obese

Kathy C.G. de Git[1], Johannes A. den Outer[1], Inge G. Wolterink-Donselaar[1], Mieneke C.M. Luijendijk[1], E. Schéle[2], Suzanne L. Dickson[2], Roger A.H. Adan[1,2]

1 Brain Center Rudolf Magnus, Dept. of Translational Neuroscience, University Medical Center Utrecht, Utrecht University, Utrecht 3584 CG, The Netherlands
2 Institute for Neuroscience and Physiology, The Sahlgrenska Academy at the University of Gothenburg, SE-405 30 Gothenburg, Sweden

Submitted

Abstract

Both feeding behavior and thermogenesis are regulated by leptin. The sensitivity to leptin's anorexigenic effects on chow diet was previously shown to predict the development of diet-induced obesity. In this study, we determined whether the sensitivity to leptin's anorexigenic effects correlates with leptin's thermogenic response, and if this response is exerted at the level of the dorsomedial hypothalamus (DMH), a brain area that plays an important role in thermoregulation. Based on the 1-hour feeding response to intravenously injected leptin on a chow diet, rats were divided into leptin sensitive (LS) and leptin resistant (LR) groups. The effects of leptin on core body, brown adipose tissue (BAT) and tail temperature were compared after intravenous versus intra-DMH leptin administration. After intravenous leptin injection, LS rats increased their BAT thermogenesis and reduced heat loss via the tail, resulting in a modest increase in core body temperature. The induction of these thermoregulatory mechanisms with intra-DMH leptin was smaller, but in the same direction as with intravenous leptin administration. In contrast, LR rats did not show any thermogenic response to either intravenous or intra-DMH leptin. These differences in the thermogenic response to leptin were associated with a 1°C lower BAT temperature and reduced UCP1 expression in LR rats under *ad libitum* feeding. The pre-existing sensitivity to the anorexigenic effects of leptin, a predictor for obesity, correlates with the sensitivity to the thermoregulatory effects of leptin, which appears to be exerted, at least in part, at the level of the DMH.

Introduction

Obesity rates continue to rise in adults and children [1], and there is a high and unexplained variability in the susceptibility for the development of obesity [2]. Like humans, several rat strains show individual differences in the susceptibility for the development of diet-induced obesity (DIO) [2, 3-5], which provides opportunities to study pre-existing vulnerability factors for DIO.

We [3] and others [2,4] previously showed that reduced sensitivity to leptin's anorexigenic effects is a pre-existing vulnerability factor for DIO. Based on the feeding response to exogenously injected leptin on a chow diet, we divided Wistar rats into leptin sensitive (LS) and leptin resistant (LR) groups [3]. LR rats were more prone to develop obesity on a free choice high-fat high-sucrose (fcHFHS) diet compared with LS rats, without eating more calories. In comparison to LS rats, LR rats showed a pre-existing reduction in the activation of leptin-induced signal transducer and activator of transcript 3 (pSTAT3), a marker for cellular leptin sensitivity [6, 7], in the dorsomedial hypothalamus (DMH) but not the arcuate nucleus (ARC). While similar pSTAT3 activation in the ARC in LS and LR rats may explain why LR rats did not eat more, it is still unclear how the pre-existing reduction in pSTAT3 activation in the DMH predisposes LR rats to exacerbated DIO.

Although there is evidence that leptin action in the DMH regulates energy balance by reducing food intake [8, 9 but see 10], leptin is particularly known to activate brown adipose tissue (BAT) thermogenesis via neurons in the DMH [8-12]. Several lines of evidence demonstrate a critical role for leptin signaling in the DMH in mediating BAT-dependent thermogenesis: 1) Injection of leptin directly into the DMH increased BAT temperature [9]; 2) Leptin-induced increases in BAT temperature were blocked by pre-injection of a leptin receptor antagonist directly into the DMH [9]; 3) Selective activation of the leptin receptor (LepRb) expressing neurons within the DMH increased BAT and core body temperature [10]; 4) Knock-out of LepRb in a specific population of DMH neurons, expressing prolactin-releasing peptide, blocked leptin-induced increases in UCP1 and core body temperature [8]. However, leptin regulation of core body temperature appears not to arise exclusively from BAT thermogenesis, as BAT temperature did not always precede and exceed the increase in core body temperature evoked by leptin receptor signaling [10]. More recently, it has been reported that, at least in ob/ob mice, systemic leptin injection leads to a pyrexic increase in core body temperature by reducing heat loss via the tail [13].

In the current study, we aimed to unravel whether rats that are less sensitive to the anorexigenic effects of peripherally injected leptin, also show a reduced thermogenic response to peripheral leptin. Further, to explore whether a reduced thermogenic response to peripheral leptin could be due to reduced cellular leptin signaling in the DMH (as opposed to, for example, impaired leptin transport across the blood-brain barrier), we compared leptin regulation of thermogenesis after intravenous and also after intra-DMH leptin injection between LS and LR rats fed regular chow. We also explored the contribution of BAT thermogenesis and heat loss via the tail to leptin's effect on core body temperature.

Methods

Animals

Adult male Wistar rats (Charles River, Sulzfeld, Germany) were individually housed in Plexiglas cages in a temperature controlled (21-23 °C) and light controlled (lights on between 08.00 and 20.00 h) room. Rats had *ad libitum* access to pelleted rat chow (3.31 kcal/g; Special Diet Service, UK) and tap water, unless otherwise stated. All experiments were performed in accordance with Dutch laws (Wet op de Dierproeven, 1996) and European regulations (Guideline 86/609/EEC) and were approved by the Animal Ethics Committee of Utrecht University.

Surgery

When the rats had reached a body weight of >300 g, they underwent surgery to implant: 1) Intra-arterial silicone catheters through the right jugular vein, according to the method of Steffens [14]; 2) Stainless steel guide cannulas (26 GA, 9 mm; Plastics One, Roanoke, USA) bilaterally above the DMH (1 mm above the DMH, from bregma: anterior-posterior: -2.50, medio-lateral: ±2.10, dorso-ventral: -8.60, at an angle of 10°, Paxinos and Watson, 1998, fourth edition). Cannulas were fixed to the skull with stainless steel screws and dental cement; 3) An intra-abdominal dual transmitter (TL11M3F40-TT, Data Science International (DSI), USA) with temperature-sensing leads to the portal vein in the liver and interscapular BAT.

Selection of leptin sensitive vs leptin resistant rats

To divide rats into two types of leptin responders, leptin sensitivity of each individual rat was determined twice, and the average response was taken. Rats were divided into two subgroups based upon their average feeding response at 1hr after leptin injection, as the variability was largest at this time-point. Rats showing a reduction in food intake (percentage suppression <100) were designated as LS, whereas rats showing no reduction or even an increase in food intake were designated as LR (percentage suppression ≥100) [3].

Telemetric measurements

The home cage was placed on a receiver plate (DSI, USA) that received radiofrequency signals from the abdominal transmitter. The plate was connected to software (DSI) that recorded core body temperature, BAT temperature, and locomotor activity every 2 minutes. In 5 rats, the battery of the transmitters was empty before the end of the experiment. These rats were therefore excluded from the telemetric measurements from the time-point of the empty battery onwards.

To test the effect of leptin on body temperature, rats were food restricted for two consecutive days (10 gr chow per day at 16.00h). The next morning at 9.00h, leptin or vehicle was injected according to a Latin square design. Two hours later food was given back, and 24h food intake was measured. The interval between the two test days of a Latin square design was 7-10 days. The effect of intravenous and intra-DMH leptin (recombinant murine leptin, NHPP, USA) on body temperature was tested with two independent Latin square designs. For intravenous injections, leptin (250 µg / 250 µl) or vehicle (phosphate buffered saline, PBS) was injected via the jugular vein cannula. Intra-DMH leptin injections were performed through an injector (10 mm, 33GA, Plastic One) inserted into the guide cannula. Bilateral infusions (300 ηg leptin / 300 ηl PBS over one minute) were performed using a syringe pump with the injectors left in place for another minute to prevent backflow.

Thermosensitive camera

During test days, the impact of leptin on tail temperature was examined by using a FLIR infrared/thermal camera (E60bx: Compact-Infrared-Thermal-Imaging-Camera; FLIR; West Malling, Kent, UK) (Figure 1A).

Post-mortem analysis

The analysis of cannula placement revealed uni- or bilateral DMH cannula(s) misplacement in 5 rats. These rats were excluded from the intra-DMH analyses.

The placement of the transmitter leads to the liver and interscapular BAT was also checked after sacrifice. All liver probes were placed correctly, but the BAT probe was misplaced in 7 rats. These rats were therefore excluded from the BAT temperature analysis. BAT tissue was dissected and stored for subsequent UCP1 analysis (see supplementary text).

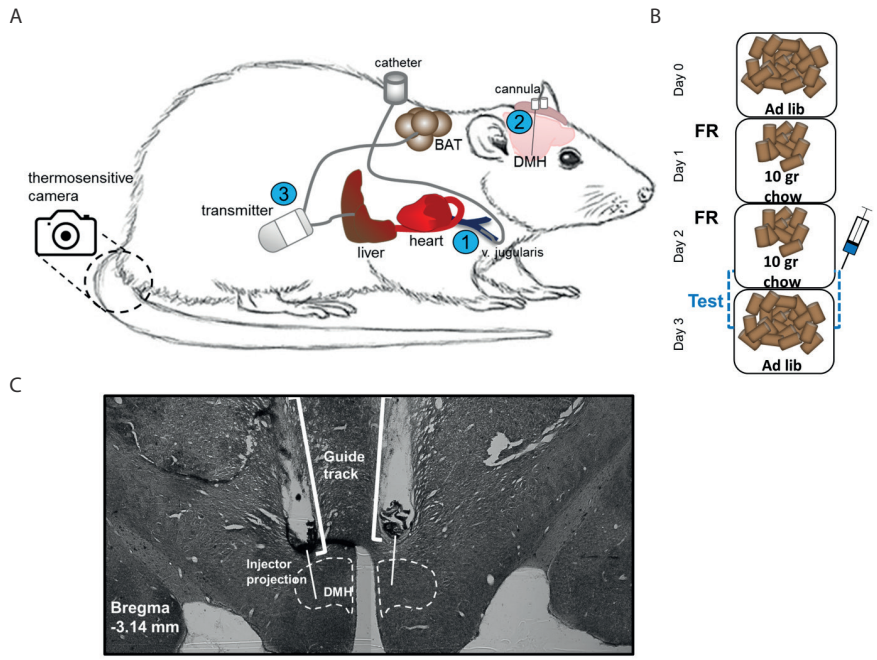

Figure 1. Animal model and experimental design. (A) Rats underwent surgery to implant: 1) A catheter in the jugular vein; 2) Local cannulas bilaterally above the DMH; 3) An intra-abdominal telemetric transmitter with probes in the liver and brown adipose tissue (BAT). An infrared/ thermosensitive camera was used to measure the tail base temperature. The region of interest for the tail base is indicated. (B) The thermogenic response to leptin was tested both via systemic injections through the jugular catheter (250 ug, i.v), and local infusions in the DMH (bilateral, 300 ng/300 nl/60sec). Rats were food restricted prior to injections to lower their body temperature. (C) Example of the anatomical verification of correctly placed DMH cannulas.

Statistical analysis

For differences in body temperature, activity, body weight, and caloric intake, two-way repeated measures ANOVAs were performed with time as within-subject variable and responder (LS/LR) as between-subject variable. BAT UCP1 expression levels were compared between LS and LR rats with an independent t-test. For fat mass analysis, a one-way ANOVA was performed with responder (LS/LR) as a between-subject variable. Feeding responses to leptin were assessed using a three-way repeated measures ANOVA with time and treatment as within-subject variables and responder (LS/LR) as between subject-variable. Thermogenic responses to leptin were assessed using a two-way ANOVA on the average data of temperature in the absence and the presence of food, respectively, with treatment as within-subject variable and responder as between subject-variable.

Mauchly's test of sphericity was used to test whether variances of the differences between treatment levels were equal. If the assumption of sphericity was violated, degrees of freedom were corrected using Greenhouse-Geisser (GG) estimates of sphericity or Huynh-Feldt estimates of sphericity when the GG estimate was >0,75. When appropriate, post hoc analyses were conducted using Student's t-tests or pairwise Bonferroni comparisons. Each parameter was tested for normality with the Kolmogorov-Smirnov test. When data were not normally distributed, data were log transformed prior to statistical analyses.

Statistical analyses were conducted using SPSS 20.3 for Windows. The threshold for statistical significance was $P<0.05$. The effects of leptin on thermoregulation were tested with one-sided post-hoc t-tests, as leptin is generally accepted to increase body temperature [8-10] and was shown to reduce tail temperature [13]. The main effects of responder on daily BAT and core body temperature, and BAT UCP1 levels were also tested one-sided, as we expected lower temperatures and UCP1 levels in LR rats. Data are presented as mean ± SEM.

Additional details regarding methods can be found in supplementary information.

Results

Distinguishing two types of leptin responders on a chow diet

Rats were divided into leptin sensitive (LS, n=10) and leptin resistant (LR, n=11) groups based on their feeding response to leptin injection, normalized to baseline vehicle, at the first hour following injection (Figure 2B,C), as described previously [3]. The selection of LS and LR rats was based on the average leptin sensitivity of two independent leptin sensitivity tests (Figure 2A). The food intake response to leptin at 1h after injection ranged from -39,4% to -9,0% (-23,8%±3,1) in LS rats and from +0,7% to +98,6% (+40,6%±16,6) in LR rats. Further inspection of the leptin sensitivity patterns of LS and LR rats at 2-24h following leptin injection revealed that LS and LR rats also differ in their leptin sensitivity at later time-points, especially at 2-5 hours following injection (Figure 2B,C). LS rats significantly reduced their food intake following leptin injection at almost all time-points. In contrast, LR rats did not show a leptin-induced reduction in food intake over 24h following injection (Figure 2B,C).

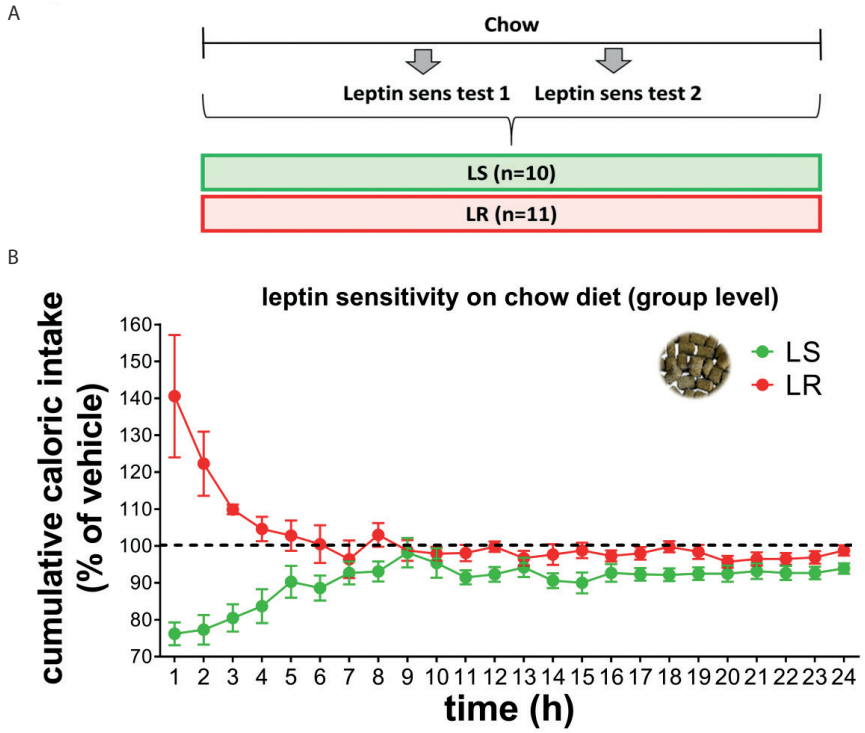

< Figure 2. Individual 1-24h leptin sensitivity in LS and LR rats fed a chow diet. Rats were divided into those showing a reduction in food intake during the first hour after intravenous leptin injection (leptin sensitive, LS) and those that did not change or increased their food intake with intravenous leptin at 1h food intake (leptin resistant, LR). (A) Experimental design. Leptin sensitivity was measured by cumulative food intake after leptin injection normalized to vehicle food intake. Average leptin sensitivity of 2 tests is shown. Leptin sensitivity (B) at group level and (C) individual level; a heat plot of the relative level of sensitivity is shown at 1-24h food intake for each individual rat (*i.e.* each row). The heat plot indicates the relative degree of leptin sensitivity at a particular time point in comparison with the other time-points in the row. 1-24h: $F_{hour*treatment*responder}$=8.619, p<0.001. Post hoc responder: p<0.05 at 1-5, 8, 11, 12, 15, 17-19 and 24h. LS, $F_{treatment*hour}$=4.391, p<0.001; $F_{treatment}$=54,644, p<0.001. Post hoc treatment: p<0.05 at 1-8h, and at 11-24h. LR, $F_{treatment*hour}$=5.568, p<0.001; $F_{treatment}$=1.016. p=0.337. Data are shown as mean ± SEM; n=10-11 per group.

In accordance with our previous findings [3], the distinct leptin sensitivity patterns in LS vs LR rats were not associated with differences in body weight, caloric intake, and adiposity on a chow diet (Figure S1). The increased susceptibility for the development of obesity in LR rats was previously specifically shown after exposure to an obesogenic fcHFHS diet [3].

There is evidence that leptin signaling in the DMH mediates food intake [8, 9]. We therefore compared the feeding response to leptin after intravenous versus intra-DMH injection (Figure S2A-C). The DMH was not critically involved in leptin regulation of food intake suppression. This finding is in accordance with the contradictory effects of leptin signaling in the DMH on food intake in previous studies [8, 9 versus 10]. Since leptin action in the DMH has been shown to regulate energy balance particularly by increasing energy expenditure [8-10], we next focused on the comparison of (leptin regulation of) thermoregulation between LS and LR rats.

LR rats show lower BAT thermogenic capacity

We implanted intra-abdominal transmitters with probes to the liver (core body temperature) and BAT (Figure 1A), to compare thermogenesis under distinct feeding conditions (*i.e. ad libitum* feeding, food restriction, and refeeding) (Figure 3A). During *ad libitum* feeding, LR rats showed a trend for a reduction in BAT temperature compared with LS rats (Figure 3A, Table S1). Both during the light and dark phase, the absolute difference in BAT temperature between LS and LR rats was large, as BAT temperature of LR rats was on average 1.0±0.2°C lower (dark: LS 38.5±0.61°C vs LR 37.3±0.39°C; light: LS 37.8±0.43°C vs LR 36.8±0.39°C). We also challenged rats by food restricting (FR) them for two days by giving them 10 grams of chow overnight (*i.e.* half of the normal amount of food intake) (Figure 3A). LS rats gradually reduced their BAT temperature during FR, reaching their lowest body temperature at 9.00h (1h into the light phase) after two days of FR. At this time-point, BAT temperature

A

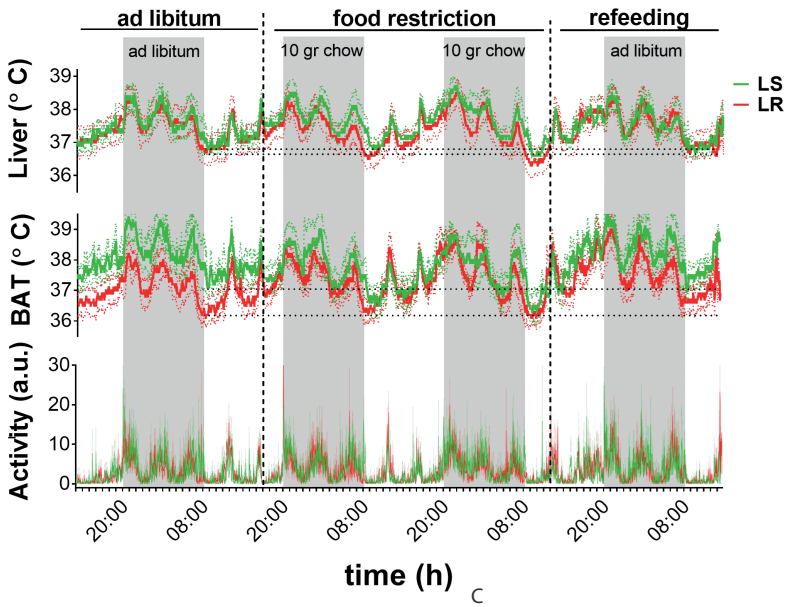

B

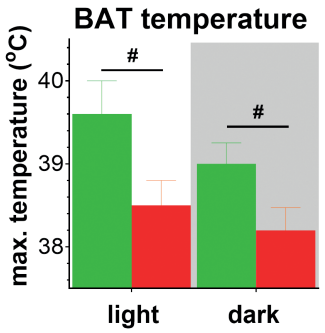

C

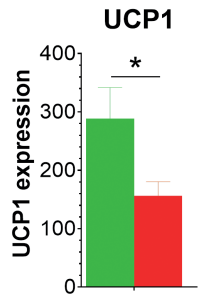

Figure 3. Comparison of core body and BAT temperature between LS and LR rats. (A) Core body (liver) temperature, BAT temperature, and locomotor activity during ad libitum feeding, food restriction (10 grams of chow overnight for two days), and refeeding in LS versus LR rats. For statistics, see Table S1 and S2. Data are shown as mean ± SEM. The dotted lines show the SEM. N=3-5 for LS rats and n=5-6 for LR rats. (B) Maximal BAT temperature in the light and dark phase in LS versus LR rats during ad libitum feeding. For each rat, the average of the five highest BAT temperatures during ad libitum feeding was taken during the light phase and dark phase, respectively. F_{light}=2.377, p=0.084; F_{dark}=2.203, p=0.091. Data are shown as mean ± SEM; n=3 for LS rats and n=5 for LR rats. #P=0.08-0.09 in LS vs LR rats. The shaded areas indicate the dark phase. (C) BAT UCP1 mRNA expression (2^-(Δ cycle threshold) with Hmbs as reference gene) in LS versus LR rats. Data are shown as mean ± SEM; n=4 per group; t=2.260, *p=0.033.

was reduced from 37.4±0.47°C during *ad libitum* feeding to 36.4±0.41°C at FR day 2 (t=5.182, p=0.035). In contrast to LS rats, LR rats did not reduce their BAT temperature during food restriction, as BAT temperature at 9.00h was 36.4±0.39°C during *ad libitum* feeding and 36.2±0.36°C at FR day 2 (t=2.998, p=0.096). These findings suggest that the minimal BAT temperature in both LS and LR rats was around 36.2-36.4°C. Perhaps LR rats did not further reduce their BAT temperature during FR because their BAT temperature was already low during *ad libitum* feeding, which suggests that BAT of LR rats shows a lower thermogenic capacity. Indeed, analysis of the maximal BAT temperature in LS versus LR rats revealed that LR rats show a trend for a lower maximal BAT temperature during both the light phase (LS 39.6±0.39°C vs LR 38.5±0.31°C) and the dark phase (LS 39.0±0.25°C vs LR 38.2±0.28°C) when *ad libitum* fed (Figure 3B). In accordance, LR rats showed significantly lower mRNA expression levels of uncoupling protein 1 (UCP1) in BAT tissue compared with LS rats (Figure 3C), and UCP1 expression levels strongly correlated with maximal BAT temperature in both the light phase and the dark phase (R2≥0.994, p≤0.049). Refeeding increased BAT temperature in both LS and LR rats, and the difference in BAT temperature between LS and LR rats gradually reinstated over time from 0.5 °C during light phase 1, to 0.7 °C during dark phase 1, and 0.8 °C during light phase 2 (Figure 3A, Table S1).

The large absolute differences in BAT temperature between LS and LR rats when *ad libitum* fed did not result in significant differences in core body (liver) temperature between LS and LR rats (Figure 3A, Table S1). However, LR rats showed a non-significant reduction of 0.3±0.2°C in core body temperature compared with LS rats during FR (average temperature LS 37.6±0.25°C vs LR 37.3±0.45°C). LS and LR rats both significantly reduced their core body temperature after two days of FR (9.00h during *ad libitum* feeding vs FR day 2, LS: 36.9±0.32°C vs 36.7±0.21°C, t=4.265, p=0.05; and LR: 36.9±0.41°C vs 36.3±0.46°C, t=7.527, p=0.002). So, both LS and LR rats reduced their core body temperature during restricted food availability, probably to conserve energy. However, the mechanism by which they reduce their body temperature differs, as LS but not LR rats strongly reduce their BAT thermogenesis during FR. Locomotor activity followed a similar circadian pattern as BAT and core body temperature, but did not differ between the LS and LR groups (Figure 3A, Table S2), suggesting that the temperature differences between these groups were independent of locomotor activity.

LR rats are resistant to the thermogenic effects of intravenous leptin

Leptin is known to robustly increase body temperature in states of low leptin levels, like fasting [10, 15, 16]. In order to compare leptin regulation of thermogenesis between LS

and LR rats, rats were food restricted for two consecutive days, and leptin was injected around 9.00h at FR day 2, as this was the time-point at which body temperature was lowest in both LS and LR rats (Figure 1B, 3A). Leptin-induced thermogenesis was tested both in the absence of food and after the food was returned (refeeding). We also tested leptin-induced heat loss via the tail by measuring tail base temperature with an infrared/thermal camera (Figure 1A).

In the absence of food, LS rats showed a tendency for a different BAT and tail base temperature response to intravenous leptin compared with LR rats (Figure 4C-F). LS rats showed a significant leptin-induced increase in BAT temperature (Figure 4C,D) and a significant reduction in tail base temperature (Figure 4E,F) compared to vehicle, indicating that thermoregulation in LS rats is leptin sensitive. The activation of these leptin-induced thermoregulatory mechanisms in LS rats caused a slight rise in core body temperature (+0.2ºC) (Figure 4A,B), that did not reach statistical significance. After returning the food, LS rats showed a significantly different BAT temperature response to leptin compared with LR rats (Figure 4D). Only LS rats showed a trend for a leptin-induced increase in BAT temperature, that was greater in magnitude than in the absence of food (average change in BAT temperature with leptin compared to vehicle after food return +1.2ºC versus +0.6ºC before food return), and was accompanied by a non-significant increase in core body temperature of +0.6ºC. In contrast to LS rats, LR rats did not show any effect of leptin on BAT, tail base, and core body temperature (Figure 4A-F), which indicates that LR rats are not only resistant to leptin's anorexigenic effects, but also to leptin's thermoregulatory effects. The differences in body temperature regulation by leptin in LS versus LR rats were independent of locomotor activity (Figure S3).

LR rats show defective temperature regulation in the DMH

We used the same approach to that used for intravenous leptin to compare the effects of intra-DMH leptin injection on body temperature in the two groups. LS and LR rats did not significantly differ in the effect of leptin on core body temperature (Figure 5A,B), BAT temperature (Figure 5C,D), tail base temperature (Figure 5E,F), and locomotor activity (Figure S4), in either the absence or presence of food. Closer inspection of the thermoregulatory effects of leptin in LS rats in the absence of food, revealed that the direction of the effect of leptin on BAT and tail base temperature was similar compared with that after intravenous injection, but the effect sizes were smaller (intra-DMH vs intravenous leptin injection, BAT: 0.3ºC vs 0.6ºC; tail base: -1.2ºC vs -0.5ºC). The smaller effect of intra-DMH leptin on thermoregulatory mechanisms resulted in a similar trend for an increase in core body temperature as with intravenous leptin (both +0.2 ºC), which suggests that the thermoregulatory

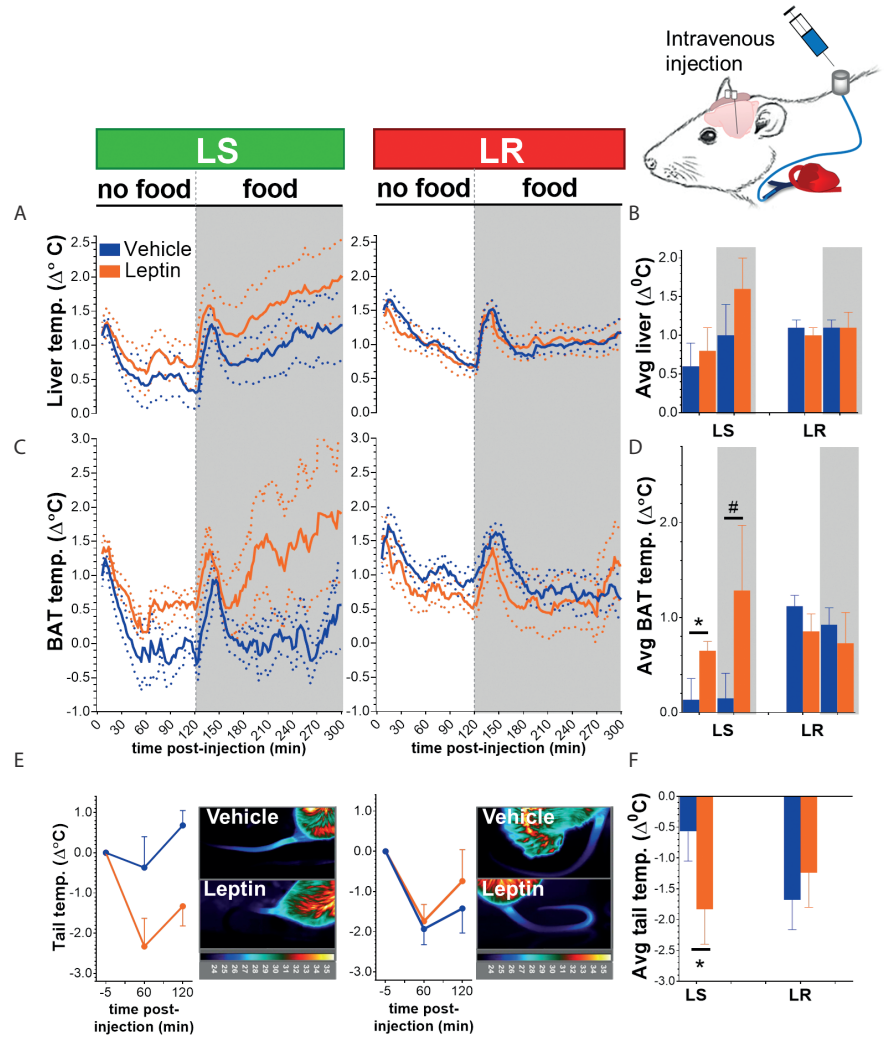

Figure 4. Comparison of leptin regulation of thermogenesis between LS and LR rats after intravenous leptin administration. (A) Continuous and (B) average change in core body (liver) temperature after intravenous leptin/vehicle injection in LS (n=5) vs LR rats (n=9), in the presence and absence of food. Without food: $F_{treatment*responder}$=1.441, p=0.107; with food: $F_{treatment*responder}$=2.945, p=0.112. (C) Continuous and (D) average change in BAT temperature after intravenous leptin/vehicle injection in LS (n=3) vs LR rats (n=6), in the presence and absence of food. Without food: $F_{treatment*responder}$=4.218, p=0.079. Post-hoc in LS and LR separately: LS t=-3.474, p=0.037; LR t=1.052, p=0.171. With food: $F_{treatment*responder}$=7.961, p=0.026. Post-hoc in LS and LR separately: LS t=-2.632, p=0.06; LR t=0.760, p=0.240. (E) Change in tail base temperature and representative temperature images after intravenous leptin/vehicle injection in LS (n=9) vs LR (n=11) rats in the absence of food. Thermal images were taken shortly before injection, and at 60 and 120 min. post-injection. (F) Average change in tail base temperature. $F_{treatment*responder}$=3.718, p=0.074. Post hoc in LS and LR separately: LS t=2.086, p=0.041; LR t=-0.791, p=0.226. Data are shown as mean ± SEM. The dotted lines show the SEM. *P<0.05, #P=0.06 for leptin vs vehicle. The shaded areas indicate measurements in the presence of food.

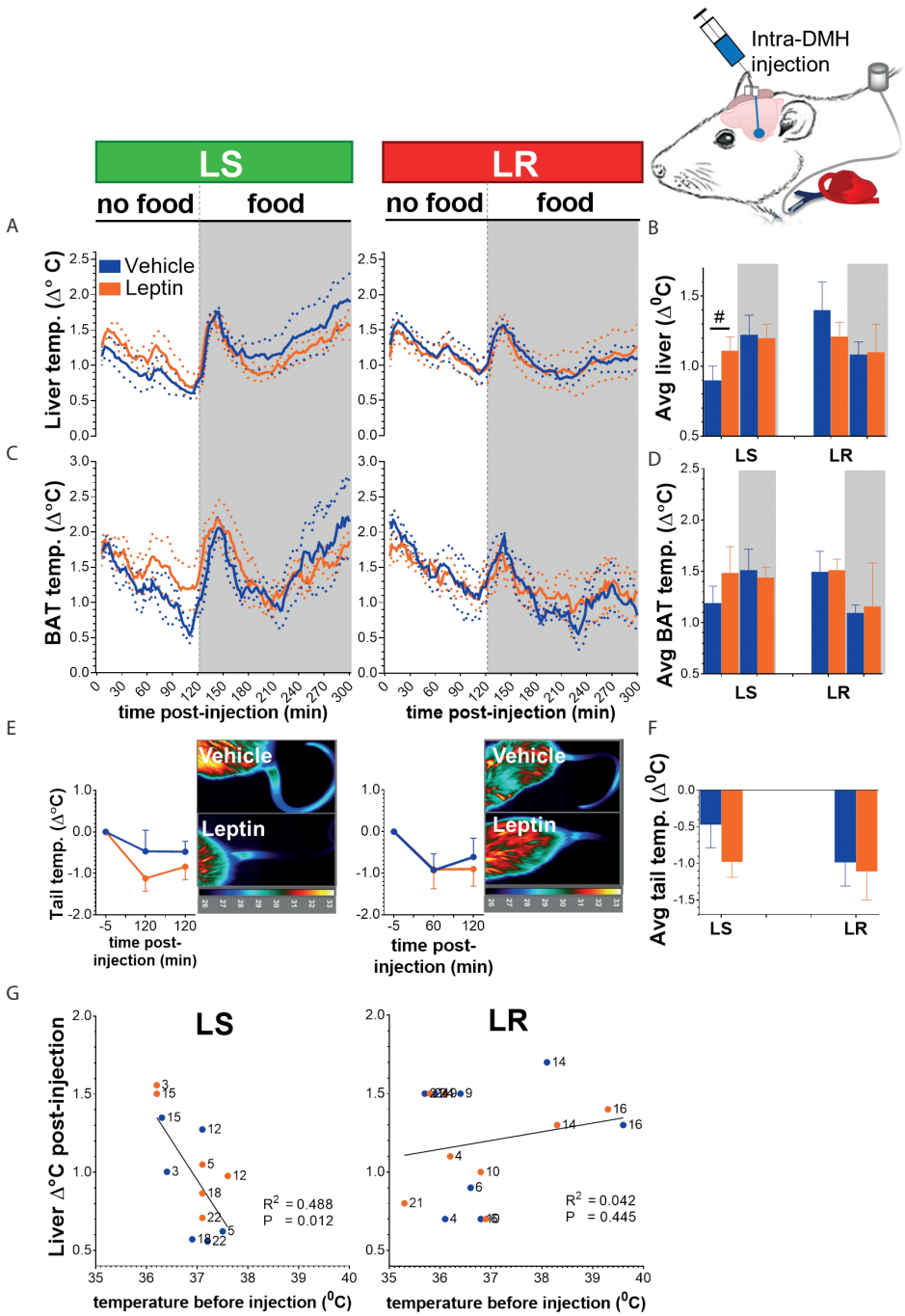

< Figure 5. Comparison of leptin regulation of thermogenesis between LS and LR rats after intra-DMH leptin administration. (A) Continuous and (B) average change in core body (liver) temperature after intra-DMH leptin/vehicle injection in LS (n=6) vs LR rats (n=9), in the presence and absence of food. Without food: $F_{treatment*responder}$=1.973, p=0.186; with food: $F_{treatment*responder}$=0.389, p=0.544. (C) Continuous and (D) average change in BAT temperature after intra-DMH leptin/vehicle injection in LS (n=4) vs LR rats (n=4), in the presence and absence of food. Without food: $F_{treatment*responder}$=2.214, p=0.187; with food: $F_{treatment*responder}$=0.009, p=0.928. (E) Change in tail base temperature and representative temperature images after intra-DMH leptin/vehicle injection in LS (n=9) vs LR (n=10) rats in the absence of food. Thermal images were taken shortly before injection, and at 60 and 120 min. post-injection. (F) Average change in tail base temperature. $F_{treatment*responder}$=0.273, p=0.608. (G) Correlation between core body temperature before injection and delta change in core body temperature 0-2h following injection of leptin (orange) or vehicle (blue). LS, R2=0.488, p=0.012, and LR, R2=0.042, p=0.445. Data are shown as mean ± SEM. The dotted lines show the SEM. #P=0.07 for leptin vs vehicle. The shaded areas indicate measurements in the presence of food.

responses evoked by enhanced leptin signaling in the DMH are more effective in modulating core body temperature than those evoked by systemic induction of leptin signaling. LR rats did not show any increase in BAT and core body temperature or a reduction in tail base temperature with intra-DMH leptin (Figure 5A-F), suggesting that leptin resistance in the DMH could contribute to the failure of leptin to affect thermoregulation in LR rats.

We noticed that core body temperature before injection was very variable between (but not within) individual rats, as it ranged from 36.1-37.2ºC in LS rats to even 35.3-39.6ºC in LR rats before intra-DMH injection (Figure 5G). Since leptin has been suggested to have a permissive rather than active thermogenic effect [12, 15, 16], we compared baseline core body temperature with delta temperature change after leptin and vehicle injection. In LS rats, we found a significantly negative correlation between body temperature before injection, and delta temperature change following intra-DMH injection (Figure 5G), indicating a reduced temperature response when core body temperature was relatively high before injection. All individual LS rats, except for one, showed a larger delta temperature change with leptin compared with vehicle. In contrast, LR rats did not show a correlation between core body temperature before injection and delta temperature change after leptin injection, illustrating a defect in the coupling between core body temperature and the facilitation of thermoregulatory mechanisms by leptin.

Discussion

As in humans, rats show high variability in the susceptibility to develop obesity [3-5, 17]. Based on the feeding response to leptin on a chow diet, rats were divided into leptin sensitive (LS) and leptin resistant (LR) groups. LS rats showed a thermogenic response to leptin, which appears to be exerted, at least in part, at the level of the DMH. In contrast, LR rats did not show any thermogenic response to leptin, thereby linking their pre-existing reduction in pSTAT3 activation in the DMH [3] to impaired leptin regulation of thermogenesis.

Leptin is thought to influence BAT thermogenesis in a permissive manner rather than being actively thermogenic, *i.e.* it probably signals the availability of lipid and glucose fuel supplies for oxidation in BAT, and acts through LepRb to enhance the excitability of neurons controlling BAT activity, thereby facilitating BAT activation [12, 15, 16]. Therefore, resistance to leptin likely contributes to the 1°C lower basal BAT temperature, the lower maximal BAT temperature, and the lower BAT UCP1 levels in LR rats compared with LS rats under *ad libitum* feeding. During food restriction, circulating leptin levels are low, which may result in lower BAT activity [10, 15, 16]. A reduction in BAT thermogenesis was indeed observed in LS but not LR rats during food restriction, which was restored during refeeding. Perhaps BAT temperature was already at its lowest point during *ad libitum* feeding in LR rats due to leptin resistance. Since BAT thermogenesis has the capacity to prevent excess body weight gain in response to an obesogenic diet [12], the pre-existing reduction in BAT thermogenesis in LR rats likely predispose them to exacerbated obesity on a fcHFHS diet.

Besides compelling evidence for a BAT-dependent thermogenic increase in core body temperature with leptin [9, 10, 18-20], leptin was recently shown to lead to a pyrexic increase in core body temperature by reducing heat loss via the tail in ob/ob mice, without affecting BAT thermogenesis [13]. After intravenous leptin injection, LS rats significantly increased their BAT thermogenesis and reduced their heat loss via the tail, resulting in a modest increase in core body temperature. This phenomenon has been observed previously for BAT thermogenesis [9]. BAT temperature was proposed to be a more sensitive marker for the sympathoexcitatory effects of leptin than total body temperature [9]. Rather than one fixed body temperature set point, different thermoregulatory mechanisms (such as BAT thermogenesis and tail vein constriction) may have different thresholds that need not be synchronized [21].

Using a variety of approaches, leptin action in the DMH has previously been shown to play a critical role in BAT-dependent thermogenesis [8-10]. In the absence of food, we found a small, non-significant increase in BAT temperature with intra-DMH leptin in LS rats. Enriori et al. also tested the effect of intra-DMH leptin injection on BAT temperature, and found a potent induction of BAT thermogenesis [9]. We speculate that differences in injection volume may explain the discrepancy with the above described results of Enriori et al., as they injected 0.5 µl (0.2 µg/µl) leptin into the DMH of mice, whereas we injected 0.3 µl (1 µg/µl) leptin into the DMH of rats. Leakage of leptin into surrounding hypothalamic nuclei, which were also shown to mediate the effect of leptin on BAT activation [9, 16, 22], could explain the stronger effect of leptin on BAT thermogenesis in mice in the study of Enriori et al. Even though the effects of intra-DMH leptin on BAT and tail temperature were small in LS rats, they were in the same direction as with intravenous leptin, and led to a similar trend for an increase (+0.2°C) in core body temperature. This suggests that the thermoregulatory mechanisms activated by leptin signaling in the DMH are more directly aimed at increasing core body temperature. Alternatively, as leptin may permissively increase core body temperature until the body temperature set point is achieved [12, 15, 16], the thermoregulatory mechanisms evoked by intra-DMH leptin may have been sufficient to raise core body temperature to this set point. As such, the larger thermoregulatory changes in BAT and tail temperature with intravenous leptin did not further raise core body temperature compared to that with intra-DMH leptin, as small thermoregulatory changes were sufficient to achieve the body temperature set-point.

One limitation of this study is the difference in group size and the low number of animals in the LS group. The LR rats, being the larger group, did not show any thermogenic response to leptin. Since we found the distinction in leptin sensitivity between LS and LR rats both at the level of food intake and thermogenesis, we believe that the thermogenic effects we observed in LS rats are valid. For intra-DMH injections, we showed that LS rats were less capable of increasing their core body temperature with leptin when their body temperature was relatively high before injection. Although this correlation nicely demonstrates that leptin permissively increases core body temperature in LS rats until the set point for core body temperature is achieved, it also explains the large variability in the thermogenic response to leptin between rats. The finding that LR rats did not show a coupling between baseline core body temperature and the temperature response to intra-DMH leptin, further supports impaired thermoregulation by leptin signaling in the DMH in LR rats.

To conclude, our study shows that leptin increases BAT thermogenesis and reduces heat loss via the tail in LS rats. LR rats show a pre-existing resistance to these thermoregulatory effects of leptin, which seems to be mediated via leptin resistance exerted, at least in part, at the level of the DMH. This resistance may explain the lower BAT capacity under *ad libitum* feeding which may, in turn, predispose LR rats to exacerbated obesity when exposed to an obesogenic fcHFHS diet. Future studies are necessary to determine whether LR rats are indeed not able to sufficiently adapt their BAT thermogenesis to the increased caloric intake on a fcHFHS diet, and whether this is the mechanism by which they become excessively obese. Altogether, these data illustrate that reduced leptin regulation of thermogenesis may be a mechanism that explains how a pre-existing reduction in leptin sensitivity in the DMH predisposes rats to exacerbated obesity.

Declaration of interest

The authors declare that they have no conflict of interest.

Funding agencies

This research was primarily supported by the Dutch Technology Foundation STW (grant 12264 to RAHA), which is part of the Netherlands Organisation for Scientific Research (NWO), and which is partly funded by the Ministry of Economic Affairs. It was also supported by the European Union's Seventh Framework programme for research, technological development and demonstration under grant agreement no. 607310 (Nudge-it to RAHA and SLD) and by the Swedish Research Council (2016-20195 to SLD).

Acknowledgments

We thank Susanne la Fleur for critically proofreading our manuscript, and Robin van Kempen for practical assistance.

References

1. Rezai-Zadeh K, Munzberg H. Integration of sensory information via central thermoregulatory leptin targets. *Physiol Behav* 2013; **121**: 49-55.
2. Ruffin MP, Adage T, Kuipers F, Strubbe JH, Scheurink AJ, van Dijk G. Feeding and temperature responses to intravenous leptin infusion are differential predictors of obesity in rats. *Am J Physiol Regul Integr Comp Physiol* 2004; **286**: R756-63.
3. de Git KCG, Peterse C, Beerens S, Luijendijk MCM, van der Plasse G, la Fleur SE, et al. Is leptin resistance the cause or the consequence of diet-induced obesity? *Int J Obes (Lond)* 2018; doi: 10.1038/s41366-018-0111-4.
4. Levin BE, Dunn-Meynell AA. Reduced central leptin sensitivity in rats with diet-induced obesity. *Am J Physiol Regul Integr Comp Physiol* 2002; **283**: R941-8.
5. Tulipano G, Vergoni AV, Soldi D, Muller EE, Cocchi D. Characterization of the resistance to the anorectic and endocrine effects of leptin in obesity-prone and obesity-resistant rats fed a high-fat diet. *J Endocrinol* 2004; **183**: 289-298.
6. Bates SH, Stearns WH, Dundon TA, Schubert M, Tso AW, Wang Y, et al. STAT3 signalling is required for leptin regulation of energy balance but not reproduction. *Nature* 2003; **421**: 856.
7. Gao Q, Wolfgang MJ, Neschen S, Morino K, Horvath TL, Shulman GI, et al. Disruption of neural signal transducer and activator of transcription 3 causes obesity, diabetes, infertility, and thermal dysregulation. *Proc Natl Acad Sci U S A* 2004; **101**: 4661-4666.
8. Dodd GT, Worth AA, Nunn N, Korpal AK, Bechtold DA, Allison MB, et al. The thermogenic effect of leptin is dependent on a distinct population of prolactin-releasing peptide neurons in the dorsomedial hypothalamus. *Cell Metab* 2014; **20**: 639-649.
9. Enriori PJ, Sinnayah P, Simonds SE, Garcia Rudaz C, Cowley MA. Leptin action in the dorsomedial hypothalamus increases sympathetic tone to brown adipose tissue in spite of systemic leptin resistance. *J Neurosci* 2011; **31**: 12189-12197.
10. Rezai-Zadeh K, Yu S, Jiang Y, Laque A, Schwartzenburg C, Morrison CD, et al. Leptin receptor neurons in the dorsomedial hypothalamus are key regulators of energy expenditure and body weight, but not food intake. *Mol Metab* 2014; **3**: 681-693.
11. Jo YH, Buettner C. Why leptin keeps you warm. *Mol Metab* 2014; **3**: 779-780.
12. Rezai-Zadeh K, Munzberg H. Integration of sensory information via central thermoregulatory leptin targets. *Physiol Behav* 2013; **121**: 49-55.
13. Fischer AW, Hoefig CS, Abreu-Vieira G, de Jong JMA, Petrovic N, Mittag J, et al. Leptin Raises Defended Body Temperature without Activating Thermogenesis. *Cell Rep* 2016; **14**: 1621-1631.
14. Steffens AB. A method of frequent sampling blood and continuous infusion of fluids in the rat without disturbing the animal. *Physiol.Behav.* 1969; **4**: 836.
15. Heeren J, Munzberg H. Novel aspects of brown adipose tissue biology. *Endocrinol Metab Clin North Am* 2013; **42**: 89-107.
16. Morrison SF, Madden CJ, Tupone D. Central neural regulation of brown adipose tissue thermogenesis and energy expenditure. *Cell Metab* 2014; **19**: 741-756.
17. Levin BE, Dunn-Meynell AA, Banks WA. Obesity-prone rats have normal blood-brain barrier transport but defective central leptin signaling before obesity onset. *Am J Physiol Regul Integr Comp Physiol* 2004; **286**: R143-50.
18. Commins SP, Watson PM, Padgett MA, Dudley A, Argyropoulos G, Gettys TW. Induction of uncoupling protein expression in brown and white adipose tissue by leptin. *Endocrinology* 1999; **140**: 292-300.
19. Commins SP, Watson PM, Frampton IC, Gettys TW. Leptin selectively reduces white adipose tissue in mice via a UCP1-dependent mechanism in brown adipose tissue. *Am J Physiol Endocrinol Metab* 2001; **280**: E372-7.

20. Himms-Hagen J. Defective brown adipose tissue thermogenesis in obese mice. *Int J Obes* 1985; **9**: 17-24.
21. Fischer AW, Cannon B, Nedergaard J. Leptin-deficient mice are not hypothermic, they are anapyrexic. *Mol Metab* 2016; **6**: 173.
22. Pandit R, Beerens S, Adan RAH. Role of leptin in energy expenditure: the hypothalamic perspective. *Am J Physiol Regul Integr Comp Physiol* 2017; **312**: R938-R947.

Supplementary information

Methods

Surgery

Surgery was performed under fentanyl/fluanisone (0.315 mg/kg fentanyl, 10 mg/kg fluanisone, Hypnorm, Janssen Pharmaceutica, Beerse, Belgium) and midazolam (2.5 mg/kg, i.p., Actavis, the Netherlands) anesthesia. Xylocaine was sprayed on the skull to provide local anesthesia (Lidocaine 100 mg/ml, AstraZeneca BV, Zoetermeer, the Netherlands). All rats received three daily peri-surgical injections of carprofen (5 mg/kg, s.c. Carporal, AST Farma BV, Oudewater, the Netherlands), starting at the day of surgery.

Selection of leptin sensitive vs resistant rats

To measure leptin sensitivity, animals were fasted overnight (10 gr chow at 16.00h). The next morning at 10.00h, leptin (250 µg / 250 µl; recombinant murine leptin, NHPP, USA) or vehicle (250 µl, phosphate buffered saline, PBS) was injected via a jugular vein catheter, and 45 minutes later food was made available once again. A latin-square design was used, such that half of the rats first received leptin, and 3-4 days later, were tested a second time with treatments reversed. Food intake was measured 1-24h after food return using an automated food-monitoring system (Scales, Department Biomedical Engineering, UMC Utrecht, The Netherlands). This program records the weight of food hoppers in the home cage automatically every 12 s. Leptin sensitivity was measured by normalizing cumulative food intake after leptin injection to cumulative food intake after vehicle injection. In each individual rat, two independent leptin sensitivity tests were performed, and subsequently the average response of two tests was taken (Figure 2A).

In six rats, the response to leptin in test 1 largely deviated from the response in test 2, which could be explained by external factors (reasons for deviation included the bleeding of cannulas following injection, stress effects, and abnormal water/food intake during the days before injection). These rats were tested a third time, and the response of the third test was averaged with the response of the most reliable test from the first two tests, which made it possible to reliably designate rats as LS or LR.

Thermosensitive camera

In order to make thermal photographs, rats were placed in an open cage to which they were extensively habituated. The camera was mounted approximately 50 cm above the cage, and thermal photographs focused on the tail base. A thermal

photograph was made shortly before injection (baseline), and at one and two hours following injection. For each time-point, several photographs were taken and the photograph with best tail base visibility was analyzed. Photographs were analyzed with a specific software package (FLIR-Tools-Software; FLIR; West Malling, Kent, UK). The region of interest covered the start of the tail base (Figure 1A), and the center temperature measurement was used for the analysis.

Post-mortem analysis

In order to check for cannula placement, rats were given a lethal dose of sodium pentobarbital (200 mg/ml, Euthanimal, Alfasan BV, Woerden, The Netherlands), and were transcardially perfused with 0.9% NaCl followed by 4% paraformaldehyde (PFA) in PBS. Brains were excised and kept in 4% PFA for 24h, and were subsequently saturated with 30% sucrose in PBS with 0.01% NaN_3. Brains were snap frozen in isopentane between -60ºC and -40ºC, and sliced into 40 µm sections using a cryostate (Leica, Germany). Tissue was collected in six series in cryo-protectant (25% glycerol; 25% ethylene-glycol in PBS) and stored at -20ºC. Two series were mounted, and subsequently photographed and digitized using a Zeiss Axioskop 2 microscope (Zeiss, Jena, Germany). Slices were matched to the stereotaxic brain atlas from Paxinos and Watson (1998; fourth edition), using the fornix, mammillothalamic tract, and optic tract as landmarks for the DMH, in order to check for guide cannula placement above the DMH (Figure 1C).

Body composition

Prior to perfusion, individual epididymal, subcutaneous (inguinal), mesenteric, and perirenal white adipose tissues were dissected from the left side, cleaned and weighed.

Uncoupling protein 1 expression

Two hours before sacrifice, rats were bilaterally injected with either 300 ηl PBS (4 LS and 4 LR rats) or 300 ηg leptin / 300ηl PBS leptin (remaining rats) in the DMH. Shortly before perfusion, BAT tissue was dissected and stored at -80ºC. Only BAT tissue of PBS injected rats was used to determine uncoupling protein 1 (UCP1) expression levels.

RNA extraction and cDNA synthesis

Frozen BAT samples were homogenized in QIAzol lysis reagent using a Tissue Lyser (Qiagen, Hilden, Germany) and chloroform was subsequently added to the homogenates prior to centrifugation at 4°C. RNA was isolated from the received upper aqueous phase using RNeasy Lipid Tissue Mini kit (Qiagen). DNA was removed by DNase treatment (Qiagen). Acquired RNA was diluted to a concentration of 50 ng/µl and reversed transcribed by using iScript cDNA synthesis kit (Bio-Rad laboratories, Hercules, CA, USA).

Quantitative real-time polymerase chain reaction (qRT-PCR) analysis

PCR reaction mixture was prepared by mixing 25 ng of cDNA with TaqMan Advanced Master Mix (Applied Biosystems, Carlsbad, CA, USA) and TaqMan Gene Expression Assay (Ucp1; Rn00562126_m1, Hmbs; Rn00565886_m1). Thermal cycling and fluorescence detection was performed with a QuantStudio 7 Flex Real-Time PCR System (Applied Biosystems). The cycle threshold (Ct) was set automatically by the system software. The Ucp1 Ct values were normalized to the reference gene Hmbs. Relative mRNA expression levels were calculated by using the 2-ΔCt equation, where the ΔCt value was obtained by subtracting Ct value of the reference gene Hmbs from the Ct value of Ucp1.

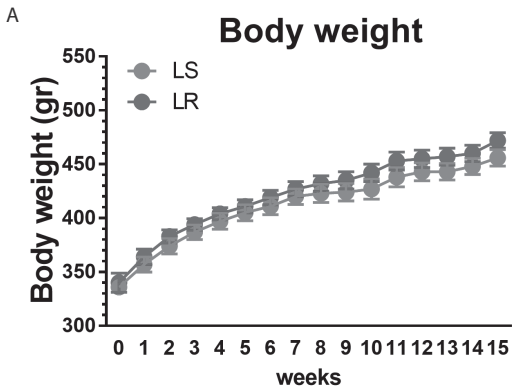

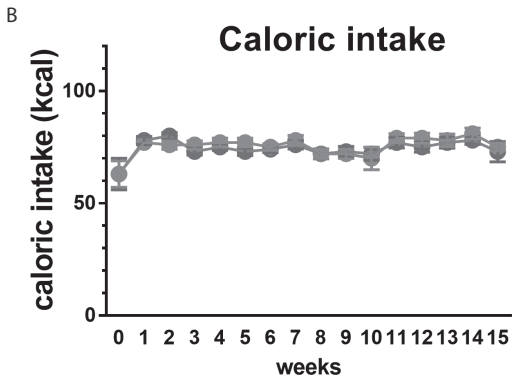

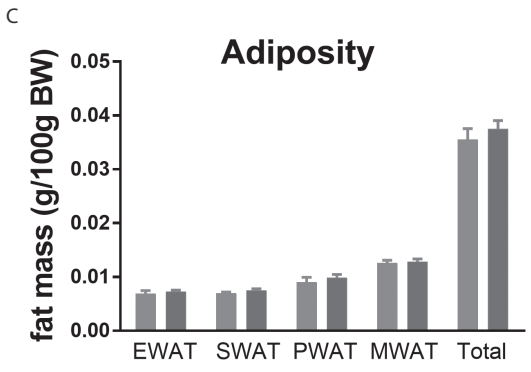

Figure S1. Obesity-related parameters in LS and LR rats on a chow diet. (A) Body weight and (B) caloric intake. $F_{week*responder} \geq 0.610$, $p \geq 0.392$. (C) EWAT, epididymal; SWAT, subcutaneous (inguinal); PWAT, perirenal, and MWAT, mesenteric white adipose tissues at week 15. $F_{responder} \geq 0.099$, $p \geq 0.168$. Data are shown as mean ± SEM. N=10-11 per group.

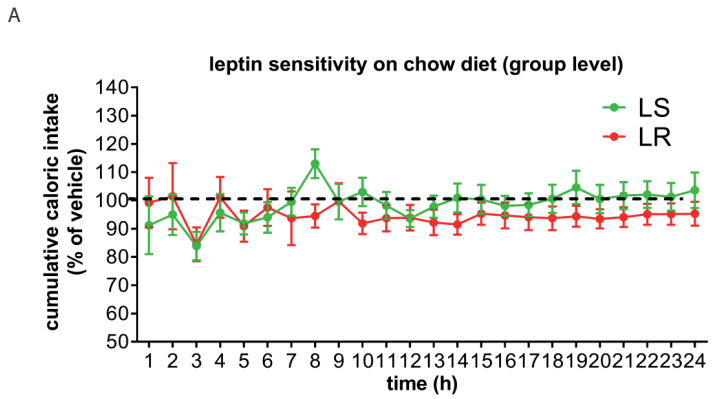

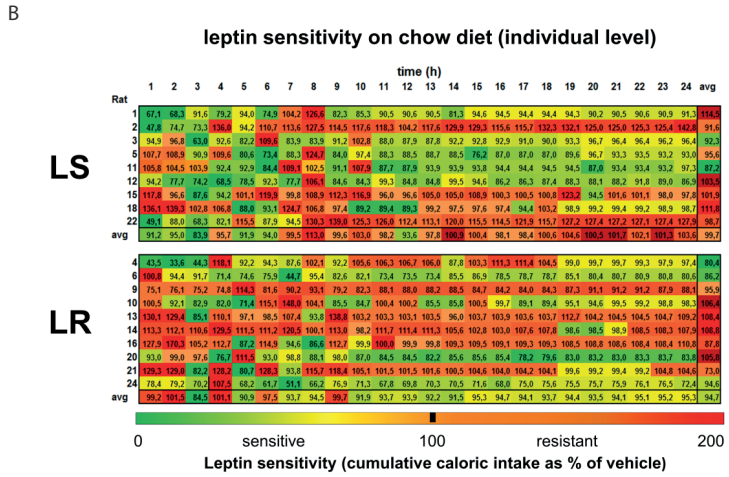

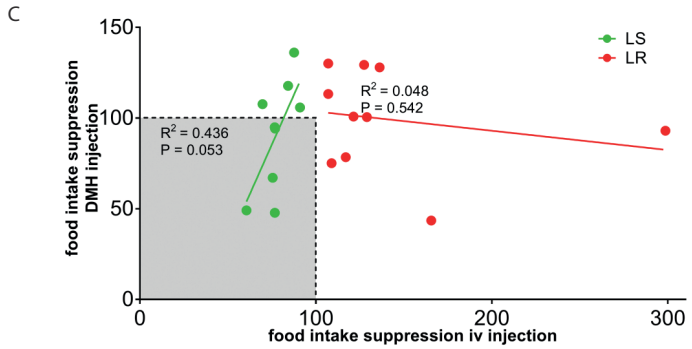

Figure S2 Individual 1-24h leptin sensitivity following intra-DMH leptin injection in LS and LR rats. Leptin sensitivity was measured by cumulative food intake after leptin injection normalized to vehicle food intake. Leptin sensitivity of one test is shown. Leptin sensitivity (A) at group level and (B) individual level; a heat plot of the relative level of sensitivity is shown at 1-24h food intake for each individual rat (i.e. each row). The heat plot indicates the relative degree of leptin sensitivity at a particular time point in comparison with the other time-points in the row. 1-24h: $F_{(hour*)treatment*responder} \geq 0.597$, $p \geq 0.422$. LS, Ftreatment*hour=1.595, p=0.049; Ftreatment=0.161, p=0.699. LR, Ftreatment*hour=0.754, p=0.785; Ftreatment=1.792. p=0.214. Data are shown as mean ± SEM; n=9-10 per group (C) Correlation between food intake suppression 1h following intravenous and intra-DMH leptin injection. LS, R2=0.436, p=0.053, and LR, R2=0.048, p=0.542.

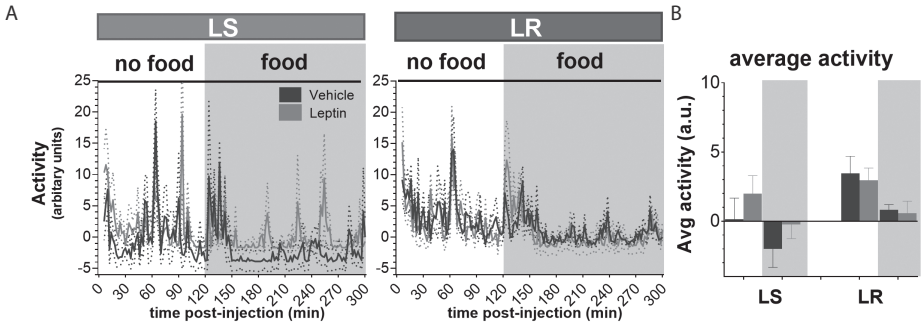

Figure S3. Comparison of leptin regulation of locomotor activity between LS and LR rats after intravenous leptin administration. (A) Continuous and (B) average delta change in locomotor activity after intravenous leptin/vehicle injection in LS (n=5) vs LR rats (n=9), in the presence and absence of food. Without food: $F_{treatment*responde}$r=0.625, p=0.445; with food: Ftreatment*responder=1.047, p=0.326. Data are shown as mean ± SEM. The dotted lines show the SEM. The shaded areas indicate measurements in the presence of food.

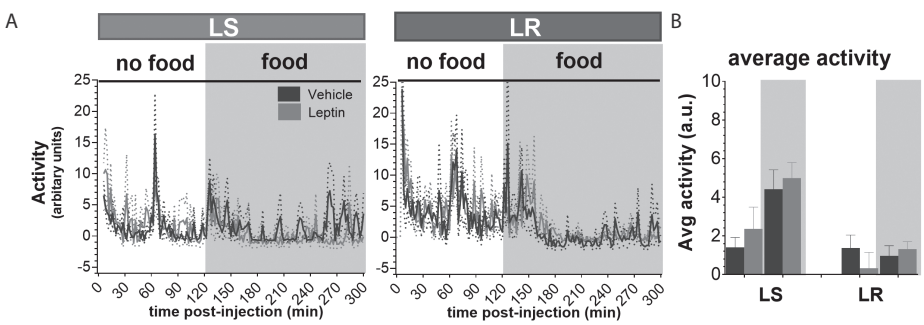

Figure S4. Comparison of leptin regulation of locomotor activity between LS and LR rats after intra-DMH leptin administration. (A) Continuous and (B) average delta change in locomotor activity after intra-DMH leptin/vehicle injection in LS (n=6) vs LR rats (n=9), in the presence and absence of food. Without food: $F_{treatment*responder}$=0.149, p=0.706; with food: Ftreatment*responder=1.891, p=0.194. Data are shown as mean ± SEM. The dotted lines show the SEM. The shaded areas indicate measurements in the presence of food.

Table S1. Statistical analysis of BAT and liver temperature in LS versus LR rats.

	LS vs LR test Statistic	P value Two-sided	One-sided
BAT temperature			
Ad libitum feeding			
Light (total)	$F_{time*responder}$ = 1.619	0.087#	
	$F_{responder}$ = 2.463	0.161	0.081#
Dark	$F_{time*responder}$ = 0.620	0.806	
	$F_{responder}$ = 2.528	0.156	0.078#
Restricted feeding			
Light 1	$F_{time*responder}$ = 1.198	0.325	
	$F_{responder}$ = 0.761	0.406	0.206
Dark 1	$F_{time*responder}$ = 0.417	0.945	
	$F_{responder}$ = 0.690	0.430	0.215
Light 2	$F_{time*responder}$ = 0.896	0.337	
	$F_{responder}$ = 0.214	0.661	0.331
Dark 2	$F_{time*responder}$ = 0.281	0.592	
	$F_{responder}$ = 0.109	0.750	0.375
Light 3	$F_{time*responder}$ = 1.416	0.271	
	$F_{responder}$ = 0.513	0.494	0.247
Refeeding			
Light 1	$F_{time*responder}$ = 1.477	0.202	
	$F_{responder}$ = 0.457	0.524	0.262
Dark 1	$F_{time*responder}$ = 0.587	0.833	
	$F_{responder}$ = 1.059	0.343	0.172
Light 2	$F_{time*responder}$ = 0.104	0.839	
	$F_{responder}$ = 1.488	0.268	0.134
Liver temperature			
Ad libitum feeding			
Light (total)	$F_{time*responder}$ = 1.430	0.247	
	$F_{responder}$ = 0.221	0.651	0.326
Dark	$F_{time*responder}$ = 0.719	0.588	
	$F_{responder}$ = 0.135	0.723	0.362
Restricted feeding			
Light 1	$F_{time*responder}$ = 1.343	0.277	
	$F_{responder}$ = 0.057	0.841	0.421
Dark 1	$F_{time*responder}$ = 1.072	0.387	
	$F_{responder}$ = 0.027	0.873	0.437
Light 2	$F_{time*responder}$ = 1.059	0.391	
	$F_{responder}$ = 0.020	0.890	0.445
Dark 2	$F_{time*responder}$ = 1.069	0.390	
	$F_{responder}$ = 0.042	0.840	0.420

Table S1. Continued

Light 3	$F_{time*responder} = 1.626$ $F_{responder} = 0.002$	0.218 0.965	 0.483
Refeeding			
Light 1	$F_{time*responder} = 1.360$ $F_{responder} = 0.248$	0.233 0.628	 0.314
Dark 1	$F_{time*responder} = 1.365$ $F_{responder} = 0.239$	0.225 0.633	 0.317
Light 2	$F_{time*responder} = 1.250$ $F_{responder} = 0.243$	0.299 0.631	 0.316

P values in bold# indicate trends for statistical differences between LS and LR rats. The one-sided test statistics for responder is also shown, as we expected lower body temperature in leptin resistant (LR) rats compared with leptin sensitive (LS) rats.

Table S2. Statistical analysis of activity in LS vs LR rats.

	LS vs LR test statistic	P value Two-sided
Activity		
Ad libitum feeding		
Light (total)	$F_{time*responder} = 1.448$ $F_{responder} = 0.151$	0.143 0.704
Dark	$F_{time*responder} = 0.624$ $F_{responder} = 0.002$	0.655 0.966
Restricted feeding		
Light 1	$F_{time*responder} = 3.674$ $F_{responder} = 0.059$	0.019 0.812
Dark 1	$F_{time*responder} = 0.672$ $F_{responder} = 0.015$	0.764 0.904
Light 2	$F_{time*responder} = 2.794$ $F_{responder} = 0.086$	0.001 0.774
Dark 2	$F_{time*responder} = 0.682$ $F_{responder} = 0.050$	0.613 0.827
Light 3	$F_{time*responder} = 1.809$ $F_{responder} = 0.832$	0.173 0.378
Refeeding		
Light 1	$F_{time*responder} = 1.259$ $F_{responder} = 0.902$	0.282 0.363
Dark 1	$F_{time*responder} = 0.730$ $F_{responder} = 0.048$	0.511 0.831
Light 2	$F_{time*responder} = 0.154$ $F_{responder} = 2.397$	0.240 0.150

LS, leptin sensitive; LR, leptin resistant rat.

Section II

Regulation of energy balance beyond the hypothalamus

Chapter 5:

Anatomical projections of the dorsomedial hypothalamus to the periaqueductal grey and their role in thermoregulation: a cautionary note

Kathy C.G. de Git[1], Diana C. van Tuijl[1], Mieneke C.M. Luijendijk[1], Inge G. Wolterink-Donselaar[1], Alexander Ghanem[2], Karl-Klaus Conzelmann[2], Roger A.H. Adan[1]

1 Brain Center Rudolf Magnus, Dept. of Translational Neuroscience, University Medical Center Utrecht, Utrecht University, Utrecht, 3584 CG, The Netherlands

2 Max von Pettenkofer Institute & Gene Center, Virology, Faculty of Medicine, LMU München, Munich, Germany

Published in Physiological Reports (2018) Jul;6(14):e13807. doi: 10.14814/phy2.13807.

Abstract

The DMH is known to regulate brown adipose tissue (BAT) thermogenesis via projections to sympathetic premotor neurons in the raphe pallidus, but there is evidence that the periaqueductal gray (PAG) is also an important relay in the descending pathways regulating thermogenesis. The anatomical projections from the DMH to the PAG subdivisions and their function are largely elusive, and may differ per anterior-posterior level from bregma. We here aimed to investigate the anatomical projections from the DMH to the PAG along the entire anterior-posterior axis of the PAG, and to study the role of these projections in thermogenesis in Wistar rats. Anterograde channel rhodopsin viral tracing showed that the DMH projects especially to the dorsal and lateral PAG. Retrograde rabies viral tracing confirmed this, but also indicated that the PAG receives a diffuse input from the DMH and adjacent hypothalamic subregions. We aimed to study the role of the identified DMH to PAG projections in thermogenesis in conscious rats by specifically activating them using a combination of canine adenovirus-2 (CAV2Cre) and Cre-dependent designer receptor exclusively activated by designer drugs (DREADD) technology. Chemogenetic activation of DMH to PAG projections increased BAT temperature and core body temperature, but we cannot exclude the possibility that at least some thermogenic effects were mediated by adjacent hypothalamic subregions due to difficulties in specifically targeting the DMH and distinct subdivisions of the PAG, because of diffuse virus expression. To conclude, our study shows the complexity of the anatomical and functional connection between the hypothalamus and the PAG, and some technical challenges in studying their connection.

Introduction

Humans have evolved efficient physiological mechanisms that promote the acquirement and defense of energy stores in white adipose tissue [1]. Pathological accumulation of energy stores results in obesity, a condition that is difficult to counteract with dieting alone, as decreased caloric intake is followed by physiological counter regulatory mechanisms that defend acquired energy stores [1, 2]. A reduction in thermogenesis during dieting is one such a mechanism [3]. Therefore, it is important to understand how thermogenesis is regulated.

Non-shivering or adaptive thermogenesis is controlled via brown adipose tissue (BAT), which has the specific metabolic function to dissipate energy in the form of heat [4-9]. BAT is an important thermoregulatory effector organ in rodents in various physiological conditions [5,6], and recent evidence acknowledged metabolically active BAT in adult humans [10-13]. BAT thermogenesis is governed by central pathways that control sympathetic innervation of BAT [4-9]. The DMH is now recognized as one of the key players in the thermoregulatory circuit [4, 5, 9, 14, 15], as disinhibition of DMH neurons was shown to elicit a marked and rapid increase in BAT sympathetic nerve activity (SNA) and BAT temperature [16, 17] that preceded the increase in core body temperature [16, 18]. The DMH is proposed to exert its sympathetic control of BAT thermogenesis via projections to sympathetic premotor neurons in the raphe pallidus [4, 5, 9, 14, 17, 19, 20], but there is evidence that the periaqueductal grey (PAG) is also an important relay in the descending pathways mediating thermogenesis [5, 14, 18, 20 but see 51].

The PAG is a relatively long midbrain region that can be divided into dorsomedial (dmPAG), dorsolateral (dlPAG), lateral (lPAG) and ventrolateral (vlPAG) subdivisions, which differ with respect to their functional properties and anatomical connections [21]. At least some of these subdivisions may have an opposite function in rostral versus caudal PAG extensions [18]. In regard to thermogenesis, it seems that neuronal activity in the rostral vPAG functions to inhibit BAT SNA and BAT temperature [20], whereas neuronal activity in the caudal (v)lPAG functions to increase BAT temperature [19]. Neuronal activity in the caudal l/dlPAG [18, 22] but not caudal (v)lPAG was shown to increase core body temperature [19]. In accordance, the increase in BAT SNA and core body temperature arising from chemical disinhibition of DMH neurons was substantially reduced by chemical activation of the rostral vPAG [20] and chemical inhibition of the caudal l/dlPAG [18], respectively. This suggests that the DMH increases thermogenesis through a combination of an inhibition of BAT sympathoinhibitory neurons in the rostral vPAG, and a facilitation of BAT sympathoexcitatory neurons in the caudal l/dlPAG. It should be noted that the role of the different PAG subdivisions

in thermoregulation is difficult to interpret, as the subdivisions were assessed in independent studies with different experimental settings, with for example the use of anesthesia [19, 20] or not [18, 22], and the anatomical resolution of the microinjection techniques used is limited [5], which may result in misinterpretation of the targeted PAG subdivision.

The above mentioned functional connection between the DMH and PAG was only studied at very specific subdivisions in the PAG, i.e. the vPAG at -5.3 to -5.6 mm from bregma, and the l/dlPAG at -7.64 to -8.30 from bregma. Clues for a potential role of other PAG subdivisions as a relay in the descending pathways from the DMH in mediating thermogenesis cannot be derived from previous anterograde tracing studies from the DMH to PAG, as these studies did not specify the anterior-posterior level at which PAG projections were observed [23, 24] or only described the PAG projections at a limited number of anterior-posterior levels from bregma [25, 26]. The limited available evidence suggests that the projections from the DMH may vary largely per anterior-posterior level in the PAG subdivisions [25, 26].

We here aimed to further investigate the anatomical and functional projection from the DMH to the PAG. We started with an anterograde tracing study to identify which subdivisions and anterior-posterior levels of the PAG receive projections from the DMH. We then performed a retrograde tracing study in order to confirm the identified projections. Finally, we aimed to compare the role of four of the identified DMH to PAG projections in thermoregulation by the combined use of a canine adenovirus-2 (CAV2Cre) and Cre-dependent designer receptor exclusively activated by designer drugs (DREADD) technology, a method that allows for the specific activation of neural pathways [27, 28, 29]. CAV2Cre was injected into the PAG, where it infects nerve terminals and retrogradely delivers Cre in the DMH, which subsequently enables the expression of the adeno-associated virus (AAV) containing DREADD $hM_3D(G_q)$ that was injected into the DMH.

Methods

Animals

Adult male Wistar rats (Charles-River, Germany) were used, weighing ~300 gram at the time of surgery. Rats were group housed in experiment 1 and 2, and individually housed in experiment 3 in a controlled environment under a normal light/dark cycle (lights on between 0700 and 1900 h). Rats had ad libitum access to standard chow (Special Diet Service, UK) and tap water, unless stated otherwise. All experiments were performed in accordance with Dutch laws (Wet op de Dierproeven, 1996) and European regulations (Guideline 86/609/EEC), and were approved by the Animal Ethics Committee of Utrecht University.

Experiment 1: anterograde tracing from DMH to PAG

Surgery

Prior to surgery, rats were anaesthetized by intramuscular fentanyl/fluanisone (0.315 mg/kg fentanyl, 10 mg/kg fluanisone, Hypnorm, Janssen Pharmaceutica, Belgium). Xylocaine was sprayed on the skull to provide local anesthesia (Lidocaine 100 mg/ml, AstraZeneca BV, the Netherlands). All rats received three daily peri-surgical injections of carprofen (5 mg/kg, s.c. Carporal, AST Farma BV, the Netherlands), starting at the day of surgery. Rats (n=3) were unilaterally injected with 0.3 µl of AAV-hSyn-ChR-YFP (4.8*1012 genomic copies/ml; UNC vector core) in the DMH (from bregma: anterior-posterior (AP): -2.30 mm, medio-lateral (ML): +1.40 mm, dorso-ventral (DV): -9.30 mm, at an angle of 5º), using a stereotactic apparatus and a microliter infusion system. Virus was injected through 34G needles, which were connected to a Hamilton microliter syringe with polyethylene tubing. By using a micro-infusion pump, the injection speed of all injections was set at 0.1 µl/min. Following infusion, the needles were left in place for 10 min to prevent backflow. Prior to these surgeries, we performed pilot experiments to compare injections between the microliter infusion system and the nanojet (where glass capillaries are used). Since no differences were observed in the targeting of the injections between the two systems, we decided to use the microliter infusion system for all our experiments.

Tissue preparation

In order to allow for sufficient virus expression, rats were sacrificed three weeks after surgery. Rats were given a lethal dose of sodium pentobarbital (200 mg/ml, Euthanimal, Alfasan BV, The Netherlands), and were transcardially perfused with 0.9% NaCl followed by 4% paraformaldehyde (PFA) in phosphate buffered saline (PBS). Brains were excised and kept in 4% PFA for 24h, and were subsequently saturated with 30% sucrose in PBS with 0.01% NaN_3. Brains were snap frozen in isopentane between -60ºC and -40ºC, and sliced into 40 µm sections using a cryostate (Leica, Germany). Tissue was collected in six series in cryo-protectant (25% glycerol; 25% ethylene-glycol in PBS) and stored at -20ºC.

Immunohistochemistry

Two series of brain slices were washed in PBS and subsequently blocked and permeabilized in blocking solution (PBS containing 10% fetal calf serum and 1% triton X-100) for 2h. Subsequently, slices were incubated overnight at 4 °C with primary chicken anti-GFP antibody (1:500, Abcam, UK) in blocking solution. After washing in PBS, brain slices were incubated with Alexa-488 labeled secondary goat anti-chicken antibody in blocking solution for 2h. After washing in PBS, slices were mounted on SuperFrost glasses (VWR, Leuven) and covered with FluorSave (Milipore).

Histological analysis

Immunofluorescent slices were photographed and digitized using a Zeiss Axioskop 2 epifluorescent microscope (Zeiss, Germany). Slices were matched to the stereotaxic brain atlas from Paxinos and Watson (1998; fourth edition), using the fornix, mammillothalamic tract, and optic tract as landmarks for the DMH, and the fourth ventricle and overall shape of the PAG for the PAG. The injection site of AAV-hSyn-ChR-YFP in the DMH was determined by the expression of cell bodies with GFP immunoreactivity. The relative abundance of GFP-labeled fibers was evaluated in different subdivisions of the PAG from bregma -4.80 till 8.80 mm by the following grading: absence of labeled fibers (-), very low (±), low (+), moderate (++), and high (+++). For each rat, one brain slice per bregma was evaluated.

Experiment 2: retrograde tracing from PAG to DMH

Surgery

A second group of rats (n=10) underwent surgery under identical procedures as described for experiment 1, but were unilaterally injected with 0.3 µl of a mixture of rabies SAD DG mCherry (SAD_G) (30-32) and AAV-hSyn-YFP (UNC vector core) (final concentration in mixture: 2.33*108 and 1.00*1012 genomic copies/ml, respectively) in the PAG. Rats were randomly divided in five groups of two and injected at 5 different coordinates in the PAG, respectively (from bregma: rat 7 and 8: AP -5.30 mm; ML +1.40 mm / <10°; DV -6.70 mm; rat 9 and 10: AP -6.30 mm; ML +1.40 mm / <10°; DV -6.50 mm; rat 11 and 12: AP -5.30 mm; ML +1.40 mm / <10°; DV -6.20 mm; rat 13 and 14: AP -7.80 mm; ML +2.20 mm / <10°; DV -6.50 mm; rat 15 and 16: AP -7.00 mm; ML +1.40 mm / <10°; DV -5.70 mm.)

Tissue preparation

Rats were sacrificed one week after surgery via identical procedures as described for experiment 1.

Immunohistochemistry

Two series of brain slices were stained via identical procedures as described for experiment 1, but slices were incubated with primary chicken anti-GFP (1:500, Abcam, UK) and rabbit anti-dsRed (1:500, Clontech) antibodies, and secondary Alexa-488 labeled goat anti-chicken (1:500, Abcam, UK) and Alexa-568 labeled goat anti-rabbit (1:500, Abcam, UK) antibodies.

Histological analysis

Immunofluorescent slices were photographed and digitized using a Zeiss Axioskop 2 epifluorescent microscope (Zeiss, Germany). Slices were matched to the stereotaxic brain atlas from Paxinos and Watson (1998; fourth edition), using the fornix, mammillothalamic tract, and optic tract as landmarks for the hypothalamus, and the fourth ventricle and overall shape of the PAG for the PAG. The PAG injection site of rabies was determined by the expression of cell bodies with GFP immunoreactivity. One rat showed no virus expression in the PAG, and was therefore excluded from the following analyses. The number of inputs in the hypothalamus was evaluated by the expression of cell bodies with mCherry immunoreactivity. Hypothalamic inputs were systematically counted at the six sections between -2.30 to -3.60 mm from bregma defined by the rat brain atlas Paxinos and Watson (1998; fourth edition). Sections of the rat brain atlas were made transparent in Photoshop (Adobe Photoshop CC 2015, Adobe Systems Software Ireland Ltd), and overlays were made with the immunohistochemical pictures. For each rat, one picture was used per section, resulting in six pictures per rat in the hypothalamus. Images were loaded in Image J (version 1.50b, National Institutes of Health, USA) and the number of inputs was counted blindly in both sites of defined subregions in the hypothalamus.

Experiment 3: functional connection between the DMH and PAG

Surgery

A third group of rats (n=16) underwent surgery under identical procedures as described for experiment 1, but were bilaterally injected with 0.3 µl of AAV-hSyn-DIO-hM$_3$D(G$_q$)-mCherry (3.8*1012 genomic copies/ml; UNC vector core) in the DMH, and bilaterally injected with 0.3 µl of a mixture of CAV2Cre (final concentration

in mixture 1.8*1012 genomic copies/ml; IGMM, France) and AAV-hSyn-EYFP (final concentration in mixture 1.65*1012 genomic copies/ml; UNC vector core) in the PAG. Rats were randomly divided in four groups of four and injected at 4 different coordinates in the PAG, respectively (from bregma: group 1: AP -5.30 mm; ML ±1.40 mm / <10°; DV -5.70 mm; group 2: AP -6.30 mm; ML ±1.40 mm / <10°; DV -5.70 mm; group 3: AP -7.30 mm; ML ±1.40 mm / <10°; DV -5.70 mm; group 4: AP -8.30 mm; ML ±1.40 mm / <10°; DV -5.70 mm). In addition, an intra-abdominal dual transmitter (TL11M3F40-TT, Data Science International, USA) with leads to the portal vein in the liver and interscapular brown adipose tissue was implanted under fentanyl/fluanisone (0.315 mg/kg fentanyl, 10 mg/kg fluanisone, Hypnorm, Janssen Pharmaceutica, Belgium) and midazolam (2.5 mg/kg, i.p., Actavis, the Netherlands) anesthesia in order to record core body temperature, BAT temperature, and activity.

Effects of CNO on body temperature and activity

The home cage was placed on a receiver plate (DSI, USA) that received radiofrequency signals from the abdominal transmitter. The plate was connected to software (DSI, USA) that recorded core body temperature, BAT temperature, and locomotor activity every 2 minutes. Test sessions started 2.5 weeks after surgery to allow the CAV2Cre to infect the DMH and induce hM3D(Gq)-mCherry expression. During a test session, body temperature and activity were measured in the absence of food to prevent confounding with food-induced thermogenesis. Rats were food restricted at 9.00h, injected with saline or CNO (i.p.) at 12.00h according to a Latin square design, and food was returned at 17.00h. Clozapine-N-oxide (CNO; kindly provided by Bryan Roth and NIMH) was dissolved to a concentration of 0.3 mg/kg/ml in sterile saline (0.9% NaCl). The interval between two test sessions was four days and treatments were reversed between the two sessions. Rats were habituated twice to this procedure with saline (i.p.) prior to testing.

The placement of the leads to the liver and interscapular brown adipose tissue was checked after sacrifice. All liver probes were placed correctly, but the BAT probe was misplaced in 5 rats because it was slipped out of the insoluble suture. These rats were therefore excluded from the BAT temperature analysis. In two rats (both belonging to the DMH miss group), the battery of the transmitter was prematurely emptied, resulting in missing telemetry data. As a consequence, all 11 rats in the DMH hit group were included in the liver temperature analysis, and 7 of these rats were included in the BAT temperature analysis. In the DMH miss group, 3 of the 5 rats were included in the liver temperature analysis, and 2 rats were included in the BAT temperature analysis.

Tissue preparation

Rats were sacrificed six weeks after surgery via identical procedures as described for experiment 1 and 2.

Immunohistochemistry

One series of brain slices was stained via identical procedures as described for experiment 2.

Histological analysis

Immunofluorescent slices were photographed and digitized using a Zeiss Axioskop 2 epifluorescent microscope (Zeiss, Germany). The injection site of AAV-hSyn-DIO-hM3D(Gq)-mCherry was determined by the expression of cell bodies with mCherry immunoreactivity, and the injection site of CAV2Cre was determined by the expression of cell bodies with GFP immunoreactivity, resulting from the co-injected AAV-hSyn-EYFP virus.

Data analysis

Telemetry data were filtered for unreliable values (which likely resulted from electromagnetic interference with the environment): all data-points with a non-physiological temperature (*i.e.* <35 or >40 ºC; ~6% of the data) were removed. Telemetry data were analyzed using a two-way repeated measures ANOVA with time (in minutes) and treatment as within-subject variable. When appropriate, post hoc analyses were conducted using pairwise Bonferroni comparisons. Each parameter was tested for normality with the Kolmogorov-Smirnov test. Statistical analyses were conducted using SPSS 20.3 for Windows. The threshold for statistical significance was set at $p<0.05$. Data are presented as mean ± SEM.

Results

Anterograde tracing study from DMH to PAG

To determine which anterior-posterior levels and subdivisions of the PAG receive input from the DMH, three rats were unilaterally injected with an anterograde tracer, AAV-hSyn-hChR2-EYFP, in the DMH and the relative abundance of GFP-labeled fibers in the PAG was determined (Figure 1A). The anterior DMH was hit in all three rats, but all rats showed some spread of expression in the surrounding areas (Figure 2). One large injection (rat 2) labeled almost the entire DMH from the most anterior to the posterior part, and is therefore represented in detail (Figure 1). The other two injection sites especially hit the dorsal DMH at the more posterior levels from bregma

and also hit the DHA, an area that is often considered to form one thermogenic center together with the DMH (4, 6-8, 15) (Figure 2).

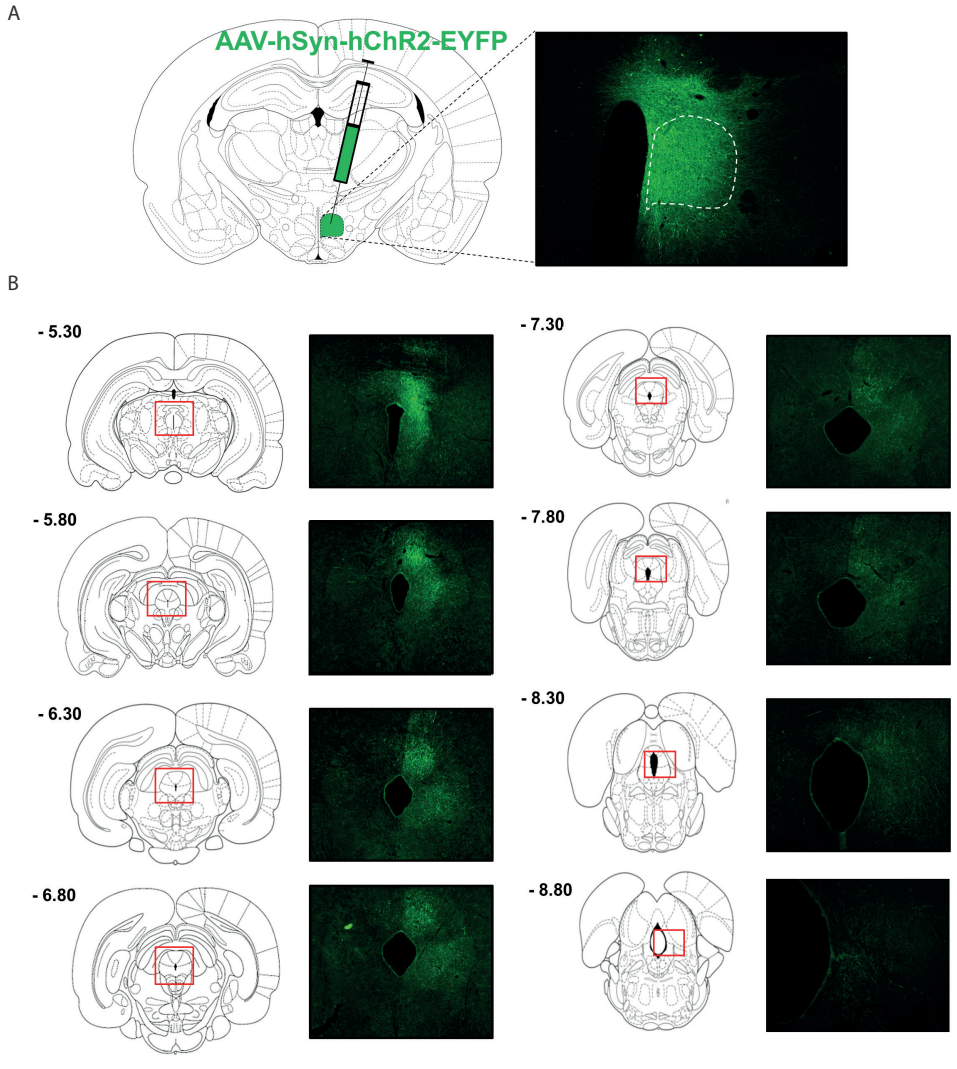

Figure 1. Anterograde tracing from DMH to PAG.
(A)The anterograde tracer virus AAV-hSyn-hChR2-EYFP was unilaterally injected into the DMH. GFP expression is shown for a successful injection in rat 2. The dotted outline shows the boundary of the DMH. GFP positive cell bodies were observed in the DMH, but not completely limited to this area. (B) Rostral to caudal GFP fiber distribution in subdivisions of the PAG. Distances from bregma (mm) are indicated at the left top.

The relative abundance of GFP-labeled fibers was assessed in defined subdivisions of the PAG from its most anterior part (-4.80 mm from bregma) to its most posterior part (-8.80 mm from bregma). Rats showed similar patterns of fiber distribution in the PAG (Table 1). The projections were strongest in the most anterior and middle parts of the PAG and became weaker at the posterior parts (Table 1; Figure 1B). Especially the dorsal and lateral PAG received projections from the DMH, but from the level of -8.00 mm from bregma onwards, the projections became weaker and more lateral.

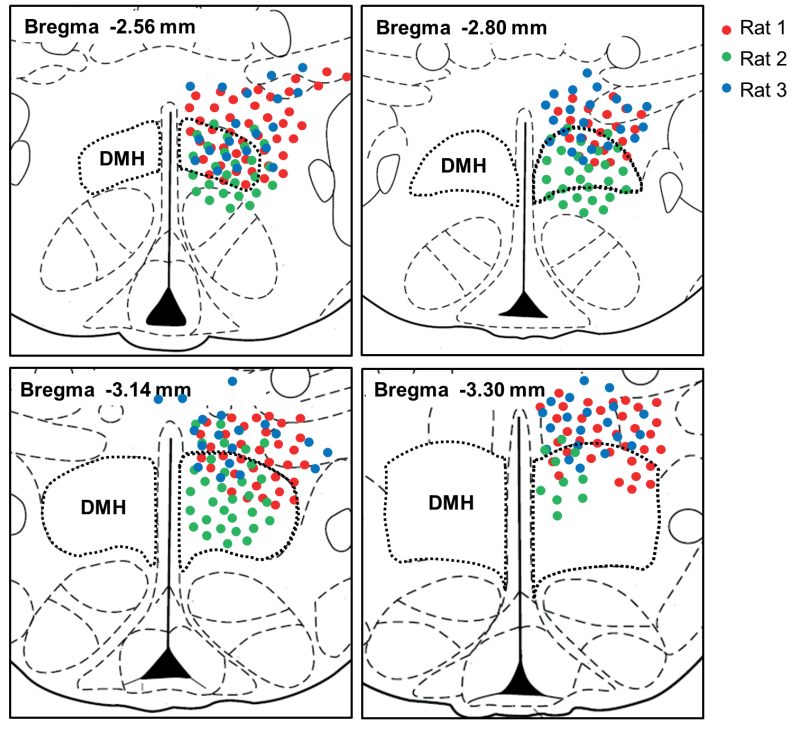

Figure 2. Mapping of AAV-hSyn-hChR2-EYFP injection sites.
Red, green, and blue circles indicate the expression of GFP positive cell bodies in rat 1, 2, and 3, respectively, in rostral to caudal levels of the rat hypothalamus. Distances from bregma (mm) are indicated at the left top. The anterior DMH was hit in all three rats. At more posterior bregma's, the dorsal DMH was hit in all rats, but rat 2 also showed GFP positive cell bodies in other subdivisions of the DMH. All rats showed some contamination of surrounding areas, especially the DHA.

Table 1. Relative densities of GFP-positive fibers in the PAG originating from DMH neurons.

	Rat 1	Rat 2	Rat 3	Average
PAG -4.80 mm				
dmPAG	+	+++	++	++
dlPAG	+	++	+	+/++
vlPAG	±	±	±	±
vmPAG	±	-	-	-
PAG -5.30 mm				
dmPAG	+	+++	+	+/++
dlPAG	+++	+++	++	++/+++
vlPAG	+	±	+	+
vmPAG	++	-	±	+
PAG -5.60 mm				
dmPAG	++	+++	++	++
dlPAG	+++	++	++	++
vlPAG	+++	++	±	+/++
vmPAG	++	±	-	±
PAG -5.80 mm				
dmPAG	++	+++	++	++
dlPAG	+++	+	±	+
lPAG	+++	++	+	++
vlPAG	++	-	±	±
vmPAG	++	-	-	+
PAG -6.30 mm				
dmPAG	+++	+++	++	++/+++
dlPAG	++	++	±	+
lPAG	+++	++	+	++
vlPAG	++	±	±	+
vmPAG	++	-	-	±
PAG -6.72 mm				
dmPAG	+++	+++	++	++/+++
dlPAG	+	+	±	+
lPAG	+++	++	++	++
vlPAG	+	-	±	±
vmPAG	++	-	-	±
PAG -6.80 mm				
dmPAG	+++	+++	++	++/+++
dlPAG	+	++	+	+
lPAG	+++	+++	++	++
vlPAG	++	±	±	+
vmPAG	++	-	-	±

Table 1. Continued

PAG -7.30 mm				
dmPAG	+++	++	++	++
dlPAG	++	+	+	+/++
lPAG	+++	+	++	++
vlPAG	++	±	±	+
vmPAG	+	-	-	±
PAG -7.80 mm				
dmPAG	+++	++	+++	++/+++
dlPAG	++	+	+	+
lPAG	+++	++	+++	++/+++
vlPAG	+++	-	±	+
vmPAG	++	-	+	+
PAG -8.00 mm				
dmPAG	+	+	+	+
dlPAG	±	+	±	±
lPAG	+++	++	+	++
vlPAG	++	±	+	+
vmPAG	++	-	-	+
PAG -8.30 mm				
dmPAG	±	+	+	+
dlPAG	±	+	±	±
lPAG	++	+	+	+
vlPAG	++	+	+	+
vmPAG	+	-	±	±
PAG -8.80 mm				
dmPAG	±	-	±	±
lPAG	++	+	+	+
vlPAG	++	+	+	+
vmPAG	-	-	±	-

Overview of the relative densities of GFP-positive fibers in anterior-posterior subdivisions of the PAG in rats injected with AAV-hSyn-hChR2-EYFP in the DMH. -, absence of labeled fibers; ±, very low; +, low; ++, moderate; and +++, high. Distances from bregma (mm) are indicated. dmPAG, dorsomedial PAG; dlPAG, dorsolateral PAG; lPAG, lateral PAG; vlPAG, ventrolateral PAG; vmPAG, ventromedial PAG.

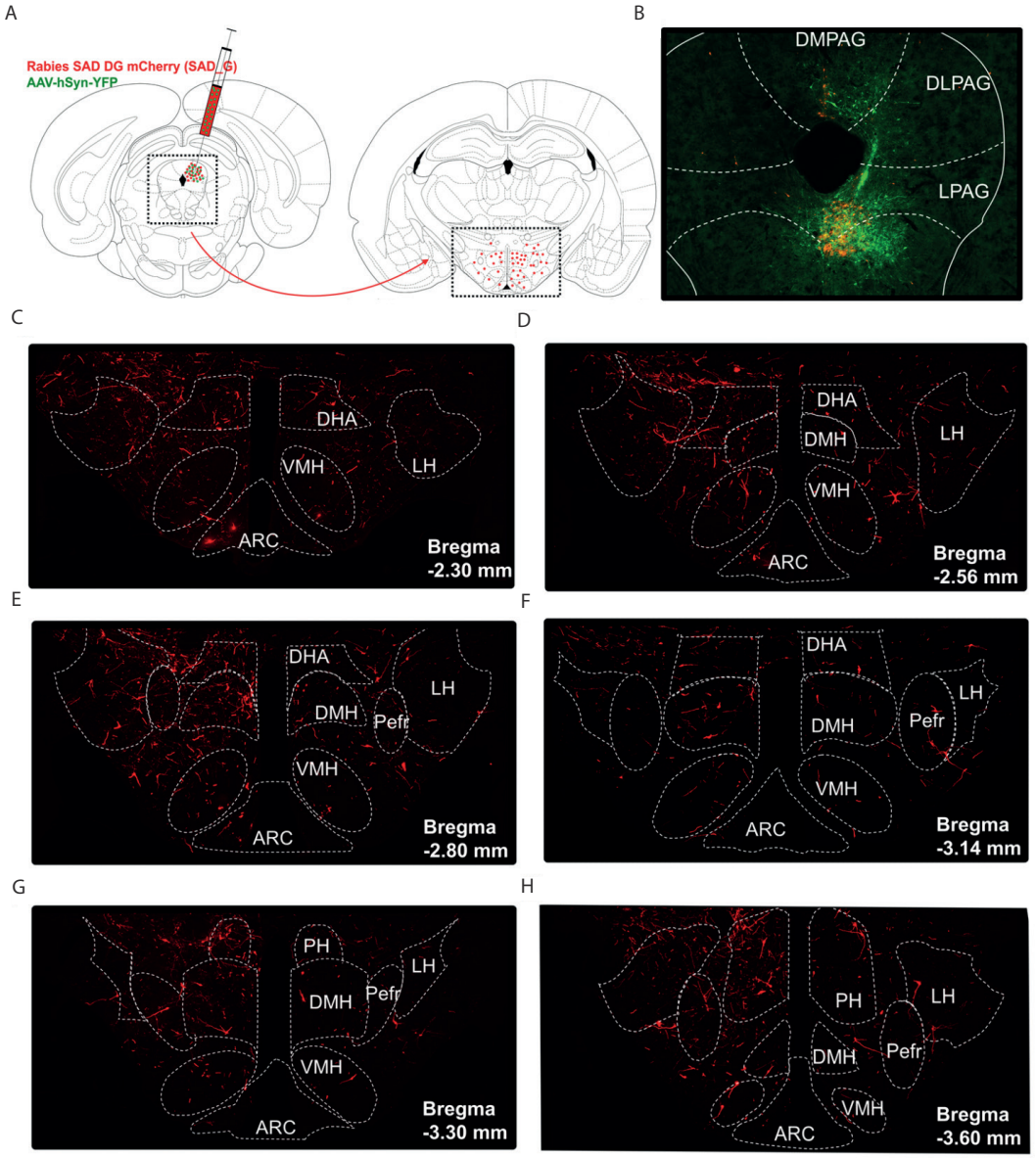

Figure 3. Retrograde tracing from PAG to hypothalamus.
(A) Experimental design. Rabies SAD DG mCherry (SAD_G), a monosynaptic retrograde tracer virus, was unilaterally injected into the PAG together with an AAV-hSyn-YFP virus to visualize the injection site. The number of direct presynaptic inputs in defined subregions of the hypothalamus, including the DMH, was assessed. (B) Representative injection site, showing the needle track and most GFP-positive cell bodies (green) in the ventral PAG. (C-H) Direct presynaptic inputs (red) in the anterior to posterior hypothalamus for the representative injection site in B. Distances from bregma (mm) are indicated, and the dotted outline shows the boundaries of hypothalamic subregions in which the number of presynaptic inputs was counted. ARC, arcuate nucleus; DHA, dorsohypothalamic area; DMH, dorsomedial hypothalamus, LH, lateral hypothalamus; Pefre, perifornical area; PH, posterior hypothalamus; VMH, ventromedial hypothalamus.

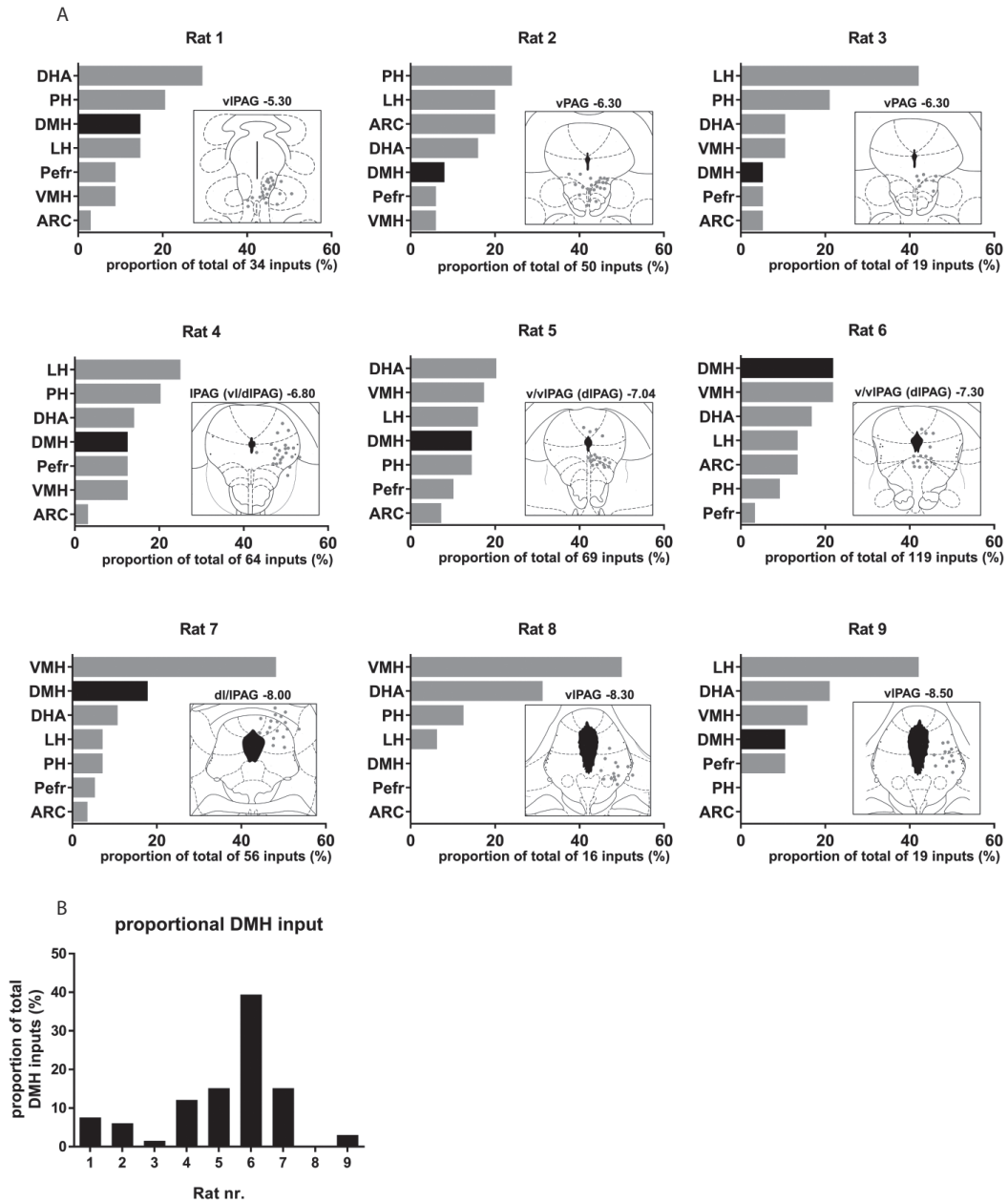

Figure 4. Hypothalamic monosynaptic inputs to the PAG.
(A) Plots of the relative proportion of presynaptic inputs in defined subregions of the hypothalamus; and schematic overviews of the injection site for all individual rats that were injected with rabies SAD DG mCherry (SAD_G) into distinct subdivisions of the PAG. Hypothalamic subregions are ranked from highest to lowest number of inputs for each individual rat, and the DMH is highlighted. Rats are ranked from most anterior injection site (top left) to most posterior injection site (bottom right). The targeted subdivision of the PAG and distance from bregma (mm), as well as the total number of inputs are indicated for each injection site. (B) The normalized inputs in the DMH in each individual rat is normalized to the total number of inputs in the DMH of all rats.

Retrograde tracing study from PAG to DMH

In order to confirm the identified projections from the DMH to the dorsal and lateral PAG, we injected a retrograde rabies virus aimed at the d/lPAG at different anterior-posterior levels (Figure 3A). Note that this recombinant rabies virus carries a rabies G coat, so that it infects all axon terminals near the injection site [30, 32]. By using this retrograde tracer virus, we could asses the direct presynaptic inputs in the hypothalamus to the PAG. An AAV-hSyn-YFP virus was injected together with the rabies virus to visualize the injection site in the PAG. Analysis of the injection sites revealed that the vlPAG was hit in most rats instead of the targeted d/lPAG. One representative injection site is shown in Figure 3B, showing that especially the vPAG was hit, but also some virus expression was present in the dPAG. Figure 3C-H shows in detail the direct presynaptic inputs in defined subregions of the hypothalamus onto the PAG for the representative injection site, showing that the PAG receives widespread input from all hypothalamic subregions rather than specific input from the DMH. All injection sites resulted in widespread presynaptic inputs in the hypothalamus (Figure 4A). The DMH was a relatively important hypothalamic input region in rat 6 and 7. Rat 7 was fully hit in the dlPAG and rat 6 also showed some GFP-expressing neurons in the dlPAG, suggesting that the DMH is a relatively important input region of the dlPAG. Analysis of the number of inputs in the DMH in individual rats normalized to the number of inputs in the DMH in all rats revealed that rat 4, 5, 6, and 7 show relatively more inputs in the DMH compared with other rats (Figure 4B). All four rats showed some GFP-expressing neurons in the dlPAG, suggesting that especially the dlPAG receives prominent input from the DMH. Taken together, the rabies retrograde tracing supports the finding of projections from the DMH to especially the dlPAG in the ChR anterograde tracing study, but also shows that there is a diffuse projection from the hypothalamus to the PAG rather than specific input from the DMH.

Role of the DMH to dlPAG projection in thermoregulation

To investigate whether the projections from the DMH to dlPAG control thermogenesis, we aimed to specifically activate this pathway by injecting CAV2Cre in the PAG and Cre-dependent DREADD $hM_3D(G_q)$ in the DMH (Figure 5A). CAV2Cre infects neurons at terminals at the injection site and retrogradely delivers Cre in neurons that project to the area of injection, which subsequently enables the expression of Cre-dependent DREADD $hm_3D(G_q)$ in projection neurons (27-29). An AAV-hSyn-YFP virus was injected together with the CAV2Cre virus to visualize the injection site in the PAG.

We intended to specifically target the dlPAG at four different anterior-posterior levels (four rats per group), but our histology analysis revealed widespread virus expression in the PAG. Consequently, it was not possible to subgroup rats based on virus expression in the PAG, and results of all rats with virus expression in the PAG were combined. Analysis of DREADD $hM_3D(G_q)$ expression (mCherry) in the hypothalamus indicated $hM_3D(G_q)$-mCherry positive neurons in the DMH in 11 of the 16 injected rats, but $hM_3D(G_q)$-mCherry expression was not restricted to the DMH (Figure 5B). The DMH was not the main target, and it was impossible to define the predominant hypothalamic subregions with $hM_3D(G_q)$-mCherry positive neurons due to diffuse mCherry staining around the injection site.

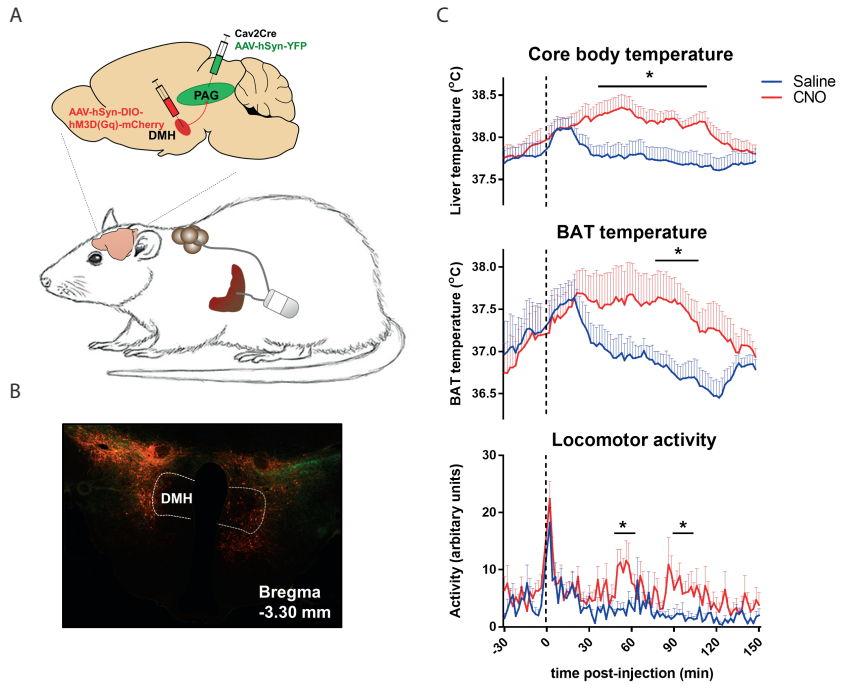

Figure 5. The effect of chemogenetic activation of DMH to PAG projections on thermoregulation. (A) Rats were implanted with an intra-abdominal transmitter with one lead to the liver (to measure core body temperature) and one lead to brown adipose tissue (BAT). To selectively study the effect of dorsomedial hypothalamus (DMH) to periaqueductal grey (PAG) projections on thermoregulation, CAV2Cre was injected into the PAG and Cre-dependent DREADD $hM_3D(G_q)$ mCherry was injected into the DMH. An AAV-hSyn-YFP virus was injected together with CAV2Cre to visualize the injection site in the PAG. (B) Example injection site of DREADD $hM_3D(G_q)$ in the DMH, showing hM3D(Gq)-mCherry positive neurons in the DMH and surrounding areas. (C) CNO treatment in rats with hM3D(Gq)-mCherry positive neurons in the DMH increased core body temperature, BAT temperature, and locomotor activity. Data are shown as mean ± SEM; n=7-11.

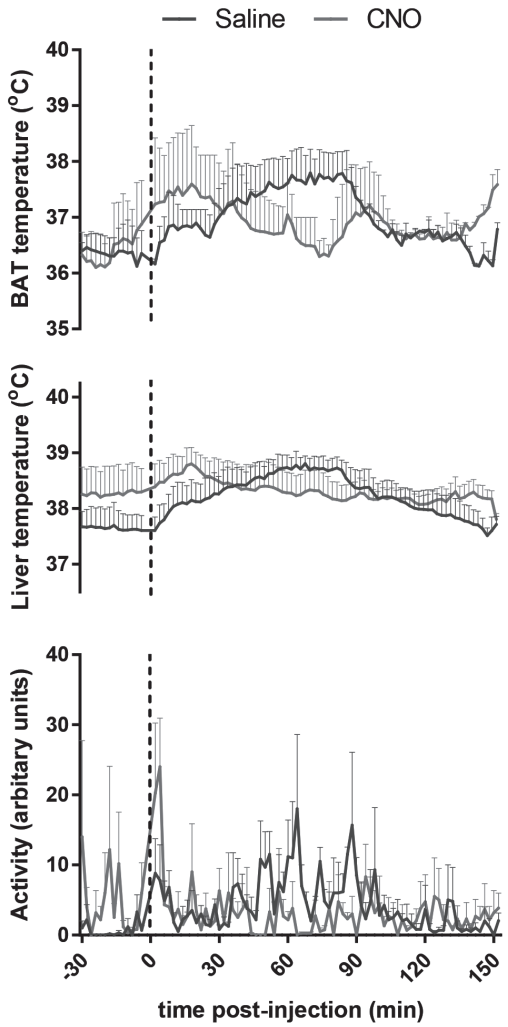

Figure 6. Thermoregulation in rats that show no hM3D(Gq)-mCherry positive neurons in the DMH.
CNO treatment in rats that showed no hM3D(Gq)-mCherry positive neurons in the DMH did not have an effect on core body temperature ($F_{treatment(1,2)}$=0.109, p=0.773), BAT temperature ($F_{treatment(1,1)}$=0.187, p=0.740), and locomotor activity ($F_{treatment(1,2)}$=3.409, p=0.206). Data are shown as mean ± SEM; n=2-3.

As a first step to asses the role of the DMH to PAG projection in thermogenesis, we combined results of all DMH hit rats and investigated the effect of chemogenetic activation with CNO (i.p., 0.3 mg/kg/ml) injections on thermoregulation. The temperature response to CNO differed significantly between DMH hit and DMH miss rats (core body and BAT temperature: $F_{treatment*time*group(74,\ 888/518)} \geq 2.824$, $p<0.01$). In DMH hit rats, CNO significantly increased core body temperature, starting after 30 minutes and returning to baseline within 150 minutes after injection (temperature response 1-150 min. after i.p., $F_{treatment*time(74,\ 740)}$=1.259, p=0.077; $F_{treatment(1,10)}$=9.496, p=0.012) (Figure 5C). The rise in core body temperature may result from the significant increase in BAT thermogenesis, as the time-course of the rise in BAT temperature was similar to that of core body temperature ($F_{treatment*time(74,\ 444)}$=1.292, p=0.063; $F_{treatment(1,\ 6)}$=6.380, p=0.045) (Figure 5C). However, as CNO injections also increased locomotor activity ($F_{treatment*time(74,\ 740)}$=1.253, p=0.081; $F_{treatment(1,\ 10)}$=15.595, p<0.01) (Figure 5C), the rise in core body temperature may not exclusively result from increased BAT thermogenesis. In rats that showed no $hM_3D(G_q)$-mCherry positive neurons in the DMH, CNO treatment did not affect thermogenesis or locomotor activity (Figure 6). Taken together, these findings support the literature showing that activation of DMH neurons projecting to the PAG increases thermogenesis [18,20], but we cannot exclude that surrounding hypothalamic subregions contribute to this effect.

Discussion

The PAG is a relatively long brain region with distinct subdivisions, representing longitudinal columns. The boundaries of these columns were previously established on the basis of anatomical connections, functional properties, and chemical properties [21]. We here performed the first study of DMH projections to PAG subdivisions along the entire anterior-posterior axis of the PAG. Our study shows projections from the DMH to especially the d/lPAG, but also indicates that there is a diffuse projection from the hypothalamus to the PAG rather than specific input from the DMH. The predominant hypothalamic input areas of the PAG vary largely per injection site, but generally include the dorsohypothalamic area (DHA), posterior hypothalamus (PH), lateral hypothalamus (LH), and ventromedial hypothalamus (VMH), which are positioned directly adjacent to the DMH. The points raised above illustrate the necessity for very specific virus injections in the relatively small DMH region of the hypothalamus and distinct subdivisions of the PAG to unravel their specific anatomical and functional connections, which appeared technically challenging.

Anterograde tracing from DMH to PAG

In our anterograde tracing study from DMH to PAG, we aimed to specifically target the DMH, but observed some viral spread in the surrounding areas, especially the DHA. Since the DHA has been shown to project to the PAG [23], the projections we observed in the PAG were probably not specific for the DMH. Tracer spread to surrounding areas is a common problem in anterograde tracing studies of the

DMH [24-26]. It is difficult to directly compare the extent of viral spread around the injection site with previous anterograde tracing studies, as the injection site was previously only shown for one anterior-posterior level from bregma and/or for only one or a few representative cases [24-26].

Our finding that the anterior and middle parts of the PAG receive projections from the DMH in their dorsal and lateral subdivisions, is roughly in accordance with the results of ter Horst et al. [25] and Thompson et al. [26], as far as could be determined at the limited number of anterior-posterior levels they presented. However, in the posterior PAG, ter Horst et al. [25] and Thompson et al. [26] showed relatively more projections in the vlPAG. One limitation of our tracing study is that we were not able to discriminate between passing fibers and terminal fields. It is likely that a substantial portion of the fibers we observed in the PAG are axons of passage with some terminal fields interspersed, as this was previously shown by studies that used tracers that enable discrimination between passing fibers and terminal labeling [23, 25, 26]. Such studies showed most abundant axonal branching and terminal fields in the posterior vlPAG [25, 26]. Therefore, one explanation for why we observed most fibers in the d/lPAG, whereas previous studies reported the most prominent innervation in the vlPAG (often at unknown anterior-posterior levels from bregma) [23, 24, 26], may result from visualizing fibers versus terminal fields, respectively. Alternatively, differences in the location of the injection site in the DMH or in the surrounding area to which the virus spread, may explain differences in projection patterns in the PAG. In comparison with previous studies, the injections sites in our study were located in more anterior parts of the DMH [23-26].

Retrograde tracing from PAG to DMH

Since we were not able to discriminate between passing fibers and terminal ends in our anterograde tracing from the DMH to the PAG, we intended to confirm the identified projections by injecting a retrograde rabies virus in the dlPAG at different anterior-posterior levels. Because this tracer does not label the injection site, we co-injected an AAV-GFP virus to visualize the injection site, which only provides an indication of the injection site as the viral spread may be different for the rabies vs AAV virus. Analysis of the estimated injection sites indicates that most rats were hit in the vlPAG instead of the targeted dlPAG, which complicates the ability to confirm the identified projections from the DMH to the dlPAG. Nevertheless, the four rats that showed relatively more inputs in the DMH compared with other rats, all showed some expression in the dlPAG around -6.80 mm till -8.00 mm from bregma, which supports the findings of the anterograde tracing study that especially the d/lPAG receives input from the DMH. The existence of anatomical connections between the DMH and dlPAG around -6.80 mm till -8.00 mm from bregma is supported by physiological data. Studies showing that the PAG is an important relay in the descending pathways mediating the thermogenic, cardiovascular, and locomotor response evoked by activation of the DMH, all targeted the dlPAG between -6.80 mm till -8.30 mm from bregma [18, 34-37], and found no effect of chemical inhibition of the vlPAG on DMH-evoked responses [36].

One important finding of the rabies tracing is that the PAG receives a diffuse input from the hypothalamus, rather than a specific input from the DMH. This finding is supported by literature showing that other hypothalamic regions, including the LH, VMH, perifornical area (PeF), DHA, and PH, project to the PAG [23, 38-41]. We here show that the hypothalamic areas providing predominant input to the PAG vary largely per injection site, but generally include the DHA, PH, LH, and VMH. The size and cell density differ between the hypothalamic subregions that were assessed. These differences create evaluation problems of the relative importance of input from the DMH compared with other hypothalamic subregions. Therefore, comparison of the relative importance of the input from the distinct hypothalamic subregions needs caution. Despite this limitation, it is obvious that the predominant input areas vary largely per PAG subdivision, and that the DMH is generally not one of the major hypothalamic input regions.

Role of the DMH to PAG projection in thermoregulation

Interestingly, the hypothalamic subregions that provided the predominant input to the PAG in the rabies tracing, i.e. the DHA, PH, LH, and VMH, were all shown to mediate thermogenesis [15, 33, 42-50]. Since these subregions all lie in the immediate proximity of the DMH, it is critical to specifically hit the DMH in intervention studies that aim to unravel the role of the PAG in DMH-evoked thermogenesis.

We here aimed to selectively activate neurons projecting from the DMH to distinct subdivisions of the PAG by the combined use of CAV2Cre and Cre-dependent DREADD technology. In principle, this method allows more selective activation of DMH to PAG projections than the method employed by previous studies [18, 20, 34-37]. In those studies, the DMH to PAG connection was modulated by chemical (dis) inhibition of the DMH and PAG via local injection of drugs, which does not allow for the specific activation (or disinhibition) of DMH neurons that project to the PAG. However, we failed to specifically hit the DMH and distinct subdivisions of the PAG because of diffuse virus expression. Explanations for the diffuse virus expression could be a too large injection volume or too high virus titer. Our injection volume of 300 nl is relatively large compared with the 20-100 nl that was injected in studies that chemically (dis)inhibited the DMH and PAG [18, 20, 34, 36], but is smaller compared with

other studies that used Cre-dependent DREADD technology [27, 29]. The titers we used for CAV2Cre and DREADD $hM_3D(G_q)$ were relatively high compared with previous studies [27, 29].

This is the first study that aimed to investigate the role of the DMH to PAG projection on core body and brown adipose tissue thermogenesis in conscious rats. Our findings suggest that the increase in core body temperature results mostly from the larger increase in BAT temperature, as the time-course of the rise in both temperatures was similar. We found a small increase in locomotor activity that might contribute to the increase in core body temperature, but in our study locomotor activity is not likely to be an important contributor because of the delayed and unstable response pattern. Locomotor activity was previously also shown not to be causal to DMH-evoked increases in core body temperature [18]. It should be noted that reduced heat loss via the tail through vasoconstriction might also contribute to the CNO-induced increase in core body temperature, as the tail is an important thermoregulatory effector organ in rodents, and both the DMH and PAG have been implicated in the regulation of tail blood flow [5, 6, 8, 18, 19]. Because of the diffuse virus injections, we cannot exclude the possibility that other hypothalamic subregions, that were hit in the DMH hit but not the DMH miss group, mediated the CNO effects on BAT and core body thermogenesis that were only observed in DMH hit rats. Importantly, the histology analysis showed that the DMH often contains less $hM_3d(G_q)$-mCherry positive neurons compared with the surrounding hypothalamic subregions, which is in accordance with the rabies tracing result showing that the DMH is generally not one of the most important input areas for the PAG. Therefore, at least some of the thermogenic effects we observed were potentially mediated by hypothalamic subregions surrounding the DMH. Neurons in these subregions were shown to play a role in thermogenesis [15, 33, 42, 50] and project to the PAG [23, 38-40], but the function of their projection to the PAG has not been investigated yet.

Conclusion

To conclude, we emphasize the importance of making specific, small virus injections into the DMH and PAG subdivisions, to study the precise anatomical and functional connection between them. This is a critical technical requirement because the PAG receives a diffuse input from the DMH and adjacent hypothalamic subregions, which were previously shown to play a role in thermoregulation as well [15, 33, 42-50]. Performing (dual) specific virus injections appeared to be technically challenging in our experiments, resulting in an unprecise determination of the role of the DMH to PAG projections in thermoregulation. Thus, our study shows the complexity of the connection between the hypothalamus and the PAG, and demonstrates some of the limitations of (dual) viral vector technology.

Acknowledgements

We thank Jos Brits for his practical assistance. This research was supported by the Dutch Technology Foundation STW (grant 12264), which is part of the Netherlands Organisation for Scientific Research (NWO), and which is partly funded by the Ministry of Economic Affairs, and by DFG (SPP1665 and CRC870) to KC.

Conflict of interest

The authors declare that no competing interests exist.

References

1. Seale P, Lazar MA. Brown fat in humans: turning up the heat on obesity. *Diabetes* 2009; **58**: 1482-1484.
2. Maclean PS, Bergouignan A, Cornier MA, Jackman MR. Biology's response to dieting: The impetus for weight regain. *Am J Physiol Regul Integr Comp Physiol* 2011; **301:** R581-600.
3. Rosenbaum M, Leibel RL. Adaptive thermogenesis in humans. *Int J Obes (Lond)* 2010; **34:** S47-55.
4. Heeren J, Munzberg H. Novel aspects of brown adipose tissue biology. *Endocrinol Metab Clin North Am* 2013; **42**: 89-107.
5. Dimicco JA, Zaretsky DV. The dorsomedial hypothalamus: a new player in thermoregulation. *Am J Physiol Regul Integr Comp Physiol* 2007; **292**: R47-63.
6. Morrison SF. Central neural control of thermoregulation and brown adipose tissue. *Auton Neurosci* 2016; **196**: 14-24.
7. Morrison SF, Madden CJ, Tupone D. Central neural regulation of brown adipose tissue thermogenesis and energy expenditure. *Cell Metab* 2014; **19**: 741-756.
8. Rezai-Zadeh K, Munzberg H. Integration of sensory information via central thermoregulatory leptin targets. *Physiol Behav* 2013; **121**: 49-55.
9. Clapham JC. Central control of thermogenesis. *Neuropharmacology* 2012; **63**: 111-123.
10. van Marken Lichtenbelt WD, Vanhommerig JW, Smulders NM, Drossaerts JM, Kemerink GJ, Bouvy ND, et al. Cold-activated brown adipose tissue in healthy men. *N Engl J Med* 2009; **360**: 1500-1508.
11. Nedergaard J, Bengtsson T, Cannon B. Unexpected evidence for active brown adipose tissue in adult humans. *Am J Physiol Endocrinol Metab* 2007; **293**: E444-52.
12. Cypess AM, Lehman S, Williams G, Tal I, Rodman D, Goldfine AB, et al. Identification and importance of brown adipose tissue in adult humans. *N Engl J Med* 2009; **360**: 1509-1517.
13. Virtanen KA, Lidell ME, Orava J, Heglind M, Westergren R, Niemi T, et al. Functional brown adipose tissue in healthy adults. *N Engl J Med* 2009; **360**: 1518-1525.
14. Morrison SF, Nakamura K, Madden CJ. Central control of thermogenesis in mammals. *Exp Physiol* 2008; **93**: 773-797.
15. Rezai-Zadeh K, Yu S, Jiang Y, Laque A, Schwartzenburg C, Morrison CD, Derbenev AV, Zsombok A, Munzberg H. Leptin receptor neurons in the dorsomedial hypothalamus are key regulators of energy expenditure and body weight, but not food intake. *Mol Metab* 2014; **3:** 681-693
16. Zaretskaia MV, Zaretsky DV, Shekhar A, DiMicco JA. Chemical stimulation of the dorsomedial hypothalamus evokes non-shivering thermogenesis in anesthetized rats. *Brain Res* 2002; **928**: 113-125.
17. Cao WH, Fan W, Morrison SF. Medullary pathways mediating specific sympathetic responses to activation of dorsomedial hypothalamus. *Neuroscience* 2004; **126**: 229-240.
18. de Menezes RC, Zaretsky DV, Fontes MA, DiMicco JA. Microinjection of muscimol into caudal periaqueductal gray lowers body temperature and attenuates increases in temperature and activity evoked from the dorsomedial hypothalamus. *Brain Res* 2006; **1092**: 129-137.
19. Chen XM, Nishi M, Taniguchi A, Nagashima K, Shibata M, Kanosue K. The caudal periaqueductal gray participates in the activation of brown adipose tissue in rats. *Neurosci Lett* 2002; **331**: 17-20.
20. Rathner JA, Morrison SF. Rostral ventromedial periaqueductal gray: a source of inhibition of the sympathetic outflow to brown adipose tissue. *Brain Res* 2006; **1077**: 99-107.
21. Dampney RA, Furlong TM, Horiuchi J, Iigaya K. Role of dorsolateral periaqueductal grey in the coordinated regulation of cardiovascular and respiratory function. *Auton Neurosci* 2013; **175**: 17-25.
22. de Menezes RC, Zaretsky DV, Fontes MA, DiMicco JA. Cardiovascular and thermal responses evoked from the periaqueductal grey require neuronal activity in the hypothalamus. *J Physiol* 2009; **587**: 1201-1215.
23. Papp RS, Palkovits M. Brainstem projections of neurons located in various subdivisions of the dorsolateral hypothalamic area-an anterograde tract-tracing study. *Front Neuroanat* 2014; **8**: 34.
24. Lee SJ, Kirigiti M, Lindsley SR, Loche A, Madden CJ, Morrison SF, et al. Efferent projections of neuropeptide Y-expressing neurons of the dorsomedial hypothalamus in chronic hyperphagic models. *J Comp Neurol* 2013; **521**: 1891-1914.
25. ter Horst GJ, Luiten PG. The projections of the dorsomedial hypothalamic nucleus in the rat. *Brain Res Bull* 1986; **16**: 231-248.
26. Thompson RH, Canteras NS, Swanson LW. Organization of projections from the dorsomedial nucleus of the hypothalamus: a PHA-L study in the rat. *J Comp Neurol* 1996; **376**: 143-173.
27. Boender AJ, de Jong JW, Boekhoudt L, Luijendijk MC, van der Plasse G, Adan RA. Combined use of the canine adenovirus-2 and DREADD-technology to activate specific neural pathways in vivo. *PLoS One* 2014; **9**: e95392.
28. Hnasko TS, Perez FA, Scouras AD, Stoll EA, Gale SD, Luquet S, et al. Cre recombinase-mediated restoration of nigrostriatal dopamine in dopamine-deficient mice reverses hypophagia and bradykinesia. *Proc Natl Acad Sci U S A* 2006; **103**: 8858-8863.
29. Boekhoudt L, Omrani A, Luijendijk MC, Wolterink-Donselaar IG, Wijbrans EC, van der Plasse G, et al. Chemogenetic activation of dopamine neurons in the ventral tegmental area, but not substantia nigra, induces hyperactivity in rats. *Eur Neuropsychopharmacol* 2016; **26**: 1784-1793.
30. Ghanem A, Conzelmann KK. G gene-deficient single-round rabies viruses for neuronal circuit analysis. *Virus Res* 2016; **216**: 41-54.
32. Wickersham IR, Finke S, Conzelmann KK, Callaway EM. Retrograde neuronal tracing with a deletion-mutant rabies virus. *Nat Methods* 2007; **4**: 47-49.
33. Zhang Y, Kerman IA, Laque A, Nguyen P, Faouzi M, Louis GW, Jones JC, Rhodes C, Munzberg H. Leptin-receptor-expressing neurons in the dorsomedial hypothalamus and median preoptic area regulate sympathetic brown adipose tissue circuits. *J Neurosci* 2011; **31:** 1873-1884.
34. Horiuchi J, McDowall LM, Dampney RA. Vasomotor and respiratory responses evoked from the dorsolateral periaqueductal grey are mediated by the dorsomedial hypothalamus. *J Physiol* 2009; **587**: 5149-5162.
35. da Silva LG,Jr, Menezes RC, Villela DC, Fontes MA. Excitatory amino acid receptors in the periaqueductal gray mediate the cardiovascular response evoked by activation of dorsomedial hypothalamic neurons. *Neuroscience* 2006; **139**: 1129-1139.
36. da Silva LG, de Menezes RC, dos Santos RA, Campagnole-Santos MJ, Fontes MA. Role of periaqueductal gray on the cardiovascular response evoked by disinhibition of the dorsomedial hypothalamus. *Brain Res* 2003; **984**: 206-214.
37. Villela DC, da Silva LG,Jr, Fontes MA. Activation of 5-HT receptors in the periaqueductal gray attenuates the tachycardia evoked from dorsomedial hypothalamus. *Auton Neurosci* 2009; **148**: 36-43.
38. Yoshida K, Konishi M, Nagashima K, Saper CB, Kanosue K. Fos activation in hypothalamic neurons during cold or warm exposure: projections to periaqueductal gray matter. *Neuroscience* 2005; **133**: 1039-1046.
39. Canteras NS, Simerly RB, Swanson LW. Organization of projections from the ventromedial nucleus of the hypothalamus: a Phaseolus vulgaris-leucoagglutinin study in the rat. *J Comp Neurol* 1994; **348**: 41-79.
40. Mota-Ortiz SR, Sukikara MH, Felicio LF, Canteras NS. Afferent connections to the rostrolateral part of the periaqueductal gray: a critical region influencing the motivation drive to hunt and forage. *Neural Plast* 2009; **2009**: 612698.
41. Saper CB, Swanson LW, Cowan WM. The efferent connections of the ventromedial nucleus of the hypothalamus of the rat. *J Comp Neurol* 1976; **169**: 409-442.

42. hornhill J, Halvorson I. Activation of shivering and non-shivering thermogenesis by electrical stimulation of the lateral and medial preoptic areas. *Brain Res* 1994; **656**: 367-374.
43. Amir S. Intra-ventromedial hypothalamic injection of glutamate stimulates brown adipose tissue thermogenesis in the rat. *Brain Res* 1990; **511**: 341-344.
44. Amir S. Activation of brown adipose tissue thermogenesis by chemical stimulation of the posterior hypothalamus. *Brain Res* 1990; **534**: 303-308.
45. Halvorson I, Gregor L, Thornhill JA. Brown adipose tissue thermogenesis is activated by electrical and chemical (L-glutamate) stimulation of the ventromedial hypothalamic nucleus in cold-acclimated rats. *Brain Res* 1990; **522**: 76-82
46. Holt SJ, Wheal HV, York DA. Hypothalamic control of brown adipose tissue in Zucker lean and obese rats. Effect of electrical stimulation of the ventromedial nucleus and other hypothalamic centres. *Brain Res* 1987; **405**: 227-233.
47. Kobayashi A, Osaka T, Namba Y, Inoue S, Kimura S. CGRP microinjection into the ventromedial or dorsomedial hypothalamic nucleus activates heat production. *Brain Res* 1999; **827**: 176-184.
48. Minokoshi Y, Saito M, Shimazu T. Sympathetic denervation impairs responses of brown adipose tissue to VMH stimulation. *Am J Physiol* 1986; **251**: R1005-8.
49. Belanger-Willoughby N, Linehan V, Hirasawa M. Thermosensing mechanisms and their impairment by high-fat diet in orexin neurons. *Neuroscience* 2016; **324**: 82-91.
50. Morrison SF, Madden CJ, Tupone D. An orexinergic projection from perifornical hypothalamus to raphe pallidus increases rat brown adipose tissue thermogenesis. *Adipocyte* 2012; **1**: 116-120.
51. Nakamura K, Morrison SF, Central efferent pathways mediating skin-evoked sympathetic thermogenesis in brown adipose tissue. *Am J Phyiol Regul Integr Comp Physiol* 2006; **292:** R127-136

Chapter 6:

Zona incerta neurons projecting to the ventral tegmental area promote action initiation towards feeding

Kathy C.G. de Git[1], Esther M. Hazelhoff[1], Minke H.C. Nota[1], Mieneke C.M. Luijendijk[1], Geoffrey van der Plasse[1*], Roger A.H. Adan[1,2*]

1 Brain Center Rudolf Magnus, Dept. of Translational Neuroscience, University Medical Center Utrecht, Utrecht University, Utrecht 3584 CG, The Netherlands
2 Institute of Neuroscience and Physiology, Sahlgrenska Academy, University of Gothenburg, Sweden

* These authors contributed equally

Submitted

Abstract

Both the zona incerta (ZI) and the ventral tegmental area (VTA) have been implicated in feeding behavior. The ZI provides prominent input to the VTA, but it has not been investigated yet whether this projection regulates feeding. Therefore, we investigated the role of ZI to VTA projection neurons in the regulation of several aspects of feeding behavior. We determined the effects of (in)activation of ZI to VTA projection neurons on feeding microstructure, food-motivated behavior under a progressive ratio schedule of reinforcement, locomotor activity, and core body temperature. To activate or inactivate ZI neurons projecting to the VTA, we used a combination of canine adenovirus-2 in the VTA, and Cre-dependent designer receptors exclusively activated by designer drugs (DREADD) or tetanus toxin (TetTox) light chain in the ZI, respectively. TetTox-mediated inactivation of ZI to VTA projection neurons reduced food-motivated behavior and feeding by reducing meal frequency. Conversely, DREADD-mediated chemogenetic activation of ZI to VTA projection neurons promoted food-motivated behavior and feeding. (In)activation of ZI to VTA projection neurons did not affect locomotor activity or directly regulate core body temperature. Taken together, ZI neurons projecting to the VTA exert bidirectional control over feeding behavior. More specifically, activity of ZI to VTA projection neurons facilitate action initiation towards feeding, as reflected in both food-motivated behavior and meal initiation, without affecting general activity.

Introduction

The worldwide prevalence of obesity is steadily increasing [1]. In our modern society, a sedentary lifestyle combined with calorie overconsumption plays an important role in the etiology of obesity [2, 3]. Understanding the neurobiology of different aspects of feeding behavior, such as motivational drive, satiety, and the anticipation to food, is a first step to tackle the obesity epidemic [4, 5].

Among neural circuits regulating feeding, the mesolimbic dopamine (mesDA) system has been implicated in food motivation [5-10]. The mesDA system consists of dopaminergic neurons in the ventral tegmental area (VTA) that project to cortico-limbic structures such as the ventral striatum [5, 10]. DA is an important modulator of feeding behavior. DA-deficient mice starve to death without additional treatment with the dopamine precursor L-DOPA [11]. Conversely, alterations in the mesDA system, such as reduced DA D2 receptor expression in the striatum, have been associated with overconsumption and obesity in both animals and humans [12-17]. The precise role of VTA DA signaling in the control of food intake is incompletely understood, but VTA DA signaling is at least crucially involved in the motivation to work for food [6-9, 18], and was shown to facilitate both the initiation and cessation of feeding [10].

The VTA receives input from metabolic centers located in the hypothalamus that regulate feeding behavior and energy balance [5, 9, 19]. The lateral hypothalamus (LH) and zona incerta (ZI) provide the major direct hypothalamic innervation of the VTA [20, 21]. While the LH>VTA projection has been extensively studied [22], the ZI>VTA projection has not been studied yet. The first evidence for a role of the ZI in feeding behavior was provided by ZI lesion studies in rats, which resulted in a reduction in *ad libitum* feeding and body weight [23, 24 but see 25]. In addition, studies in sheep showed that the ZI responds to the ingestion and especially the sight of food by releasing γ-aminobutyric acid (GABA) [26, 27]. Recently, stimulation of ZI GABA neurons was shown to evoke binge-like eating and body weight gain in mice [28]. Also patients with Parkinson's disease receiving deep brain stimulation of the subthalamus, including the ZI, sometimes show binge-like eating [29, 30]. Thus, several lines of evidence indicate that the ZI is involved in feeding and energy balance. The ZI has robust projections throughout the brain [25], and was previously shown to mediate feeding behavior via projections to the paraventricular thalamus [28], but the role of its projections to the VTA has not been studied yet.

In the current study, we investigated whether the ZI projections to the VTA regulate feeding behavior. Several aspects of feeding behavior, including the motivation to work for food and feeding microstructure, were assessed. Locomotor activity and body temperature were also tested in order to determine whether ZI>VTA projection neurons specifically mediate feeding behavior, or also have a role in energy metabolism. We first permanently inactivated ZI>VTA projection neurons by using a combination of canine adenovirus 2 (CAV2Cre) in the VTA [31-33], and Cre-dependent tetanus toxin (TetTox) light chain in the VTA [34,35]. Then, we tested whether chemogenetic activation of ZI>VTA projection neurons, by the combined use of CAV2Cre in the VTA and Cre-dependent designer receptors exclusively activated by designer drugs (DREADD) in the ZI [31-33] results in opposite effects on feeding behavior.

Experimental procedures

Animals and ethical approval

Upon arrival, adult male Wistar rats (Charles-River, Sulzfeld, Germany) were group housed in a temperature (21-23 °C) and light controlled (lights on between 13.00 and 1.00 h) room. At the time of surgery, rats weighed 385±5 grams in experiment 1 and 484±10 grams in experiment 2. Following surgery, rats were housed individually in Plexiglas cages. Rats had *ad libitum* access to pelleted rat chow (3.31 kcal/g; Special Diet Service, UK) and tap water, unless stated otherwise. In experiment 1, rats were food restricted from week 11-16, during which rats received 4 gr chow per 100 gr body weight. All experiments were approved by the Animal Ethics Committee of Utrecht University and conducted in agreement with Dutch laws (Wet op de Dierproeven, 1996; revised 2014) and European regulations (Guideline 86/609/EEC; Directive 2010/63/EU).

Experiment 1: Inactivation of ZI-region to VTA projection neurons

Surgery – inactivating ZI-region to VTA projection neurons

The first group consisted of 18 rats, which were randomly divided into two subgroups of 9 rats based on their average body weight and the motivation to work for food rewards (number of rewards) during operant conditioning in the two weeks before surgery. The first subgroup, referred to as the TetTox group, was bilaterally injected with 1.0 µl of AAV-CBA-DIO-GFP:TetTox (1.0*1012 genomic copies/ml, kindly provided by Richard D. Palmiter [35] in the ZI, and bilaterally injected with 0.3 µl of a mixture of CAV2cre (final concentration in mixture 1.25*1012 genomic copies/ml; IGMM, France) and AAV-hSyn-mCherry (final concentration in mixture 1.0*1012 genomic copies/ml; UNC vector core) in the VTA. The second subgroup, referred to as the control group, was bilaterally injected with 0.3 µl of AAV-hSyn-DIO-hM3D(Gq)-mCherry (1.0*1012 genomic copies/ml; UNC vector core) in the ZI, and bilaterally injected with 0.3 µl of a mixture of CAV2cre (final concentration in mixture 1.25*1012 genomic copies/ml; IGMM, France) and AAV-hSyn-YFP (final concentration in mixture 1.0*1012 genomic copies/ml; UNC vector core) in the VTA. For both subgroups, the same coordinates were used for the ZI (from bregma: anterior-posterior (AP): -2.30 to -2.50 mm, medio-lateral (ML): +1.40 mm, dorso-ventral (DV): -9.30 mm, at an angle of 5°), and the VTA (from bregma: AP: -5.40 mm, ML: +2.20 mm, DV: -8.90 mm, at an angle of 10°). As there were no differences observed between virus expression and behavioral measures between the different AP coordinates, they were considered to be equal and combined for statistical analyses. In addition, an intra-abdominal transmitter (TA10TA-F40, Data Science International, USA) was implanted to continuously monitor core body temperature and locomotor activity.

Surgery was performed under fentanyl/fluanisone (0.315 mg/kg fentanyl, 10 mg/kg fluanisone, Hypnorm, Janssen Pharmaceutica, Belgium) and midazolam (2.5 mg/kg, i.p., Actavis, the Netherlands) anesthesia. Xylocaine was sprayed on the skull to provide local anesthesia (Lidocaine 100 mg/ml, AstraZeneca BV, the Netherlands). All rats received three daily peri-surgical injections of carprofen (5 mg/kg, s.c. Carporal, AST Farma BV, the Netherlands), starting at the day of surgery.

Operant conditioning – testing the motivation to work for food rewards

Apparatus. Experiments were conducted in two-lever operant conditioning chambers designed for rats (30.5x24.1x21.0 cm; Med associates, USA), which were placed in light- and sound-attenuating cubicles equipped with a ventilation fan. Each chamber was equipped with a metal grid floor, two retractable levers with a cue light above each lever, a pellet dispenser to deliver sucrose pellets (45 mg, TestDiet, USA) to a receptacle between the two levers, and a house light. Data collection and processing was controlled by MED-PC software.

Training. Starting approximately six weeks before surgery, rats learned to lever press for sucrose pellets under a fixed ratio (FR)1 schedule, as described previously [36]. During each trial both levers were present, but only presses on the active lever (ALPs) led to delivery of a sucrose pellet, illumination of the cue light above the active lever, and retraction of both levers. Twenty seconds after the pellet was received, the levers were reinserted into the chamber. Presses on the inactive lever

(ILPs) were recorded, but this had no consequence. After acquisition of sucrose self-administration under this schedule, rats were further trained on a FR3 schedule and then on a FR5 schedule, where the response requirement to obtain a sucrose pellet was increased to three and five ALPs, respectively. All sessions lasted 30 min or until rats had earned the maximum number of pellets (*i.e.* 60 for FR1 and FR3, and 30 for FR5), whichever occurred first. Four weeks before surgery, all rats were considered trained and a progressive ratio (PR) schedule was implemented.

Progressive ratio

The effort rats were willing to make for a sucrose reward was tested under a PR schedule, in which the response requirement to obtain a sucrose pellet was progressively increased after each obtained reward [1, 2, 4, 9, 12, 15, 20, 25, 32, 40, 50, 62, 77, 95, 118, 145, 178, 219, 268, 328, 402, 492, 603, 737 (36)]. The session ended when the rat had failed to earn a reward within 30 min. All PR sessions started before 12.00h and were completed before 13.00h. Rats of the control and TetTox group were equally divided over the chambers and sessions. PR responding was assessed five days per week for four weeks prior to virus injections. Four weeks after virus injections, PR testing recommenced and was assessed three days per week, both under *ad libitum* feeding (week 4-9) and restricted feeding in the home cage (week 12-16).

Feeding patterns – measuring feeding microstructure

Feeding behavior was studied by using data collected by Scales (Department Biomedical Engineering, UMC Utrecht, The Netherlands) [37, 38]. This program records the weight of food hoppers in the home cage automatically every 12 s. To study feeding behavior without interference by behavioral tasks or handling, weekend data were analyzed for each week. Feeding microstructure was analyzed from week 6 to 9 during *ad libitum* feeding. As previously [37, 38], a meal was defined as an episode of food intake with a minimal consumption of 1 kcal (0.3 gr chow), and a minimal inter-meal interval of 5 min.

Telemetric measurements – locomotion and temperature measurement

Each home cage was placed on a receiver plate (DSI, USA) that received radiofrequency signals from the abdominal transmitter. The plates were connected to software (DSI, USA) that recorded core body temperature and locomotor activity every 10 minutes. To study telemetry data without interference by behavioral tasks or handling, 48h weekend data was analyzed for each week, and detailed telemetry data per hour was analyzed for week 6 to 9.

Tissue preparation – checking virus injection sites

In week 29 post-surgery, rats were given a lethal dose of sodium pentobarbital (200 mg/ml, Euthanimal, Alfasan BV, The Netherlands), and were transcardially perfused with 0.9% NaCl followed by 4% paraformaldehyde (PFA) in phosphate buffered saline (PBS). Brains were excised and kept in 4% PFA for 24h, and were subsequently saturated with 30% sucrose in PBS with 0.01% NaN3. Brains were snap frozen in isopentane between -60ºC and -40ºC, and sliced into 40 µm sections using a cryostat (Leica, Germany). Tissue was collected in six series in cryo-protectant (25% glycerol; 25% ethylene-glycol in PBS) and stored at -20ºC.

Immunohistochemistry – checking virus injection sites

One series of brain slices was washed in PBS and subsequently blocked and permeabilized in blocking solution (PBS containing 10% fetal calf serum and 1% triton X-100) for 2h. Subsequently, slices were incubated overnight at 4 ºC with primary chicken anti-GFP antibody (1:500, Abcam, UK) and rabbit anti-dsRed (1:500, Clontech) in blocking solution. After washing in PBS, brain slices were incubated with Alexa-488 labeled secondary goat anti-chicken, and Alexa-568 labeled goat anti-rabbit (1:500, Abcam, UK) antibodies in blocking solution for 2h. After washing in PBS, slices were mounted on SuperFrost glasses (VWR, Leuven) and covered with FluorSave (Milipore).

In situ hybridization - checking virus injection sites

In situ hybridization (ISH) was performed for the detection of (floxed) GFP expressed by the AAV-CBA-DIO-GFP:TetTox virus in the ZI-region. One series of (perfused) brain slices was washed in PBS, acetylated for 10 min., and washed again in PBS. Slices were pre-hybridized in hybridization solution (50% formamide, 5x SSC, 5x Denhardt's, 250 µg/ml tRNA Bakers yeast, 500 µg/ml sonificated salmon sperm DNA) for 2h at room temperature. Subsequently, slices were incubated overnight at 68ºC in hybridization solution containing 400 ng/ml 720bp long digoxigenin (DIG)-labeled enhanced green fluorescent protein probe (eGFP) riboprobe (antisense to NCBI gene DQ768212). Slices were quickly washed in pre-warmed (68ºC) 2x SSC, and then incubated in pre-warmed 0.2x SSC for 2h at 68ºC. DIG was detected with an alkaline phosphatase labeled antibody (1:5000, Roche, Germany) after overnight incubation at room temperature using NBT/BCIP as a substrate. Slices were mounted on SuperFrost glasses (VWR, Leuven), dehydrated in ethanol, cleared in xylene and embedded in Entellan.

Histological analysis – checking virus injection sites

Immunofluorescent and ISH slices were photographed and digitized using the epifluorescent and brightfield function of a Zeiss Axioskop 2 microscope (Zeiss, Germany), respectively. The injection site of CBA-DIO-GFP:TetTox in the ZI-region was determined by the expression of GFP RNA positive cell bodies, and the injection site of CAV2cre in the VTA was determined by the expression of cell bodies with mCherry immunoreactivity, resulting from the co-injected AAV-hSyn-mCherry virus.

Experiment 2: Chemogenetic activation of ZI to VTA projections

Surgery – activating ZI to VTA projection neurons

A second group of rats (n=14) underwent surgery under identical procedures as described for experiment 1, but were bilaterally injected with 0.3 µl of the activating DREADD AAV-hSyn-DIO-hM3D(Gq)-mCherry (1.0*1012 genomic copies/ml; UNC vector core) in the ZI (from bregma: AP: -2.30 mm, ML: +1.40 mm, DV: -8.80 mm, at an angle of 0º), and bilaterally injected with 0.3 µl of a mixture of CAV2cre (final concentration in mixture 1.33*1012 genomic copies/ml; IGMM, France) and AAV-hSyn-YFP (final concentration in mixture 1.60*1012 genomic copies/ml; UNC vector core) in the VTA (from bregma: AP: -5.40 mm, ML: +2.20 mm, DV: -8.90 mm, at an angle of 10º).

Drugs

Clozapine-N-oxide (CNO; kindly provided by Bryan Roth and NIMH) was dissolved to a concentration of 0.3 mg/kg/ml in sterile saline (0.9% NaCl). All injections were given intraperitoneally, and the effect of CNO and saline injections on PR responding, feeding behavior, locomotor activity, and body temperature was tested according to a Latin square design. Rats received two habituation saline injections (i.p.) prior to testing.

Operant conditioning – testing the motivation to work for food rewards

PR training was performed via identical procedures as in experiment 1. PR testing recommenced 2.5 weeks after virus injections, and the effect of CNO versus saline on PR responding was assessed 4 weeks after virus injections. Rats were injected 30 min before being placed in the operant chambers. At least one washout day was kept between injections.

Feeding patterns and telemetric measurements – feeding microstructure, locomotion and temperature measurement

The effect of CNO on feeding behavior was tested during the same test session as for body temperature and locomotor activity. Telemetry data was recorded every 2 minutes. During a test session, body temperature and activity were first measured in the absence of food to prevent confounding with feeding-induced thermogenesis. Rats were food restricted at 9.00h, injected with saline or CNO at 14.30h, and food was returned at 15.30h. Rats were once habituated to the test schedule prior to testing. Testing commenced 7 weeks after virus injections, and the interval between the two test sessions of a Latin square design was at least 4 days. Feeding patterns were analyzed up to 6h following food return.

Tissue preparation – checking virus injection sites

In week 10 post-surgery, rats were transcardially perfused and tissue was prepared via identical procedures as in experiment 1.

Immunohistochemistry – checking virus injection sites

One series of brain slices was washed in PBS, blocked and permeabilized in blocking solution (PBS containing 10% normal goat serum (NGS) and 1% triton X-100) for 1h, and washed again in PBS. Subsequently, slices were incubated overnight at 4 ºC with primary chicken anti-GFP antibody (1:500, Abcam, UK) and rabbit anti-dsRed (1:500, Clontech) in carrier solution (PBS containing 3% NGS and 0.25% triton X-100). After washing in PBS, brain slices were incubated with Alexa-488 labeled secondary goat anti-chicken, and Alexa-568 labeled goat anti-rabbit (1:500, Abcam, UK) antibodies in carrier solution for 1h. After washing in PBS, slices were mounted on SuperFrost glasses (VWR, Leuven) and covered with FluorSave (Milipore).

Histological analysis – checking virus injection sites

Histological analysis was performed as described for experiment 1. The injection site of AAV-hSyn-DIO-hM3D(Gq)-mCherry was determined by the expression of mCherry positive cell bodies, and the injection site of CAV2cre in the VTA was determined by the expression of cell bodies with GFP immunoreactivity, resulting from the co-injected AAV-hSyn-YFP virus.

Data analysis

In experiment 1, differences in PR performance, feeding behavior, body weight, and telemetric measurements were tested by performing two-way repeated measures ANOVAs with time as within-subject variable and group (control; TetTox) as between-subject variable. In experiment 2, differences in these parameters were tested by

performing a paired t-test with treatment as within-subject variable or a two-way repeated measures ANOVAs with treatment and time as within-subject variables.

Mauchly's test of sphericity was used to test whether variances of the differences between treatment levels were equal. If the assumption of sphericity was violated, degrees of freedom were corrected using Greenhouse-Geisser (GG) estimates of sphericity or Huynh-Feldt estimates of sphericity when the GG estimate was >0,75. When appropriate, post hoc analyses were conducted using Student's t-tests or pairwise Bonferroni comparisons. Each parameter was tested for normality with the Kolmogorov-Smirnov test. When data were not normally distributed, data was transformed using a square root for count data and log transformation for the other data prior to statistical analyses.

Statistical analyses were conducted using SPSS 20.3 for Windows. The threshold for statistical significance was set at $P<0.05$. Data are presented as mean ± SEM.

In experiment 1, one rat of the control group died shortly after surgery. Three rats of the TetTox group did not show GFP expression in the ZI-region, and were therefore excluded from all analyses. Because of technical issues with the weighing system, the following food intake data were excluded: baseline for one TetTox rat; week 4 for one control rat; week 6 for two control and two TetTox rats. To allow testing by repeated measures ANOVAs, the average of week 3/5 and week 5/7 was taken for the concerning rats in week 4 and 6, respectively. In experiment 2, experiments were performed in two subgroups of rats. The first group consisted of 9 rats. The second group of 5 rats was added later and was tested under similar experimental procedures. One rat of this group died shortly after surgery. As there were no differences observed between virus expression and behavioral measures between the two subgroups, they were considered to be equal and combined for statistical analyses.

Results

Experiment 1: Inactivation of ZI-region to VTA projection neurons

Selective inactivation of ZI-region neurons projecting to the VTA

To study the role of ZI neurons projecting to the VTA, we aimed to specifically inactivate these neurons by injecting CAV2Cre in the VTA and Cre-dependent TetTox light chain (AAV-DIO-GFP:TetTox) in the ZI (Figure 1A). CAV2cre infects neurons at terminals at the injection site and retrogradely delivers Cre in neurons that project to the area of injection, which subsequently enables the expression of Cre-dependent TetTox in projection neurons [31-33]. Expression of TetTox prevents neurotransmitter release from infected neurons [34, 35]. Thus, the combined use of Cre-dependent TetTox and CAV2Cre allows for selective and permanent inactivation of ZI neurons projecting to the VTA. Control rats received a non-inactivating virus (AAV-hSyn-DIO-hM3D(Gq)-mCherry) in the ZI, and CAV2Cre in the VTA.

A

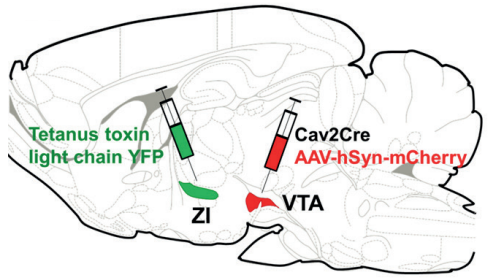

B

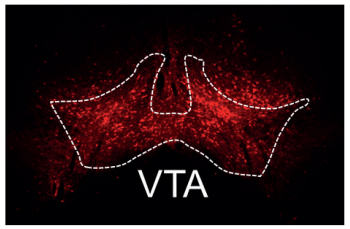

C

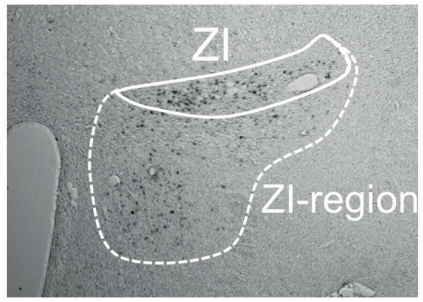

Figure 1. TetTox-GFP is expressed in ZI-region neurons projecting to the VTA. (A) To selectively inactive ZI neurons projecting to the VTA, CAV2Cre was injected into the VTA and Cre-dependent TetTox-GFP was injected into the ZI. An AAV-hSyn-mCherry virus was injected together with CAV2Cre to visualize the injection site in the VTA. (B) Immunofluorescence of mCherry (red) in the VTA following virus injection of CAV2Cre/AAV-hSyn-mCherry (bregma -5.30 mm). (C) TetTox-GFP mRNA expression in the ZI and the zone medioventral to the ZI, together representing the ZI-region (bregma -2.12 mm).

Immunohistological staining of mCherry (from AAV-hSyn-mCherry which was co-injected with CAV2Cre) confirmed correct targeting of the VTA in all rats (Figure 1B), but showed no TetTox-GFP positive neurons around the injection site in the ZI. Perhaps we did not observe TetTox-GFP at the protein level because rats were sacrificed a long time after virus injections. Therefore, we performed ISH to detect TetTox-GFP mRNA expression. TetTox-GFP mRNA expression was present in the ZI, but showed spread in the zone medioventral to the ZI (Figure 1C). Three rats showed no TetTox-GFP positive neurons in the ZI, and were therefore excluded from all analyses. In the remaining six rats, the ZI-region was targeted.

Inactivation of ZI-region to VTA projection neurons reduces food-motivated behavior

To test whether inactivation of ZI-region neurons projecting to the VTA affects food-motivated behavior, responding for sucrose under a PR schedule of reinforcement was tested. Prior to virus injections, control and TetTox rats did not significantly differ in rewards and ALPs ($t \geq 1.804$, $p \geq 0.096$) (Figure 2A, B), but TetTox rats showed a trend for a reduction in ILPs ($t=2.047$, $p=0.063$) (Figure 2C). PR testing recommenced four weeks after virus injections, to allow for sufficient virus expression, and was performed both under *ad libitum* feeding and during food restriction (FR) in the home cage. Immediately following PR retesting, TetTox rats showed a lower number of ALPs, and consequently, earned fewer rewards than control rats (Figure 2A, B). Reduced PR performance in TetTox rats was maintained over the course of *ad libitum* feeding, as well as during FR. In accordance with studies showing that FR improves PR performance [5, 6, 39], control rats obtained more rewards during FR compared with *ad libitum* feeding (week 9: 9.94±0.50 vs week 16: 12.04±0.64; $t=3.979$, $p=0.005$). An FR-induced increase in the number of rewards was also observed in TetTox rats (week 9: 5.08±0.24 vs week 16: 6.94±0.60; $t=2.625$, $p=0.047$), and the adaptive increase in PR responding during FR did not differ from control rats ($F_{feeding\text{-}condition*group}=0.079$, $p=0.783$). These findings indicate that TetTox-inactivation of ZI-region to VTA projection neurons reduces the motivation to work for food reward, but does not affect the motivation to increase food reward seeking in times when the metabolic need for food is increased.

The overall lower PR performance in TetTox rats was associated with a lower number of ILPs during the first three weeks following virus injections, but this trend was already observed prior to virus injections, and the difference with the control group disappeared over time due to a gradual reduction in the number of ILPs in the control group (Figure 2C). Together, these findings suggest that the lower number of ALPs in TetTox rats did not result from a reduction in general activity but was due to a specific reduction in food-motivated behavior. In accordance, TetTox rats did not differ

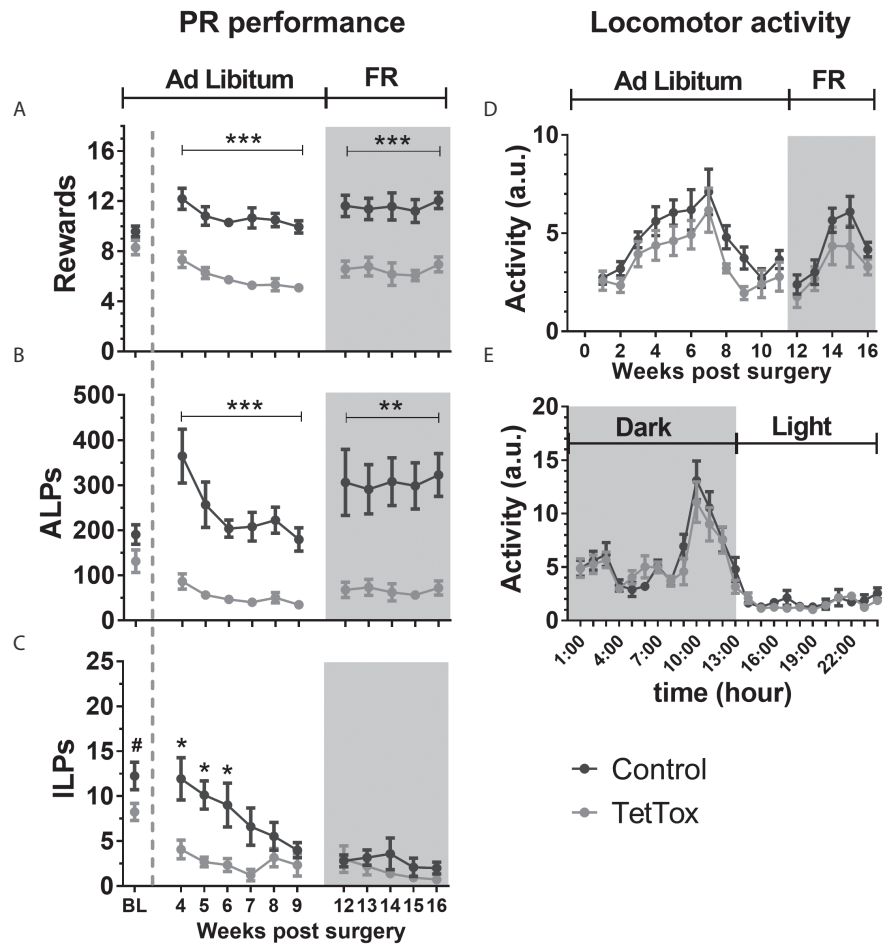

Figure 2. Effect of inactivation of ZI-region neurons projecting to the VTA on responding for sucrose under a PR schedule of reinforcement and locomotor activity. (A) Rewards, (B) active lever presses (ALPs), and (C) inactive lever presses (ILPs) in PR testing, averaged per week. Baseline (BL); PR performance one week before virus injections (average of 5 sessions is shown). PR testing recommenced 4 weeks after virus injections, and was assessed under *ad libitum* feeding and food restriction (FR) in the home cage (average of 3 sessions per week is shown). *Ad libitum*: rewards and ALPs, $F_{group} \geq 51.274$, $p=0.000$, post hoc $p<0.01$ for all weeks; ILPs $F_{group}=10.175$, $p=0.008$, post hoc $p<0.05$ at week 4-6. FR: rewards and ALPs, $F_{group} \geq 21.836$, $p \leq 0.001$, post hoc $p<0.02$ for all weeks; ILPs $F_{group}=0.866$, $p=0.370$. (D) Locomotor activity in arbitrary units (a.u.) averaged per week. *Ad libitum* and FR: $F_{group} \geq 2.683$, $p \geq 0.127$. (E) Locomotor activity over 24h averaged over the weekend data of week 6-9. $F_{group}=2.337$, $p=0.152$. Data is shown as mean ± SEM. N=8 for controls and n=6 for TetTox rats. #P<0.07, *P<0.05, **P<0.01, ***P<0.06 compared with controls.

from control rats in locomotor activity in the home cage (Figure 2D, E). Thus, TetTox-inactivation of ZI-region to VTA projection neurons reduces food-motivated behavior independent of general activity but does not affect the motivation to increase food reward seeking during a FR-induced metabolic challenge.

Inactivation of ZI-region to VTA projection neurons reduces *ad libitum* feeding

Chow intake in the home cage did not differ between control and TetTox rats before virus injections (Figure 3A). Starting from week 3 post virus injections onwards, TetTox rats ate less chow compared with control rats under *ad libitum* feeding (Figure 3A, B). Both the control and TetTox group showed a rhythmic feeding pattern with higher chow intake in the dark phase compared with the light phase (Figure 3B), and no differences in light/dark phase feeding distribution were observed between the groups (Figure 3C). As approximately 70% of chow was consumed in the dark phase, the lower chow intake in TetTox rats compared with controls was most pronounced in this phase (difference between groups was 3.97 and 0.97 gr in dark and light phase, respectively) (Figure 3B). Lower chow intake in TetTox rats resulted from a significantly lower number of meals, especially in the dark phase (Figure 3D). TetTox rats showed a non-significant tendency to compensate for their reduced meal frequency by increasing their meal size (Figure 3E), but this was not sufficient to restore food intake levels to those of control rats.

Although all rats increased body weight over the duration of *ad libitum* feeding, body weight was significantly lower in TetTox rats compared with control rats from 7 weeks post virus injections onwards (Figure 3F). Further inspection of the relationship between chow intake and body weight revealed that TetTox rats ate less chow per 100 gr body weight (Figure 3G), suggesting that TetTox rats were metabolically more efficient.

Inactivation of ZI-region to VTA projection neurons leads to a reduction in core body temperature

From week three post virus injections onwards, TetTox rats showed a reduction of 0.32±0.02 ºC in core body temperature during *ad libitum* feeding compared with controls (Figure 4A). The timing of the reduction in core body temperature in TetTox rats was similar to that of the reduction in food intake (Figure 3A, 4A). Core body temperature was significantly reduced during the dark phase (Figure 4B), the period during which the strongest reduction in food intake was observed (Figure 3B). Furthermore, core body temperature correlated significantly with the amount of chow intake during *ad libitum* feeding, especially during the dark phase

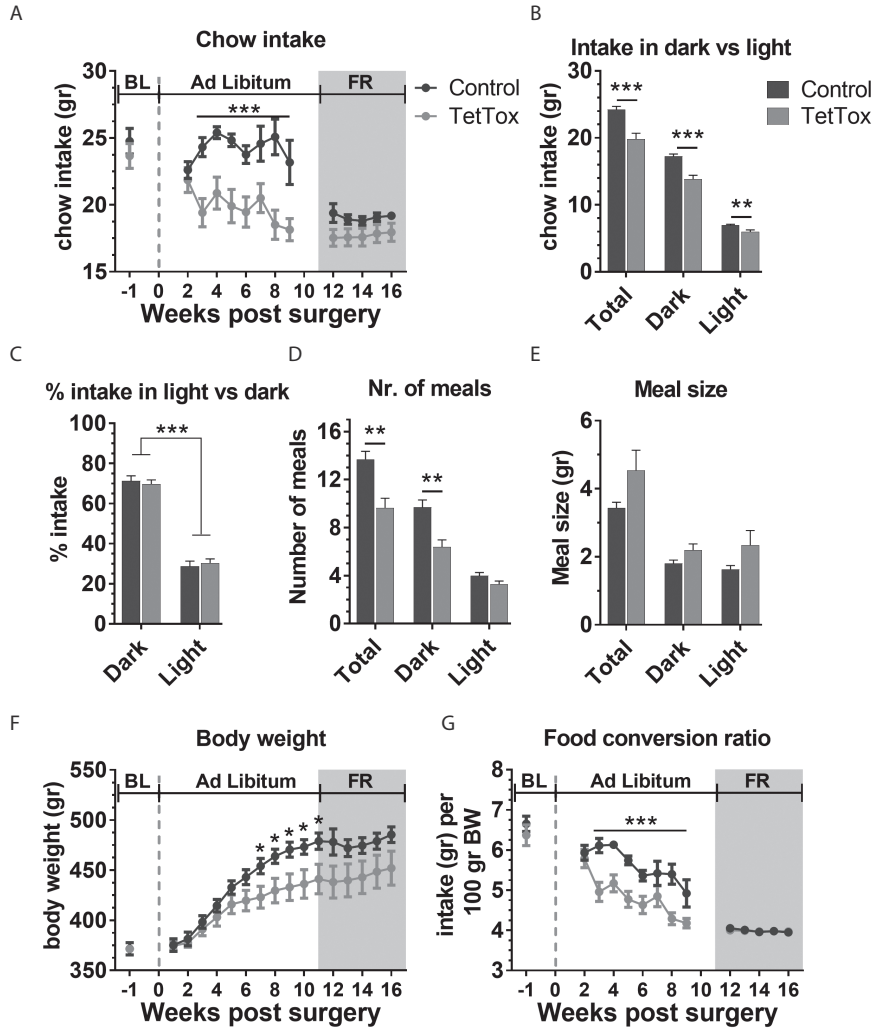

Figure 3. Effect of inactivation of ZI-region neurons projecting to the VTA on homeostatic feeding. (A) Chow intake per day, averaged per week, under *ad libitum* feeding and during food restriction (FR). Baseline (BL): t_{group}=0.775, p=0.454; *Ad libitum*: F_{group}=22.444, p=0.000, post hoc p<0.05 at week 3-9. FR: F_{group}=3.697, p=0.079. (B) Average chow intake per day during the light and dark phase over the course of *ad libitum* feeding. $F_{circadian\text{-}phase*group}$=29.066, p=0.000. Post hoc: p=0.000 for total and dark, p=0.004 for light. (C) Percentage (%) of chow intake during the dark and light phase over the course of *ad libitum* feeding. $F_{circadian\text{-}phase*group}$=0.210, p=0.655. $F_{circadian\text{-}phase}$=139.55, p=0.000. (D) Number of meals, and (E) meal size averaged over the 24h weekend data of week 6-9. Number of meals: $F_{circadian\text{-}phase*group}$=10.886, p=0.003. Post hoc p<0.01 for total and dark, p=0.090 for light. Meal size: $F_{circadian\text{-}phase*group}$=2.707, p=0.111. F_{group}=4.161, p=0.064. (F) Body weight averaged per week. BL: t_{group}=0.004, p=0.997; *Ad libitum*: $F_{time*group}$=6.813, p=0.015. Post hoc p<0.05 at week 7-11. FR: $F_{time*group}$=1.002, p=0.353; F_{group}=3.708, p=0.078. (G) Chow intake per 100 gr body weight per day, averaged per week. BL: t_{group}=0.917, p=0.379; *Ad libitum*: F_{group}=26.280, p=0.000. Post hoc p<0.05 at week 3-7. FR: F_{group}=0.317, p=0.585. Data is shown as mean ± SEM. N=8 for controls and n=5-6 for TetTox rats. *P<0.05, **P<0.01, ***P<0.001 compared with controls.

(Figure 4C,D). Together, the data show a strong relationship between food intake and core body temperature, which is most apparent during the active feeding period (dark phase).

To further test the correlation between food intake and core body temperature, we challenged rats with FR. Like control rats, TetTox rats reduced their core body temperature in response to the reduction in chow intake, and the adaptive temperature response did not differ from control rats (Figure 4E).

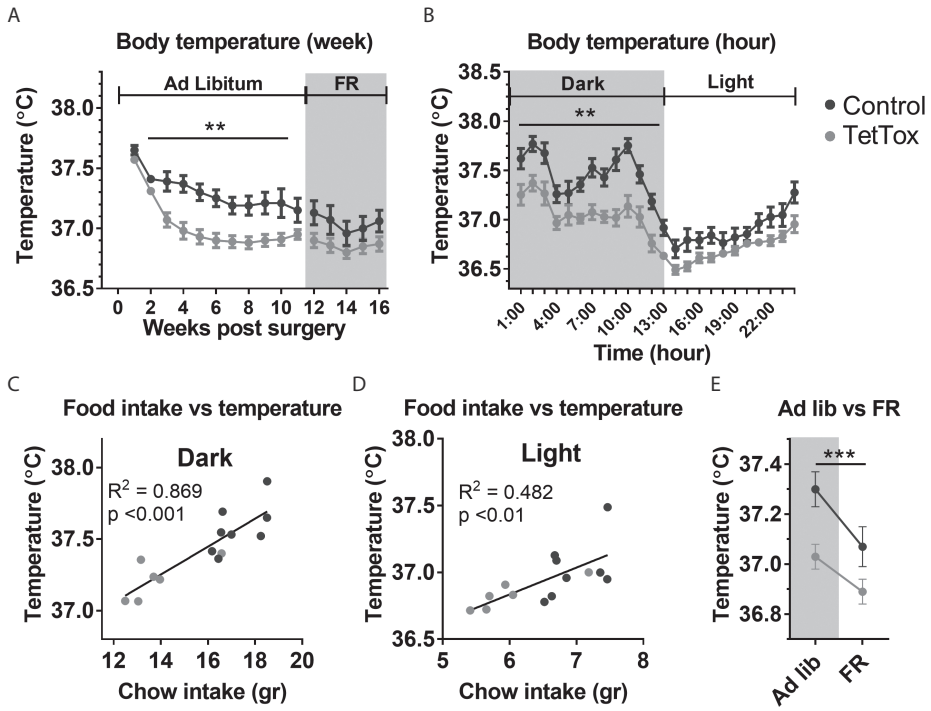

Figure 4. Effect of inactivation of ZI-region neurons projecting to the VTA on body temperature. (A) Core body temperature during *ad libitum* feeding and food restriction (FR), averaged per week. $F_{time*group}$=3.754, p=0.026. Post hoc p<0.01 in week 3-8, and p<0.05 in week 2 and 9. (B) Core body temperature over 24h averaged over the weekend data of week 6-9. Total: $F_{time*group}$=3.154, p=0.000; dark: F_{group}=17.962, p=0.001; light: F_{group}=3.581, p=0.083. (C,D) Correlation between food intake and chow intake during the dark and light phase, respectively. (E) Average core body temperature during *ad libitum* feeding and FR. $F_{feeding\text{-}condition*group}$=2.440, p=0.144. $F_{feeding\text{-}condition}$=51.808, p=0.000. Weekend data of week 6-9 were analyzed. N=8 for controls and n=5-6 for TetTox rats. Data is shown as mean ± SEM. A-B: **P<0.01 compared with controls; E: ***P<0.001 for *ad libitum* vs FR.

In summary, TetTox-inactivation of ZI-region neurons projecting to the VTA reduced the motivation to work for food and reduced chow intake due to lower meal frequency, without affecting general activity. Food intake showed a strong correlation with core body temperature.

Experiment 2: Chemogenetic activation of ZI>VTA projection neurons

Selective targeting of ZI>VTA projection neurons

We next tested whether chemogenetic activation of the ZI>VTA projection has opposite effects on food-motivated behavior and *ad libitum* feeding compared to TetTox-inactivation of this projection. To do this, Cre-dependent DREADD hM3D(Gq) was injected into the ZI (Figure 5A). CAV2cre was injected into the VTA, where it infects nerve terminals and retrogradely delivers Cre in the ZI, which subsequently enables the expression of Cre-dependent DREADD hM3D(Gq) in ZI neurons projecting to the VTA. Analysis of DREADD hM3D(Gq)-mCherry positive neurons revealed that the ZI was successfully targeted in all rats, and that virus expression was restricted to the ZI (Figure 5B). All rats also showed correct targeting of the VTA (Figure 5C).

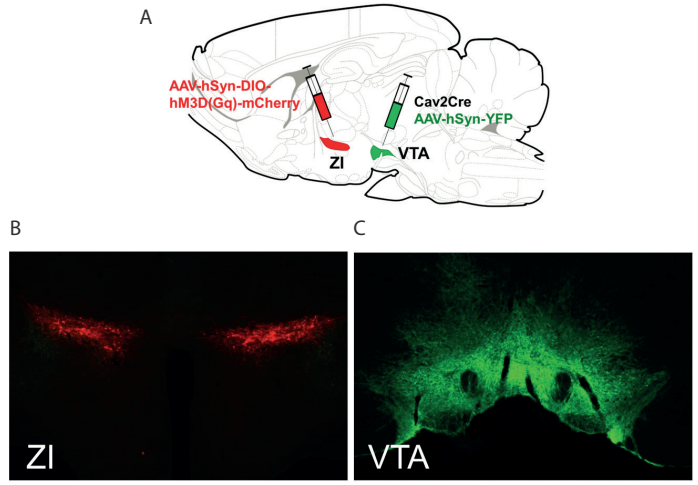

Figure 5. DREADD hM3D(Gq)-mCherry is selectively expressed in ZI neurons projecting to the VTA. (A) To selectively inactive ZI neurons projecting to the VTA, CAV2Cre was injected into the VTA and Cre-dependent DREADD hM3D(Gq)-mCherry was injected into the ZI. An AAV-hSyn-YFP virus was injected together with CAV2Cre to visualize the injection site in the VTA. (B) Immunofluorescence of DREADD hM3D(Gq)-mCherry (red) positive neurons in the ZI . (C) Immunofluorescence of GFP (green) in the VTA following virus injection of CAV2Cre/AAV-hSyn-YFP (bregma -5.30 mm).

Chemogenetic activation of ZI>VTA projection neurons promotes food-motivated behavior

To test whether chemogenetic activation of ZI>VTA projection neurons promotes food-motivated behavior, responding for sucrose under a PR schedule of reinforcement was tested following treatment with CNO compared with saline. CNO treatment resulted in a significant increase in the number of ALPs (Figure 6B), resulting in a significant increase in the number of rewards earned (Figure 6A). The number of ILPs was not affected by CNO treatment (Figure 6C), indicating that the CNO-induced increase in ALPs did not result from an increase in general activity. Thus, chemogenetic activation of ZI>VTA projection neurons does not affect general activity (as reflected by ILPs), but specifically increases food reward seeking.

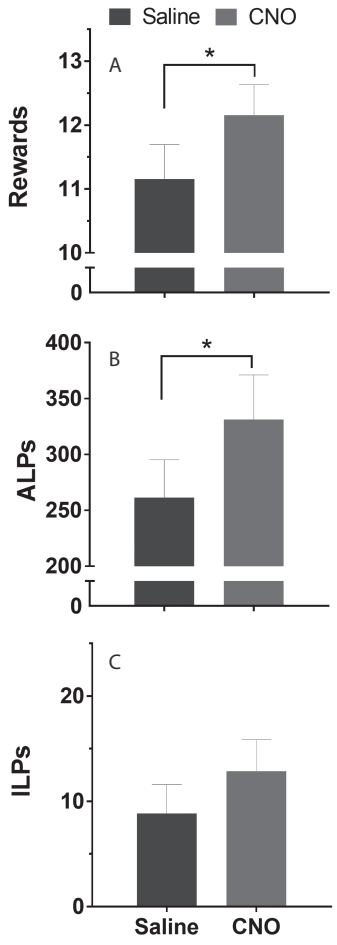

Figure 6. Effect of chemogenetic activation of ZI to VTA projection neurons on responding for sucrose under a PR schedule of reinforcement. (A) Rewards, (B) active lever presses (ALPs), and (C) inactive lever presses (ILPs) in PR testing following saline and CNO injection. $T_{treatment} \geq 2.449$, $p \leq 0.031$ for ALPs and rewards. Data is shown as mean ± SEM. *P<0.05 for saline vs CNO.

Chemogenetic activation of ZI neurons projecting to the VTA promotes feeding

To test whether chemogenetic activation of ZI neurons projecting to the VTA promotes feeding, rats were injected with saline or CNO following 5.5 h food restriction (see methods). Food was returned one hour after injection, and meal structures were analyzed up to 6h following food return.

All rats typically started feeding immediately (within 2 min) upon access to chow and consumed one meal during the first hour following food return (Figure 7A). The second meal was initiated 2.6±0.58 h after the first meal (Figure 7B). CNO treatment postponed the initiation of the second meal to 4.8±0.41 h after the first meal (Figure 7A, B), and significantly increased the first meal size (+1.65±0.68 gr difference with saline) (Figure 7C). The satiety ratio (first meal interval/first meal size) shows that post-meal satiety was not affected by CNO treatment (Figure 7D), indicating that, as a result of the larger first meal size with CNO, rats initiated their second meal after a longer first meal interval. The size of the second meal and other meals was not affected by CNO treatment (Figure 7C). In accordance, CNO treatment resulted in a significant increase in cumulative food intake during the first hour after food return only (Figure 7E). As might be expected from such a short-lasting feeding effect, CNO treatment did not affect 24h body weight changes following injections (data not shown). To summarize, chemogenetic activation of ZI>VTA projection neurons promotes feeding by increasing the first meal size specifically.

Chemogenetic activation of ZI>VTA projection neurons does not affect locomotor activity and body temperature

Finally, we tested whether locomotor activity and core body temperature are affected by chemogenetic activation of ZI>VTA neurons. To test this, the effects of CNO treatment were assessed in the same test paradigm as for feeding, both before and after food return. No effects of CNO treatment were observed on locomotor activity (Figure 8A) and core body temperature (Figure 8B) in either the absence or presence of food. Thus, these data support that chemogenetic activation of ZI>VTA projection neurons primarily stimulates food-related activity, but not general activity, and does not modulate core body temperature.

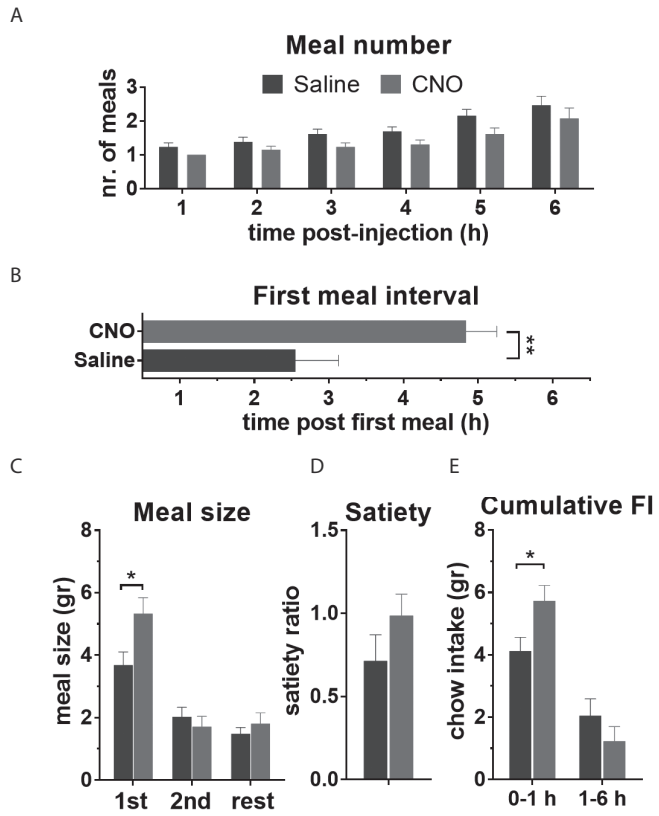

Figure 7. Effect of chemogenetic activation of ZI to VTA projection neurons on feeding. Effects of CNO vs saline treatment on (A) cumulative number of meals per hour. $F_{treatment*hour}$=0.863, p=0.486. $F_{treatment}$=5.256, p=0.041; (B) first meal interval. $t_{treatment}$=3.100, p=0.009; (C) size of the first, second, and rest of meals. $t_{treatment*hour}$=6.329, p=0.006. Post hoc p<0.05 for first meal size; (D) satiety ratio (first meal interval/first meal size; a measure of post-meal satiety). $t_{treatment}$=0.268, p=0.268; (E) 0-1h and 2-6h cumulative food intake (FI). $F_{treatment*hour}$=7.603, p=0.017. Post hoc p<0.05 at 0-1h. Data is shown as mean ± SEM. *P<0.05 and **P<0.01 for saline vs CNO.

Discussion

We here studied the effects of permanent inactivation and reversible activation of ZI>VTA projection neurons on several aspects of feeding behavior. TetTox-inactivation of ZI-region neurons projecting to the VTA reduced the motivation to work for food and reduced chow intake due to lower meal frequency, resulting in decreased body weight gain without affecting general activity. These findings suggest that inactivation of ZI>VTA projection neurons specifically reduces food-related action initiation. Chemogenetic activation of ZI>VTA projection neurons resulted in the opposite: increased food-motivated behavior and feeding, without affecting general activity. Together, these findings support that ZI>VTA projection neurons drive feeding by facilitating action initiation towards food.

Regulation of feeding behavior by ZI>VTA projection neurons

Previously, lesioning of the entire ZI-region or of GABA neurons within the ZI resulted in a consistent reduction of *ad libitum food* intake and body weight compared with control rats [23, 24, 28 but see 25]. We here extend these observations by showing that specific inactivation of ZI-region to VTA projection neurons results in similar effects, suggesting that the ZI can regulate feeding behavior and body weight via its projections to the VTA.

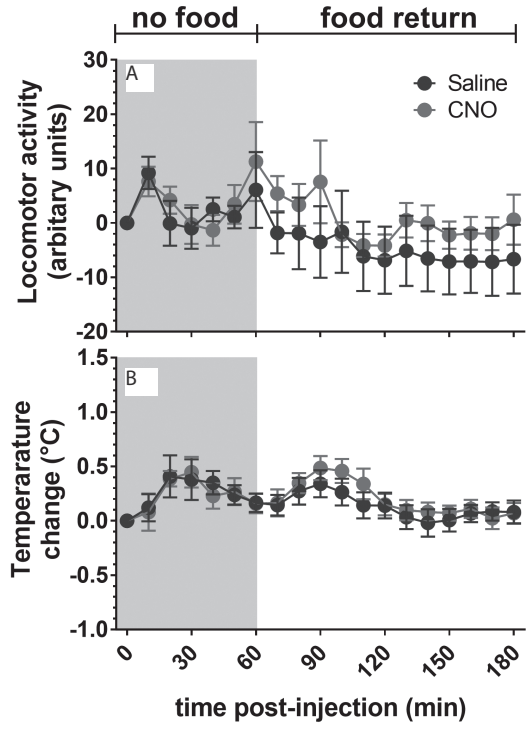

Figure 8. Effect of chemogenetic activation of ZI to VTA projection neurons on locomotor activity and core body temperature. The effect of CNO versus saline treatment on (A) the delta change in locomotor activity and (B) core body temperature, in the presence and absence of food. $F_{treatment}$≥0.072, p≥0.265. Data is shown as mean ± SEM.

The reduction in food intake following inactivation of ZI-region to VTA projection neurons was caused by a reduction in meal frequency, indicating reduced meal initiation. Chemogenetic activation of ZI>VTA projection neurons showed the opposite effect on feeding, that is, it promoted feeding. However, the increase in food intake resulted specifically from an increased first meal size after CNO injection. These results are in accordance with those of Zhang et al., who showed that stimulation of ZI GABA neurons results in an intake of 35% of total daily food intake within just 10 minutes, whereas ablation of ZI GABA neurons reduces long-term food intake [28]. An explanation for the discrepancy in feeding microstructure following activation vs inactivation could be that the inactivation with TetTox was permanent and resulted in counter-regulatory mechanisms, whereas chemogenetic activation had a short-lasting effect of a few hours following CNO injection. Furthermore, the effect of chemogenetic activation of ZI>VTA projection neurons on feeding was tested in the light phase, whereas the effects on meal frequency with TetTox-inactivation were strongest in the more active dark phase.

In our chemogenetic activation study of ZI>VTA projection neurons, CNO treatment seemed to induce an acute hunger effect, as the first but not the second meal size was increased, which resulted in a significant increase in cumulative food intake during the first hour after food return only. The satiety ratio (first meal interval/first meal size) shows that post-meal satiety was not affected by CNO treatment, indicating that, as a result of the larger first meal size with CNO, rats might have felt sated for a longer time, and therefore initiated their second meal after a longer first meal interval. Thus, in line with the results of Zhang et al. [28], chemogenetic activation of ZI>VTA projection neurons specifically induced an acute hunger effect, resulting in a binge. TetTox-inactivation of these neurons seemed to have an opposite, long-term suppressing effect on hunger, as indicated by the lower meal initiation, for which was inadequately compensated by an increase in meal size.

Regulation of food intake with regard to body weight by ZI>VTA projection neurons

TetTox-inactivation of ZI-region neurons projecting to the VTA did not only result in a lower absolute chow intake, but also lower chow intake per 100 gr body weight, indicating a higher metabolic efficiency. This was also apparent during food restriction, during which all rats received 4 gr of chow per 100 gr body weight. Food restriction had more impact on body weight gain in control rats compared with TetTox rats, which led to convergence of the body weights of the two groups. Previously, lesioning of the ZI was also shown to reduce the ratio of food intake to body weight [23]. Like ZI lesioned rats [23], rats with TetTox-inactivation of ZI to VTA projection neurons maintained a body weight that was consistently below that of control rats after surgery, despite the higher metabolic efficiency, which may reflect the establishment of a lower postsurgical body weight set-point.

The higher metabolic efficiency following TetTox-inactivation of ZI-region to VTA projection neurons likely provides a compensatory mechanism for the lower action initiation towards food, that was reflected in the lower motivation to work for food and lower meal initiation. The ability to adjust food intake to the caloric density of diets was previously not affected by ZI lesioning [23]. In accordance, TetTox rats still increased their food reward seeking in times of reduced food availability during FR. Thus, the ZI is not necessary for the coupling between metabolic needs and feeding initiation, but generally facilitates action initiation towards feeding via its projections to the VTA.

The reduced core body temperature in rats with TetTox-inactivation of ZI-region to VTA projection neurons could explain their higher metabolic efficiency. Lower core body temperature might be a consequence of the lower food intake, acting as a compensatory mechanism to conserve energy. Because of the permanent inactivation of ZI-region to VTA projection neurons, it was impossible to disentangle cause and consequence of TetTox-inactivation on food intake versus core body temperature. The strong relationship between food intake and core body temperature, which was most apparent during the active feeding period (dark phase), suggests that reduced core body temperature might be a consequence of the lower food intake. TetTox rats were still able to adapt their core body temperature in response to a metabolic challenge (as assessed by FR), suggesting normal temperature regulation upon FR. To study the role of ZI>VTA projection neurons in thermoregulation more precisely, we chemogenetically activated these neurons in the absence of food, to prevent interference with feeding. Chemogenetic activation of these neurons did not affect core body temperature, supporting that the reduction in core body temperature following TetTox-inactivation of ZI-region to VTA projection neurons represents a compensatory response to reduced food intake rather than a direct effect of TetTox-inactivation on core body temperature.

Character of ZI input on dopaminergic neurons in the VTA

Although the VTA also contains GABAergic (~30%) and glutamatergic (~2-10%) neurons, the majority of neurons are dopaminergic (60-70%) and these neurons are implicated in feeding [6, 9, 22]. Activation of DA neurons in the VTA has been shown to drive activational (rather than directional) aspects of motivation for food, as it increases responding on both the active and inactive levers under a PR schedule of

reinforcement [18], as well as general activity [31, 32, 40]. Since chemogenetic activation of ZI>VTA projection neurons increased responding on the active but not inactive lever in PR testing, and did not affect general locomotor activity, input from the ZI to VTA DA neurons seems to confine the facilitation of general action initiation towards a food-directed action initiation. This idea is supported by the TetTox-inactivation findings.

With regard to feeding microstructure, VTA DA neurons were previously shown to facilitate both the initiation and cessation of feeding behavior by simultaneously increasing meal frequency and reducing meal size [10]. Our data suggest that input from the ZI onto VTA DA neurons facilitates both the initiation and continuation of feeding, as loss of ZI input via TetTox-inactivation of ZI-region to VTA projection neurons resulted in lower meal initiation, and the short-lasting chemogenetic activation of ZI>VTA projection neurons increased first meal size.

The neurochemical character of the cells in the ZI that provide input onto the VTA to promote action initiation towards feeding remains to be determined. The ZI is a brain area with an exceptionally diverse range of neurochemically defined cell types, yet GABAergic and glutamatergic cells are both quite abundant [25]. Since the (in)activation of ZI(-region) neurons projecting to the VTA had similar effects on feeding behavior as described for (in)activation of ZI GABA neurons [28] (*i.e.* activation substantially promoted short-term (<10 minutes) feeding, and inactivation reduced long-term feeding), the ZI might provide GABAergic input onto VTA neurons to regulate feeding behavior. The ZI was shown to provide major input on VTA DA neurons [20]. Inhibitory GABAergic input onto VTA DA neurons may confine DA signaling in the VTA to the regulation of food-related action initiation (instead of general action initiation). In addition, the ZI might also provide GABAergic input onto VTA GABA neurons, as the ZI does not only innervate DA neurons in the VTA (21 versus 20), and VTA GABA neurons interact locally to regulate DA neurons (17).

Technical challenges in modulating ZI>VTA projection neurons

The results of the TetTox-inactivation study should be interpreted with two limitations in mind, *i.e.* that we did not specifically target the ZI, but the ZI-region, and that TetTox-GFP expression was assessed at the mRNA level instead of the protein level. Perhaps we did not observe TetTox-GFP at the protein level because rats were sacrificed a long time (29 weeks) after virus injections. The presence of TetTox-GFP mRNA expressing neurons in the ZI-region indicates that TetTox expression in neurons does not lead to cell death, as was previously also reported [35]. We speculate that permanent blockade of synaptic transmission by TetTox eventually results in blockade of translation, for example due to ER stress resulting from the overexpression of TetTox transcripts and/or accumulation of non-released proteins. Of note, in our pilot study, we did observe TetTox-GFP protein in the ZI in rats that were sacrificed 17 weeks after virus injections, which is a similar time-period as for the behavioral data presented in this study. To independently confirm the results of the TetTox study, we chemogenetically activated ZI>VTA projection neurons, and thereby specifically targeted the ZI instead of the ZI-region. We chose to activate rather than inhibit ZI>VTA projection neurons, as it is technically more difficult to inhibit a neuronal projection than to activate one (35), and we aimed to determine whether the modulation of feeding by ZI>VTA projection neurons is bidirectional.

Conclusions

In this study, we show for the first time that the ZI regulates feeding behavior via its projections to the VTA. Activity of the projection from ZI>VTA promotes feeding by facilitating specific action initiation towards food, as reflected in both food-motivated behavior and meal frequency. This probably results from ZI modulation of VTA DA neurons. ZI>VTA projection neurons do not control general activity or directly modulate core body temperature, pointing to a specific role for ZI>VTA projection neurons in the facilitation of food-related action initiation. These findings provide new insights into the neurobiology of feeding behavior, which may have implications for the development of novel treatments for eating disorders and obesity.

Competing interests

The authors declare that no competing interests exist.

Author contributions

The experiments were performed at the Brain Center Rudolf Magnus, Dept. of Translational Neuroscience, University Medical Center Utrecht, Utrecht University, The Netherlands.

Experiments were conceived and designed by K.G, G.P., and R.A. Collection, analysis and interpretation of data from TetTox-inactivation experiments was performed by K.G., E.H., M.N., M.L., and G.P. Collection, analysis and interpretation of data from chemogenetic activation experiments was performed by K.G., M.N., M.L., and G.P. The manuscript was written by K.G., with critical revisions by G.P., and R.A.

All authors have approved the final version of the manuscript and agree to be accountable for all aspects of the work. All persons designated as authors qualify for authorship, and all those who qualify for authorship are listed.

Funding

This research was supported by the Dutch Technology Foundation STW (grant 12264), which is part of the Netherlands Organisation for Scientific Research (NWO), and which is partly funded by the Ministry of Economic Affairs, and by NWO under project number 863.13.018 (NWO/ALW Veni grant).

Acknowledgements

We thank Jos Brits, Jacques P. Flores-Dourojeanni, Keith Garner, and Céline Peterse for their practical assistance.

References

1. Nguyen DM, El-Serag HB. The epidemiology of obesity. *Gastroenterol Clin North Am* 2010; **39**: 1-7.
2. Romieu I, Dossus L, Barquera S, Blottiere HM, Franks PW, Gunter M, et al. Energy balance and obesity: what are the main drivers? *Cancer Causes Control* 2017; **28**: 247-258.
3. Naef L, Pitman KA, Borgland SL. Mesolimbic dopamine and its neuromodulators in obesity and binge eating. *CNS Spectr* 2015; **20**: 574-583.
4. Kelley AE, Baldo BA, Pratt WE, Will MJ. Corticostriatal-hypothalamic circuitry and food motivation: integration of energy, action and reward. *Physiol Behav* 2005; **86**: 773-795.
5. van Zessen R, van der Plasse G, Adan RA. Contribution of the mesolimbic dopamine system in mediating the effects of leptin and ghrelin on feeding. *Proc Nutr Soc* 2012; **71**: 435-445.
6. Wise RA. Dopamine, learning and motivation. *Nat Rev Neurosci* 2004; **5**: 483-494.
7. Salamone JD, Correa M. The mysterious motivational functions of mesolimbic dopamine. *Neuron* 2012; **76**: 470-485.
8. Berridge KC. The debate over dopamine's role in reward: the case for incentive salience. *Psychopharmacology (Berl)* 2007; **191**: 391-431.
9. Meye FJ, Adan RA. Feelings about food: the ventral tegmental area in food reward and emotional eating. *Trends Pharmacol Sci* 2014; **35**: 31-40.
10. Boekhoudt L, Roelofs TJM, de Jong JW, de Leeuw AE, Luijendijk MCM, Wolterink-Donselaar IG, et al. Does activation of midbrain dopamine neurons promote or reduce feeding? *Int J Obes (Lond)* 2017; **41**: 1131-1140.
11. Zhou QY, Palmiter RD. Dopamine-deficient mice are severely hypoactive, adipsic, and aphagic. *Cell* 1995; **83**: 1197-1209.
12. Wang GJ, Volkow ND, Logan J, Pappas NR, Wong CT, Zhu W, et al. Brain dopamine and obesity. *Lancet* 2001; **357**: 354-357.
13. Volkow ND, Wang GJ, Fowler JS, Telang F. Overlapping neuronal circuits in addiction and obesity: evidence of systems pathology. *Philos Trans R Soc Lond B Biol Sci* 2008; **363**: 3191-3200.
14. Johnson PM, Kenny PJ. Dopamine D2 receptors in addiction-like reward dysfunction and compulsive eating in obese rats. *Nat Neurosci* 2010; **13**: 635-641.
15. Cone JJ, Chartoff EH, Potter DN, Ebner SR, Roitman MF. Prolonged high fat diet reduces dopamine reuptake without altering DAT gene expression. *PLoS One* 2013; **8**: e58251.
16. Stice E, Yokum S, Blum K, Bohon C. Weight gain is associated with reduced striatal response to palatable food. *J Neurosci* 2010; **30**: 13105-13109.
17. McCutcheon JE. The role of dopamine in the pursuit of nutritional value. *Physiol Behav* 2015; **152**: 408-415.
18. Boekhoudt L, Wijbrans EC, Man JHK, Luijendijk MCM, de Jong JW, van der Plasse G, et al. Enhancing excitability of dopamine neurons promotes motivational behaviour through increased action initiation. *Eur Neuropsychopharmacol* 2018; **28**: 171-184.
19. van der Plasse G, van Zessen R, Luijendijk MC, Erkan H, Stuber GD, Ramakers GM, et al. Modulation of cue-induced firing of ventral tegmental area dopamine neurons by leptin and ghrelin. *Int J Obes (Lond)* 2015; **39**: 1742-1749.
20. Ogawa SK, Cohen JY, Hwang D, Uchida N, Watabe-Uchida M. Organization of monosynaptic inputs to the serotonin and dopamine neuromodulatory systems. *Cell Rep* 2014; **8**: 1105-1118.
21. Gonzalez JA, Jensen LT, Fugger L, Burdakov D. Convergent inputs from electrically and topographically distinct orexin cells to locus coeruleus and ventral tegmental area. *Eur J Neurosci* 2012; **35**: 1426-1432.
22. Ferrario CR, Labouebe G, Liu S, Nieh EH, Routh VH, Xu S, et al. Homeostasis Meets Motivation in the Battle to Control Food Intake. *J Neurosci* 2016; **36**: 11469-11481.

23. McDermott LJ, Grossman SP. Regulation of calorie intake in rats with rostral zona incerta lesions: effects of caloric density or palatability of the diet. *Physiol Behav* 1979; **23**: 1135-1140.
24. Huang YH, Mogenson GJ. Differential effects of incertal and hypothalamic lesions on food and water intake. *Exp Neurol* 1974; **43**: 276-280.
25. Mitrofanis J. Some certainty for the "zone of uncertainty"? Exploring the function of the zona incerta. *Neuroscience* 2005; **130**: 1-15.
26. Kendrick KM, Hinton MR, Baldwin BA. GABA release in the zona incerta of the sheep in response to the sight and ingestion of food and salt. *Brain Res* 1991; **550**: 165-168.
27. Kendrick KM, Baldwin BA, Cooper TR, Sharman DF. Uric acid is released in the zona incerta of the subthalamic region of the sheep during rumination and in response to feeding and drinking stimuli. *Neurosci Lett* 1986; **70**: 272-277.
28. Zhang X, van den Pol AN. Rapid binge-like eating and body weight gain driven by zona incerta GABA neuron activation. *Science* 2017; **356**: 853-859.
29. Amami P, Dekker I, Piacentini S, Ferre F, Romito LM, Franzini A, et al. Impulse control behaviours in patients with Parkinson's disease after subthalamic deep brain stimulation: de novo cases and 3-year follow-up. *J Neurol Neurosurg Psychiatry* 2015; **86**: 562-564.
30. Zahodne LB, Susatia F, Bowers D, Ong TL, Jacobson CE,4th, Okun MS, et al. Binge eating in Parkinson's disease: prevalence, correlates and the contribution of deep brain stimulation. *J Neuropsychiatry Clin Neurosci* 2011; **23**: 56-62.
31. Boender AJ, de Jong JW, Boekhoudt L, Luijendijk MC, van der Plasse G, Adan RA. Combined use of the canine adenovirus-2 and DREADD-technology to activate specific neural pathways in vivo. *PLoS One* 2014; **9**: e95392.
32. Boekhoudt L, Omrani A, Luijendijk MC, Wolterink-Donselaar IG, Wijbrans EC, van der Plasse G, et al. Chemogenetic activation of dopamine neurons in the ventral tegmental area, but not substantia nigra, induces hyperactivity in rats. *Eur Neuropsychopharmacol* 2016; **26**: 1784-1793.
33. Hnasko TS, Perez FA, Scouras AD, Stoll EA, Gale SD, Luquet S, et al. Cre recombinase-mediated restoration of nigrostriatal dopamine in dopamine-deficient mice reverses hypophagia and bradykinesia. *Proc Natl Acad Sci U S A* 2006; **103**: 8858-8863.
34. Campos CA, Bowen AJ, Han S, Wisse BE, Palmiter RD, Schwartz MW. Cancer-induced anorexia and malaise are mediated by CGRP neurons in the parabrachial nucleus. *Nat Neurosci* 2017; **20**: 934-942.
35. Carter ME, Han S, Palmiter RD. Parabrachial calcitonin gene-related peptide neurons mediate conditioned taste aversion. *J Neurosci* 2015; **35**: 4582-4586.
36. la Fleur SE, Vanderschuren LJ, Luijendijk MC, Kloeze BM, Tiesjema B, Adan RA. A reciprocal interaction between food-motivated behavior and diet-induced obesity. *Int J Obes (Lond)* 2007; **31**: 1286-1294.
37. van der Zwaal EM, Luijendijk MC, Evers SS, la Fleur SE, Adan RA. Olanzapine affects locomotor activity and meal size in male rats. *Pharmacol Biochem Behav* 2010; **97**: 130-137.
38. la Fleur SE, Luijendijk MC, van der Zwaal EM, Brans MA, Adan RA. The snacking rat as model of human obesity: effects of a free-choice high-fat high-sugar diet on meal patterns. *Int J Obes (Lond)* 2014; **38**: 643-649.
39. Solinas M, Goldberg SR. Motivational effects of cannabinoids and opioids on food reinforcement depend on simultaneous activation of cannabinoid and opioid systems. *Neuropsychopharmacology* 2005; **30**: 2035-2045.
40. Wang S, Tan Y, Zhang JE, Luo M. Pharmacogenetic activation of midbrain dopaminergic neurons induces hyperactivity. *Neurosci Bull* 2013; **29**: 517-524.

Chapter 7:

Summary and general discussion:
Novel insights into concepts related to leptin, the hypothalamus and energy balance

Kathy C.G. de Git

Brain Center Rudolf Magnus, Dept. of Translational Neuroscience, University Medical Center Utrecht, Utrecht University, Utrecht 3584 CG, The Netherlands

Summary

Living in our modern society, some individuals become heavily obese, whereas others appear obesity resistant [1]. This high variability in the susceptibility for the development of obesity remains largely unexplained. The overall aim of this thesis was to improve the understanding of the neural control of physiological processes that balance energy intake and expenditure, as well as of certain susceptibility factors that increase the risk for the development of obesity. Further, several technical challenges in studying the role of neural circuits in the control of energy balance were discussed, and several generally accepted concepts related to leptin, the hypothalamus, and energy balance were challenged.

Section I: Leptin and hypothalamic control of energy balance

The hypothalamus is known for its critical role in the control of energy balance [2-4]. It senses and integrates information from metabolic signals provided by the periphery, like the adiposity hormone leptin, which inform the brain about energy storage and availability. The hypothalamus responds to these metabolic signals by adapting energy intake and energy expenditure accordingly [2]. Therefore, the first section of this thesis focused on leptin and hypothalamic control of energy balance.

Chapter 2. In this chapter, we reviewed literature showing that overconsumption of high-fat diets in models of diet-induced obesity (DIO) results in the induction of an inflammatory response in the hypothalamus, which promotes the development of central leptin resistance and obesity. This inflammatory response involves dynamic changes in the expression and activity of several mediators of the innate immune system, including upregulation of IκB kinase-β/nuclear factor-κB (IKKβ/NF-κB) signaling, often described as "the master switch" of the innate immune system. Although the exact cellular mechanisms by which hypothalamic inflammation promotes central leptin resistance have not been resolved yet, current understandings propose that this inflammatory signaling might be induced by the accumulation of saturated fatty acids (SFAs) in the hypothalamus. In short, SFAs may act on glial cells, that act as drivers of inflammatory signaling by releasing pro-inflammatory cytokines. The upregulated cytokine-induced IKKβ/NF-κB signaling converges with classical signal transducer and activator of transcript 3 (STAT3) signaling (that is also upregulated due to hyperleptinemia) in hypothalamic neurons to upregulate suppressor of cytokine signaling 3 (SOCS3) expression, which subsequently mediates leptin resistance by providing negative feedback on the long form of the leptin receptor (LepRb).

Appendix I. The evidence for the development of an inflammatory response upon exposure to diets high in fat and sugar in chapter 2 has mostly been obtained by studies in which rodents were offered a pelleted high-fat diet. Since the free-choice high-fat high-sucrose (fcHFHS) diet mimics the human diet more closely than pelleted diets, we tested in appendix I whether exposure to the fcHFHS diet also upregulates inflammatory signaling in the mediobasal hypothalamus (MBH). Eight weeks of fcHFHS diet feeding did not upregulate inflammatory signaling, as measured by IKKβ/NF-κB signaling, in the MBH. However, it increased endogenous leptin signaling, as measured by phosphorylation of STAT3 (pSTAT3), a marker of leptin signal transduction, in the MBH. Thus, in contrast to high-fat diet feeding, fcHFHS diet feeding does not result in chronic upregulation of inflammatory signaling, but selectively upregulates endogenous leptin signaling in the MBH.

It is generally believed that leptin resistance results from the overconsumption of energy-dense diets, high in saturated fat and sugar, via processes like inflammatory signaling, and that this diet-induced leptin resistance contributes to the development of obesity [5-16]. At the cellular level, the development of diet-induced leptin resistance has specifically been shown in the arcuate nucleus (ARC), a brain area known to be a critical regulator of food intake [14, 17-19]. However, there is some evidence that reduced leptin sensitivity does not necessarily result from energy-dense diet feeding, but may already be present before energy-dense diet exposure and predispose rats to exacerbated DIO [1, 20]. From these studies, it was still unclear to what extent a pre-existing reduction in leptin sensitivity is a predictor for DIO, as it was not tested whether leptin sensitivity is a stable parameter in a rat.

Chapter 3. In this chapter, we first showed that leptin sensitivity is highly variable between individual rats but is a stable parameter in a rat over time. We then investigated whether individual leptin sensitivity on a chow diet predicts the development of obesity on a fcHFHS diet, and how this is related to the development of diet-induced leptin resistance. To do this, rats were grouped in leptin sensitive (LS) and leptin resistant (LR) rats based on individual leptin sensitivity on chow diet, and the development of DIO and leptin resistance on a fcHFHS diet was compared. Exposure to the fcHFHS diet revealed that LR rats, which showed a pre-existing reduction in leptin sensitivity compared with LS rats, gained more body weight and adiposity after 8 weeks of fcHFHS diet exposure, without eating more calories or altering leptin sensitivity. Thus, a pre-existing reduction in leptin sensitivity predicts

the susceptibility to develop excessive DIO after fcHFHS diet exposure. Previous studies in rats with a pre-existing or experimentally induced reduction in leptin sensitivity showed that obesity largely results from increased caloric intake [1, 20-22]. In contrast, in our model, rats with a pre-existing reduction in leptin sensitivity showed exacerbated obesity without eating more calories. This illustrates that there is more than one way by which a pre-existing reduction in leptin sensitivity predisposes rats to develop DIO, and makes our model interesting to study food intake independent mechanisms that lead to obesity. Finally, we showed that the pre-existing reduction in leptin sensitivity in LR rats compared with LS rats is associated with reduced cellular leptin sensitivity in the dorsomedial hypothalamus (DMH) and ventromedial hypothalamus (VMH), but not the ARC, as measured by leptin-induced pSTAT3 activation. Exposure to the fcHFHS diet did not further reduce leptin sensitivity in the DMH, VMH or ARC of LR rats. In other words, we found that pre-existing leptin sensitivity in an area involved in thermogenesis, the DMH (and VMH), but not the ARC, likely explains the difference in becoming excessively obese or not on a fcHFHS diet. Thus, our results challenge the generally accepted concept of diet-induced leptin resistance in the ARC as a causal factor for the initiation and/or maintenance of DIO.

Appendix II. LS and LR rats did not differ in total caloric intake in chapter 3, but we did not test whether they differ in feeding microstructure. Leptin is known to reduce meal size [23, 24]. Previously, an increase in meal size, but not meal number, was associated with DIO [25]. However, it was not studied whether DIO prone rats already consume larger meals before high-fat diet exposure, which may predispose them to exacerbated DIO. Therefore, we studied in appendix II whether individual leptin sensitivity on a chow diet and the susceptibility for the development of DIO are related to the consumption of larger meal sizes on chow diet. We showed that LS rats and obesity-prone LR rats do not differ in meal size, meal frequency, and meal duration on chow diet, indicating that individual leptin sensitivity on chow diet is not related to feeding microstructure on chow diet. Correlation analyses revealed that feeding microstructure on chow diet was neither related to the development of DIO on a fcHFHS diet.

From chapter 3 it was still unclear how the pre-existing reduction in pSTAT3 activation in the DMH predisposes LR rats to exacerbated DIO. Leptin is particularly known to activate brown adipose tissue (BAT) thermogenesis via neurons in the DMH [17, 26-29]. However, at least in *ob/ob* mice, leptin was recently shown to lead to a pyrexic increase in core body temperature by reducing heat loss via the tail, without affecting BAT thermogenesis [30].

Chapter 4. We here aimed to unravel whether rats that are less sensitive to the anorexigenic effects of peripherally injected leptin, also show a reduced thermogenic response to peripheral leptin. Further, to explore whether a reduced thermogenic response to peripheral leptin could be due to reduced cellular leptin signaling in the DMH (as opposed to, for example, impaired leptin transport across the blood-brain barrier (BBB)), we compared leptin regulation of thermogenesis after intravenous and after intra-DMH leptin injection between LS and LR rats fed regular chow. We also explored the contribution of BAT thermogenesis and heat loss via the tail to leptin's effect on core body temperature. After intravenous leptin injection, LS rats increased their BAT thermogenesis and reduced heat loss via the tail, resulting in a modest increase in core body temperature. The induction of these thermoregulatory mechanisms with intra-DMH leptin was smaller, but in the same direction as with intravenous leptin administration. Thus, LS rats showed a thermogenic response to leptin, which appears to be exerted, at least in part, at the level of the DMH. In contrast, LR rats did not show any thermogenic response to either intravenous or intra-DMH leptin, thereby linking their pre-existing reduction in pSTAT3 activation in the DMH to impaired leptin regulation of thermogenesis. The resistance to leptin's thermogenic effects in LR rats was associated with a 1°C lower BAT temperature and reduced BAT UCP1 expression under *ad libitum* feeding on chow diet, which may predispose LR rats to exacerbated obesity when exposed to a fcHFHS diet.

Appendix III. In this appendix, we aimed to study whether long-term blockade of leptin receptor (LepR) signaling within DMH neurons, or inactivation of LepR expressing DMH neurons, reduces core body temperature, and thereby results in increased body adiposity. We used several distinct viral vector technologies to downregulate leptin signaling in the DMH and compared the effects and technical limitations of the distinct viral vectors. In rats, we compared the effects of two different viral vectors, blocking LepR signaling via overexpression of a leptin receptor antagonist (LepA) or a microRNA sequence targeting LepR (miLepR), respectively. In LepR-Cre mice, we studied the effects of inactivation of LepR-expressing DMH neurons by using a virus expressing Cre-dependent tetanus toxin (TetTox) light chain. With none of the viral vectors we were able to selectively downregulate leptin signaling in DMH neurons. The technical limitations of the viral vectors were as followed: 1) LepA spread to neighboring hypothalamic subregions; 2) miLepR did not substantially downregulate leptin signaling; 3) TetTox injected mice showed hardly any TetTox-GFP protein positive cells, which may point towards toxicity effects, and only one mouse was bilaterally hit in the DMH according to *TetTox-GFP* mRNA expression. Because of the limitations of the employed viral vectors, we were not able to determine whether long-term blockade of leptin signaling specifically

within DMH neurons reduces core body temperature, and whether this is sufficient to defend adiposity.

Section II: Regulation of energy balance beyond the hypothalamus

The hypothalamus does not act in isolation but regulates energy balance via functional connections with other major brain areas, such as the midbrain [3, 31]. In section I, the DMH appeared to be a critical region for the regulation of energy balance. Therefore, the aim of section II was to study projections through which the DMH regulates energy balance. Two midbrain regions that are innervated by the DMH and were of particular interest to this thesis are the ventral tegmental area (VTA) and the periaqueductal grey (PAG), which were previously shown to regulate energy intake [32-38] and energy expenditure [39-42], respectively.

The DMH is generally accepted to exert its sympathetic control of BAT thermogenesis via projections to sympathetic premotor neurons in the raphe pallidus (RPa) [40, 41, 43-47], but there is evidence that the PAG is also an important relay in the descending pathways mediating thermogenesis [39, 40, 45, 48]. The PAG is a relatively long midbrain region that can be divided into dorsomedial (dmPAG), dorsolateral (dlPAG), lateral (lPAG) and ventrolateral (vlPAG) subdivisions, which differ with respect to their functional properties and anatomical projections [49]. The anatomical projections from the DMH to the distinct PAG subdivisions and their function are largely elusive and may differ per anterior-posterior level from bregma [39, 49-51].

Chapter 5. In this chapter, we aimed to investigate the anatomical projections from the DMH to the PAG along the entire anterior-posterior axis of the PAG, and to study the role of these projections in thermogenesis in rats. Anterograde viral tracing (with channel rhodopsin (ChR)) showed that the DMH projects especially to the dorsal and lateral PAG. Retrograde viral tracing (with rabies) confirmed this, but also indicated that the PAG receives a diffuse input from the DMH and adjacent hypothalamic subregions rather than specific input from the DMH. This finding emphasizes the importance of making very specific virus injections in the relatively small DMH region of the hypothalamus and distinct subdivisions of the PAG to unravel their specific anatomical and functional connections. We aimed to study the role of the identified DMH to PAG projections in thermogenesis in conscious rats by specifically activating them using a combination of canine adenovirus-2 (CAV2Cre) in the PAG and Cre-dependent designer receptor exclusively activated by designer drugs (DREADD) technology in the DMH. Chemogenetic activation of DMH to PAG projections increased BAT temperature and core body temperature, but we cannot exclude the possibility that at least some thermogenic effects were mediated by adjacent hypothalamic subregions due to difficulties in specifically targeting the DMH and distinct subdivisions of the PAG, because of diffuse virus expression. Thus, in chapter 5, we showed that it is technically challenging to specifically target the projections from the DMH to distinct PAG subdivisions because of the limitations of (dual) viral vector technology, and that the DMH generally appears not to be the predominant hypothalamic input area for the PAG.

Appendix IV. In this appendix, we studied whether the projections from the DMH to the PAG are leptin sensitive. To do this, we performed a retrograde viral tracing (with Cre-dependent herpes simplex virus) for two different anterior-posterior levels in the lPAG in LepR-Cre mice. This allowed us to visualize the LepR positive neurons in the hypothalamus that provide direct input to the lPAG. We found that the DMH is the second most important LepR positive hypothalamic input region for the lPAG, independent of the anterior-posterior level of the PAG. Thus, the DMH provides prominent LepR positive hypothalamic input to the PAG along several levels of its anterior-posterior axis. This finding is in contrast to the diffuse hypothalamic input to the PAG when no distinction between cell types was made (chapter 5).

Appendix V. As also discussed in chapter 5, we experienced several technical challenges in targeting the DMH and its projections with dual viral vector technology. In appendix V, we provide an overview of the targeting of the DMH with different viral vectors that have been employed in this thesis. In Wistar rats, we showed successful targeting of the DMH following intra-DMH injection of constitutively expressing viruses. A minor limitation was that virus expression was not fully restricted to the DMH. In LepR-Cre mice, the targeting of the DMH with Cre-dependent viruses was also successful, although one limitation was that TetTox-GFP was only observed at the mRNA level instead of protein level in the DMH. This points towards potential toxicity effects of TetTox. In contrast, targeting of the DMH was not successful in Wistar rats with all approaches employing Cre-dependent DREADD or TetTox in the DMH in combination with Cav2Cre in a projection region. In most cases, needle tracks were directed towards the DMH, but (almost) no virus expression was observed in the DMH. Thus, there appears to be a specific problem in targeting the DMH with Cre-dependent viruses in combination with Cav2Cre in a projection region.

Chapter 6. In this chapter, we aimed to target the DMH to VTA projection, but the histology analysis revealed that the DMH was not the main target; instead, the ZI appeared to be the main target. In accordance, the ZI was previously shown to provide the major direct hypothalamic innervation of the VTA, together with the LH [52, 53]. Both the zona incerta (ZI) and the ventral tegmental area (VTA) have been implicated in feeding behavior, but it has not been studied before whether the ZI to VTA projection regulates feeding. Therefore, we investigated the effects of permanent inactivation and reversible activation of ZI to VTA projection neurons on several aspects of feeding behavior. To activate or inactivate ZI neurons projecting to the VTA, we used a combination of CAV2Cre in the VTA, and Cre-dependent DREADD or TetTox in the ZI, respectively. TetTox-mediated inactivation of ZI to VTA projection neurons reduced the motivation to work for food and reduced food intake due to lower meal frequency. Conversely, DREADD-mediated chemogenetic activation of ZI to VTA projection neurons promoted food-motivated behavior and feeding. Thus, we showed for the first time that the ZI to VTA projection exerts bidirectional control over feeding by modulating action initiation towards food. (In)activation of ZI to VTA projection neurons did not affect locomotor activity or directly regulate core body temperature, demonstrating that ZI to VTA projection neurons drive feeding by facilitating action initiation towards food, without affecting general activity.

General discussion

In this discussion, several generally accepted concepts related to leptin, the hypothalamus, and energy balance are challenged. Further, this chapter discusses the unanticipated results regarding the neural projections that control energy intake and energy expenditure. Also the technical challenges and limitations in performing the studies in this thesis are described. Finally, it is proposed how the findings of this thesis may translate to the human situation, and how they may contribute to the prevention and/or treatment of obesity.

1. Insights obtained from leptin sensitive and leptin resistant rats

1.1 Defining leptin resistance

Leptin resistance is a complex concept. The most general definition of leptin resistance is that elevated plasma leptin levels in obese individuals fail to counteract obesity [22, 54]. In rodent models of diet-induced obesity (DIO), leptin resistance is often defined as a failure of exogenously injected leptin to reduce food intake [9-11, 13-15, 19, 22, 55]. In these models, leptin resistance is often relative, *i.e.* a reduced but not complete absent sensitivity to the food intake suppressing effects of exogenous leptin, usually observed at one or a few time-points following leptin injection [9, 14, 22, 55-57]. The results of our systematic review in **chapter 3** (Table S1) indicate that previous studies assessed leptin sensitivity at variable time-points after leptin injection, ranging between 2-38 hours after injection. The effect sizes of the anorectic response to leptin were very variable. These results indicate that the well-established food intake suppressing effect of leptin is not that straightforward, and therefore that the conclusion of leptin resistance largely depends on the time-points at which leptin sensitivity is tested. Further, leptin sensitivity was often tested at the group level instead of by comparing the treatment effects within individual rats.

Although our 1-24h monitoring of leptin sensitivity at the individual level in **chapter 3** is already a step ahead in accurately determining leptin sensitivity, there are still a number of issues that should be considered when assessing leptin sensitivity, most importantly the criteria based on which leptin sensitive rats should be distinguished from leptin resistant rats. Potential criteria for the definition of leptin sensitive versus leptin resistance could be the timing at which leptin's anorexigenic effects might be expected or the number of time-points at which leptin reduces food intake. For example, since leptin has been shown to induce

pSTAT3 signal transduction within an hour following leptin injection [17, 19], a rat could be defined as leptin resistant if it does not reduce its food intake during the first hour following leptin injection. An alternative definition for leptin resistance could be that a rat is leptin resistant if it shows a reduction in food intake at less than 12 of the 24 time-points at which food intake was measured. Potential compensation for a leptin-induced reduction in food intake may complicate the latter point, although we showed in **chapter 3** (Fig. 3C) that compensation may play a limited role within the first 24h following leptin injection. The long-lasting food intake suppressing effect of leptin probably results from the long residence time of leptin binding to its receptor [58].

Another point of consideration is to distinguish between relative and absolute leptin resistance. Relative leptin resistance may refer to a reduction in leptin sensitivity compared with for example control animals or sensitivity at another time-point (e.g. before fcHFHS diet exposure). Absolute leptin resistance, *i.e.* absolutely no anorexigenic response to leptin, is more difficult to demonstrate, especially at multiple time-points. In **chapter 3**, we integrated all of the considerations above to select leptin sensitive (LS) and leptin resistant (LR) rats, and to study the development of diet-induced leptin resistance on the fcHFHS diet. On chow diet, LS and LR rats were selected based on their absolute leptin sensitivity at the first hour after leptin injection, and LS rats were shown to be relatively more leptin sensitive compared with LR rats at 2-24h following leptin injection. The development of diet-induced leptin resistance in LS and LR rats was studied by measuring relative leptin resistance compared with leptin sensitivity before fcHFHS diet exposure and was calculated by counting the number of time-points at which rats did not respond to leptin. Even though we took all these considerations into account, it remains difficult to fully characterize the distinction between leptin sensitive and leptin resistant.

Finally, also the dose of leptin should be taken into account when assessing leptin sensitivity because this has a major influence on the effectiveness of leptin to reduce food intake, as is nicely shown by the dose-response study of Ruffin et al. 2004 [1]. A highly variable effect of leptin on food intake (range -94% to +129%) was found in Wistar rats following intravenous injection of a low dose of leptin (20 µg) [1]. Interestingly, we observed similar feeding responses in Wistar rats after a much higher dose (250 µg) of intravenously injected leptin.

1.2 Selective leptin resistance in the DMH and VMH instead of the ARC

Leptin resistance is also a complex concept at the cellular level being subject to interpretation. The development of diet-induced leptin resistance is often

demonstrated by an attenuation in the incremental increase or maximal level of leptin-induced pSTAT3 specifically in the ARC of rodents [14, 17-19]. An important point that should be taken into account when testing leptin sensitivity at the cellular level, is the degree of endogenous leptin action. In **chapter 3**, we showed that leptin injection does not increase pSTAT3 levels in the ARC in both LS and LR rats on the fcHFHS diet. However, both LS and LR rats already showed increased pSTAT3 levels on the fcHFHS diet after vehicle injection compared with chow diet and were therefore probably not able to further increase their pSTAT3 signaling following leptin injection. Increased pSTAT3 activation in the ARC after exposure to an obesogenic diet was previously also reported, and was shown to indicate increased endogenous leptin action [11]. Therefore, we state that both LS and LR rats did not develop leptin resistance in the ARC. If we had defined leptin resistance simply as an attenuation in the incremental increase of pSTAT3 following leptin versus vehicle, we would have concluded that LS and LR rats developed leptin resistance in the ARC after fcHFHS diet exposure. In previous studies, pSTAT3 activation in the ARC after vehicle injection was either not reported [19] or not elevated on a high-diet (*e.g.* [17]). Thus, the major difference between our result and those of previous studies is that we found increased pSTAT3 signaling in the ARC on the fcHFHS diet after vehicle injection, indicating increased endogenous leptin signaling. It should be noted that assessment of the maximal level of leptin-induced pSTAT3 activation in the ARC also led to the conclusion that LS and LR rats do not develop leptin resistance in the ARC, in contrast to the development of selective leptin resistance in the ARC in previous studies [17, 19].

By studying the maximal level of leptin-induced pSTAT3 in the ARC of rodents in **chapter 3**, we found that LR rats show a pre-existing reduction in cellular leptin sensitivity in the VMH and DMH, but not the ARC. LS rats, but not LR rats, also developed diet-induced leptin resistance in the VMH and DMH. The development of diet-induced leptin resistance in the DMH was most convincing, as this was demonstrated by both an attenuation in the maximal level of leptin-induced pSTAT3 and loss of the incremental increase in comparison with vehicle.

1.3 Mechanisms underlying the pre-existing reduction in leptin sensitivity in the DMH

In **chapter 3**, we concluded that the susceptibility to develop excessive DIO depends on a pre-existing reduction in leptin responsiveness rather than diet-induced leptin resistance, as LR rats showed exacerbated weight gain and adiposity compared with LS rats during fcHFHS diet feeding. Importantly, the molecular mechanisms underlying diet-induced leptin resistance might differ from those underlying a pre-

existing leptin resistance. Diet-induced leptin resistance is initially characterized by peripheral leptin resistance, but prolonged high-fat diet feeding eventually also induces central leptin resistance, especially in the ARC [14, 17-19, 22]. In contrast, studies in selectively bred DIO and diet-resistant (DR) rats by Levin et al. indicate that a pre-existing leptin resistance does not result from impaired leptin transport across the BBB, but from reduced central leptin resistance, as reflected in reduced LepRb expression, leptin receptor binding, and pSTAT3 activation, in the ARC, VMH, and DMH [59-62].

In contrast to the results of Levin et al., we showed a pre-existing reduction in pSTAT3 activation in the DMH and VMH, but not the ARC in LR rats. The discrepancy with the above described results of Levin et al. might result from their selective breeding of DR and DIO rats or differences in rat strain and/or supplier. At first glance, the most plausible explanation for the pre-existing reduction in pSTAT3 activation in the DMH and VMH, but not the ARC, of LR rats seems impaired transport of leptin through the cerebrospinal fluid (CSF) in the third ventricle. Such a transport defect may specifically be observed after peripheral leptin injection. To explore whether a reduced response to leptin in the DMH/VMH could be due to reduced cellular leptin signaling in these regions, as opposed to, for example, impaired leptin transport across the BBB or through the CSF, we compared the effects of leptin after peripheral (intravenous) versus intra-DMH leptin injection in **chapter 4**. We aimed to compare pSTAT3 signaling in the DMH following peripheral versus intra-DMH leptin injection, but the pSTAT3 stainings were not successful. Since leptin signaling in the DMH is particularly known to regulate thermogenesis, we compared leptin-induced thermogenesis after peripheral versus intra-DMH leptin injection. In contrast to LS rats, LR rats did not show any thermogenic response to either peripheral or intra-DMH leptin. These findings suggest that the reduced response to peripheral leptin is exerted, at least in part, by reduced responsiveness of LepRb-expressing neurons in the DMH (*i.e.* central leptin resistance).

Central or cellular leptin resistance may be mediated by various mechanisms. The reduction in leptin-induced pSTAT3 activation in the DMH does not reveal the underlying mechanism, as it may reflect, for example, reduced cell surface LepRb levels, impaired leptin signal transduction, or impaired leptin binding. These mechanisms were all shown to explain the pre-existing reduction in central leptin sensitivity in the ARC, VMH, and DMH of DIO rats [59-62]. In LR rats, it is fascinating that specifically the ARC does not become leptin resistant. The best way to explain this phenomenon might be that leptin resistance in LR rats results from a combination of impaired leptin transport through the CSF and central leptin resistance in the hypothalamus. To test the contribution of impaired leptin transport through the CSF, a time-course of pSTAT3 activation should be made for the ARC, VMH, and DMH following peripheral leptin injection.

1.4 Reduced thermogenesis likely links the pre-existing reduction in leptin sensitivity in the DMH (and VMH) in LR rats to exacerbated obesity

Mice fed a high-fat diet were previously show to develop resistance to leptin's anorexigenic effects but remained sensitive to leptin's thermoregulatory effects [19], which are critically mediated by the DMH [17]. This finding is in accordance with the development of selective leptin resistance in the ARC upon high-fat diet feeding [14, 17-19]. In contrast, we found in **chapter 4** that LR rats, which show a pre-existing reduction in the sensitivity to leptin's anorexigenic effects, are also resistant to leptin's thermogenic effects. This finding may be explained by the pre-existing reduction in cellular leptin sensitivity in the DMH (and VMH) in LR rats (**chapter 3**).

In **chapter 4**, we show that LS rats exhibit a significant increase in BAT thermogenesis and a significant reduction in heat loss via the tail following peripheral leptin injection. The induction of these thermoregulatory mechanisms with intra-DMH leptin was smaller and non-significant, but in the same direction as with peripheral leptin administration. In interpreting these data, several limitations should be kept in mind, most importantly the low number of rats in the LS group (due to unexpected premature emptying of a considerable number of transmitter batteries and misplacement of BAT probes). Explanations for the non-significant effects of intra-DMH leptin on thermoregulation in LS rats could not only be the low n, but also that leptin is known to modestly affect body temperature [17, 27, 28, 30], which is in line with its proposed permissive rather than active thermogenic role [26, 44, 63]. Finally, also the large individual differences in the thermogenic response to leptin may provide an explanation for the non-significant effects in LS rats. As explained thoroughly in the discussion section in **chapter 4**, we believe that the thermogenic effects we observed following intra-DMH leptin injection in LS rats are valid. Nevertheless, further experiments with a higher n are required to investigate whether the impaired thermogenic response to peripheral leptin in LR versus LS rats is exerted via leptin resistance at the level of the DMH. To determine the importance of leptin signaling in the DMH in mediating thermoregulation following peripheral leptin administration, a leptin antagonist could be injected into the DMH prior to peripheral leptin injection. In ***appendix III***, we also aimed to downregulate leptin receptor signaling specifically in the DMH by using viral vector technology, but this appeared technically challenging, as also discussed in section 3.1.

In **chapter 4**, the resistance to leptin's thermogenic effects likely contributes to the 1°C lower basal BAT temperature and the lower BAT UCP1 levels in LR rats compared with LS rats under *ad libitum* feeding. Since BAT thermogenesis has the capacity to prevent excess body weight gain in response to an obesogenic diet [26], the pre-existing reduction in BAT thermogenesis in LR rats likely predisposes them to exacerbated obesity on a fcHFHS diet. Although limited, evidence supports a role for leptin signaling in the VMH in the regulation of BAT thermogenesis [64-66]. Interestingly, mice with selective deletion of LepRs in VMH steroidogenic factor-1 (SF-1) neurons show defective adaptive thermogenesis in response to a high-fat diet, suggesting that leptin signaling in VMH SF-1 neurons is especially required for the promotion of energy expenditure in response to HFD exposure [64, 65]. Therefore, the pre-existing reduction in leptin sensitivity in the VMH may, like that in the DMH, predispose LR rats to exacerbated obesity on a fcHFHS diet due to defective adaptive thermogenesis. Future studies are necessary to determine whether LR rats are indeed not able to sufficiently adapt their BAT thermogenesis to the increased caloric intake on a fcHFHS diet, and whether this is the mechanism by which they become excessively obese.

1.5 Other mechanisms that may explain the development of excessive obesity in LR rats

Although defective adaptive thermogenesis provides a plausible explanation as for how the pre-existing reduction in leptin sensitivity in the DMH and VMH may predispose LR rats to excessive obesity, it has not been shown yet whether this is the mechanism by which LR rats become excessively obese on the fcHFHS diet. Moreover, other mechanisms that lead to increased energy intake and/or reduced energy expenditure may contribute to the development of exacerbated obesity in LR rats as well (Table 1).

In **chapter 3** and ***appendix II***, we show that LS and LR rats do not differ in energy intake or meal patterns on chow diet, and neither differ in total caloric intake on the fcHFHS diet or the consumption of the chow, lard, and sugar water components of the fcHFHS diet. However, it was not tested whether LS and LR rats differ in meal patterns on the fcHFHS diet. Since especially the combination of fat and sugar appears to be deleterious for obesity development and its metabolic consequences [57, 67], it might be that LR rats consume more often meals consisting of a combination of fat and sugar water. Alternatively, LR rats might have an increased capacity to absorb energy from the fcHFHS diet, as increased energy extraction has been associated with high-fat diet feeding, obesity, and reduced leptin sensitivity [68-70]. The level of energy absorption from ingested food could be tested by performing bomb calorimetry on feces, which allows determination of the energy lost in feces [71].

It might seem paradoxical that LS and LR rats, which were selected based on their acute feeding response to exogenous leptin on chow diet, display similar daily caloric intake while on a chow or on a fcHFHS diet. However, the feeding response to supra-physiological doses of pharmacological leptin may not be physiologically relevant at all, *i.e.* the feeding response elicited by pharmacological leptin may not indicate anything about the modulation of daily food intake by leptin signaling. This notion is in line with the idea that leptin acts as a tonic gain-setter for other signals regulating energy balance, such as shorter term anorectic signals. Despite this notion, the feeding response to pharmacological leptin uncovers a susceptibility to become obese on a fcHFHS diet. Our model may especially be interesting to study food intake independent mechanisms by which a pre-existing reduction in leptin sensitivity in the DMH/VMH predisposes rats to exacerbated DIO.

In **chapter 4**, LS and LR rats did not differ in locomotor activity. The lower BAT temperature in LR versus LS rats on chow diet did not result in a lower core body temperature, which might be explained by higher insulation in LR rats. Next to a possible defect in adaptive BAT thermogenesis in response to fcHFHS diet feeding, also reduced energy expenditure as measured by heat production (resulting from the oxidation of carbohydrates, fat, and proteins) in a metabolic cage, may be a potential mechanism by which LR rats become excessively obese following fcHFHS diet exposure. Investigation of the contribution of the latter two mechanisms, as well as of energy absorption, should be the focus of further research to elucidate via which mechanism LR rats become more obese than LS rats on the fcHFHS diet.

Table 1. Potential mechanisms underlying increased proneness for obesity in LR rats compared with LS rats

Mechanism	Difference between LS and LR rats	Reference
Energy intake and absorption		
Total caloric intake		Chapter 3
Chow	LS = LR	
fcHFHS	LS = LR (slight tendency for LS < LR)	
chow	LS = LR	
lard	LS = LR	
sugar water	LS = LR	
Meal patterns		Appendix II
Chow	LS = LR	
fcHFHS	n.a.	
Energy absorption from food		n.a.
Chow	n.a.	
fcHFHS	n.a.	
Energy expenditure		
Core body temperature		Chapter 4
Chow	LS = LR	
fcHFHS	LS = LR*	
BAT thermogenesis		Chapter 4
Chow	LS > LR	
fcHFHS	n.a.	
Tail temperature		n.a.
Chow	n.a.	
fcHFHS	n.a.	
Locomotor activity		Chapter 4
Chow	LS = LR	
fcHFHS	LS = LR*	
Oxidation of nutrients / heat production		n.a.
Chow	n.a.	
fcHFHS	n.a.	

*Preliminary data (not shown in this thesis). n.a., not available, = equal level in LS and LR rats, > / < higher / lower level in LS versus LR rats.

1.6 Contribution of diet-induced leptin resistance and hypothalamic inflammation to the development of DIO

Diet-induced leptin resistance has been proposed to initiate and/or maintain DIO [7, 9-11, 13-15, 19, 22, 55]. In **chapter 3**, we show that LR rats, which were predisposed to develop excessive obesity, showed a pre-existing reduction in leptin sensitivity which was not further reduced by fcHFHS diet exposure. Thus, diet-induced leptin resistance appears not to play a role in the development of obesity in rats that are predisposed to develop excessive obesity. However, the findings in LS rats suggest that diet-induced leptin resistance may contribute to the development of obesity in rats that do not show a pre-existing reduction in leptin sensitivity. LS rats did develop diet-induced leptin resistance, and although they became less obese than LR rats, they still showed a 25% increase in adiposity and a 50% increase in plasma leptin levels compared with chow diet-fed rats after 8 weeks of fcHFHS diet exposure.

In **chapter 2**, we review literature showing that overconsumption of pelleted high-fat diets induces an inflammatory response in the hypothalamus, which contributes to the development of central leptin resistance and obesity [72-74]. In ***appendix I***, we tested whether exposure to the fcHFHS diet also results in an inflammatory response in the hypothalamus, and focused on IKKβ/NF-κB signaling, as this is often described as "the master switch" of the innate immune system. The group of rats in which we tested inflammatory signaling consisted mainly of LS rats (which were the rats that developed diet-induced leptin resistance upon fcHFHS diet feeding). We did not observe an upregulation of IKKβ/NF-κB signaling in the MBH of fcHFHS diet fed rats, suggesting that hypothalamic inflammation does not contribute to the development of fcHFHS diet-induced leptin resistance and obesity in LS rats. Importantly, the detection of inflammatory markers in the hypothalamus was recently shown to depend on the intake of the fat and sugar water components of the fcHFHS diet shortly before sacrifice [75]. Removal of fat and sugar water in the night before sacrifice reversed fcHFHS diet-induced hypothalamic inflammation. These findings were observed in rats that were offered the fcHFHS diet for one week, and suggest that one week of fcHFHS diet feeding is not sufficient to induce irreversible adaptations in inflammatory signaling. In accordance, previous studies also showed a complex "on-off" expression pattern for several inflammatory mediators during the first days of high-fat diet feeding, followed by permanent upregulation after prolonged high-fat diet feeding (**chapter 2**, Table 1). In ***appendix I***, we neither observed inflammatory signaling after 8 weeks of fcHFHS diet feeding, which is a time-point at which inflammatory signaling was previously shown to have become chronically upregulated after high-fat diet exposure (**chapter 2**; Table 1). The discrepancy with previous studies could result from differences in diet or feeding status shortly before sacrifice. Regardless of the reason for the discrepancy, it is obvious that long-term fcHFHS diet feeding does not induce irreversible hypothalamic inflammation. Since the fcHFHS diet mimics the human diet more closely than pelleted high-fat diets (**chapter 1**, section 4.1), our findings question the relevance of hypothalamic inflammation for the development of diet-induced leptin resistance and obesity in the human situation.

1.7 The origin of LS and LR rats

The origin of the pre-existing differences in leptin sensitivity is still unknown and may reflect both genetic and epigenetic variation. We used commercially

available outbred rats in our experiments, which makes it difficult to determine the potential contribution of *e.g.* litter size (early prenatal and postnatal environment) and breeding (*e.g.* parity) to the development of pre-existing differences in leptin sensitivity.

1.8 Implications for the prevention and treatment of human obesity

1.8.1 Weight reduction in human obesity

The current treatment of human overweight and obesity focuses on weight reduction, which is most successfully achieved by bariatric surgery. Although weight reduction itself is difficult, it is even harder to keep the weight off once it has been lost [76]. Long-term studies in weight-reduced children and adults indicate an 80-90% recidivism rate to pre-weight loss levels of body fatness after otherwise successful weight loss [77]. This high recidivism rate can be explained by counter-regulatory mechanisms, involving declines in energy expenditure, circulating leptin levels, and activity of the hypothalamus, that are evoked during the maintenance of a reduced body weight [76, 78, 79]. These counter-regulatory mechanisms create the ideal situation for weight regain, and thereby actively oppose the treatment of obesity over long periods of time, eventually resulting in reinstatement of pre-weight loss levels of body fat.

Both in humans and rodents, maintenance of a reduced body weight results in a drop in circulating leptin levels, which informs the brain about decreased fat reserves, thereby triggering a compensatory decrease in energy expenditure and increase in food intake [76, 78-80]. Studies in 10% weight-reduced lean and obese human subjects show that administration of replacement doses of leptin, that restore circulating leptin levels to pre-weight loss levels, reverse the metabolic, behavioral, neuroendocrine and autonomic changes that characterize the weight-reduced state, including the decrease in energy expenditure and its associated decline in SNS activity and thyroid hormones, and the increase in food intake [76, 78, 79]. Accordingly, leptin replacement also reverses reduced activity of the hypothalamus in the weight-reduced state [79]. The weight-reduced state may therefore be regarded as a state of relative leptin deficiency.

Lean and obese human subjects maintained at a 10% reduction in body weight show a ~20-25% decline in 24h energy expenditure [81, 82]. This decrease in energy expenditure is 10-15% below that what might be expected based on the reduction in lean mass and body fat. In weight-reduced human subjects, declines in SNS activity and circulating thyroid hormones constitute mechanisms by which low leptin levels may result in reduced BAT-dependent thermogenesis [76]. As little as 25 gr of BAT going from a maximally active to a minimally active state was predicted to be more than sufficient to account for the unpredicted extra decline in resting energy expenditure following weight loss [76]. Therefore, reduced BAT thermogenesis could, at least partially, explain the magnitude of reduced energy expenditure following weight loss. BAT is an important thermoregulatory effector organ in rodents [45, 83]. In adult humans, however, the contribution of BAT to thermogenesis remains unclear, even though evidence acknowledged metabolically active BAT in adult humans (see discussion section 2.1) [76, 84-87].

1.8.2 Translating insights obtained from LS and LR rats to human obesity

As explained above, the weight-reduced state in lean and obese human subjects is characterized by counter-regulatory mechanisms associated with relative leptin deficiency, which can be reversed by leptin administration. Importantly, substantial variation has been observed in the effectiveness of leptin to reverse these counter-regulatory mechanisms [78]. By translating the findings in LS and LR rats in this thesis to human obesity, at least some of the variability in the effectiveness of leptin in weight-reduced humans can be explained. In **chapter 3**, we show high variability in leptin sensitivity between rats, but not within a rat over time. We divided rats into leptin sensitive (LS) and leptin resistant (LR) rats based on pre-existing sensitivity to the anorexigenic effects of leptin on chow diet, and showed in **chapter 4** that LR rats are also resistant to the thermogenic effects of leptin on chow diet. Although genetic variations in leptin and LepR genes have been reported in humans [54], we do not know whether a similar distinction between LS and LR can be made in the human population. Therefore, the considerations below are hypothetical.

In human individuals showing similar leptin sensitivity as LS rats, leptin administration in the weight-reduced state is expected to successfully reverse the decline in energy expenditure and increase in food intake. In contrast, in human individuals showing a similar resistance to leptin as LR rats, leptin administration in the weight-reduced state is expected not to be successful in reversing these counter-regulatory mechanisms. Furthermore, these individuals are probably more prone to develop excessive obesity in our modern society, that provides *ad libitum* availability of energy-dense foods and encourages a sedentary lifestyle, as was shown for LR rats on the fcHFHS diet (**chapter 3**). The pre-existing reduction in BAT thermogenesis that was observed in LR rats may contribute to the development of excessive obesity (**chapter 4**) and will likely oppose successful weight loss. Thus, individuals showing similar resistance to leptin as LR rats will likely become more obese in our modern society and experience more difficulties in losing excess weight due to, for example, a pre-existing reduction in BAT thermogenesis, which cannot be reversed by leptin administration.

For human individuals showing a pre-existence resistance to leptin similar to that in LR rats, it is especially important to prevent the development of obesity. In rats, the feeding response to leptin during the first hour following injection predicts the susceptibility to DIO (**chapter 3**). It would be interesting to test whether the feeding response to leptin is suitable as a biomarker for humans with an increased susceptibility to develop excessive obesity, as such that those identified as susceptible know that they should be very cautious with their diet and lifestyle in order to prevent the development of obesity. However, testing the acute anorexigenic response to exogenous leptin is more difficult to accomplish in human individuals. Therefore, it would be ideal if plasma leptin levels could be used as a biomarker of leptin sensitivity. The finding that plasma leptin levels were not different between LS and LR rats on chow diet (**chapter 3**) indicates that plasma leptin levels are probably not suitable as biomarker. Since the feeding response to leptin correlates with the thermogenic response to leptin (**chapter 4**), measurement of the acute temperature response to exogenous leptin could be an alternative, easier to accomplish way to measure leptin sensitivity in human individuals.

Although prevention is the best strategy to combat the rising prevalence of obesity, this thesis also provides some insights into treatment possibilities. Current pharmacological therapies for obesity focus on weight loss during the obese state and are based on the assumption of a balance between energy intake and energy expenditure [79]. Weight loss, however, results in an uncoupling of this balance, as such that an increase in energy intake and a reduction in energy expenditure promote weight regain. Since these counter-regulatory mechanisms are associated with a state of relative leptin deficiency, treatment with pharmacological leptin or a leptin agonist will support weight loss and the prevention of weight regain by reversing these counter-regulatory mechanisms. However, as explained above, leptin treatment will not be successful in all individuals due to leptin resistance. In leptin resistant individuals, additional treatment of leptin resistance is necessary, whereby the underlying mechanism of leptin resistance should be taken into account. As explained in discussion section 1.3, the molecular mechanisms underlying diet-induced leptin resistance might differ from those underlying a pre-existing leptin resistance and may therefore require different therapeutic targets. It is obvious that pre-existing leptin resistance (a stable parameter that is not affected by fcHFHS diet feeding), as observed in LR rats, needs to be treated in order to allow leptin administration to reverse the counter-regulatory mechanisms in the weight-reduced state. For diet-induced leptin resistance, as observed in LS rats on the fcHFHS diet, it is uncertain whether treatment of leptin resistance is required. Previously, rats that developed diet-induced leptin resistance following fcHFHS diet exposure quickly restored their leptin sensitivity following withdrawal of the fat and sugar component of the fcHFHS diet [9]. However, findings in our lab indicate that rats remain resistant to the anorexigenic effects of leptin following withdrawal of the fat and sugar component of the fcHFHS diet [88], but that leptin treatment corrects hypothermia during the withdrawal phase [88], which might be sufficient to support (the maintenance of) weight loss. In order to identify therapeutic targets for the treatment of leptin resistance, elucidation of the molecular mechanisms underlying pre-existing leptin resistance, as observed in LR rats, should be the priority for further research.

2. Challenges in measuring (brown adipose tissue) thermogenesis in rodents and its translation to human thermoregulation

2.1 Thermoregulation in rodents versus humans

In **chapter 4**, **chapter 5**, **chapter 6**, and ***appendix III*** of this thesis, we studied thermogenesis in rodents. It is important to know how much human and rodent thermoregulation overlap in order to translate findings in rodent studies to humans. Although the repertoire of thermal effectors in rodents is, with the exception of sweating and heat loss via the tail, similar to that in humans [83], there are a few challenges in translating rodent thermoregulation to humans. Processes related to the surface area: body mass ratio and ambient temperature are some of the key factors that can affect the translational potential of rodent studies (for detailed overview see [89]).

As a consequence of the ~3000-fold lower body mass, rodents have a larger surface area: body mass ratio than humans [89,90]. Since surface area is an important determinant of heat exchange, rodents show disproportional greater heat loss. Therefore, heat generation (*e.g.* via brown adipose tissue (BAT) thermogenesis) is a major mechanism for survival. Rodents also show a higher rate of thermal conductance and have a minimal "thermal shell". Consequently, their core body temperature, whilst tightly regulated, varies much more than in humans. In general, the variability in core body temperature increases when a mammal's body size becomes smaller [89,90].

Since humans live in or near their thermo-neutral zone, heat is primarily generated as a by-product of metabolic processes, with a small contribution of adaptive thermogenesis [90]. Rodent studies are usually performed at ambient temperatures around 20-24 ºC, but this ambient temperature lies below the thermo-neutral zone

of rodents (approximately 28-32ºC) [89-91]. As rodents prefer warmer temperatures, they are cold-stressed at ambient temperatures of 20-22 ºC, leading to adaptive thermogenesis, a tightly regulated heat producing process that is primarily executed by BAT (though behavioral thermoregulatory responses, such as adaptations in the nest structure, and body contact in group-housed rodents are also major effector mechanisms against cold stress) [26, 63, 83, 89, 90, 92]. In contrast, humans experience cold stress infrequently and have a greater "thermal shell", which helps to increase the insulation of their core in response to cold, and thereby to maintain a stable core body temperature [89, 90]. Housing rodents at thermo-neutrality may help to increase the translational potential of rodent models, but this is difficult to accomplish in most laboratories.

In **chapter 4**, **chapter 5**, and ***appendix III*** of this thesis, we studied BAT thermogenesis in rodents. BAT is an important thermoregulatory effector organ in rodents in various physiological conditions [45, 83]. It contributes to thermogenesis to maintain core body temperature at rest (obligatory thermogenesis) and at ambient temperatures below thermo-neutrality (facultative thermogenesis) [76]. Recent evidence also acknowledged metabolically active BAT in adult humans, as measured by 2-[18F]fluoro-2-deoxy-glucose (FDG) uptake [84-87]. Of note, although the FDG uptake seen in BAT implies the existence of metabolically active tissue in human subjects, FDG does not necessarily reflect actual thermogenic activity [76]. The contribution of BAT to thermogenesis in adult humans remains therefore unclear (for overview see [76]). Further, variable results were obtained in the ability to detect metabolically active BAT in adult human subjects under thermo-neutral conditions (representing obligatory thermogenesis) [76, 84-86]. The detection of BAT was improved at temperatures below thermo-neutrality after a cold challenge (representing facultative thermogenesis) [76, 84-86]. In our modern society, humans spend most of their time in or near their thermo-neutral zone, which reduces the need for facultative thermogenesis via *e.g.* BAT thermogenesis [76]. Therefore, especially a potential role for BAT in obligatory thermogenesis seems relevant for adult humans, although stimulation of BAT activity or "recruitment" of BAT is also regarded as a promising therapeutic target for the prevention and treatment of obesity [93].

2.2 Technical limitations in studying thermogenesis in rodents

In studying thermoregulation in rodents in our lab, we experienced several technical limitations. First of all, we observed high variability in room temperature (range 21.2-23.9 ºC) and humidity levels (range 44-61%) between days in the light and temperature "controlled" experimental rooms. Accordingly, there was a large variability observed in pre-injection baseline temperatures within individual rats between two test days in a Latin square design (average difference: 0.3±0.3 ºC; range of difference: 0.0-1.1 ºC for both BAT and core temperature). Pre-injection baseline temperatures were also quite variable between rats over test days (ranging between 35.3-39.6 ºC for core temperature, and 35.0-38.4 ºC for BAT temperature). For thermogenesis experiments, where we expected maximal temperature effects of 0.5-1 ºC following leptin or clozapine N-oxide (CNO) injection, such a variability in pre-injection baseline temperature is too large to reliably study the thermogenic response to leptin or CNO. At least for leptin, which is thought to permissively increase core body temperature [26, 44, 63], pre-injection baseline temperatures may largely influence the maximal thermogenic response to exogenous leptin (**chapter 4**). Although the thermogenic response following chemogenetic activation of DREADD-expressing neurons with CNO does probably not act in a permissive manner, also here a ceiling effect for core body temperature is expected to affect the maximal thermogenic response to CNO. Because of these limitations, thermogenic responses to leptin and CNO were mostly studied at the group level in this thesis, as pre-injection baseline temperatures were too variable to study thermogenic effects within individual rats in a Latin square design.

Other technical limitations that complicated the measurement of thermogenesis in this thesis are the susceptibility of dual transmitters (TL11M3F40-TT, Data Science International (DSI), USA) for spontaneously occurring "circuit errors" and premature emptying of the transmitter battery. The BAT probe was also often misplaced because it was slipped out of the insoluble suture, despite multiple stitches. All these technical limitations substantially reduced the number of animals in the experiments described in **chapter 4** and especially **chapter 5**, which reduced the power to detect thermogenic effects.

3. Challenges in employing (dual) viral vector technology in the DMH

In this thesis, several distinct viral vectors have been employed to study the role of leptin receptor (LepR) signaling within the DMH, and to study projections through which the DMH regulates energy balance. In employing these viral factors, three main technical limitations hampered our research: 1) We were not able to selectively downregulate leptin signaling in DMH neurons; 2) Expression of tetanus toxin (TetTox) light chain was only observed at the mRNA level instead of the protein level in the DMH; 3) Targeting of the DMH was not successful with all approaches employing Cre-dependent virus in the DMH in combination with canine adenovirus-2 (Cav2Cre) in a projection region. In

addition to these limitations, concerns have been raised in recent literature regarding CNO, the inert ligand for designer receptor exclusively activated by designer drugs (DREADDs), because of potential off-target effects of its metabolite clozapine [94, 95].

3.1 Downregulation of leptin receptor signaling in DMH neurons

In ***appendix III***, we show that we were not able to selectively downregulate leptin signaling in DMH neurons with any of the viral vectors that were employed. The major reason for why overexpression of a leptin antagonist (LepA) does not specifically downregulate leptin receptor signaling within the DMH, is that LepA is secreted by infected neurons and spreads to neurons in surrounding areas, and possibly projection areas, where it also downregulates pSTAT3 signaling. Due to the nature of this technology, it will never be possible to specifically block LepR signaling in the DMH with viral overexpression of LepA.

For the virus that expresses a microRNA sequence targeting *LepR* (miLepR) we did not observe substantial downregulation of pSTAT3 in miLepR-GFP expressing neurons. However, we did not quantify the downregulation of pSTAT3 in the DMH, or more specifically, in miLepR-GFP expressing neurons in the DMH. In previous studies that aimed to downregulate LepR signaling in specific hypothalamic subregions by employing (other) viral vector technologies, downregulation of pSTAT3 or *LepR* mRNA was neither obvious in the immunohistochemical staining, but quantification of pSTAT3 or *LepR* mRNA levels revealed a downregulation of ~50% [27, 96]. This magnitude of downregulation in leptin signaling in DMH neurons was sufficient to induce a time-dependent increase in body weight and adiposity but did not affect core body temperature at room temperature [27]. In order to determine whether expression of miLepR induces sufficient downregulation of leptin signaling in the DMH to allow induction of a behavioral phenotype, quantification of pSTAT3 downregulation (in miLepR-GFP expressing neurons) in the DMH is required.

The final viral vector technology we employed involves permanent inactivation of LepR-expressing neurons in the DMH of LepR-Cre mice by Cre-dependent TetTox. For this viral vector, we did not test whether leptin signaling was specifically downregulated in TetTox-GFP infected neurons. It was not possible to study the co-localization between pSTAT3 and TetTox-GFP, as there were hardly any TetTox-GFP protein positive neurons observed in the DMH. The poor protein expression of TetTox-GFP may point towards toxicity effects of TetTox (see discussion section 3.2). Analysis of *TetTox-GFP* mRNA revealed that only one mouse was hit bilaterally in the DMH, and four mice were hit unilaterally in the DMH. Virus expression was not restricted to the DMH in these mice, and analysis of *TetTox-GFP* mRNA instead of protein expression may result in misinterpretation of the hypothalamic subregion in which LepR-positive neurons were functionally inactivated (see discussion section 3.2). Therefore, this study has too many limitations and uncertainties to draw conclusions on the role of leptin signaling in the DMH in the regulation of thermogenesis and adiposity.

Because of the limitations of the employed viral vectors, we were not able to determine whether long-term blockade of LepR signaling specifically within DMH neurons reduces core body temperature, and whether this is sufficient to defend adiposity. An alternative way to establish blockade of LepR signaling in the DMH is daily injection of a (pegylated) leptin antagonist (LepA) through local DMH cannulas [11, 97-99]. The advantage of local injection of LepA compared with viral overexpression is that LepA will not be secreted by neurons, and therefore be more restricted to the DMH. However, in contrast to peripheral administration [11, 98, 99], it is not feasible to daily inject LepA into the DMH over long periods of time because of the invasiveness of local injections. Therefore, viral vector technology is probably the best technique for long-term blockade of LepR signaling in the DMH, despite the limitations of the employed viral vectors.

Previously, 50% blockade of pSTAT3 activation in the DMH following viral vector mediated deletion of LepR's in the DMH (with AAV-Cre in in LepRbfl/fl mice) did not result in a reduction in core body temperature at room temperature, and the cold-induced reduction in core body temperature was reversed within 3h [27]. To the best of our knowledge, other studies only reported the acute effects of leptin signaling in the DMH on thermogenesis [17, 28], potentially because of difficulties in studying the effects of long-term blockade of LepR signaling in the DMH. It is possible that >50% downregulation of leptin signaling in the DMH is needed to find an effect on core body temperature at room temperature. With viral expression of a microRNA sequence targeting *LepR* (miLepR), the magnitude of downregulation of leptin signaling depends on the half-life of LepR, as only the synthesis of new LepR's will be blocked by miLepR. Although we are not aware of knowledge about the half-life of LepR *in vivo*, this might be too long to induce efficient downregulation of leptin signaling by miLepR within several weeks after virus injection. TetTox-mediated inactivation of LepR-positive neurons in LepR-Cre mice might be a more effective approach to downregulate leptin signaling in the DMH, as it acts by inactivating LepR-expressing neurons rather than blocking the synthesis of LepR's themselves. Furthermore, the effect of TetTox is induced upon its expression, which occurs within a few weeks following virus injection. The disadvantage of this approach is that the role of LepR-expressing neurons instead of LepR signaling itself is studied.

Moreover, because of concerns regarding viral toxicity, further research is needed to determine whether TetTox is suitable to study the role of leptin signaling in the DMH, as discussed below in section 3.2.

3.2 Absence of TetTox expression at the protein level in the DMH

In all experiments in which Cre-dependent TetTox was employed, either in LepR-Cre mice to inactivate LepR-expressing neurons in the DMH, or in combination with Cav2Cre in rats to inactivate DMH neurons projecting to the PAG or VTA, hardly any TetTox-GFP protein positive neurons were observed in the DMH and in surrounding areas (***appendix III***, ***appendix V***, and **chapter 6**). In contrast, *TetTox-GFP* mRNA expression was usually relatively clear, and a substantial number of animals showed *TetTox-GFP* mRNA expression in the DMH. This indicates that we were able to target the DMH, but that there was a problem in TetTox-GFP protein expression. Of note, TetTox-GFP protein expression was usually observed at the edges of the area of *TetTox-GFP* mRNA expression.

The presence of *TetTox-GFP* mRNA in the DMH indicates that TetTox expression in neurons does not lead to cell death, as was previously also reported [100]. However, since biological actions are performed by proteins, it is uncertain whether cells that show *TetTox-GFP* mRNA but not protein are functionally inactivated. In contrast to, for example, *in vitro* validation of chemogenetic activation of DREADD-infected neurons via slice electrophysiology [101], functional inactivation by TetTox is difficult, if not impossible, to validate. Lack of functional validation makes it difficult to determine whether histological analysis should focus on the location of TetTox-GFP protein or mRNA expression, as both may lead to misinterpretation of the area in which neurons are functionally inactivated (due to misinterpretation of the main target of virus expression, or of the area in which neurons are functionally inactivated, respectively). It is most likely that TetTox-GFP protein gradually disappears over time in the area of *TetTox GFP* mRNA expression, as usually less TetTox-GFP protein positive neurons were observed when animals were sacrificed a relatively long period (*e.g.* 29 vs 12 weeks) after virus injection (***appendix V***). We speculate that permanent blockade of synaptic transmission by TetTox eventually results in blockade of translation, for example due to ER stress resulting from the overexpression of TetTox transcripts and/or accumulation of non-released proteins, and that this may explain gradual loss of TetTox-GFP protein over time. Therefore, *TetTox-GFP* mRNA probably best represents the area of functional inactivation.

Importantly, gradual loss of TetTox-GFP protein over time may point towards toxicity effects that do not necessarily occur in Cre-expressing neurons specifically. That is, viral expression of *TetTox-GFP* is controlled by the CBA promotor, which is a strong promotor that may not only promote expression of recombined *TetTox-GFP* in Cre-expressing neurons, but also of inverted *TetTox-GFP* in neurons that do not express Cre recombinase. In other words, in LepR-Cre negative neurons in LepR-Cre mice, and in neurons that do not express Cav2Cre in rats, the CBA promotor may induce expression of non-recombined *TetTox-GFP*. Since the CBA promotor is quite strong, there might be an overproduction of inverted *TetTox-GFP* mRNA in Cre-negative neurons, which may result in toxicity, for example due to blockade of translation of cellular proteins resulting from ER stress. Such a toxicity effect may contribute to the behavioral phenotype observed following injection of TetTox, which is problematic as it is aspecific (*i.e.* it does not specifically occur in LepR-positive neurons in LepR-Cre or in targeted projection neurons in rats). This effect could explain why the physiological/behavioral effects observed following TetTox injections were usually quite robust compared with those following injection of other viral vectors, and often became stronger at 6-8 weeks after virus injection (***appendix III*** and **chapter 6**). However, the permanent inactivation of neurons by TetTox technology, and the large areas of virus expression (according to *TetTox-GFP* mRNA) provide alternative plausible explanations for these observations. Preliminary results obtained by *in situ* hybridization with a GFP sense and GFP antisense probe (to detect non-recombined and recombined *TetTox-GFP*, respectively), indicate that such an aspecific toxicity effect of TetTox cannot be excluded, but further research is needed to sort this out.

It will be difficult to sort out what exactly happens in cells after (long-term) TetTox-GFP expression. Therefore, it is questionable to what extent TetTox technology is a suitable technology to employ. The problems with TetTox technology are not specific for the DMH, as TetTox-GFP protein was neither observed in the zona incerta (ZI) following targeting of the ZI>VTA projection (**chapter 6**). To limit the chance of potential toxicity effects, a time-course of TetTox-GFP protein expression should be made for several different titers, to determine the optimal virus titer and latest possible time-point for sacrifice at which there is still clear TetTox-GFP protein expression. These experiments should be performed for each brain region of interest, as susceptibility for viral toxicity may differ per brain region. Evidence in this thesis suggests that the DMH is more susceptible than other brain regions. In general, 8-12 weeks is the minimal time-period needed to carefully perform longitudinal experiments on energy balance with viral vector technology in animals. Since TetTox-GFP protein was previously substantially reduced or even (almost)

absent at 12 weeks after virus injection (***appendix V***), it might be that TetTox-GFP protein is expressed too short to perform longitudinal experiments.

3.3 Unsuccessful targeting of the DMH with approaches employing Cre-dependent virus in combination with Cav2Cre

In this thesis, a specific problem in targeting the DMH with Cre-dependent viruses in combination with Cav2Cre in a projection region was observed in rats (**chapter 5**, ***appendix V***). This problem was observed following both the targeting of DMH to PAG projection neurons and DMH to VTA projection neurons. In contrast, the DMH was often successfully targeted following intra-DMH injection of constitutively expressing viruses in rats, and Cre-dependent viruses in LepR-Cre mice (**chapter 5**, ***appendix III***, ***appendix IV***, ***appendix V***). Also ZI to VTA projection neurons were successfully targeted with the combination of Cre-dependent viruses and Cav2Cre (**chapter 6**), supporting a specific problem in the targeting of DMH projection neurons.

It should be noted that the DMH is a relatively difficult brain region to target in general, as it is a relatively small brain region that lies adjacent to the third ventricle. Misplaced needle tracks could explain the absence of virus expression in the DMH in some cases, but probably do not explain the majority of unsuccessful DMH injections with Cre-dependent viruses in rats. Further, we show in **chapter 5**, ***appendix III***, and ***appendix V***, that it is difficult to restrict virus expression to the DMH in rats with all viral vectors that have been employed in this thesis. This could be explained by the physical structure that is inherent to the DMH, that may differ from other brain nuclei. In the DMH, injected volumes might diffuse easily to adjacent areas. Diffusion of injected volumes might also be a problem in previous studies targeting the connection between the DMH and PAG by chemical (dis)inhibition of the DMH and PAG via local injection of drugs [39, 40, 102-105]. Therefore, caution is required in interpreting the results of previous pharmacological studies that investigated the connection between the DMH and PAG. Although misplaced needle tracks and diffuse virus expression provide explanations for difficulties in targeting the DMH, they do not explain the specific problems in targeting DMH projection neurons with Cre-dependent viruses. The most plausible explanations for difficulties in targeting DMH projection neurons with Cre-dependent viruses could be the absence of neuronal projections from the DMH to the targeted projection areas or a problem with Cav2Cre infection/expression in the targeted projection areas (*e.g.* due to viral tropism).

Previous anterograde tracing studies from the DMH to PAG indicate that there are projections from the DMH to the PAG [50, 51, 106, 107]. However, it was largely unclear at which anterior-posterior level in the PAG these projections were observed, as this was not specified. In **chapter 5**, anterograde viral tracing showed that the DMH projects especially to the dorsal and lateral PAG along the entire anterior-posterior axis of the PAG. Retrograde viral tracing (with rabies) confirmed this, but also showed that the DMH generally appears not to be one of the major hypothalamic input regions for the PAG. A major limitation of viral techniques is that they require neurons to express specific molecules, such as cell surface receptors, for viral uptake and transport [108]. These molecules show variable expression across different neuronal types, which may lead to a bias of viral infection in specific neuronal types (*i.e.* viral tropism). Viral tropism makes it difficult to achieve reliable labeling and to interpret negative results, as certain projections that are not labeled might still exist. Since viral tropism has previously been reported for rabies virus [109], and anterograde tracing studies indicate that the DMH projects to the PAG [50, 51, 106, 107] (**chapter 5**), our rabies retrograde tracing study might, as a consequence of viral tropism, underestimate the importance of the DMH as a hypothalamic input area for the PAG. That is, variable subsets of DMH neurons projecting to the PAG might not express the molecules required for the viral uptake and transport of rabies virus. Similarly, viral tropism has been reported for Cav2Cre [108], and absence of molecules required for uptake and transport of Cav2Cre in variable subsets of DMH to PAG projection neurons may explain the difficulties in targeting these neurons with the combination of a Cre-dependent virus in the DMH and Cav2Cre in the PAG. Although potential problems with Cav2Cre expression in DMH to PAG projection neurons may theoretically also result from Cav2Cre toxicity, this is less likely than viral tropism, as Cav2Cre was recently reported to show low toxicity and immunogenicity in the brain [108].

Further research is needed to determine whether viral tropism may indeed explain the difficulties in targeting DMH to PAG projection neurons with Cav2Cre and rabies virus, or whether this results from poor input from DMH neurons to the PAG. To study the importance of the DMH as an hypothalamic input region for the PAG, retrograde tracing should be repeated with classical retrograde tracers, such as retrobeads, cholera toxin subunit B, or the organic dye fluoro-gold [110-113]. Interestingly, a viral receptor complementation strategy was recently developed to overcome Cav2Cre virus tropism [108]. This strategy involves the injection of AAV constructs expressing coxsackievirus and adenovirus receptor (CAR), the cell surface receptor for Cav2Cre, in candidate projection neurons. CAR can either be used as a helper virus by mixing it with Cre-dependent viruses, or be implemented in Cre-dependent viral constructs themselves. It would be interesting to study whether CAR expression in the DMH improves the targeting of DMH to PAG projection neurons with Cre-dependent viruses due to improved retrograde labeling of Cav2Cre.

Like the targeting of DMH to PAG projection neurons, targeting of DMH to VTA projection neurons with Cre-dependent viruses was also problematic (***appendix V***), whereas the targeting of ZI to VTA projection in the same DREADD experiment neurons was successful (**chapter 6**). Although, at least in mice, the ZI was shown to provide the major direct hypothalamic innervation to the VTA together with the lateral hypothalamus (LH) [52, 53], the DMH was also shown to provide prominent input to the VTA [53]. Therefore, it seems most likely that the problems in targeting DMH to VTA projection neurons do not result from absence of neuronal projections, but may also result from viral tropism of Cav2Cre. This hypothesis could be tested by performing the same experiments as described above for DMH to PAG projection neurons.

3.4 Limitations related to DREADD technology

Recently, concerns have been raised against CNO because a small portion of systemically administered CNO is metabolized to clozapine, which is an antipsychotic drug that penetrates the BBB much more easily and binds DREADD receptors more potently than CNO [94, 95]. Therefore, DREADD activation by CNO is probably largely mediated via converted clozapine. Importantly, clozapine may also act on numerous endogenous receptors (as an antagonist), leading to potential off-target effects [94, 95]. To keep clozapine levels below the threshold for altering signaling at endogenous receptors, we used a low dose of 0.3 mg/kg CNO in all experiments described in this thesis. As soon as a more selective DREADD agonist is fully characterized [95], it would be best to start using this instead of CNO. Further, in order to determine whether the observed behavioral effects result specifically from DREADD activation, the effects of CNO in DREADD-injected animals versus non-DREADD-injected animals should be compared (95). One of the limitations of the DREADD experiments in **chapter 5** and **chapter 6** is that we did not include a non-DREADD injected control group.

In **chapter 5**, where we aimed to chemogenetically activate DMH neurons projecting to the PAG, we compared the effects of CNO treatment in DMH hit rats with those in rats showing no $hM_3D(G_q)$-mCherry positive neurons in the DMH. Rats that showed at least one $hM_3D(G_q)$-mCherry positive neuron in the DMH were designated as DMH hit. Presence of $hM_3D(G_q)$-mCherry positive neurons in the DMH was accompanied by clear $hM_3D(G_q)$-mCherry expression in surrounding hypothalamic areas. Regions that often showed $hM_3D(G_q)$-mCherry positive neurons include the ZI, VMH, LH, and posterior part of the anterior hypothalamic area (AHP), and to a lesser extent the dorsohypothalamic area (DHA) and posterior hypothalamus (PH). Neurons in many of these hypothalamic subregions were previously shown to play a role in thermogenesis [27, 114-116]. Importantly, the histology analysis showed that the DMH often contained less $hM_3d(G_q)$-mCherry positive neurons than the surrounding hypothalamic subregions. Thus, the DMH was not the main target in DMH hit rats. In rats that showed no $hM_3D(G_q)$-mCherry positive neurons in the DMH, expression in other hypothalamic areas was also poor. Therefore, a more correct definition for the DMH hit group would be "greater DMH area hit" or even "hypothalamus hit" versus "poor $hM_3D(G_q)$-mCherry expression" in rats that showed no $hM_3D(G_q)$-mCherry positive neurons in the DMH. Due to the diffuse virus expression, it is not possible to determine which hypothalamic subregion predominantly mediated the CNO-induced thermogenic response. Although we failed to specifically target neurons projecting from the DMH to distinct subdivisions in the PAG, our findings are still novel, as we selectively activated hypothalamic neurons projecting to the PAG. Previously, the hypothalamus to PAG connection was modulated by chemical (dis)inhibition of the hypothalamus and PAG via local injection of drugs, which does not allow for the specific activation (or disinhibition) of hypothalamic neurons that project to the PAG [42].

In **chapter 6**, we did not include a non-DREADD virus control group for the DREADD ZI-VTA experiment. In previous DREADD studies in our lab, in which the effects of chemogenetic activation of dopaminergic VTA neurons on food-motivated behavior, feeding microstructure, and locomotor activity were investigated, several control groups were included [101, 117, 118]. These controls included DREADD injection into Cre-negative animals and the injection of a non-DREADD control virus. No effects of any dose of CNO (0 - 1.0 mg/kg) were observed in controls [101, 117, 118]. Although these findings do not definitely exclude that potential off-target effects of CNO's metabolite clozapine contribute to the effects observed on food-motivated behavior, feeding microstructure, and locomotor activity after chemogenetic activation of ZI>VTA projection neurons in **chapter 6**, they support that the effects likely result from the activation of DREADDs in the ZI.

4. Concluding remarks and future outlook

In this thesis, we show that sensitivity to the anorexigenic effect of leptin is a predictor for the development of excessive obesity following obesogenic diet exposure in rats. Translating knowledge gained from leptin sensitive and leptin resistant rats to humans may, if such a distinction between leptin sensitive and leptin resistant individuals can be made in the human population as well, provide an explanation for why some individuals become heavily obese, whereas others appear obesity resistant in our modern society [1]. Treatment with leptin or a leptin agonist

was proposed to support reversal of the counter-regulatory decline in energy expenditure and increase in food intake in weight-reduced human individuals [76], thereby supporting weight loss and the prevention of weight regain in order to combat obesity. However, leptin (agonist) treatment will likely not be successful in all individuals due to (pre-existing) leptin resistance.

To combat obesity, clinical application of DREADD may have a powerful therapeutic potential in the support of weight loss and prevention of weight regain, also in leptin resistant individuals. Currently, the use of DREADD in a clinical setting is in a very premature state of development, and replacement of CNO for a more selective DREADD agonist, as well as further safety and efficacy studies are needed to allow its clinical application [119]. This thesis provides some potential therapeutic targets for once DREADD technology becomes applicable in a clinical setting. We show that chemogenetic activation of (dorso)hypothalamic neurons projecting to the PAG increases energy expenditure primarily due to increased BAT thermogenesis. Although the contribution of BAT to thermogenesis in adult humans remains unclear [76], BAT "recruitment" is considered a promising therapeutic target for the prevention and treatment of obesity [93]. Chemogenetic activation of (dorso)hypothalamic neurons projecting to the PAG may therefore be a powerful therapeutic target to promote BAT thermogenesis, thereby supporting weight loss and the prevention of weight regain to combat obesity. In this thesis, we also show for the first time that activity of ZI neurons projecting to the VTA promotes action initiation towards feeding. Therefore, chemogenetic inactivation of ZI neurons projecting to the VTA might provide a therapeutic target in the support of decreased food intake, though a (presumably compensatory) reduction in body temperature, as was observed following permanent inactivation of ZI>VTA projection neurons in rats, may interfere with the effectiveness of this treatment. However, the finding that chemogenetic activation of ZI>VTA projection neurons affected feeding behavior but not thermoregulation suggests that transient inactivation of ZI>VTA projection neurons with DREADD technology might allow specific modulation of feeding behavior.

To conclude, the findings in this thesis improve the understanding of the neural control of physiological processes that balance energy intake and energy expenditure, as well as of certain susceptibility factors that increase the risk for the development of obesity, thereby providing novel insights into potential strategies for the prevention and treatment of human obesity.

References

1. Ruffin MP, Adage T, Kuipers F, Strubbe JH, Scheurink AJ, van Dijk G. Feeding and temperature responses to intravenous leptin infusion are differential predictors of obesity in rats. *Am J Physiol Regul Integr Comp Physiol* 2004; **286**: R756-63.
2. Zhou Y, Rui L. Leptin signaling and leptin resistance. *Front Med* 2013; **7**: 207-222.
3. Berthoud HR, Munzberg H, Morrison CD. Blaming the Brain for Obesity: Integration of Hedonic and Homeostatic Mechanisms. *Gastroenterology* 2017; **152**: 1728-1738.
4. Elmquist JK, Elias CF, Saper CB. From lesions to leptin: hypothalamic control of food intake and body weight. *Neuron* 1999; **22**: 221-232.
5. Schwartz MW, Peskind E, Raskind M, Boyko EJ, Porte D,Jr. Cerebrospinal fluid leptin levels: relationship to plasma levels and to adiposity in humans. *Nat Med* 1996; **2**: 589-593.
6. Considine RV, Stephens TW, Nyce M, Ohannesian JP, Marco CC, McKee LJ, et al. Serum immunoreactive-leptin concentrations in normal-weight and obese humans. *The New England Journal of Medicine* 1996; **334**: 292.
7. Heymsfield SB, Greenberg AS, Fujioka K, Dixon RM, Kushner R, Hunt T, et al. Recombinant leptin for weight loss in obese and lean adults: a randomized, controlled, dose-escalation trial. *JAMA* 1999; **282**: 1568-1575.
8. Caro JF, Kolaczynski JW, Nyce MR, Ohannesian JP, Opentanova I, Goldman WH, et al. Decreased cerebrospinal-fluid/serum leptin ratio in obesity: a possible mechanism for leptin resistance. *Lancet* 1996; **348**: 159-161.
9. Apolzan JW, Harris RBS. Rapid onset and reversal of peripheral and central leptin resistance in rats offered chow, sucrose solution, and lard. *Appetite* 2013; **60**: 65-73.
10. Myers MG,Jr. Leptin keeps working, even in obesity. *Cell Metab* 2015; **21**: 791-792.
11. Ottaway N, Mahbod P, Rivero B, Norman LA, Gertler A, D'Alessio DA, et al. Diet-induced obese mice retain endogenous leptin action. *Cell Metab* 2015; **21**: 877-882.
12. Lin L, Martin R, Schaffhauser AO, York DA. Acute changes in the response to peripheral leptin with alteration in the diet composition. *Am J Physiol Regul Integr Comp Physiol* 2001; **280**: R504-9.
13. Shapiro A, Tumer N, Gao Y, Cheng KY, Scarpace PJ. Prevention and reversal of diet-induced leptin resistance with a sugar-free diet despite high fat content. *Br J Nutr* 2011; **106**: 390-397.
14. Haring SJ, Harris RB. The relation between dietary fructose, dietary fat and leptin responsiveness in rats. *Physiol Behav* 2011; **104**: 914-922.
15. Scarpace PJ, Matheny M, Tumer N, Cheng KY, Zhang Y. Leptin resistance exacerbates diet-induced obesity and is associated with diminished maximal leptin signalling capacity in rats. *Diabetologia* 2005; **48**: 1075-1083.
16. Frederich RC, Hamann A, Anderson S, Lollmann B, Lowell BB, Flier JS. Leptin levels reflect body lipid content in mice: evidence for diet-induced resistance to leptin action. *Nat Med* 1995; **1**: 1311-1314.
17. Enriori PJ, Sinnayah P, Simonds SE, Garcia Rudaz C, Cowley MA. Leptin action in the dorsomedial hypothalamus increases sympathetic tone to brown adipose tissue in spite of systemic leptin resistance. *J Neurosci* 2011; **31**: 12189-12197.
18. Enriori PJ, Evans AE, Sinnayah P, Jobst EE, Tonelli-Lemos L, Billes SK, et al. Diet-induced obesity causes severe but reversible leptin resistance in arcuate melanocortin neurons. *Cell Metab* 2007; **5**: 181-194.
19. Munzberg H, Flier JS, Bjorbaek C. Region-specific leptin resistance within the hypothalamus of diet-induced obese mice. *Endocrinology* 2004; **145**: 4880-4889.
20. Levin BE, Dunn-Meynell AA. Reduced central leptin sensitivity in rats with diet-induced obesity. *Am J Physiol Regul Integr Comp Physiol* 2002; **283**: R941-8.

21. Bates SH, Stearns WH, Dundon TA, Schubert M, Tso AW, Wang Y, et al. STAT3 signalling is required for leptin regulation of energy balance but not reproduction. *Nature* 2003; **421**: 856.
22. Scarpace PJ, Zhang Y. Leptin resistance: a prediposing factor for diet-induced obesity. *Am J Physiol Regul Integr Comp Physiol* 2009; **296**: R493-500.
23. de Lartigue G, Barbier de la Serre C, Espero E, Lee J, Raybould HE. Leptin resistance in vagal afferent neurons inhibits cholecystokinin signaling and satiation in diet induced obese rats. *PLoS One* 2012; **7**: e32967.
24. Morton GJ, Blevins JE, Williams DL, Niswender KD, Gelling RW, Rhodes CJ, et al. Leptin action in the forebrain regulates the hindbrain response to satiety signals. *J Clin Invest* 2005; **115**: 703-710.
25. Farley C, Cook JA, Spar BD, Austin TM, Kowalski TJ. Meal pattern analysis of diet-induced obesity in susceptible and resistant rats. *Obes Res* 2003; **11**: 845-851.
26. Rezai-Zadeh K, Munzberg H. Integration of sensory information via central thermoregulatory leptin targets. *Physiol Behav* 2013; **121**: 49-55.
27. Rezai-Zadeh K, Yu S, Jiang Y, Laque A, Schwartzenburg C, Morrison CD, et al. Leptin receptor neurons in the dorsomedial hypothalamus are key regulators of energy expenditure and body weight, but not food intake. *Mol Metab* 2014; **3**: 681-693.
28. Dodd GT, Worth AA, Nunn N, Korpal AK, Bechtold DA, Allison MB, et al. The thermogenic effect of leptin is dependent on a distinct population of prolactin-releasing peptide neurons in the dorsomedial hypothalamus. *Cell Metab* 2014; **20**: 639-649.
29. Jo YH, Buettner C. Why leptin keeps you warm. *Mol Metab* 2014; **3**: 779-780.
30. Fischer AW, Hoefig CS, Abreu-Vieira G, de Jong JMA, Petrovic N, Mittag J, et al. Leptin Raises Defended Body Temperature without Activating Thermogenesis. *Cell Rep* 2016; **14**: 1621-1631.
31. Wilson JL, Enriori PJ. A talk between fat tissue, gut, pancreas and brain to control body weight. *Mol Cell Endocrinol* 2015; **418 Pt 2**: 108-119.
32. Zhou QY, Palmiter RD. Dopamine-deficient mice are severely hypoactive, adipsic, and aphagic. *Cell* 1995; **83**: 1197-1209.
33. Wang GJ, Volkow ND, Logan J, Pappas NR, Wong CT, Zhu W, et al. Brain dopamine and obesity. *Lancet* 2001; **357**: 354-357.
34. Volkow ND, Wang GJ, Fowler JS, Telang F. Overlapping neuronal circuits in addiction and obesity: evidence of systems pathology. *Philos Trans R Soc Lond B Biol Sci* 2008; **363**: 3191-3200.
35. Johnson PM, Kenny PJ. Dopamine D2 receptors in addiction-like reward dysfunction and compulsive eating in obese rats. *Nat Neurosci* 2010; **13**: 635-641.
36. Cone JJ, Chartoff EH, Potter DN, Ebner SR, Roitman MF. Prolonged high fat diet reduces dopamine reuptake without altering DAT gene expression. *PLoS One* 2013; **8**: e58251.
37. Stice E, Yokum S, Blum K, Bohon C. Weight gain is associated with reduced striatal response to palatable food. *J Neurosci* 2010; **30**: 13105-13109.
38. McCutcheon JE. The role of dopamine in the pursuit of nutritional value. *Physiol Behav* 2015; **152**: 408-415.
39. de Menezes RC, Zaretsky DV, Fontes MA, DiMicco JA. Microinjection of muscimol into caudal periaqueductal gray lowers body temperature and attenuates increases in temperature and activity evoked from the dorsomedial hypothalamus. *Brain Res* 2006; **1092**: 129-137.
40. Rathner JA, Morrison SF. Rostral ventromedial periaqueductal gray: a source of inhibition of the sympathetic outflow to brown adipose tissue. *Brain Res* 2006; **1077**: 99-107.
41. Chen XM, Nishi M, Taniguchi A, Nagashima K, Shibata M, Kanosue K. The caudal periaqueductal gray participates in the activation of brown adipose tissue in rats. *Neurosci Lett* 2002; **331**: 17-20.
42. de Menezes RC, Zaretsky DV, Fontes MA, DiMicco JA. Cardiovascular and thermal responses evoked from the periaqueductal grey require neuronal activity in the hypothalamus. *J Physiol* 2009; **587**: 1201-1215.
43. Clapham JC. Central control of thermogenesis. *Neuropharmacology* 2012; **63**: 111-123.
44. Heeren J, Munzberg H. Novel aspects of brown adipose tissue biology. *Endocrinol Metab Clin North Am* 2013; **42**: 89-107.
45. Dimicco JA, Zaretsky DV. The dorsomedial hypothalamus: a new player in thermoregulation. *Am J Physiol Regul Integr Comp Physiol* 2007; **292**: R47-63.
46. Zaretskaia MV, Zaretsky DV, Shekhar A, DiMicco JA. Chemical stimulation of the dorsomedial hypothalamus evokes non-shivering thermogenesis in anesthetized rats. *Brain Res* 2002; **928**: 113-125.
47. Cao WH, Fan W, Morrison SF. Medullary pathways mediating specific sympathetic responses to activation of dorsomedial hypothalamus. *Neuroscience* 2004; **126**: 229-240.
48. Morrison SF, Nakamura K, Madden CJ. Central control of thermogenesis in mammals. *Exp Physiol* 2008; **93**: 773-797.
49. Dampney RA, Furlong TM, Horiuchi J, Iigaya K. Role of dorsolateral periaqueductal grey in the coordinated regulation of cardiovascular and respiratory function. *Auton Neurosci* 2013; **175**: 17-25.
50. ter Horst GJ, Luiten PG. The projections of the dorsomedial hypothalamic nucleus in the rat. *Brain Res Bull* 1986; **16**: 231-248.
51. Papp RS, Palkovits M. Brainstem projections of neurons located in various subdivisions of the dorsolateral hypothalamic area-an anterograde tract-tracing study. *Front Neuroanat* 2014; **8**: 34.
52. Ogawa SK, Cohen JY, Hwang D, Uchida N, Watabe-Uchida M. Organization of monosynaptic inputs to the serotonin and dopamine neuromodulatory systems. *Cell Rep* 2014; **8**: 1105-1118.
53. Gonzalez JA, Jensen LT, Fugger L, Burdakov D. Convergent inputs from electrically and topographically distinct orexin cells to locus coeruleus and ventral tegmental area. *Eur J Neurosci* 2012; **35**: 1426-1432.
54. Pan H, Guo J, Su Z. Advances in understanding the interrelations between leptin resistance and obesity. *Physiol Behav* 2014; **130**: 157-169.
55. Desai BN, Harris RB. An acute method to test leptin responsiveness in rats. *Am J Physiol Regul Integr Comp Physiol* 2014; **306**: R852-60.
56. Harris RB, Apolzan JW. Changes in glucose tolerance and leptin responsiveness of rats offered a choice of lard, sucrose, and chow. *Am J Physiol Regul Integr Comp Physiol* 2012; **302**: R1327-39.
57. van den Heuvel JK, Eggels L, van Rozen AJ, Luijendijk MC, Fliers E, Kalsbeek A, et al. Neuropeptide Y and leptin sensitivity is dependent on diet composition. *J Neuroendocrinol* 2014; **26**: 377-385.
58. Verkerke H, Naylor C, Zabeau L, Tavernier J, Petri WA,Jr, Marie C. Kinetics of leptin binding to the Q223R leptin receptor. *PLoS One* 2014; **9**: e94843.
59. Levin BE, Dunn-Meynell AA, Banks WA. Obesity-prone rats have normal blood-brain barrier transport but defective central leptin signaling before obesity onset. *Am J Physiol Regul Integr Comp Physiol* 2004; **286**: R143-50.
60. Levin BE, Dunn-Meynell AA, Ricci MR, Cummings DE. Abnormalities of leptin and ghrelin regulation in obesity-prone juvenile rats. *Am J Physiol Endocrinol Metab* 2003; **285**: E949-57.
61. Bouret SG, Gorski JN, Patterson CM, Chen S, Levin BE, Simerly RB. Hypothalamic neural projections are permanently disrupted in diet-induced obese rats. *Cell Metab* 2008; **7**: 179-185.
62. Irani BG, Dunn-Meynell AA, Levin BE. Altered hypothalamic leptin, insulin, and melanocortin binding associated with moderate-fat diet and predisposition to obesity. *Endocrinology* 2007; **148**: 310-316. 63. Morrison SF, Madden CJ, Tupone D. Central neural regulation of brown adipose tissue thermogenesis and energy expenditure. *Cell Metab* 2014; **19**: 741-756.
64. Dhillon H, Zigman JM, Ye C, Lee CE, McGovern RA, Tang V, et al. Leptin directly activates SF1 neurons in the VMH, and this action by leptin is required for normal body-weight homeostasis. *Neuron* 2006; **49**: 191-203.
65. Gao Q, Wolfgang MJ, Neschen S, Morino K, Horvath TL, Shulman GI, et al. Disruption of neural signal transducer and activator of transcription 3 causes obesity, diabetes, infertility, and thermal dysregulation. *Proc Natl Acad Sci U S A* 2004; **101**: 4661-4666.

66. Minokoshi Y, Haque MS, Shimazu T. Microinjection of leptin into the ventromedial hypothalamus increases glucose uptake in peripheral tissues in rats. *Diabetes* 1999; **48**: 287-291.
67. la Fleur SE, Luijendijk MC, van Rozen AJ, Kalsbeek A, Adan RA. A free-choice high-fat high-sugar diet induces glucose intolerance and insulin unresponsiveness to a glucose load not explained by obesity. *Int J Obes (Lond)* 2011; **35**: 595-604.
68. Turnbaugh PJ, Ley RE, Mahowald MA, Magrini V, Mardis ER, Gordon JI. An obesity-associated gut microbiome with increased capacity for energy harvest. *Nature* 2006; **444**: 1027-1031.
69. Schele E, Grahnemo L, Anesten F, Hallen A, Backhed F, Jansson JO. The gut microbiota reduces leptin sensitivity and the expression of the obesity-suppressing neuropeptides proglucagon (Gcg) and brain-derived neurotrophic factor (Bdnf) in the central nervous system. *Endocrinology* 2013; **154**: 3643-3651.
70. Park DY, Ahn YT, Park SH, Huh CS, Yoo SR, Yu R, et al. Supplementation of Lactobacillus curvatus HY7601 and Lactobacillus plantarum KY1032 in diet-induced obese mice is associated with gut microbial changes and reduction in obesity. *PLoS One* 2013; **8**: e59470.
71. Moir L, Bentley L, Cox RD. Comprehensive Energy Balance Measurements in Mice. *Curr Protoc Mouse Biol* 2016; **6**: 211-222.
72. Wang X, Ge A, Cheng M, Guo F, Zhao M, Zhou X, et al. Increased hypothalamic inflammation associated with the susceptibility to obesity in rats exposed to high-fat diet. *Exp Diabetes Res* 2012; **2012**: 847246.
73. Milanski M, Degasperi G, Coope A, Morari J, Denis R, Cintra DE, et al. Saturated fatty acids produce an inflammatory response predominantly through the activation of TLR4 signaling in hypothalamus: implications for the pathogenesis of obesity. *J Neurosci* 2009; **29**: 359-370.
74. Thaler JP, Yi CX, Schur EA, Guyenet SJ, Hwang BH, Dietrich MO, et al. Obesity is associated with hypothalamic injury in rodents and humans. *J Clin Invest* 2012; **122**: 153-162.
75. Belegri E, Eggels L, Unmehopa UA, Mul JD, Boelen A, la Fleur SE. The effects of overnight nutrient intake on hypothalamic inflammation in a free-choice diet-induced obesity rat model. *Appetite* 2018; **120**: 527-535.
76. Rosenbaum M, Leibel RL. Adaptive thermogenesis in humans. *Int J Obes (Lond)* 2010; **34**: S47-55.
77. McGuire MT, Wing RR, Klem ML, Hill JO. Behavioral strategies of individuals who have maintained long-term weight losses. *Obes Res* 1999; **7**: 334-341.
78. Rosenbaum M, Murphy EM, Heymsfield SB, Matthews DE, Leibel RL. Low dose leptin administration reverses effects of sustained weight-reduction on energy expenditure and circulating concentrations of thyroid hormones. *J Clin Endocrinol Metab* 2002; **87**: 2391-2394.
79. Rosenbaum M, Sy M, Pavlovich K, Leibel RL, Hirsch J. Leptin reverses weight loss-induced changes in regional neural activity responses to visual food stimuli. *J Clin Invest* 2008; **118**: 2583-2591.
80. Leibel RL. Molecular physiology of weight regulation in mice and humans. *Int J Obes (Lond)* 2008; **32**: S98-108.
81. Leibel RL, Rosenbaum M, Hirsch J. Changes in energy expenditure resulting from altered body weight. *N Engl J Med* 1995; **332**: 621-628.
82. Weigle DS, Sande KJ, Iverius PH, Monsen ER, Brunzell JD. Weight loss leads to a marked decrease in nonresting energy expenditure in ambulatory human subjects. *Metabolism* 1988; **37**: 930-936.
83. Morrison SF. Central neural control of thermoregulation and brown adipose tissue. *Auton Neurosci* 2016; **196**: 14-24.
84. van Marken Lichtenbelt WD, Vanhommerig JW, Smulders NM, Drossaerts JM, Kemerink GJ, Bouvy ND, et al. Cold-activated brown adipose tissue in healthy men. *N Engl J Med* 2009; **360**: 1500-1508.
85. Virtanen KA, Lidell ME, Orava J, Heglind M, Westergren R, Niemi T, et al. Functional brown adipose tissue in healthy adults. *N Engl J Med* 2009; **360**: 1518-1525.
86. Cypess AM, Lehman S, Williams G, Tal I, Rodman D, Goldfine AB, et al. Identification and importance of brown adipose tissue in adult humans. *N Engl J Med* 2009; **360**: 1509-1517.
87. Nedergaard J, Bengtsson T, Cannon B. Unexpected evidence for active brown adipose tissue in adult humans. *Am J Physiol Endocrinol Metab* 2007; **293**: E444-52.
88. Pandit R. *Of dieting and leptin,* Utrecht University press, Utrecht, 2015.
89. Gordon CJ. The mouse thermoregulatory system: Its impact on translating biomedical data to humans. *Physiol Behav* 2017; **179**: 55-66.
90. Abreu-Vieira G, Xiao C, Gavrilova O, Reitman ML. Integration of body temperature into the analysis of energy expenditure in the mouse. *Mol Metab* 2015; **4**: 461-470.
91. Pandit R, Beerens S, Adan RAH. Role of leptin in energy expenditure: the hypothalamic perspective. *Am J Physiol Regul Integr Comp Physiol* 2017; **312**: R938-R947.
92. Ferrario CR, Labouebe G, Liu S, Nieh EH, Routh VH, Xu S, et al. Homeostasis Meets Motivation in the Battle to Control Food Intake. *J Neurosci* 2016; **36**: 11469-11481.
93. Boon MR, Bakker LEH, Prehn C, Adamski J, Vosselman MJ, Jazet IM, et al. LysoPC-acyl C16:0 is associated with brown adipose tissue activity in men. *Metabolomics* 2017; **13**: 48-017-1185-z. Epub 2017 Mar 3.
94. Gomez JL, Bonaventura J, Lesniak W, Mathews WB, Sysa-Shah P, Rodriguez LA, et al. Chemogenetics revealed: DREADD occupancy and activation via converted clozapine. *Science* 2017; **357**: 503-507.
95. Mahler SV, Aston-Jones G. CNO Evil? Considerations for the Use of DREADDs in Behavioral Neuroscience. *Neuropsychopharmacology* 2018, **43**:934-936.
96. Bian J, Bai XM, Zhao YL, Zhang L, Liu ZJ. Lentiviral vector-mediated knockdown of Lrb in the arcuate nucleus promotes diet-induced obesity in rats. *J Mol Endocrinol* 2013; **51**: 27-35.
97. Zhang J, Matheny MK, Tumer N, Mitchell MK, Scarpace PJ. Leptin antagonist reveals that the normalization of caloric intake and the thermic effect of food after high-fat feeding are leptin dependent. *Am J Physiol Regul Integr Comp Physiol* 2007; **292**: R868-74.
98. Elinav E, Niv-Spector L, Katz M, Price TO, Ali M, Yacobovitz M, et al. Pegylated leptin antagonist is a potent orexigenic agent: preparation and mechanism of activity. *Endocrinology* 2009; **150**: 3083-3091.
99. Shpilman M, Niv-Spector L, Katz M, Varol C, Solomon G, Ayalon-Soffer M, et al. Development and characterization of high affinity leptins and leptin antagonists. *J Biol Chem* 2011; **286**: 4429-4442.
100. Carter ME, Han S, Palmiter RD. Parabrachial calcitonin gene-related peptide neurons mediate conditioned taste aversion. *J Neurosci* 2015; **35**: 4582-4586.
101. Boekhoudt L, Omrani A, Luijendijk MC, Wolterink-Donselaar IG, Wijbrans EC, van der Plasse G, et al. Chemogenetic activation of dopamine neurons in the ventral tegmental area, but not substantia nigra, induces hyperactivity in rats. *Eur Neuropsychopharmacol* 2016; **26**: 1784-1793.
102. Horiuchi J, McDowall LM, Dampney RA. Vasomotor and respiratory responses evoked from the dorsolateral periaqueductal grey are mediated by the dorsomedial hypothalamus. *J Physiol* 2009; **587**: 5149-5162.
103. da Silva LG,Jr, Menezes RC, Villela DC, Fontes MA. Excitatory amino acid receptors in the periaqueductal gray mediate the cardiovascular response evoked by activation of dorsomedial hypothalamic neurons. *Neuroscience* 2006; **139**: 1129-1139.
104. da Silva LG, de Menezes RC, dos Santos RA, Campagnole-Santos MJ, Fontes MA. Role of periaqueductal gray on the cardiovascular response evoked by disinhibition of the dorsomedial hypothalamus. *Brain Res* 2003; **984**: 206-214.
105. Villela DC, da Silva LG,Jr, Fontes MA. Activation of 5-HT receptors in the periaqueductal gray attenuates the tachycardia evoked from dorsomedial hypothalamus. *Auton Neurosci* 2009; **148**: 36-43.

106. Lee SJ, Kirigiti M, Lindsley SR, Loche A, Madden CJ, Morrison SF, et al. Efferent projections of neuropeptide Y-expressing neurons of the dorsomedial hypothalamus in chronic hyperphagic models. *J Comp Neurol* 2013; **521**: 1891-1914.
107. Thompson RH, Canteras NS, Swanson LW. Organization of projections from the dorsomedial nucleus of the hypothalamus: a PHA-L study in the rat. *J Comp Neurol* 1996; **376**: 143-173.
108. Li SJ, Vaughan A, Sturgill JF, Kepecs A. A Viral Receptor Complementation Strategy to Overcome CAV-2 Tropism for Efficient Retrograde Targeting of Neurons. *Neuron* 2018; **98**: 905-917.e5.
109. Albisetti GW, Ghanem A, Foster E, Conzelmann KK, Zeilhofer HU, Wildner H. Identification of Two Classes of Somatosensory Neurons That Display Resistance to Retrograde Infection by Rabies Virus. *J Neurosci* 2017; **37**: 10358-10371.
110. Katz LC, Burkhalter A, Dreyer WJ. Fluorescent latex microspheres as a retrograde neuronal marker for in vivo and in vitro studies of visual cortex. *Nature* 1984; **310**: 498-500.
111. Schmued LC, Fallon JH. Fluoro-Gold: a new fluorescent retrograde axonal tracer with numerous unique properties. *Brain Res* 1986; **377**: 147-154.
112. Luppi PH, Fort P, Jouvet M. Iontophoretic application of unconjugated cholera toxin B subunit (CTb) combined with immunohistochemistry of neurochemical substances: a method for transmitter identification of retrogradely labeled neurons. *Brain Res* 1990; **534**: 209-224.
113. Wan XC, Trojanowski JQ, Gonatas JO. Cholera toxin and wheat germ agglutinin conjugates as neuroanatomical probes: their uptake and clearance, transganglionic and retrograde transport and sensitivity. *Brain Res* 1982; **243**: 215-224.
114. Zhang Y, Kerman IA, Laque A, Nguyen P, Faouzi M, Louis GW, et al. Leptin-receptor-expressing neurons in the dorsomedial hypothalamus and median preoptic area regulate sympathetic brown adipose tissue circuits. *J Neurosci* 2011; **31**: 1873-1884.
115. Thornhill J, Halvorson I. Activation of shivering and non-shivering thermogenesis by electrical stimulation of the lateral and medial preoptic areas. *Brain Res* 1994; **656**: 367-374.
116. Morrison SF, Madden CJ, Tupone D. An orexinergic projection from perifornical hypothalamus to raphe pallidus increases rat brown adipose tissue thermogenesis. *Adipocyte* 2012; **1**: 116-120.
117. Boekhoudt L, Wijbrans EC, Man JHK, Luijendijk MCM, de Jong JW, van der Plasse G, et al. Enhancing excitability of dopamine neurons promotes motivational behaviour through increased action initiation. *Eur Neuropsychopharmacol* 2018; **28**: 171-184.
118. Boekhoudt L, Roelofs TJM, de Jong JW, de Leeuw AE, Luijendijk MCM, Wolterink-Donselaar IG, et al. Does activation of midbrain dopamine neurons promote or reduce feeding? *Int J Obes (Lond)* 2017; **41**: 1131-1140.
119. Boekhoudt L. *Behavioral effects of chemogenetic dopamine neuron activation,* Utrecht University press, Utrecht, 2016.

Addendum

Appendix chapters 248

Dutch summary / Nederlandse samenvatting 286

Acknowledgements / dankwoord 292

List of publications 298

Curriculum Vitae 300

Appendix I

The effects of free-choice high-fat high-sucrose diet feeding on hypothalamic inflammation

Kathy C.G. de Git[1,2], Evita Belegri[1], Roger A.H. Adan[1,2], Susanne E. la Fleur[2]

1 Brain Center Rudolf Magnus, Dept. of Translational Neuroscience, University Medical Center Utrecht, Utrecht University, Utrecht 3584 CG, The Netherlands
2 Dept. of Endocrinology and Metabolism, Academic Medical Center, University of Amsterdam, Amsterdam, 1105 AZ, The Netherlands

Background and aim

As described in chapter 2, the evidence for the development of an inflammatory response upon exposure to diets high in fat and sugar has mostly been obtained by studies in which rodents were offered a pelleted high-fat diet. This inflammatory response has been proposed to contribute to the development of central leptin resistance and obesity. The free-choice high-fat high-sucrose (fcHFHS) diet mimics the human diet more closely than pelleted diets (see introduction section 4.1). Therefore, we here study whether exposure to the fcHFHS diet for eight weeks also upregulates inflammatory signaling in the mediobasal hypothalamus. IκB kinase-β/nuclear factor-κB (IKKβ/NF-κB) signaling, often described as "the master switch" of the innate immune system, was studied. Also endogenous leptin signaling, which converges with inflammatory signaling (see chapter 2), was studied in the mediobasal hypothalamus.

Methods

A subgroup of 11 rats (cohort 1) from the study described in chapter 3 was used for this experiment. Rats were divided in those that were maintained on chow diet over the entire experimental period (n=6), and those that were subjected to a fcHFHS diet for 8 weeks (n=5). In chapter 3, these rats were subsequently divided into subgroups of leptin sensitive (LS) and leptin resistant (LR) rats based upon their leptin sensitivity on chow diet (before fcHFHS diet exposure). In this study, both the chow and fcHFHS diet group contain one rat that was classified as LR.

After eight weeks of fcHFHS diet feeding, rats were sacrificed by rapid decapitation between 13:30 and 14:30. Brains were quickly removed, snap-frozen, and stored at -80 ºC until further analysis.

Brain processing, isolation of hypothalamic samples, and Western blot analysis were performed as described previously (1). However, the mediobasal hypothalamus, instead of the whole hypothalamus, was bilaterally isolated and was used for protein detection.

Data are presented as mean ± SEM. Differences between the chow and fcHFHS diet group were evaluated using Student's t-tests. All tests were performed using Graphpad Prism 7.04 (Graphpad software Inc, la Jolla, CA, USA). One data point is missing for IKKβ in the fcHFHS group, because of an air bubble on the membrane.

Table 1. Primary antibodies used for Western blotting

Directed against		Specification
pIKKα/β	inflammatory signaling	#2697 Cell Signaling (Ser176/180); 1:1000
IKKβ	inflammatory signaling	#2370 Cell Signaling; 1:500
pNF-κB p65	inflammatory signaling	#3033 Cell signaling (Ser536); 1:1000
NF-κB p65	inflammatory signaling	#8242 Cell Signaling; 1:1000
IκBα	inflammatory signaling	#9242 Cell Signaling; 1:1000
pSTAT3	leptin signaling	#9145 Cell Signaling; 1:1000
STAT3	leptin signaling	#4904 Cell Signaling; 1:1000
SOCS3	leptin signaling	#2932 Cell Signaling; 1:1000
β-Actin	loading control	Sc-1616 Santa-Cruz; 1:1500-1:3000

Results

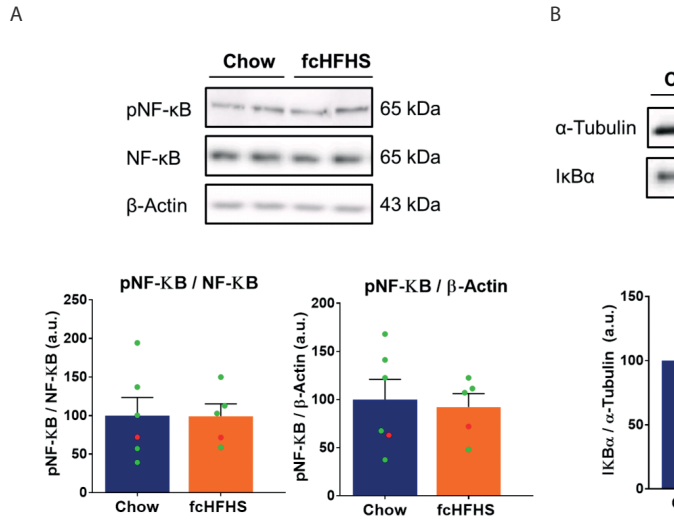

Figure 1. Eight weeks of fcHFHS diet feeding does not affect inflammatory signaling in the mediobasal hypothalamus. Consumption of the fcHFHS diet for eight weeks did not significantly affect IκB kinase-β/nuclear factor-κB (IKKβ/NF-κB) signaling in the mediobasal hypothalamus compared with chow diet fed rats. (A) Phosphorylation of NF-κB, (B) protein degradation of IκBα, (C) phosphorylation of IKK in the mediobasal hypothalamus. Individual data points are shown, and the color indicates the type of leptin responder, as defined in chapter 3. LS, leptin sensitive; LR, leptin resistant. Chow n=6; fcHFHS n=4-5. Data are show as mean ± SEM. Chow versus fcHFHS group: $t_{diet \geq 0.0299, p \geq 0.10.}$

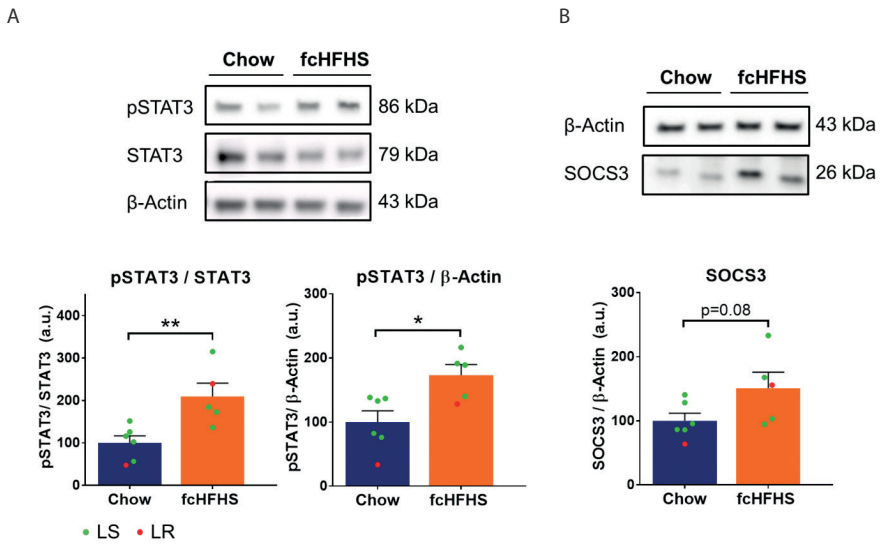

Figure 2. Eight weeks of fcHFHS diet feeding is associated with increased endogenous leptin signaling in the mediobasal hypothalamus. In comparison with chow diet feeding, consumption of the fcHFHS diet for eight weeks (A) significantly increased phosphorylation of STAT3 (pSTAT3) and (B) tended to increase SOCS3 levels in the mediobasal hypothalamus. Individual data points are shown, and the color indicates the type of leptin responder, as defined in chapter 3. LS, leptin sensitive; LR, leptin resistant. Chow n=6; fcHFHS n=5. Data are show as mean ± SEM. Chow versus fcHFHS group for pSTAT3: tdiet ≥ 2.974, p ≤ 0.02; for SOCS3: tdiet ≥ 1.95, p = 0.083. * P < 0.05, ** P < 0.01 compared with chow diet.

Conclusion

Eight weeks of fcHFHS diet feeding increases pSTAT3, a marker of leptin signal transduction. Thus, fcHFHS diet feeding increases endogenous leptin signaling in the mediobasal hypothalamus. We did not find an upregulation of IKKβ/NF-κB signaling, a critical mediator of inflammatory signaling, in the mediobasal hypothalamus after fcHFHS diet feeding, indicating that fcHFHS diet exposure upregulates leptin signaling, but does not lead to chronic activation of inflammatory signaling, in the mediobasal hypothalamus.

Acknowledgements

We thank Harrie van der Eerden and Unga Unmehopa for practical assistance.

Reference

1. Belegri E, Eggels L, Unmehopa UA, Mul JD, Boelen A, la Fleur SE. The effects of overnight nutrient intake on hypothalamic inflammation in a free-choice diet-induced obesity rat model. *Appetite* 2018; **120:** 527-535.

Appendix II

Meal patterns on chow diet in two types of leptin responders

Kathy C.G. de Git, Roger A.H. Adan

Brain Center Rudolf Magnus, Dept. of Translational Neuroscience, University Medical Center Utrecht, Utrecht University, Utrecht 3584 CG, The Netherlands

Background and aim

In chapter 3, we showed that sensitivity to leptin's anorexigenic effects on chow diet, prior to exposure to a free-choice high-fat high-sucrose (fcHFHS) diet, predicts the susceptibility for the development of diet-induced obesity (DIO). Based upon individual leptin sensitivity on chow diet, rats were grouped in leptin sensitive (LS) and leptin resistant (LR) rats. LR rats, which showed a pre-existing reduction in leptin sensitivity compared with LS rats, gained more body weight and adiposity after 8 weeks of fcHFHS diet exposure, without eating more calories. LS and LR rats did not differ in average caloric intake on either a chow or fcHFHS diet, but it remains to be tested whether they differ in feeding microstructure.

Previously, hyperphagia in DIO prone rats was caused by an increase in meal size, but not meal number, compared with both diet-resistant rats and chow diet fed rats [1]. However, it was not studied whether DIO prone rats already consume larger meals before high-fat diet exposure, which may predispose them to exacerbated DIO. Leptin is known to reduce meal size by regulating the response to satiety hormones like cholecystokinin (CCK) at the level of the brainstem, and leptin resistance of vagal afferents may increase meal size [2-4].

In this appendix, we studied whether individual leptin sensitivity on a chow diet and the susceptibility for the development of DIO are related to the consumption of larger meal sizes on chow diet. To test this, we compared feeding microstructure (meal size, meal frequency, and meal duration) between LS and LR rats on chow diet. In rats that were also subjected to a fcHFHS diet, we tested whether individual feeding microstructure on chow diet is related to body weight at week 8 of the fcHFHS diet.

Methods

For this study, data from chapter 3 were used. Rats were equally divided into two diet groups (for details see chapter 3). One group of control rats remained on chow and tap water over the entire experimental period (n=21), whereas the other group was subjected to a fcHFHS diet for eight weeks (n=20). Subsequently, the chow and fcHFHS diet group were both divided into subgroups of LS and LR rats based upon their leptin sensitivity on chow diet (chow group LS n=11; LR n=10; fcHFHS group LS n=12; LR n=8), as described in chapter 3.

Feeding behavior was studied by using data collected by Scales (Department Biomedical Engineering, UMC Utrecht, The Netherlands) [5, 6]. This program records the weight of food hoppers in the home cage automatically every 12 s. To study feeding behavior without interference by behavioral tasks or handling, weekend data were analyzed per 24h for one weekend when all rats were still on a chow diet. As previously [5,6], a meal was defined as an episode of food intake with a minimal consumption of 1 kcal (0.3 gr chow), and a minimal inter-meal interval of 5 min. Because of technical issues with the weighing system, data from two rats (one chow group LS rat, and one fcHFHS group LS rat) were excluded from the analyses.

Differences in feeding microstructure were tested by performing two-way repeated measures ANOVAs with circadian phase as within-subject variable and responder (LS/LR rat) as between-subject variable. When appropriate, post hoc analyses were conducted using pairwise comparisons. Statistical analyses were conducted using SPSS 20.3 for Windows. The threshold for statistical significance was set at $P<0.05$. Data are presented as mean ± SEM.

Results

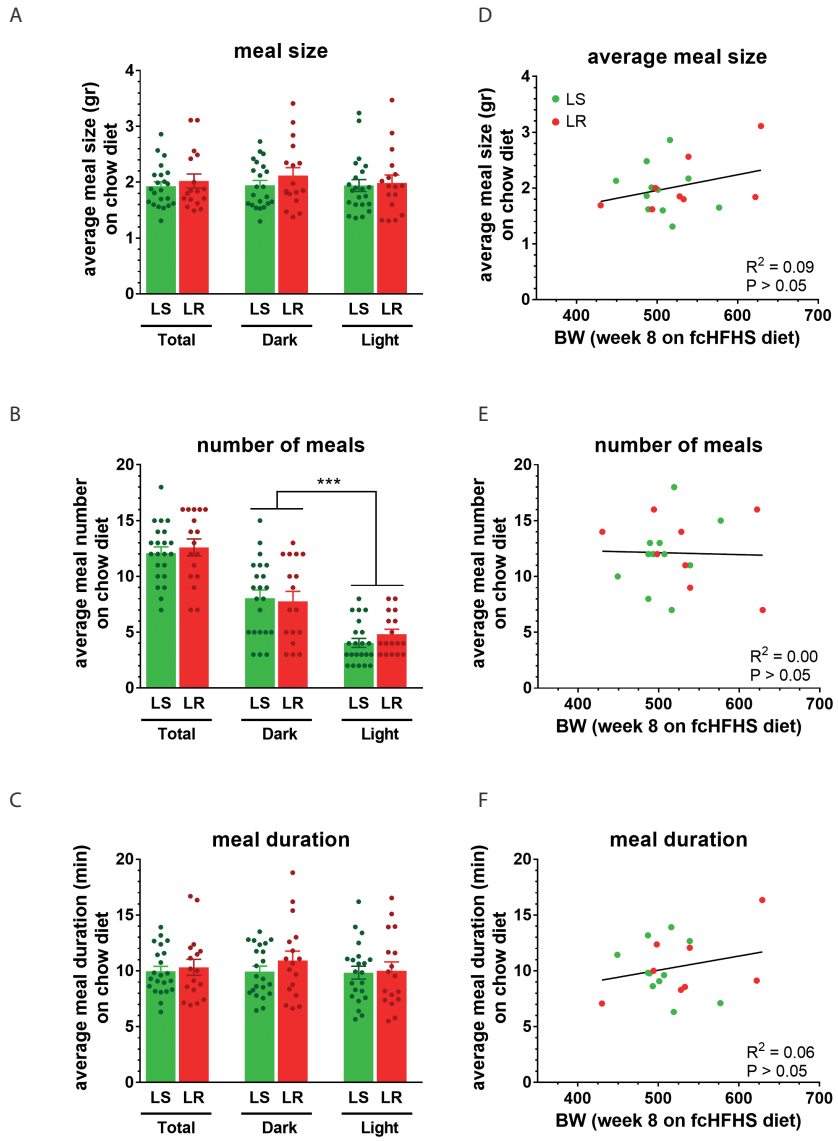

> Figure 1. Feeding microstructure does not differ between LS and LR rats on chow diet, and does not predict the development of exacerbated obesity on a fcHFHS diet. (A-C) Average (A) meal size, (B) number of meals, and (C) meal duration in leptin sensitive (LS) and leptin resistant (LR) rats when all rats were still on chow diet. Data are averaged over the 24h weekend data (total), the dark phase (dark), and the light phase (light). As expected, rats consumed more meals during the dark phase compared with the light phase ($F_{circadian\text{-}phase}(2,74)=90.557$, $p<0.001$), but showed no differences in average meal size and average meal duration between the light and dark phase ($F_{circadian\text{-}phase}(2,74)\geq0.737$, $p>0.378$). LS and LR rats did not differ in meal size, meal number, and meal duration on chow diet ($F_{responder}(1,37)\geq0.289$, $p>0.475$). Data are shown as mean ± SEM. LS n=22; LR n=17. ***$P<0.001$ for light vs dark phase. (D-F) Correlation between average (D) meal size, (E) number of meals, and (F) meal duration on chow diet (before fcHFHS diet exposure), and body weight (BW) after 8 weeks of fcHFHS diet exposure. Individual data points are shown from rats that were offered a fcHFHS diet for 8 weeks following chow diet exposure. No correlation was found between feeding microstructure parameters on chow diet and body weight at week 8 of the fcHFHS diet. LS n=11; LR n=8.

Conclusion

LS rats and obesity-prone LR rats do not differ in meal size, meal frequency, and meal duration on chow diet, indicating that individual leptin sensitivity on chow diet is not related to feeding microstructure on chow diet. Since none of these feeding microstructure parameters on chow diet correlate with body weight following 8 weeks of fcHFHS diet feeding, feeding microstructure does not predict the development of DIO on a fcHFHS diet.

References

1. Farley C, Cook JA, Spar BD, Austin TM, Kowalski TJ. Meal pattern analysis of diet-induced obesity in susceptible and resistant rats. Obes Res 2003; **11:** 845-851.
2. de Lartigue G, Barbier de la Serre C, Espero E, Lee J, Raybould HE. Leptin resistance in vagal afferent neurons inhibits cholecystokinin signaling and satiation in diet induced obese rats. Plos One 2012; **7:** e32967.
3. Morton GJ, Blevins JE, Williams DL, Niswender KD, Gelling RW, Rhodes CJ, Baskin DG, Schwartz MW. Leptin action in the forebrain regulates the hind brain response to satiety signals. J Clin Invest 2005; **115:** 703-710.
4. Blevins JE, Schwartz MW, Baskin DG. Evidence that paraventricular nucleus oxytocin neurons link hypothalamic leptin action to caudal brain stem nuclei controlling meal size. Am J Physiol Regul Integr Comp Physiol; 2004: R87-96.
5. van der Zwaal EM, Luijendijk MC, Evers SS, la Fleur SE, Adan RA. Olanzapine affects locomotor activity and meal size in male rats. Pharmacol Biochem Behav 2010; **97:** 130-137.
6. la Fleur SE, Luijendijk MC, van der Zwaal EM, Brans MA, Adan RA. The snacking rat as model of human obesity: effects of a free-choice high-fat high-sugar diet on meal patterns. Int J Obes (Lond) 2014; **38:** 643-649.

Appendix III

Technical challenges of viral vector mediated blockade of leptin receptor signaling in the dorsomedial hypothalamus

Kathy C.G. de Git, Sanne Beerens, Micha N. Ronner, Mieneke C.M. Luijendijk, Inge I.G. Wolterink-Donselaar, Roger A.H. Adan

Brain Center Rudolf Magnus, Dept. of Translational Neuroscience, University Medical Center Utrecht, Utrecht University, Utrecht 3584 CG, The Netherlands

Aim and background

Both feeding behavior and thermogenesis are regulated by leptin. Leptin is known to particularly activate brown adipose tissue (BAT) thermogenesis via neurons in the dorsomedial hypothalamus (DMH) (see introduction section 2.3.2). However, it is incompletely understood whether a disruption of leptin signaling in the DMH results in hypothermia, and whether this is sufficient to defend body adiposity. In this appendix, we studied whether long-term blockade of leptin receptor (LepR) signaling within DMH neurons, or inactivation of LepR-expressing DMH neurons, results in increased adiposity via reduced thermogenesis. We used several distinct viral vector technologies to downregulate leptin signaling in the DMH, and compared the effects and technical limitations of the distinct viral vectors. In rats, we compared the effects of two different viral vectors, blocking LepR signaling via overexpression of a leptin receptor antagonist (LepA) or expression of a microRNA sequence targeting *LepR* (miLepR), respectively. In LepR-Cre mice, we studied the effects of inactivation of LepR-expressing DMH neurons by using a virus expressing Cre-dependent tetanus toxin (TetTox) light chain.

Methods

Experiment 1: long-term blockade of leptin receptor signaling within DMH neurons in rats

Upon arrival, adult male Wistar rats (n=18; Charles-River, Sulzfeld, Germany) were group housed in a controlled environment under a 12h light/dark cycle. At the time of surgery, rats weighed 264±2.3 grams. Following surgery, rats were housed individually in Plexiglas cages in a temperature (21-23 °C) and light controlled (lights on between 04.00 and 16.00 h) room. Rats had *ad libitum* access to pelleted rat chow (3.31 kcal/g; Special Diet Service, UK) and tap water.

Surgery was performed as described for experiment 1 in chapter 6 with the following adaptations. Rats were divided into three equal subgroups based on their body weight and food intake in the week before surgery. Rats were bilaterally injected with 0.3 µl of virus into the DMH (from bregma anterior-posterior (AP): -2.30 mm, medio-lateral (ML): +1.60 mm <10º, dorso-ventral (DV): -9.30 mm). The first subgroup (n=3), referred to as the leptin receptor antagonist (LepA) group, was injected with AAV-CBA-LepAnta-ires-GFP (1.58*1011 genomic copies/ml). The second subgroup (n=10), referred to as the leptin receptor microRNA (miLepR) group, was injected with AAV-esyn-miLepR-GFP (1.00*1012 genomic copies/ml). The third group (n=5),

referred to as the control group, was injected with either AAV-CBA-GFP (1.00*1013 genomic copies/ml, n=3) or AAV-miLuc-GFP (9.5*1013 genomic copies/ml; n=2). As there were no differences observed between virus expression and physiological measures between the different control viruses, they were considered to be equal and combined for statistical analyses. In addition, an intra-abdominal transmitter (TA10TA-F40, Data Science International, USA) was implanted to continuously monitor core body temperature and locomotor activity.

In week 11 post-surgery, rats were anesthetized and prior to perfusion, individual epididymal and subcutaneous (inguinal) white adipose tissues were dissected from the left side, cleaned and weighed. Transcardial perfusion, immunohistochemistry, and histological analysis were performed via similar procedures as described for experiment 1 in chapter 6.

Differences in body weight, food intake, core body temperature, locomotor activity, and adiposity were tested by performing two-way repeated measures ANOVAs with time as within-subject variable and group (control, LepA, miLepR) as between-subject variable. When appropriate, post hoc analyses were conducted using pairwise Bonferroni comparisons. Statistical analyses were conducted using SPSS 20.3 for Windows. The threshold for statistical significance was set at $P<0.05$. Data are presented as mean ± SEM. Activity data from one rat were excluded because of technical problems with the telemetric device.

Experiment 2: permanent inactivation of leptin receptor expressing DMH neurons in mice

Mature male LepR-Cre +/- mice (n=18) were used. Mice were group housed until surgery, after which they were housed individually in a controlled environment under 12 light/dark cycle (lights on between 13.00 and 01.00h). Mice had *ad libitum* access to standard mouse chow and tap water, except for a three-week period (week 5-7) of food restriction. During this period, mice were fed as such that they were maintained on a body weight of 90% of the pre-surgery body weight.

Surgery was performed as described for experiment 1 in chapter 6 with the following adaptations. Mice were divided into three equal subgroups based on their body weight in the week before surgery, and were bilaterally injected with virus into the DMH (from bregma anterior-posterior (AP): -0.19 mm, medio-lateral (ML): +0.15 mm <10º, dorso-ventral (DV): -0.58 mm). The first group of mice (n=6), referred to as the control group, was unilaterally injected with 0.3 µl of AAV5-DREADD-Gq-mCherry (final titer 1.0*1012 genomic copies/ml), and on the contralateral side injected with

0.3 µl of a mixture of AAV5-DREADD-Gq-mCherry and AAV-DIO-hChR(H134R)-EYFP (final titer in mixture 1.0*1012 genomic copies/ml and 3.7*1012 genomic copies/ml, respectively). The second group (n=9) was unilaterally injected with 0.3 µl of AAV-CBA-DIO-GFP:TetTox (final titer 1.4*1012 genomic copies/ml), and on the contralateral side injected with 0.3 µl of a mixture of AAV-CBA-DIO-GFP:TetTox and AAV-DIO-hChR(H134R)-mCherry (final titer in mixture 1.4*1012 genomic copies/ml and 2.6*1012 genomic copies/ml, respectively). The third group (n=3) received the same viral mixtures as group 2, but was bilaterally injected with 0.5 µl instead of 0.3 µl. As there were no differences observed between virus expression and physiological measures between group 2 and 3, they were considered to be equal and combined for statistical analyses, and referred to as the TetTox group. During surgery, also a temperature sensitive transponder (IPTT-300, BioMedic Data Systems, The Nederlands) was implanted subcutaneously in BAT tissue.

Over the course of the experiment, body weight, food intake, and BAT temperature were measured three days per week (Monday-Wednesday-Friday). BAT temperature was measured at three time-points at the respective days (10.00h, 13.30h, and 16.00h). The data from the measurement at 10.00h and 16.00h were used to determine the temperature during the dark and light phase, respectively.

In week 14 post-surgery, mice were anesthetized and prior to perfusion, individual epididymal and subcutaneous (inguinal) white adipose tissues were dissected from the left side, cleaned and weighed. Transcardial perfusion, immunohistochemistry, and histological analysis were performed via similar procedures as described for experiment 1 in chapter 6. Post-mortem analysis revealed that the BAT transponder was misplaced in three control mice and five TetTox mice (three of them showed no virus expression). These mice were excluded from the temperature analyses.

Differences in body weight, caloric intake, and BAT temperature were tested by performing two-way repeated measures ANOVAs with time as within-subject variable and group (control vs TetTox DMH uni- and bilateral hit) as between-subject variable. When appropriate, post hoc analyses were conducted using pairwise Bonferroni comparisons. Adiposity and average BAT temperature were tested by performing an independent t-test with group (control vs TetTox DMH uni- and bilateral hit) as between subject factor. Statistical analyses were conducted using SPSS 20.3 for Windows. The threshold for statistical significance was set at $P<0.05$. Data are presented as mean ± SEM.

Results

Experiment 1: long-term blockade of leptin receptor signaling within DMH neurons in rats

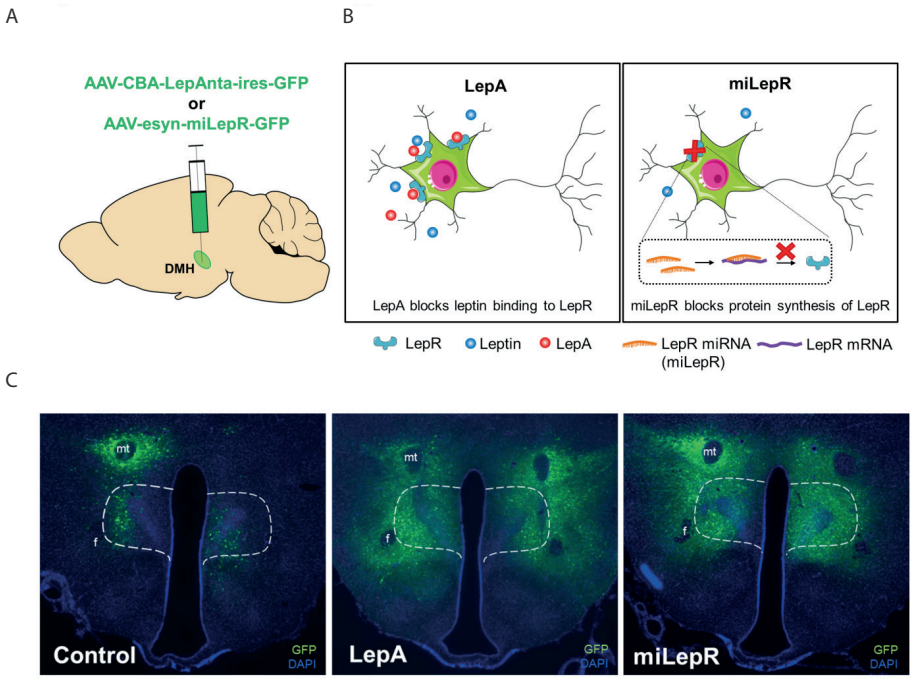

Figure 1. Viral vector mediated blockade of leptin receptor signaling in the DMH. (A) Rats were bilaterally injected into the DMH with a virus overexpressing a leptin receptor antagonist (AAV-CBA-lepAnta-ires-GFP) or a virus expressing a microRNA sequence targeting *LepR* (AAV-esyn-miLepR-GFP). (B) (Left) Overexpression of a leptin receptor antagonist (LepA) blocks binding of leptin to the LepR, and thereby blocks LepR signaling. (Right) The microRNA sequence targeting *LepR* (miLepR) blocks the protein synthesis of new LepRs by binding to *LepR* mRNA, resulting in its cleavage. (C) Representative examples of GFP expression in rats that were bilaterally hit in the DMH following virus injection of (left) a GFP-expressing control virus, (middle) a virus overexpressing LepA, and (right) a virus expressing miLepR. The dotted outline shows the boundary of the DMH (bregma -3.30 mm). GFP expression was not restricted to the DMH, and not all rats were hit bilaterally. In the LepA group (n=3), 2 rats were hit bilaterally, and one rat was hit unilaterally. In the miLepR group (n=10), 4 rats were hit bilaterally, and 5 rats were hit unilaterally. Only rats with bilateral expression and rats of the control group were included in the data analysis below.

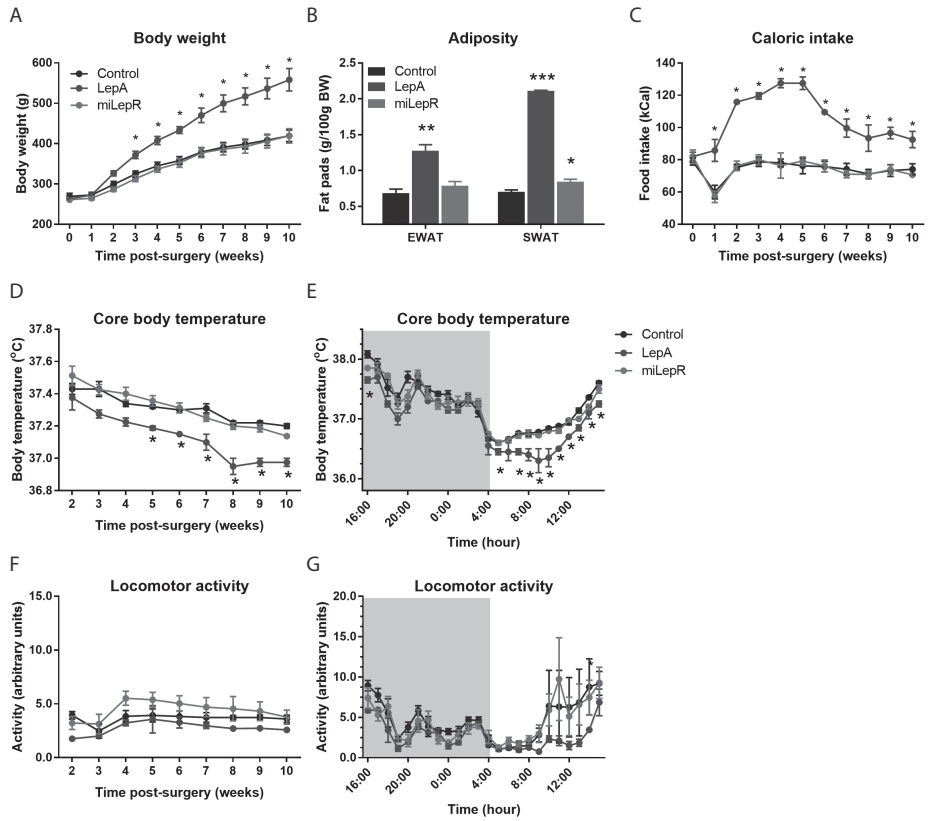

Figure 2. Viral overexpression of LepA, but not miLepR, increases body adiposity via increased food consumption and reduced thermogenesis. Overexpression of LepA in the DMH (A) increased body weight from 3 weeks following surgery onwards ($F_{week*group}$(20,80)=16.111, p<0.001), and (B) increased both epididymal and subcutaneous white adipose tissue (EWAT) and (SWAT) at the end of the experiment compared with control rats ($F_{fat*group}$(2,8)=45.544, p<0.001; F_{group}(2,8)=125.130, p<0.001). The increase in body weight and adiposity might result from (C) an increase in food consumption from 1 week following surgery onwards ($F_{week*group}$(20,80)=6.302, p<0.001), and (D) a reduction in core body temperature from 5 weeks following surgery onwards ($F_{week*group}$(16,64)=1.647, p=0.082; F_{group}(2,8) = 33.731, p<0.001), which was (E) especially observed during the light phase (data are shown for week 10; $F_{hour*group}$(46,148)=1.879, p<0.01). In contrast to overexpression of LepA, expression of miLepR in the DMH did not affect (C) food intake, and (D,E) core body temperature. In accordance, expression of miLepR did not affect (A) body weight, and (B) EWAT, but slightly increased SWAT. (F, G) Locomotor activity was not affected by (over)expression of either LepA or miLepR in the DMH (F_{group}(2,7)≥3.370, p≤0.501). Control n=5; LepA n=2, miLepR n=4. Data are show as mean ± SEM. *P<0.05 vs controls.

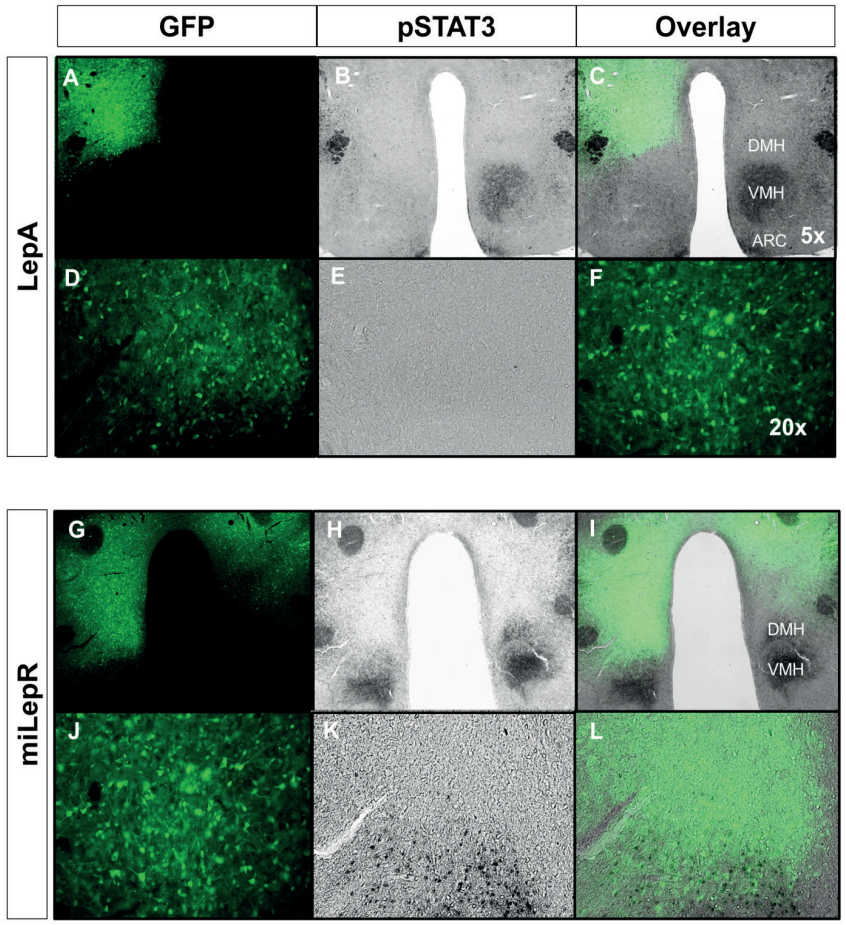

Figure 3. Viral overexpression of LepA blocks leptin signaling in the DMH and surrounding regions, whereas expression of miLepR does not substantially block leptin signaling. To test whether viral vector mediated (over)expression of LepA and miLepR blocks leptin receptor signaling specifically in the area of virus expression, GFP staining (from the viral vector) was combined with pSTAT3 staining. pSTAT3 is a marker of leptin signal transduction. (A-L) Representative images of hypothalamic GFP expression and pSTAT3 induction following leptin treatment (2 mg/kg for 2h) are shown for (A-F) a virus overexpressing LepA, and (G-L) a virus expressing miLepR. (A-C) Unilateral overexpression of LepA resulted in a complete downregulation of pSTAT3 in the area of GFP expression (DMH), but also in the surrounding areas (most importantly the VMH). (D-F) None of the GFP expressing cells showed pSTAT3 induction. (G-H) In contrast, expression of miLepR did not substantially downregulate pSTAT3 signaling in the area of GFP expression. (J-L) Many of the GFP expressing cells showed pSTAT3 induction. These findings indicate that overexpression of LepA in the DMH blocks pSTAT3 signaling in the DMH and surrounding regions, whereas expression of miLepR in the DMH does not substantially block pSTAT3 signaling.

Experiment 2: permanent inactivation of leptin receptor expressing DMH neurons in mice

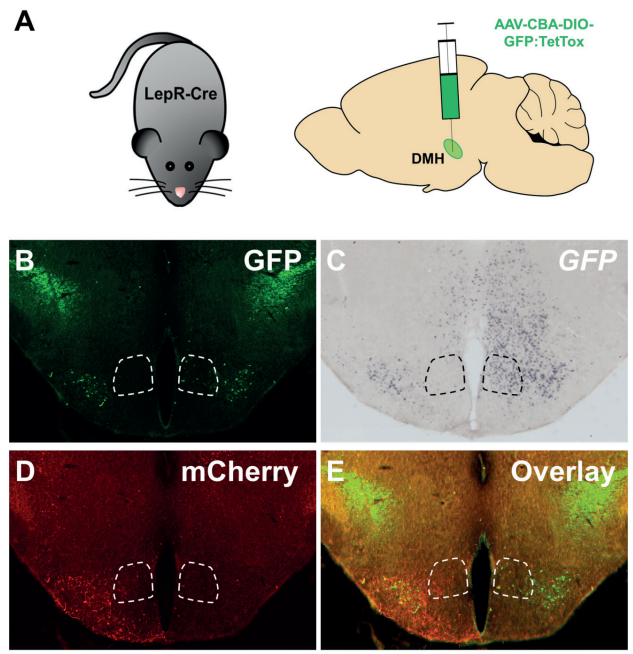

Figure 4. Viral vector mediated inactivation of leptin receptor positive DMH neurons. (A) LepR-Cre mice were bilaterally injected with Cre-dependent tetanus toxin (TetTox) light chain (AAV-CBA-DIO-GFP:TetTox) into the dorsomedial hypothalamus (DMH), resulting in permanent inactivation of LepR-positive neurons in the infected area. Further, mice were unilaterally injected with AAV-DIO-hChR(H134R)-mCherry, as a control virus for the injection site. Overall, TetTox injected mice showed hardly any TetTox-GFP protein positive cells. Therefore, *TetTox-GFP* mRNA was also analyzed. (B-E) Examples of (B) TetTox-GFP protein expression, (C) *TetTox-GFP* mRNA expression, (D) ChR-mCherry protein expression, and (E) an overlay of TetTox-GFP protein and ChR-mCherry protein expression in one mouse of the TetTox group that was hit unilaterally in the DMH. The dotted outline shows the boundary of the DMH (bregma -2.10 mm). TetTox-GFP protein expression was relatively clear in this example mouse compared with other mice. Note that TetTox-GFP protein expression was relatively sparse compared with *TetTox-GFP* mRNA expression, and was located at the edge of the expression area of *TetTox-GFP* mRNA. (D) ChR-mCherry (only injected on the left side) was more abundantly expressed than (B) TetTox-GFP protein and seems to be expressed in the same area as (C) *TetTox-GFP* mRNA. (E) Only a few ChR-mCherry protein positive neurons co-localize with TetTox-GFP protein. Since *TetTox-GFP* mRNA was more clearly expressed than TetTox-GFP protein, histological analysis of the location of virus expression was based on *TetTox-GFP* mRNA expression. TetTox expression was not restricted to the DMH, and not all rats showed (bilateral) *TetTox-GFP* expression. Within the TetTox group (n=12), *TetTox-GFP* mRNA expression was completely absent in three mice (DMH miss), not expressed in the DMH in four mice (DMH miss), unilaterally expressed in the DMH in four mice (DMH unilateral hit), and bilaterally expressed in the DMH in one mouse (DMH bilateral hit). Only mice that were hit uni- or bilaterally in the DMH and mice of the control group were included in the data analysis below.

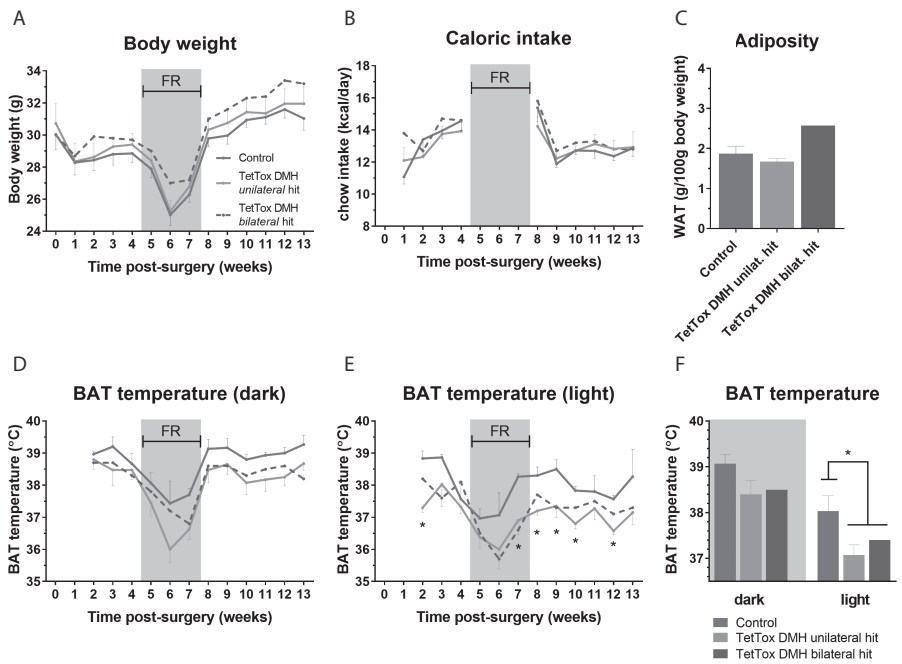

Figure 5. Permanent inactivation of leptin receptor positive DMH neurons decreases BAT temperature, without affecting body weight and adiposity. (A-C) Uni- or bilateral inactivation of LepR expressing neurons in the DMH did not significantly affect (A) body weight ($F_{group}(1,9)=0.621$, p=0.451), (B) caloric intake ($F_{group}(1,9)=0.006$, p=0.940), and (C) white adipose tissue (WAT) ($t_{group}(9)=0.065$, p=0.950). However, the single mouse that showed bilateral expression of TetTox in the DMH showed a tendency for an increase in body weight and adiposity. (D-F) Uni- or bilateral inactivation of LepR expressing neurons in the DMH did (D,F) not significantly affect BAT temperature in the dark phase ((D): $F_{group}(1,6)=4.529$, p=0.077; (F): t(6)dark=1.894, p=0.107), but (E,F) decreased BAT temperature in the light phase ((E): $F_{group}(1,6)=7.084$, p=0.037; (F): t(6) light=2.645, p=0.038). (F) Shows the average BAT temperature during week 8-13. Control n=3-6; TetTox unilateral DMH hit n=4, TetTox bilateral DMH hit n=1. Data are show as mean ± SEM. *P<0.05 for TetTox (unilateral and bilateral combined) vs controls. *P<0.05 vs controls. FR, food restriction.

Conclusion

We here show in rats that the effects of long-term blockade of leptin receptor signaling in the DMH largely depend on the used viral vector technology. By employing a viral vector that overexpresses a LepA, we showed that rats increase their body weight and adiposity by increasing food intake and decreasing core body temperature. Since the increase in food intake preceded the decrease in core body temperature, and was maintained over the course of the experiment, it is not possible to determine the exact effect of the decrease in core body temperature on body weight and adiposity. In contrast to overexpression of LepA, expression of miLepR did not affect food intake and core body temperature, and accordingly, did not affect body weight and total adiposity. The difference in the degree of pSTAT3 downregulation in the DMH (and surrounding areas) likely explains the discrepancy between the results of the two viral vectors. Overexpression of LepA completely downregulated pSTAT3 signaling in the DMH, whereas expression of miLepR did not substantially downregulate pSTAT3 signaling. One limitation of overexpression of LepA is that it did not only downregulate pSTAT3 signaling in the area of virus injection (DMH), but also in surrounding areas. Moreover, as LepA is secreted by neurons, it might also block pSTAT3 signaling in the projection areas. Another limitation of both viral vectors is that virus expression was not restricted to the DMH. Because of the limitations of both employed viral vectors, it is not possible to determine whether long-term blockade of LepR signaling specifically within DMH neurons results in a reduction in core body temperature, and whether this is sufficient to defend adiposity.

To further investigate the importance of leptin signaling in the DMH for the regulation of thermogenesis and the defense of adiposity, we permanently inactivated LepR expressing neurons in the DMH of LepR-Cre mice. Inactivation of LepR-positive DMH neurons resulted in a decrease in BAT temperature, supporting that leptin signaling in the DMH is critical for the regulation of BAT-dependent thermogenesis. Since food intake was not affected, LepR-positive DMH neurons do not seem to regulate food intake. Inactivation of LepR-positive DMH neurons did not affect body weight and adiposity, indicating that a reduction in thermogenesis is not sufficient to defend body adiposity. However, the single mouse that showed bilateral TetTox expression in the DMH showed a tendency for an increase in body weight and adiposity compared with controls and TetTox mice that were hit unilaterally in the DMH. Further research with a larger group of bilaterally DMH hit mice is needed to determine the relationship between the reduction in BAT thermogenesis and the defense of adiposity. Important limitations of the current study are that virus expression was not restricted to the DMH, and that histological analysis was performed on *TetTox-GFP* mRNA expression instead of TetTox-GFP protein expression, which may result in misinterpretation of the hypothalamic subregion in which LepR-positive neurons were functionally inactivated. The poor expression of TetTox-GFP protein may point towards toxicity effects of TetTox.

Appendix IV

Identifying the leptin receptor expressing hypothalamic inputs to the periaqueductal grey: the importance of the dorsomedial hypothalamus

Kathy C.G. de Git, Micha N. Ronner, Diana C. van Tuijl, Inge G. Wolterink-Donselaar, Azar Omrani, Roger A.H. Adan

Brain Center Rudolf Magnus, Dept. of Translational Neuroscience, University Medical Center Utrecht, Utrecht University, Utrecht 3584 CG, The Netherlands

Aims

1) To determine which subdivisions of the periaqueductal gray (PAG) receive input from leptin receptor (LEPR) positive neurons in the dorsomedial hypothalamus (DMH).

2) To identify which LEPR positive hypothalamic neurons provide input to the PAG, and to determine the relative importance of the DMH as an input region.

Methods

Animals

Mature male LepR-Cre +/- mice were used. Mice were group housed until surgery, after which they were housed individually in a controlled environment under a reversed light/dark cycle (lights on between 1900 and 0700h). Mice had ad libitum access to standard mouse chow and tap water. All experiments were performed in accordance with Dutch laws (Wet op de Dierproeven, 1996) and European regulations (Guideline 86/609/EEC), and were approved by the Animal Ethics Committee of Utrecht University.

Experiment 1: anterograde viral tracing from LEPR positive neurons in the DMH to the PAG

For this experiment, six LepR-Cre +/- mice were used. All experimental procedures were performed as described for experiment 1 in chapter 5 with the following adaptations. Mice were unilaterally injected with 0.3 µl of AAV-EF1a-hChR2-EYFP (3.7*1012 genomic copies/ml; UNC vector core), and, on the contralateral side, unilaterally injected with 0.3 µl of AAV-EF1a-hChR2-mCherry (2.6*1012 genomic copies/ml; UNC vector core) into the DMH (from bregma: anterior-posterior (AP): -0.19 mm, medio-lateral (ML): +0.15 mm, dorso-ventral (DV): -0.58 mm, at an angle of 10^{o}).

Experiment 2: retrograde viral tracing from the PAG to LEPR positive neurons in the DMH

For this experiment, four LepR-Cre +/- mice were used. All experimental procedures were performed as described for experiment 2 in chapter 5 with the following adaptations.

Mice were unilaterally injected with 1.0 µl of HSV-DIO-mCherry into the PAG. Mice were randomly divided into two groups of two and injected at two different coordinates in the PAG. Case 1 and 2: AP: -3.9 mm, ML +1.0 mm / <10º, DV -3.1 mm from bregma; case 3 and 4: AP: -4.5 mm, ML +1.0 mm / <10º, DV -3.1 mm from bregma (mouse brain atlas by Paxinos and Franklin (2001, second edition)).

The number of LEPR positive inputs in the hypothalamus was evaluated by the expression of cell bodies with mCherry immunoreactivity. Hypothalamic inputs were systematically counted at the nine sections between -1.34 to -2.30 mm from bregma defined by the mouse brain atlas Paxinos and Watson (2001; second edition).

Results

Experiment 1: anterograde viral tracing from LEPR positive neurons in the DMH to the PAG

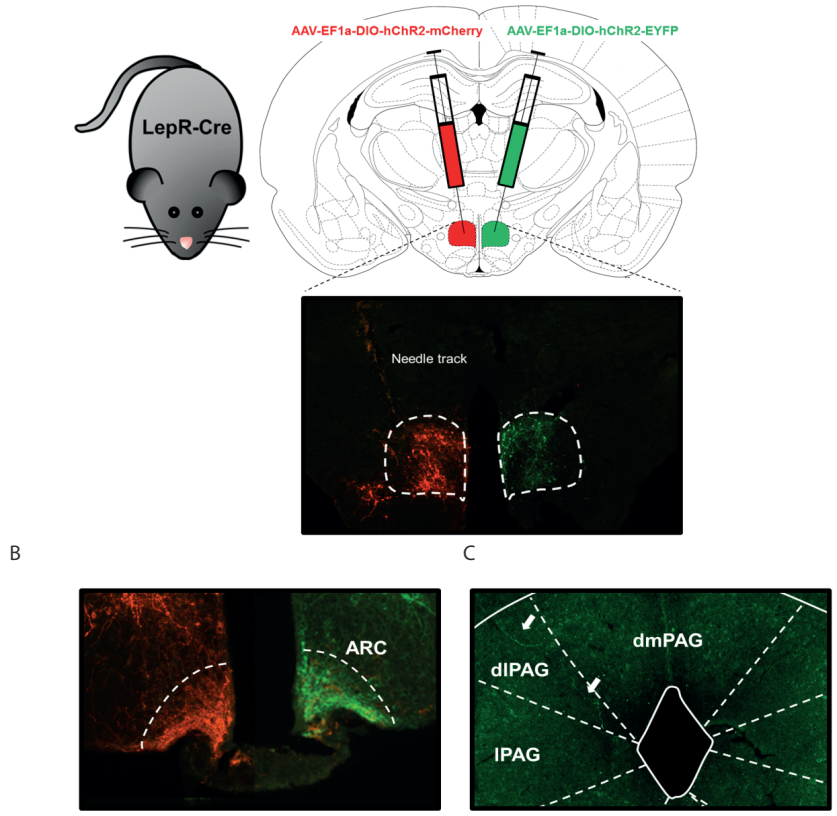

Figure 1. The periaqueductal grey receives scarce projections from the dorsomedial hypothalamus. (A) The anterograde tracer virus AAV-EF1a-hChR2-mCherry was unilaterally injected into the DMH, and, on the contralateral side, the anterograde tracer virus AAV-EF1a-hChR2-EYFP was unilaterally injected into the DMH of LepR-Cre mice. DMH injections were successful in four of the six injected mice (three mice were hit bilaterally, and one mouse was hit unilaterally). GFP and mCherry expression are shown for successful bilateral DMH injections in one mouse. The dotted outline shows the boundary of the DMH. (B) All mice that were hit in the DMH showed numerous projections in the arcuate nucleus (ARC). Projections to the ARC were abundant compared with other brain regions. (C) Only one mouse that was hit in the DMH showed projections in the periaqueductal gray (PAG). Two projections were detected in the dorsolateral PAG (dlPAG) at -4.36 mm from bregma. The arrows indicate the observed projections. Of note, in general, projections were restricted mainly to the hypothalamus, with limited projections to the midbrain and hindbrain.

Experiment 2: retrograde viral tracing from the PAG to LEPR positive neurons in the DMH

A

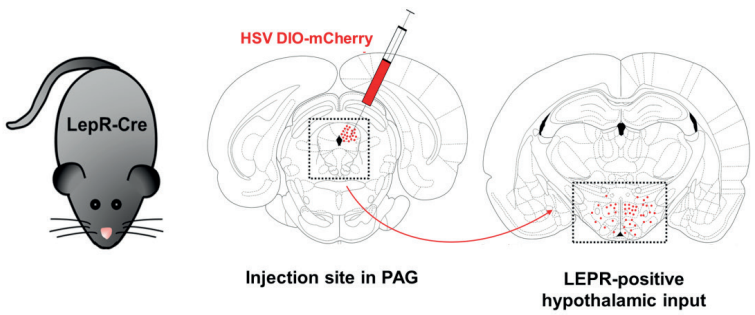

B

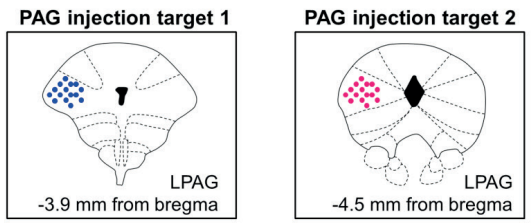

C

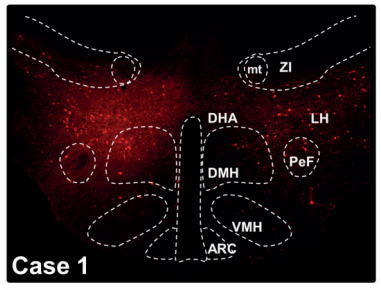

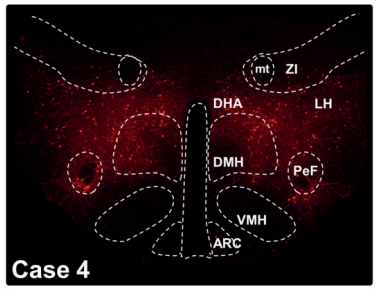

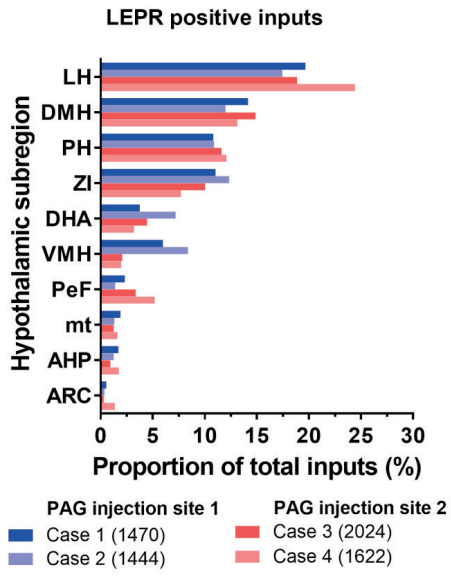

< Figure 2. The dorsomedial hypothalamus is the second most important leptin receptor positive hypothalamic input region for the periaqueductal grey. (A) Experimental design. HSV-DIO-mCherry, a Cre-dependent retrograde tracer virus, was unilaterally injected into the PAG of LepR-Cre mice. The number of leptin receptor (LEPR) positive, direct presynaptic inputs was assessed in defined subregions of the hypothalamus, including the dorsomedial hypothalamus (DMH). (B) Schematic overview of the two distinct target sites of injection: the lateral PAG (lPAG) at -3.9 mm and -4.5 mm from bregma, respectively. (C) Plot of the relative proportion of LEPR positive presynaptic inputs in defined subregions of the hypothalamus. Hypothalamic subregions are ranked from highest to lowest number of inputs. Two cases are presented for both targeted injection sites in the PAG, and the total number of LEPR positive hypothalamic inputs is indicated for each case. Despite the targeting of the PAG at two distinct anterior-posterior levels from bregma, the relative input from the distinct hypothalamic subregions was very similar across cases. Overall, the lateral hypothalamus (LH) provided the most prominent LEPR positive input, followed by the DMH. AHP, anterior hypothalamic area; DHA, dorsohypothalamic area; mt, mammillothalamic tract; PeF, perifornical nucleus; PH, posterior hypothalamus; VMH, ventromedial hypothalamus; ZI, zona incerta.

Conclusion

Using anterograde viral tracing, LEPR positive neurons in the DMH were shown to project predominantly to the hypothalamus, most importantly the ARC. The dlPAG receives scarce projections from LEPR positive neurons in the DMH, but the projections to other brain regions in the midbrain and hindbrain are also limited. These findings indicate that it is possible to visualize projections from LEPR positive neurons in the DMH, and suggest that LEPR positive neurons in the DMH scarcely project to the PAG or that projections to brain regions further away from the injection site were not clearly visible at three weeks following virus injection. To further investigate whether the PAG receives LEPR positive input from the DMH, we performed a retrograde viral tracing for two different anterior-posterior levels in the lPAG. Retrograde tracing revealed that the DMH is the second most important LEPR positive hypothalamic input region for the lPAG, independent of the anterior-posterior level of the PAG. Thus, the DMH provides prominent LEPR positive hypothalamic input to the PAG along several levels of its anterior-posterior axis.

Appendix V

Difficulties in targeting the dorsomedial hypothalamus with dual viral vector technology

Kathy C.G. de Git, Diana C. van Tuijl, Micha N. Ronner, Minke H.C. Nota, Inge Wolterink-Donselaar, Mieneke C.M. Luijendijk, Esther M. Hazelhoff, Roger A.H. Adan

Brain Center Rudolf Magnus, Dept. of Translational Neuroscience, University Medical Center Utrecht, Utrecht University, Utrecht 3584 CG, The Netherlands

Aim and background

As discussed in chapter 5, we experienced several technical challenges in targeting the dorsomedial hypothalamus (DMH) with dual viral vector technology. In this appendix, we provide an overview of the targeting of the DMH with different viral vectors that have been employed in this thesis. In Wistar rats, we compare the targeting of the DMH following injection of constitutively expressing (non Cre-dependent) viruses and Cre-dependent viruses. For the latter, a combination of two virus injections was performed: 1) Cre-dependent dependent designer receptors exclusively activated by designer drugs (DREADD) or tetanus toxin (TetTox) light chain was injected into the DMH, and 2) canine adenovirus 2 (Cav2Cre) was injected into the periaqueductal grey (PAG) or ventral tegmental area (VTA). In LepR-Cre mice, DMH injections of several Cre-dependent viruses were compared.

Methods

Adult male Wistar rats and mature male LepR-Cre +/- mice were used. Rats weighed ~300 grams at the time of surgery in Figure 1-3, 487±11 grams in Figure 4A-C, and 372±9 grams in Figure 4D-F. Mice weighed 30.1±0.47 grams at the time of surgery. Viral injections were performed as described for experiment 1 in chapter 5 for constitutively expressing viruses and experiment 3 in chapter 5 for the combination of Cre-dependent viruses with Cav2Cre. Table 1 and Table 2 give an overview of the details of the viral injections in rats and mice, respectively.

Transcardial perfusion, immunohistochemistry, and histological analysis were performed via similar procedures as described in chapter 5 and 6. More specifically, Figure 1 was performed as described for experiment 1 in chapter 5, Figure 2A-C and Figure 3 were performed as described for experiment 3 in chapter 5, Figure 2D-F and Figure 4D-F were performed as described for experiment 1 in chapter 6, and Figure 4A-C was performed as described for experiment 2 in chapter 6. For Figure 4D-F, GFP in situ hybridization was performed as described for experiment 1 in chapter 6. In Figure 3, GFAP (glial fibrillary acidic protein) was detected with rabbit-α-GFP (1:1000, Abcam, UK), and NeuN was detected with mouse-α-NeuN (1:1000, Abcam, UK).

Table 1. Details of viral injections in Wistar rats.

Figure in results	Region	Virus	Volume (µl)	Titer (final mixture)	Coordinates (AP / ML / DV / angle)	Histology
1	DMH	AAV-hSyn-hChR2-EYFP	0.3	4.8*1012	-2.3 / +1.4 / -9.3 / <5°	3 wk
2 A-C	**DMH**	**AAV-hSyn-DIO-hM3D(Gq)-mCherry**	**0.3**	**3.8*1012**	**-2.3 / +1.4 / -9.3 / <5°**	**6 wk**
	PAG	Cav2Cre / AAV-hSyn-YFP	0.3	1.8*1012/ 1.65*1012	-5.3 / +1.4/ -6.7 / <10°	
2 D-F	DMH	AAV-CBA-DIO-GFP:TetTox	0.3	1*1012	-2.3 / +1.4 / -9.3 / <5°	12 wk
	PAG	Cav2Cre / AAV-hSyn-mCherry	0.3	1*1012 / 1*1012	-5.3 (panel D) or -6.8 (panel E) / +1.4 / -5.7 / <10°	
3	DMH	AAV-hSyn-DIO-hM3D(Gq)-mCherry	0.3	3.8*1012	-2.3 / +1.4 / -9.3 / <5°	6 wk
	PAG	Cav2Cre / AAV-hSyn-YFP	0.3	1.8*1012/ 1.65*1012	-5.3 / +1.4/ -6.7 / <10°	
4 A-C	**DMH**	**AAV-hSyn-DIO-hM3D(Gq)-mCherry**	**0.3**	**1*1012**	**-2.3 / +1.2 / -9.7 / <5°**	**9 wk**
	VTA	Cav2Cre / AAV-hSyn-YFP	0.3	1.3*1012/ 1.6*1012	-5.4 / +2.2/ -8.9 / <10°	
4 D-F	DMH	AAV-CBA-DIO-GFP:TetTox	0.3	1*1012	-2.3 / +1.4 / -9.3 / <5°	29 wk
	VTA	Cav2Cre / AAV-hSyn-mCherry	0.3	1.25*1012 /1*1012	-5.4 / +2.2 / -8.9 / <10°	

Virus injections are presented per figure in the results section. Histology indicates the time post-surgery at which rats were sacrificed. DMH, dorsomedial hypothalamus, PAG, periaqueductal grey, VTA, ventral tegmental area, AP, anterior-posterior, ML, medio-lateral, DV, dorso-ventral.

Table 2. Details of viral injections in LepR-Cre mice.

Figure in results	Region	Virus	Volume (µl)	Titer (final mixture)	Coordinates (AP / ML / DV / angle)	Histology
5 A-C	DMH	AAV-hSyn-DIO-hM3D(Gq)-mCherry (bilateral) / AAV-DIO-hChR(H134R)-EYFP (unilateral)	0.3	1*1012/ 3.7*1012	-0.19 / +0.15 / -0.58 / <10°	12 wk
5 D-G	DMH	AAV-CBA-DIO-GFP:TetTox (bilateral) / AAV-DIO-hChR(H134R)-mCherry (unilateral)	0.3-0.5	1.4*1012/ 2.6*1012	-0.19 / +0.15 / -0.58 / <10°	12 wk

Virus injections are presented per figure in the results section. Histology indicates the time post-surgery at which mice were sacrificed. DMH, dorsomedial hypothalamus, AP, anterior-posterior, ML, medio-lateral, DV, dorso-ventral.

A

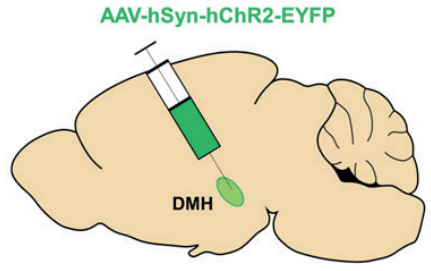

B

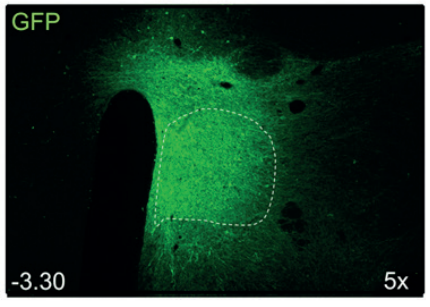

Figure 1. Successful targeting of the DMH with constitutively expressing viruses in Wistar rats. (A) AAV-hSyn-hChR2-EYFP was unilaterally injected into the DMH. (B) GFP positive cell bodies were observed in the DMH, but not completely limited to this area. The dotted outline shows the boundary of the DMH. The distance from bregma (mm) is indicated at the left bottom. Similar results were obtained for other constitutively expressing GFP viruses (AAV-CBA-GFP, AAV-miLuc-GFP, CBA-LepAnta-ires-GFP, AAV-esyn-miLepR-GFP), as described in appendix III.

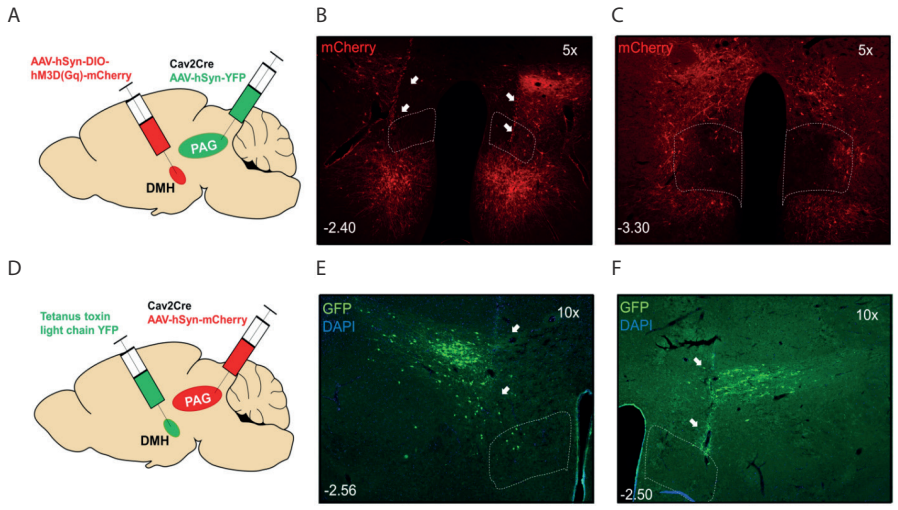

Figure 2. Despite needle tracks pointing towards the DMH, the DMH was not targeted by Cre-dependent viruses in Wistar rats. (A) To selectively target DMH neurons projecting to the PAG, CAV2Cre was injected into the PAG and Cre-dependent DREADD hM3D(Gq) mCherry was injected into the DMH. (B) Representative example injection site of DREADD hM3D(Gq) in the DMH (bregma -2.40 mm), showing needle tracks pointing towards the DMH (especially the right needle track). However, the DMH was not the target of hM3D(Gq)-mCherry expression; instead, hM3D(Gq)-mCherry positive neurons were observed in the areas surrounding the DMH. (C) hM3D(Gq)-mCherry expression at a further distance from bregma (-3.30 mm) for the example injection in B. Also at this distance from bregma, the DMH was not the target of hM3D(Gq)-mCherry expression. hM3D(Gq)-mCherry positive neurons were observed at the edges of the DMH and in the areas surrounding the DMH. (D) To selectively target DMH neurons projecting to the PAG, CAV2Cre was injected into the PAG and Cre-dependent TetTox-GFP was injected into the DMH. (E) Representative example injection site of TetTox-GFP in the DMH (bregma -2.56 mm), showing a needle track that was directed a bit too lateral for the DMH. TetTox-GFP positive neurons were observed in a small area dorsolateral from the DMH (F) A second representative example injection site of TetTox-GFP in the DMH (bregma -2.50 mm), showing a needle track that was directed towards the DMH. However, the DMH was not the target of TetTox-GFP expression. TetTox-GFP positive neurons were observed in a small area dorsolateral from the DMH (as also observed for the injection site in E). The dotted outlines show the boundary of the DMH. The distances from bregma (mm) are indicated at the left bottom. The arrows indicate the needle tracks.

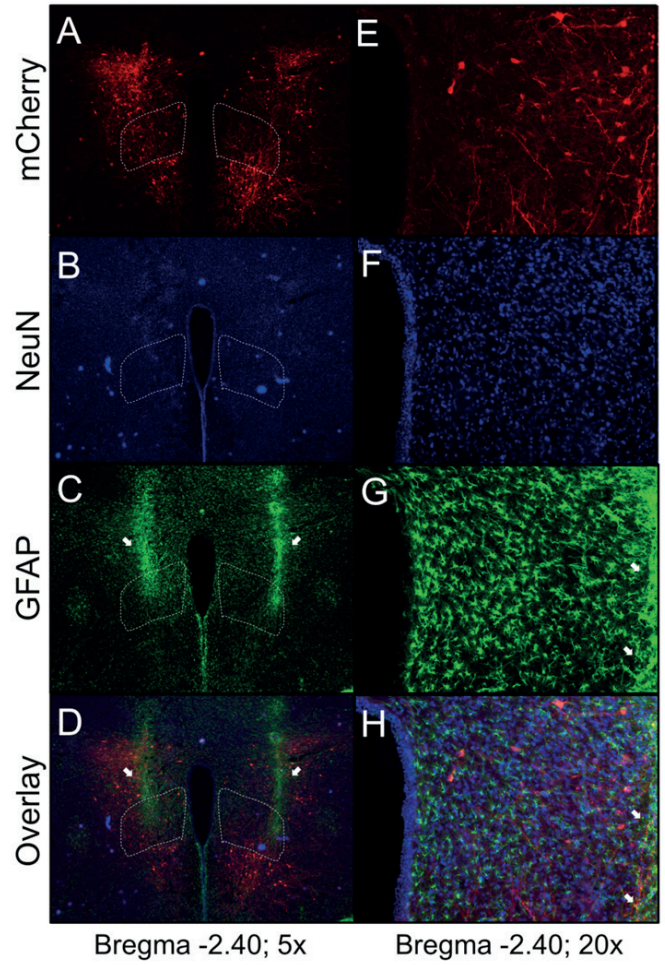

Figure 3. The absence of Cre-dependent DREADD expression in the DMH does not result from neuronal cell death. To determine whether the absence of hM3D(Gq)-mCherry in the DMH following intra-DMH injection of Cre-dependent DREADD hM3D(Gq) mCherry (Fig. 2A-C) results from viral toxicity, slices were stained for NeuN and GFAP. These markers were used to visualize inflammation and/or neuronal death. NeuN is a neuron-specific nuclear marker, and GFAP is an intermediate protein found in astrocytes, and was used to detect the presence of reactive astrocytes. The stainings were performed on unique brain slices showing unilateral DREADD expression in the DMH following bilateral intra-DMH DREADD injection (n=2). (A-D) Example of (A) hM3D(Gq)-mCherry, (B) NeuN, and (C) GFAP expression, and (D) an overlay of the expression patterns in an example rat that was hit unilaterally in the DMH. (E-H) Zoom in on the expression pattern of (E) hM3D(Gq)-mCherry, (F) NeuN, (G) GFAP, and (D) the overlay of the right DMH. Cell counts of NeuN were not different between the site with (766±55) and without (779±68) DREADD hM3D(Gq) mCherry expression (n=2), indicating that the absence of DREADD hM3D(Gq) mCherry expression did not result from neuronal loss. Also GFAP density was not different between the site with and without DREADD hM3D(Gq) mCherry expression (C), supporting the results of the NeuN staining showing that the unilateral absence of

DREADD hM3D(Gq) mCherry expression did not result from neuronal damage. The dotted outlines show the boundary of the DMH. The distances from bregma (mm) are indicated at the left bottom. The arrows indicate the needle tracks.

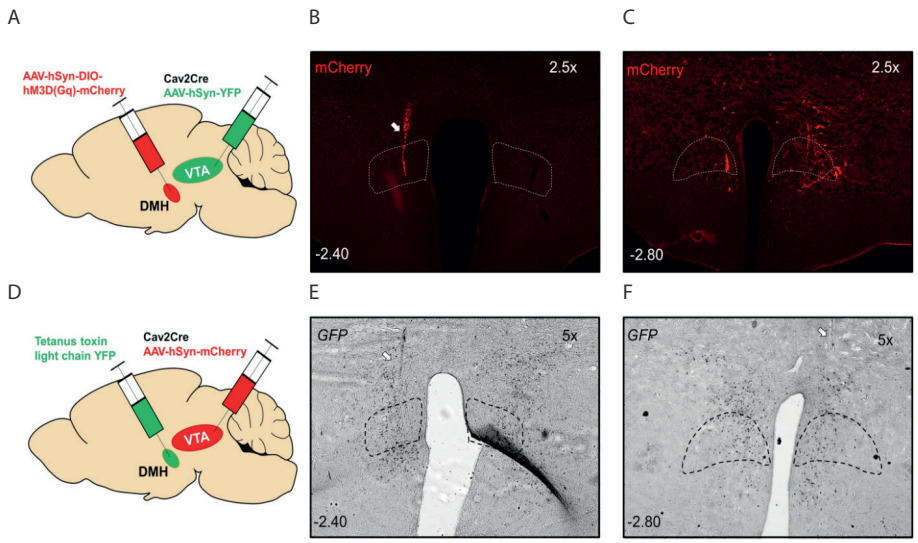

Figure 4. Despite needle tracks pointing towards the DMH, the expression of Cre-dependent viruses was not evident in Wistar rats. (A) To selectively target DMH neurons projecting to the VTA, CAV2Cre was injected into the VTA and Cre-dependent DREADD hM3D(Gq) mCherry was injected into the DMH. (B) Representative example injection site of DREADD hM3D(Gq) in the DMH, showing a needle track pointing towards the DMH (left). However, no hM3D(Gq)-mCherry expression was observed in the DMH or surrounding areas. (C) Example of best hM3D(Gq)-mCherry expression observed in the DMH following DMH injection of DREADD hM3D(Gq) mCherry in 9 rats. Almost no hM3D(Gq)-mCherry expression was observed. (D) To selectively target DMH neurons projecting to the VTA, CAV2Cre was injected into the VTA and Cre-dependent TetTox-GFP was injected into the DMH. Immunohistological analysis showed no TetTox-GFP positive neurons in the hypothalamus of any of the 9 injected rats. Therefore, in situ hybridization was performed to detect *TetTox-GFP* mRNA. (E) Representative example injection site of TetTox-GFP in the DMH, showing a needle track that was directed towards the DMH (left). In contrast to TetTox-GFP protein, *TetTox-GFP* mRNA was detected, and was expressed in the DMH and surrounding areas. (F) *TetTox-GFP* mRNA in a second representative example animal. *TetTox-GFP* mRNA was expressed in the DMH and surrounding areas. The dotted outlines show the boundary of the DMH. The distances from bregma (mm) are indicated at the left bottom. The arrows indicate the needle tracks.

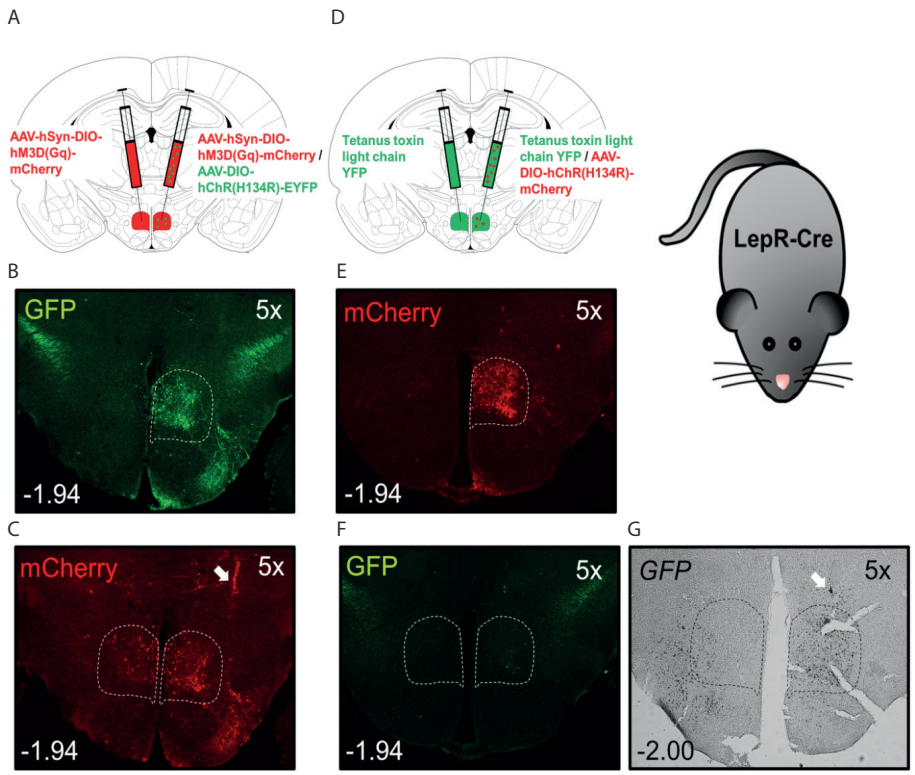

Figure 5. Successful targeting of the DMH with Cre-dependent viruses in LepR-Cre mice. (A) Cre-dependent DREADD hM3D(Gq) mCherry was bilaterally injected into the DMH, and Cre-dependent channelrhodopsin (ChR; AAV-DIO-hChR(H134R)-EYFP) was co-injected on one side. (B) Representative example of ChR-GFP expression following unilateral injection into the DMH. GFP positive cell bodies were observed in the DMH, and mostly restricted to this area, indicating successful targeting of the DMH with Cre-dependent ChR. (C) Representative example of DREADD hM3D(Gq) mCherry expression following bilateral injection into the DMH. hM3D(Gq) mCherry positive cell bodies were bilaterally observed in the DMH, and mostly restricted to this area. The expression on the right side was similar to that of ChR-GFP in (B). (D) Cre-dependent TetTox-GFP was bilaterally injected into the DMH, and Cre-dependent ChR (AAV-DIO-hChR(H134R)-mCherry) was co-injected on one side. (E) Representative example of ChR-mCherry expression following unilateral injection into the DMH. As for ChR-GFP, ChR-mCherry positive cell bodies were observed in the DMH, and mostly restricted to this area, indicating successful targeting of the DMH with Cre-dependent ChR. (F) Representative example of TetTox-GFP expression following bilateral injection into the DMH. No TetTox-GFP expression was observed in the DMH in any of the 12 injected mice. Therefore, in situ hybridization was performed to detect *TetTox-GFP* mRNA. (G) Representative example injection site of TetTox-GFP in the DMH, showing a needle track that was directed towards the DMH (right), and unilateral expression of *TetTox-GFP* mRNA in the DMH. The area of TetTox-GFP mRNA expression was similar to ChR-mCherry expression in (E), indicating successful (unilateral) targeting of the DMH with TetTox-GFP, but loss of TetTox-GFP protein. The dotted outlines show the boundary of the DMH. The distances from bregma (mm) are indicated at the left bottom. The arrows indicate the needle tracks.

Conclusion

We here show successful targeting of the DMH following intra-DMH injection of constitutively expressing viruses in Wistar rats. Virus expression was predominantly observed in the DMH, but not fully restricted to this area. In contrast, targeting of the DMH was not successful in Wistar rats with all approaches employing Cre-dependent DREADD or TetTox. Although misplaced needle tracks could explain the absence of virus protein expression in the DMH in some cases, it probably does not explain the majority of unsuccessful DMH injections. In most cases, needle tracks were directed towards the DMH, but no virus protein expression was observed in the DMH (and sometimes even not in the surrounding hypothalamic regions).

Targeting of DMH-PAG projection neurons with DREADD hM3D(Gq)-mCherry resulted in a typical expression pattern, whereby hM3D(Gq)-mCherry positive neurons were observed at the edges of the DMH and in the areas surrounding the DMH. NeuN and GFAP staining showed that the absence of hM3D(Gq)-mCherry in the DMH did not result from damage of DMH neurons. Targeting of DMH-PAG projection neurons with TetTox-GFP also resulted in a typical expression pattern. Like rats with misplaced needle tracks, rats with needle tracks pointing towards the DMH showed TetTox-GFP expression in an area dorsolateral to the DMH. These findings suggest that, as for DREADD hM3D(Gq)-mCherry, something may block TetTox-GFP protein expression in the DMH. Following the targeting of DMH-VTA projection neurons with TetTox, no TetTox-GFP protein expression was observed in the hypothalamus. However, *TetTox-GFP* mRNA was observed in the DMH. Since DMH-VTA rats were sacrificed at a later time-point after surgery (week 29) than DMH-PAG rats (week 12), it is possible that TetTox-GFP protein expression gradually reduces over time. This may explain why TetTox-GFP protein was only expressed in a small hypothalamic area in DMH-PAG rats, and was completely absent in DMH-VTA rats. Finally, targeting of DMH-VTA projection neurons with DREADD hM3D(Gq)-mCherry resulted in a complete absence of hM3D(Gq)-mCherry expression in the hypothalamus, in spite of needle tracks pointing towards the DMH. To determine whether gradual loss of virus protein expression over time may explain the absence of virus protein expression in the DMH, in situ hybridization should be performed to detect *hM3D(Gq)-mCherry* mRNA.

Finally, we compared virus expression in the DMH of LepR-Cre mice following injection of several distinct Cre-dependent viruses. We show successful targeting of the DMH with DREADD and ChR. No TetTox-GFP protein expression was observed in the DMH following intra-DMH TetTox injection, but *TetTox-GFP* mRNA showed a similar expression pattern as ChR. This finding supports successful targeting of the DMH with TetTox, but loss of TetTox-GFP protein over time.

To conclude, both the injection of constitutively expressing viruses in Wistar rats and Cre-dependent viruses in LepR-Cre mice resulted in successful targeting of the DMH. The absence of TetTox-GFP protein expression following intra-DMH TetTox injection probably results from the loss of TetTox-GFP protein over time, as *TetTox-GFP* mRNA was still observed in the DMH. Analysis of mRNA instead of protein may result in misinterpretation of the hypothalamic subregion in which LepR-positive neurons were functionally inactivated by TetTox, and may point towards toxicity effects of TetTox. Further, there appears to be a specific problem in targeting the DMH with Cre-dependent viruses in combination with the injection of Cav2Cre in a projection region in Wistar rats.

Nederlandse samenvatting

In onze moderne maatschappij ontwikkelen sommige individuen ernstige obesitas, terwijl anderen hier resistent voor lijken te zijn. Deze grote variabiliteit in de aanleg voor de ontwikkeling van obesitas is grotendeels onverklaard. Het overkoepelende doel van dit proefschrift was om het begrip te verbeteren van de neurale circuits die de balans tussen energie-inname en energieverbruik reguleren. Ook werden bepaalde gevoeligheidsfactoren bestudeerd die het risico op de ontwikkeling van obesitas verhogen. Verder werden er technische uitdagingen in het bestuderen van de neurale regulatie van energiebalans bediscussieerd en verschillende algeheel geaccepteerde concepten gerelateerd aan leptine, de hypothalamus en energiebalans uitgedaagd.

Sectie I: Leptine en hypothalame controle van energiebalans

De hypothalamus, een belangrijk regelcentrum in het brein, staat bekend om zijn kritieke rol in de regulatie van energiebalans. Het detecteert en integreert informatie van metabole signalen uit de periferie, zoals het vethormoon leptine, die het brein informeert over energieopslag en -beschikbaarheid. De hypothalamus reageert op deze metabole signalen door energie-inname en energieverbruik aan te passen. Daarom ligt de focus van de eerste sectie van dit proefschrift op leptine en hypothalame controle van energiebalans.

Hoofdstuk 2. Dit hoofdstuk geeft een overzicht van literatuur die aantoont dat overconsumptie van vetrijke diëten, in zogenoemde knaagdiermodellen voor dieet-geïnduceerde obesitas (DIO), resulteert in het ontstaan van een ontstekingsreactie in de hypothalamus. Deze ontstekingsreactie stimuleert de ontwikkeling van leptine resistentie (ongevoeligheid voor de werking van leptine) en obesitas en wordt gemedieerd door het aangeboren immuunsysteem. Er wordt een geïntegreerd model gepresenteerd van hoe de interactie tussen de verschillende geactiveerde mediatoren van het aangeboren immuunsysteem kan leiden tot de ontwikkeling van leptine resistentie in het brein.

Appendix I. Het bewijs voor de ontwikkeling van een ontstekingsreactie na de overconsumptie van vetrijke diëten in hoofdstuk 2 is voornamelijk verkregen in studies waarin knaagdieren vetrijk eten kregen aangeboden in kant-en-klare brokjes. In ons lab bieden we ratten een vrije keuze vet- en suikerrijk dieet aan, waarbij ratten kunnen kiezen tussen normale rattenbrokjes (chow), kraanwater, verzadigd vet (frituurvet) en 30% suikerwater. Dit vrije keuze vet- en suikerrijke dieet bootst het humane dieet beter na dan kant-en-klare brokjes. Daarom hebben we in appendix I getest of blootstelling aan dit dieet ook leidt tot een ontstekingsreactie in de hypothalamus. In tegenstelling tot de overconsumptie van vetten via kant-en-klare brokjes leidde blootstelling aan het vrije keuze vet- en suikerrijke dieet voor 8 weken niet tot een chronische ontstekingsreactie in de hypothalamus. De endogene leptine signalering was wel verhoogd in de hypothalamus.

Er wordt algemeen gedacht dat leptine resistentie het resultaat is van de overconsumptie van energierijke diëten, rijk aan vet en suiker, via processen zoals ontsteking, en dat deze dieet-geïnduceerde leptine resistentie bijdraagt aan de ontwikkeling van obesitas. Op cellulair niveau hebben voorgaande studies de ontwikkeling van leptine resistentie specifiek aangetoond in de arcuate nucleus (ARC), een subgebied in de hypothalamus waarvan bekend is dat het een belangrijke regulator is van voedselinname. Echter, er is enkel bewijs dat verminderde leptine gevoeligheid niet noodzakelijkerwijs ontstaat door de consumptie van energierijke diëten, maar al aanwezig kan zijn voor blootstelling aan energierijke diëten en een risicofactor vormt voor het ontwikkelen van ernstigere obesitas. Uit voorgaande studies was niet duidelijk in welke mate een reeds bestaande verminderde leptine gevoeligheid de ontwikkeling van DIO voorspelt. Ook was eerder niet getest of leptine gevoeligheid een stabiele parameter is in een rat.

Hoofdstuk 3. In dit hoofdstuk werd eerst aangetoond dat leptine gevoeligheid erg variabel is tussen individuele ratten, maar een stabiele parameter is in een rat over de tijd. Daarna werd onderzocht of individuele leptine gevoeligheid op een chow dieet (normale rattenbrokjes) de ontwikkeling van obesitas op een vrije keuze vet- en suikerrijk dieet voorspelt. Ook werd onderzocht of dit samenhangt met de ontwikkeling van dieet-geïnduceerde leptine resistentie. Om dit te kunnen onderzoeken werden ratten in twee subgroepen ingedeeld: leptine gevoelige (LS) en leptine resistente (LR) ratten, gebaseerd op leptine gevoeligheid op een standaard chow dieet. Blootstelling aan het vrije keuze vet- en suikerrijke dieet toonde aan dat LR ratten, die een reeds bestaande verminderde leptine gevoeligheid hadden vergeleken met LS ratten, meer lichaamsgewicht en vetweefsel erbij hadden gekregen na 8 weken blootstelling aan het vet- en suikerrijke dieet, zonder dat zij meer calorieën hadden gegeten of hun leptine gevoeligheid was veranderd. Dus een reeds bestaande vermindering in leptine gevoeligheid voorspelt de aanleg voor het ontwikkelen van ernstigere obesitas na blootstelling aan een vrije keuze vet- en suikerrijk dieet. Tenslotte toonden we aan dat de reeds bestaande verminderde

gevoeligheid in LR ratten vergeleken met LS ratten geassocieerd is met een verminderde cellulaire leptine gevoeligheid in de dorsomediale hypothalamus (DMH) en ventromediale hypothalamus (VMH), maar niet de ARC (gemeten met pSTAT3, een marker voor leptine signalering). Blootstelling aan het vet- en suikerrijke dieet verlaagde de leptine gevoeligheid in de DMH, VMH en ARC van LR ratten niet verder. In andere woorden, we hebben gevonden dat een reeds bestaande verminderde leptine gevoeligheid in een hersengebied dat bekend staat om zijn rol in thermogenese (warmteproductie): de DMH (en VMH), maar niet de ARC, vermoedelijk het verschil verklaart tussen wel of niet ernstige obesitas ontwikkelen op het vrije keuze vet- en suikerrijke dieet. Daarom dagen onze resultaten het algemeen geaccepteerde concept uit van dieet geïnduceerde leptine resistentie in de ARC als een causale factor voor de ontwikkeling van DIO.

Appendix II. LS en LR ratten verschilden niet in totale calorie inname in hoofdstuk 3, maar er was niet getest of de twee subgroepen wellicht verschillen in maaltijdpatronen. In appendix II toonden we aan dat dit niet het geval is.

Uit hoofdstuk 3 was niet gebleken hoe een reeds bestaande verminderde leptine gevoeligheid in de DMH de aanleg voor het ontwikkelen van ernstigere obesitas verklaart. Aangezien leptine signalering in DMH neuronen vooral bekend staat om het induceren van thermogenese (warmteproductie), zou verminderde thermogenese een mogelijke verklaring kunnen zijn. Dit onderzochten we in hoofdstuk 4.

Hoofdstuk 4. We probeerden hier te ontrafelen of ratten die minder gevoelig zijn voor de eetlust verminderende effecten van leptine ook minder gevoelig zijn voor de thermogene effecten van leptine. Dit deden we door de thermogene effecten van leptine te vergelijken tussen LS en LR ratten op een standaard chow dieet. Ook wilden we testen of een eventuele verminderde thermogene respons op leptine komt door verminderde leptine signalering in de DMH (in tegenstelling tot bijvoorbeeld verminderd transport van leptine over de bloed-hersen barrière). Daarom hebben we de effecten van leptine op thermogenese vergeleken na intraveneuze injectie versus injectie direct in de DMH in LS versus LR ratten. LS ratten verhoogden hun lichaamstemperatuur na intraveneuze leptine injectie. Dit kwam door zowel een verhoging van thermogenese in gespecialiseerd bruin vetweefsel als verminderd warmteverlies via de staart. De inductie van deze temperatuurresponsen met leptine injectie direct in de DMH was kleiner, maar in dezelfde richting als met intraveneuze leptine injectie. Dus LS ratten toonden een thermogene respons op leptine, die tenminste gedeeltelijk werd gemedieerd op het niveau van de DMH. In tegenstelling tot LS ratten toonden LR ratten geen enkele thermogene respons op leptine. De verslechterde leptine regulatie van thermogenese in LR ratten kan gekoppeld worden aan de eerdere bevinding van verminderde leptine gevoeligheid in de DMH in deze ratten. Verder was de resistentie voor leptine's thermogene effecten in LR ratten ook geassocieerd met een 1°C lagere BAT temperatuur en een verlaagde BAT UCP1 expressie onder baseline condities, wat aangeeft dat LR ratten een verminderde thermogene capaciteit hebben. Dit kan hen vatbaarder maken voor het ontwikkelen van ernstige obesitas zodra zij worden blootgesteld aan een vet- en suikerrijk dieet.

Appendix III. In deze appendix probeerden we te bestuderen of chronische blokkade van leptine receptor signalering in DMH neuronen lichaamstemperatuur verlaagt en dit vervolgens resulteert in een toename in lichaamsvet. We hebben verschillende virale vector technologieën gebruikt om leptine signalering te blokkeren in de DMH. Door een verscheidenheid aan technische limitaties waren we met geen van de virale vectoren in staat om leptine signalering selectief in DMH neuronen te blokkeren. Daarom konden we niet vaststellen of chronische blokkade van leptine signalering specifiek in DMH neuronen de lichaamstemperatuur verlaagt.

Sectie II: Regulatie van energiebalans voorbij de hypothalamus

De hypothalamus werkt niet alleen, maar reguleert energiebalans via functionele connecties met andere belangrijke hersengebieden, zoals het midbrein. In sectie I bleek de DMH een belangrijke hersenregio voor de regulatie van energiebalans. Daarom was het doel van sectie II om de projecties te bestuderen via welke de DMH energiebalans reguleert. Twee regio's in het midbrein die bijzonder interessant waren voor dit proefschrift zijn de ventral tegmental area (VTA) en de periaqueductal grey (PAG), waarvan eerder was aangetoond dat ze respectievelijk energie-inname en energieverbruik reguleren.

Het is bekend dat de DMH zijn sympathische controle van bruin vet thermogenese reguleert via projecties naar sympathische premotor neuronen in de raphe pallidus, maar er is bewijs dat de projecties naar de PAG ook belangrijk zijn voor het mediëren van thermogenese. De PAG is een relatief lang hersengebied dat in vier subgebieden kan worden opgedeeld, die verschillen in hun functionele eigenschappen en anatomische projecties. De precieze anatomische projecties van de DMH naar de verschillende subgebieden in de PAG en hun functie waren grotendeels onduidelijk in voorgaande studies.

Hoofdstuk 5. In dit hoofdstuk probeerden we de anatomische projecties van de DMH naar de PAG over de gehele lengte (anterior-posterior as) van de PAG te visualiseren en de rol van deze projecties in thermogenese te bestuderen. Anterograde virale tracing toonde aan dat de DMH voornamelijk naar de dorsale en laterale PAG projecteert. Retrograde virale tracing bevestigde dit, maar gaf ook aan dat de PAG een diffuse input ontvangt van de hypothalamus in plaats van specifieke input van de DMH. We probeerden de rol van de geïdentificeerde projecties in thermogenese te bestuderen door gebruik te maken van een speciale virale vector technologie genaamd designer receptor exclusively activated by designer drugs (DREADD). Via deze techniek (in combinatie met een tweede virus genaamd canine adenovirus-2 (CAV2Cre)) probeerden we projecties van de DMH naar de PAG te activeren. Na activatie van deze projecties vonden we een verhoging in bruin vet temperatuur en lichaamstemperatuur, maar we konden niet uitsluiten dat tenminste sommige thermogene effecten werden gemedieerd door omringende hypothalame subregio's vanwege moeilijkheden met het specifiek targetten van de DMH. Dus we toonden in hoofdstuk 5 aan dat het technisch uitdagend is om specifieke projecties van de DMH naar de PAG te activeren vanwege de limitaties van virale vector technologie. Ook toonden we aan dat de DMH over het algemeen niet het belangrijkste hypothalame input gebied is voor de PAG.

Appendix IV. In deze appendix bestudeerden we of de projecties van de DMH naar de PAG leptine gevoelig zijn. Hiervoor voerden we een retrograde virale tracing uit in een speciale leptine muizenlijn, namelijk de leptine receptor (LepR)-Cre muislijn. Via deze techniek konden we LepR positieve neuronen visualiseren in de hypothalamus die input leveren aan de PAG. De resultaten lieten zien dat de DMH het een na belangrijkste gebied is in de hypothalamus dat LepR positieve input geeft aan de PAG.

Appendix V. Zoals ook was bediscussieerd in hoofdstuk 5, ervaarden we verschillende technische uitdagingen bij het targetten van de DMH en zijn projecties met virale vector technologie. Appendix V geeft een overzicht van de targeting van de DMH met verschillende virale vectoren die gebruikt zijn in dit proefschrift. Met de meeste virale vectoren waren we in staat om de DMH te raken. Echter, we vonden een specifiek probleem in het targetten van de DMH wanneer we dit probeerden te doen in combinatie met een projectieregio via duale virale vectortechnologie.

Hoofdstuk 6. In dit hoofdstuk probeerden we de DMH naar VTA projectie te targetten, maar de histologische analyse gaf aan dat de DMH niet de hoofdtarget was; daarentegen bleek de zona incerta (ZI) de hoofdtarget te zijn. Van de ZI is ook bekend dat het belangrijke hypothalame innervatie aan de VTA geeft. Voor zowel de ZI als de VTA is eerder aangetoond dat ze betrokken zijn bij eetgedrag, maar het is niet eerder bestudeerd of de projectie van de ZI naar VTA eetgedrag reguleert. Daarom testten we de effecten van activatie en inactivatie van ZI naar VTA projectie neuronen op verschillende aspecten van eetgedrag. We gebruikten virale vector technologieën om de projecties van de ZI naar VTA permanent te inactiveren of reversibel te activeren. Inactivatie van ZI naar VTA projectie neuronen verlaagde de motivatie om voor voedsel te werken en verlaagde ook voedselinname door een lagere maaltijdfrequentie. Omgekeerd stimuleerde activatie van ZI naar VTA projectie neuronen de motivatie om te werken voor voedsel en ook voedselinname zelf. Dus in dit hoofdstuk toonden we aan dat de projectie van de ZI naar de VTA bidirectionele controle uitoefent op eetgedrag.

Dankwoord

Toen ik aan mijn promotieonderzoek begon, dacht ik dat ik me tijdens dit traject vooral verder zou ontwikkelen tot een gedegen zelfstandig onderzoeker. Echter, meer dan dat heb ik het ervaren als een traject dat leidde tot vele levenslessen en waardevolle inzichten over mezelf, anderen, wetenschap in het algemeen en wat al niet meer, waar ik dankbaar voor ben en nog lang profijt van zal hebben. Ik kon altijd rekenen op de steun van fijne collega's, vrienden en familie en wil iedereen die op enige wijze heeft bijgedragen aan mijn persoonlijke groei en de totstandkoming van dit proefschrift hartelijk bedanken.

Allereerst wil ik mijn promotoren bedanken.

Roger, jij hebt mij de mogelijkheid gegeven om dit promotieonderzoek te doen en om ook gelijk mijn master afstudeerscriptie bij jou te schrijven, wat een mooi review artikel is geworden. Hoewel de resultaten van de eerste onderzoeken behoorlijk tegenvielen, heb jij er altijd vertrouwen in gehad dat er een boekje zou komen. Ook heb je altijd mogelijkheden geboden om mijzelf te ontwikkelen. Je deur stond altijd open en ik kon altijd rekenen op snelle feedback. Daar ben ik je dankbaar voor. Gaandeweg mijn promotietraject kwam ik er achter dat jouw vraag "of ik goed ben in verkopen" toch niet zo irrelevant was als ik tijdens het sollicitatiegesprek dacht. Ik moet eerlijk zeggen dat ik veel geleerd heb van je kundige formuleringen. Tijdens het traject bleek ook dat onze persoonlijkheden en werkwijze best van elkaar verschillen, met als uitzonderingen de koppigheid en sterke drive die we gemeen hebben. Om toch een beetje toe te geven (aan de uitgebreide discussie betreffende het gebruik van de thermogevoelige camera dan) en vanwege je aanstekelijke enthousiasme over de nieuwste wetenschappelijke technieken, heb ik een plaatje van de thermogevoelige camera op de cover geplaatst. De cover is voor jou.

Susanne, hoewel we elkaar niet heel vaak zagen, vond ik de gesprekken altijd fijn en je feedback op mijn werk altijd erg waardevol. Jouw scherpe inzichten hebben zeker bijgedragen aan het identificeren van de twee typen leptine responders en hielpen bij het nuanceren van conclusies. Ook stel ik het erg op prijs dat ik welkom was om experimenten te doen in het AMC.

Mijn geliefde collega's, **Inge**, **Nienke**, **Mark V.** en **Yuije**, ik ben heel blij dat ik jullie ontmoet heb en jullie mij hebben bijgestaan op alle leuke en minder leuke momenten de afgelopen jaren. Lieve **Inge**, allereerst wil ik je bedanken voor al je hulp en enthousiaste aanmoedigingen op het lab. Ik vond het altijd erg fijn dat je de tijd nam om operaties goed uit te voeren en dingen uit te leggen / voor te doen. Jouw stereotactische expertise heeft o.a. geleid tot een prachtige targeting van de uitdagende DMH. Nog meer dan voor bovenstaande wil ik je bedanken voor alle gezelligheid, de urenlange gesprekken en voor al je steun. Ik kon altijd alles tegen je vertellen en je was er altijd voor me. Daarom vind ik het ontzettend fijn dat je straks achter mij staat als paranimf. Beste **Mark**, wat een geluk dat wij kamergenootjes waren. Ik kon werkelijk voor alles bij je terecht; van de kleine computer- en labvraagjes tot de diepere dilemma's. Ik bewonder je inzicht en kennis over een breed scala aan wetenschappelijke onderwerpen/technieken enorm en vind het bijzonder dat je vaak al eerder op de hoogte was van een nieuw paper in mijn vakgebied dan ikzelf. Bedankt voor het delen van je wetenschappelijke expertise en ook voor je steun en interesse en de fijne gesprekken. Ik vind het erg fijn dat je mij ook op het laatste moment zult bijstaan als paranimf (jammer dat ruggespraak niet meer gebruikelijk is ;)). **Nienke**, het begon allemaal met onze lunches samen, waarin we al onze frustraties konden afreageren. Gaandeweg moesten er steeds meer verschillende onderwerpen besproken worden en konden we het eigenlijk geen lunch-meetings meer noemen ;). Toen zijn we overgestapt naar andere bijklets locaties, waar we vaak tot sluitingstijd nog zitten. Genoeg te bespreken dus! Logisch, want wat begrijpen we elkaar toch goed. Als er iemand is van wie ik veel geleerd heb de afgelopen jaren dan ben jij het wel. Ik vind het ontzettend knap hoe je voor jezelf hebt gekozen en nu in het leven staat. **Yuije,** you were a lovely roommate. I enjoyed our conversations about our shared passion: dancing, our future career, and other things in life. It was nice to share our thoughts and experiences and to find out that we have so much in common! I am so happy that you will be back in time from China to attend my defense :).

Tijdens mijn promotieonderzoek had ik het genoegen om een aantal studenten te mogen begeleiden. Allemaal ontzettend bedankt voor jullie harde werken, enthousiasme, input en gezelligheid! Zonder jullie was dit proefschrift er niet geweest. **Sanne**, jij was mijn eerste studente en ik had het geluk dat je veel technieken al uitstekend beheerste en de overige technieken heel snel aanleerde. Je pSTAT3 kleuringen zijn werkelijk prachtig geworden. Super dat je nu aan je eigen PhD gaat beginnen in Glasgow! **Diana**, jij weet van aanpakken! Bedankt voor al je harde werken en steun in moeilijke tijden. Ik vond het altijd fijn om met je samen te werken en erg gezellig om met je te kletsen. **Céline**, jij functioneerde tijdens je eerste stage al als een volwaardig analiste. Ontzettend leuk dat je nu aan je master gaat beginnen! **Micha**, bedankt voor al je goed doordachte input en je hulp met het uittesten van de thermogevoelige camera. Knap van je dat je een opleiding tot arts-onderzoeker bent gaan doen. **Jan**, jij hebt me echt door de laatste loodjes van mijn promotieonderzoek heen geholpen met je harde werken en enthousiasme. Extra

bedankt voor je hulp met de faeces en het uithalen van het maagdarmstelsel. En natuurlijk voor je hulp met het maken van een foto voor de cover! **Esther** en **Minke**, ik wil jullie bedanken voor jullie geweldige hulp met de ZI-VTA experimenten van het samenwerkingsproject met Geoffrey. De studenten **Joran**, **Sara**, **Janneke**, **Robin** en **Marianne**, allemaal ontzettend bedankt voor jullie enthousiasme en input bij de kleinere stageprojecten.

Er zijn een aantal collega's bij wie ik altijd kon binnenlopen voor goed advies. **Geoffrey**, wat was het fijn dat jouw kantoor vlak naast de mijne zat en je deur altijd open stond. Ik kon voor van alles en nog wat bij je terecht; een praatje, discussies over data, goed advies over allerlei zaken en ik heb veel van je geleerd (o.a. hoe je onder een presentatie uit komt, wat voor hotel te boeken op een congres ;)) en om je grapjes gelachen. Jouw idee om kleuren toe te voegen aan de leptine-gevoeligheids tabellen heeft ze omgetoverd tot mooie heatplots. Bedankt voor alles. **Frank**, dankjewel voor al je goede adviezen, inzichten en interessante vragen en dat ik altijd bij je terecht kon. Ik vind het super om te zien wat voor grants je al hebt binnen gehaald en heb er geen twijfel over dat je op een dag hoogleraar wordt. **Azar**, thank you for always making time to discuss data, even when you were very busy after the birth of your lovely twin boys. I also enjoyed your enthusiastic reactions to my ballroom dancing stories. I wish you all the best with your new job and life in Germany! **Rahul**, dankjewel dat ik altijd bij je binnen kon lopen voor hulp en advies. Ik wil je in het bijzonder bedanken voor je hulp, steun en gezelligheid bij het opstarten van mijn promotieonderzoek.

Dit proefschrift was er niet geweest zonder de hulp van de analisten en technische ondersteuning in het lab op de 4e en 5e verdieping. **Mieneke**, jij bent uiteraard de eerste om te bedanken. Er is geen dierexperiment geweest waar jij niet bij hebt geholpen. Ik kon altijd bij je aankloppen voor hulp en advies en je maakte altijd ruimte in je drukke agenda om mij te helpen. Ook ben ik niet vergeten dat je mij zelfs op je vrije dag bent komen helpen met glucose testen. Ontzettend bedankt voor alles! **Mark B.**, jij bent degene die de tijd heeft genomen om mij uitgebreid uit te leggen hoe je v. jugularis canules moet onderhouden. Dankzij jouw uitleg is het gelukt om de canules maandenlang open te houden, wat vele mensen bewonderingswaardig vinden en tot mooie resultaten heeft geleid in dit proefschrift. Ook kon ik altijd bij je terecht met technische vragen over allerlei technieken en proefdier gerelateerde vragen. **Jos**, je hebt me enorm uit de brand geholpen met je hulp bij het doorspoelen van de v. jugularis canules en alle injecties. Ook ben ik je dankbaar voor je fantastische schoonmaakkunsten en vond ik het gezellig om een praatje met je te maken. **Marjolein** en **Annemieke**, bedankt voor al jullie hulp

in de stallen en de goede zorgen voor mijn zieke dieren. **Keith**, bedankt voor al je praktische ondersteuning en je goede uitleg van technieken. Ik heb veel van je geleerd en vond het gezellig om met je samen te werken. **Henk** en **Leo**, ontzettend bedankt voor alle hulp en de gezelligheid op en om het lab. Ik hoop dat jullie heerlijk van jullie pensioen aan het genieten zijn! Ik wil ook **Harrie**, **Youri**, **Marina**, **Roland**, **Hugo**, **Ruth**, en **Anita** bedanken voor het beantwoorden van al mijn vragen en voor de hulp op het lab.

All of the other members of the Adan group, **Han**, **Ruud**, **Linde**, **Jacques**, **Tessa**, **Véronne**, **Nefeli**, **Jeroen**, **Janna,** and **Maryse**, thank you so much for your input and help during the past few years. **Véronne**, super dat je de leptine responders hebt kunnen repliceren in muizen. Ik hoop dat dit model nog verdere mooie data voor je oplevert.

Jiska, **Jelle** and **Valeria** thank you for your understanding of physiological data and help with the associated statistics. **Jiska**, ook bedankt voor de gezelligheid en je begrip van andere PhD-perikelen.

Dan zijn er nog een paar andere mensen op de afdeling die ik graag wil bedanken. **Sandra**, **Vicki**, **Ria** en **Krista**, bedankt dat jullie altijd klaar stonden om te helpen met allerlei administratieve zaken. **Joke**, ik vond het mooi om te zien hoe je sommige collega's in een moeilijke periode hebt geholpen. Ook vond ik je interesse in o.a. mijn ballroom dansen altijd erg leuk. Veel succes en plezier met het bouwen van jullie eigen huis! **Geert**, bedankt voor je interesse in de voortgang van mijn promotieonderzoek en je hulp bij het vinden van stagestudenten.

Jan-Willem, **Tom** en **Cindy**, bedankt dat ik altijd bij jullie terecht kon voor vragen over anatomie en kleuringen.

My colleagues in the AMC, it's been a while since I performed experiments in your lab, but I remember that you were always very helpful and thoughtful. **Evita**, it was a pleasure to work on the same project with you. I enjoyed our discussions about diets and (the existence of) hypothalamic inflammation. Thanks a lot for your help with the Western blots. **Unga**, bedankt dat je vaak al gelen voor mij maakte en ook voor de andere praktische hulp en adviezen. **Leslie**, bedankt voor je hulp met de glucose metingen en het uitvoeren van het metabole kooi experiment. **Myrtille**, bedankt voor alle gezelligheid op de congressen, met als toppunt de SSIB in Montréal en de super leuke vakantie die daar op volgde. Ik wil je ook bedanken voor je bemoedigende woorden en vind het altijd erg gezellig om met je bij te kletsen.

Heel veel sterke en succes met de laatste loodjes van je eigen promotieonderzoek!

Mijn oude stagebegeleiders hebben een belangrijke basis gevormd voor dit promotietraject. **Henk**, bij mijn bachelor stage bij jou ben ik enthousiast geworden over het werken bij Translational Neuroscience. Ook waardeer ik je vertrouwen in mij en je interesse in mijn onderzoek enorm. **Marcel**, bedankt voor je vertrouwen in mij en het overbrengen van jouw methode van literatuuronderzoek doen. Deze methode stond aan de basis van de mooie stukken die ik de afgelopen jaren heb geschreven en ook mijn stagestudenten hebben hier veel profijt van gehad. Verder wil ik je samen met **Rosanne** bedanken voor het overbrengen van jullie expertise in de moleculaire biologie. Daar heb ik zeker wat aan gehad tussen de gedragsbiologen! **Marcia**, het enthousiast overbrengen van al je kennis en kunde betreffende de high en low drinkers maakte de basis voor mijn promotieonderzoek compleet! Als variant op jouw high en low drinkers heb ik leptin sensitive en leptin resistant ratten onderzocht ;). **Louk**, dankzij jou ben ik mijn promotieonderzoek bij Roger gestart.

Ook wil ik mijn vrienden en kennissen buiten het lab bedanken voor hun steun en interesse en de gezellige momenten. In het bijzonder wil ik **Hugo** bedanken, die vanuit zijn eigen ervaring met wetenschap en promoveren extra steun bood op moeilijke momenten.

Paul en **Cynthia**, parallel aan mijn promotieonderzoek stond de transformatie naar echte wedstrijddansers. Onder jullie begeleiding hebben we nu al een niveau bereikt waarvan we vroeger niet hadden durven hopen dat ooit te halen. Bedankt voor jullie vertrouwen en positieve support. We kijken er naar uit om onder jullie begeleiding nieuwe grenzen te verleggen.

Joke, **Marina** en **Michel**, bedankt voor jullie steun, warmte en gezelligheid. Ik voel me altijd erg welkom bij jullie.

Mijn lieve familie, **Papa**, **Mama** en **Angela**, bedankt voor jullie enorme steun, liefde en vertrouwen. **Papa**, dankjewel dat je er altijd voor mij bent. Het meedenken over praktische oplossingen voor mijn problemen en je bemoedigende woorden waren een grote steun. De wandelingen samen met Cooper en Diesel maakten de laatste fase van mijn promotieonderzoek extra fijn. **Mama**, dankjewel voor je liefde en zorgzaamheid. Met je goede zorgen heb jij mij mijn basis gegeven. **Angela**, ik vind het altijd ontzettend fijn om met je te kletsen en leuke dingen te doen.

Liefste **Martijn**, vlak voordat ik aan het promotie-avontuur begon, ben jij (eindelijk!) dichter in mijn leven gekomen. Je hebt alles van dichtbij meegemaakt en was er altijd voor mij. Bedankt voor je luisterend oor, steun en liefde. Je gevoel voor humor maakte alles leuker en was een uitstekende remedie tegen frustraties. Ook heb ik intens genoten van de vele (dans)avonturen samen die parallel stonden aan dit promotietraject en een welkome afleiding boden. Bedankt voor alles, liefste. Ik kijk uit naar onze toekomst samen!

List of publications

Kathy C.G. de Git, Roger A. Adan. Leptin resistance in diet-induced obesity: the role of hypothalamic inflammation. *Obesity Reviews, 2015, 16(3), 207-224*

Kathy C.G. de Git, Céline Peterse, Sanne Beerens, Mieneke C.M. Luijendijk, Geoffrey van der Plasse1, Susanne E. la Fleur, Roger A.H. Adan. Is leptin resistance the cause or the consequence of diet-induced obesity? *International Journal of Obesity, 2018, doi: 10.1038/s41366-018-0111-4*

Kathy C.G. de Git, Diana C. van Tuijl, Mieneke C.M. Luijendijk, Inge G. Wolterink-Donselaar, Alexander Ghanem, Karl-Klaus Conzelmann, Roger A.H. Adan. Anatomical projections of the dorsomedial hypothalamus tot he periaqueductal grey and their role in thermoregulation: a cautionary note. *Physiological Reports, 2018, 6(14), e13807, doi: 10.14814/phy2.13807*.

Kathy C.G. de Git, Johannes A. den Outer, Inge G. Wolterink-Donselaar, Mieneke C.M. Luijendijk, E. Schéle, Suzanne L. Dickson, Roger A.H. Adan. Rats that are predisposed to excessive obesity show reduced leptin-induced thermoregulation before becoming obese. *Submitted*

Kathy C.G. de Git, Esther M. Hazelhoff, Minke H.C. Nota, Mieneke C.M. Luijendijk, Geoffrey van der Plasse, Roger A.H. Adan. Zona incerta neurons projecting to the ventral tegmental area promote action initiation towards feeding. *Submitted*

Kathy C.G. de Git, Teun P. de Boer, Marc. A. Vos, Marcel. A.G. van der Heyden. Cardiac ion channel trafficking and drugs. *Pharmacology and Therapeutics, 2013, 139(1), 24-31*

Robin J. Mulders, **Kathy C.G. de Git**, Erik Schéle, Suzanne L. Dickson, Yolanda Sanz, Roger A.H. Adan. Microbiota in obesity: interactions with enteroendocrine, immune and central nervous systems. *Obesity Reviews, 2018, 19(4), 435-451*.

Marcia Spoelder, Jacques P. Flores Dourojeanni, **Kathy C.G. de Git**, Annemarie Baars, Heidi M.B. Lesscher, Louk J.M.J. Vanderschuren. Individual differences in voluntary alcohol intake in rats: relationships with impulsivity, decision making and Pavlovian conditioned approach. *Psychopharmacology, 2017, 234(14), 2177-2196*

Rosanne Varkevisser, Marien J.C. Houtman, Tobias Linder, **Kathy C.G. de Git**, Henriette D. Beekman, Richard R. Tidwell et al. Structure-activity relationships of pentamidine-affected ion channel trafficking and dofetilide mediated rescue. *British Journal of Pharmacology, 2013, 169(6), 1322-1334*

Hiroki Takanari, Lukas Nalos, Anna Stary-Weinzinger, **Kathy C.G. de Git.**, Rosanne Varkevisser, Tobias Linder et al. Efficient and specific cardiac IK_1 inhibition by a new pentamidine analogue. *Cardiovascular Research, 2013, 99(1), 203-214*

Curriculum Vitae

Catharina Geertje (Kathy) de Git was born on the 16th of April in 1990 in Utrecht. In 2008, she obtained her Athenaeum degree with Latin *cum laude* at College de Heemlanden in Houten. In the same year, she started the Bachelor Biomedical Sciences at the Utrecht University. Kathy has always been interested in physiology and neuroscience. Therefore, she performed her Bachelor internship at the department of Translational Neuroscience in the UMC Utrecht under the supervision of Dr. Henk Karst, where she studied the role of stress hormones in the persistence of intrusive memories in post-traumatic stress disorder. In 2011, she obtained her Bachelor's degree *cum laude*, and started the Master Biology of Disease at the Utrecht University. She performed her first internship at the department of Medical Physiology in the UMC Utrecht under the supervision of Dr. Rosanne Varkevisser and Dr. Marcel van der Heyden, where she studied the role of cardiac ion channel trafficking defects in cardiac arrhythmias. She was asked to independently write a review article for publication on this topic and became first author. Kathy performed her second internship under the supervision of Dr. Marcia Spoelder, in the group of Prof. Dr. Louk Vanderschuren at Utrecht University, where she studied individual differences in alcohol intake in relationship to risky decision making in rats. She obtained her Master's degree *cum laude* in 2013, after finishing her Master thesis entitled "Leptin resistance in diet-induced obesity: the role of hypothalamic inflammation", under the supervision of Prof. Dr. Roger Adan at the department of Translational Neuroscience in the UMC Utrecht.

In 2014, Kathy continued studying the topic of her Master thesis during her PhD project in the same lab under the supervision of Prof. Dr. Roger Adan and Prof. Dr. Susanne la Fleur. She performed some of her experiments at the department of Endocrinology and Metabolism at the Academic Medical Center in Amsterdam. During the past 4.5 years, the topic of her PhD project gradually changed into "Challenging the concepts related to leptin, the hypothalamus, and energy balance", the results of which are presented in this thesis. During her PhD period, Kathy published her Master thesis as a review article and won a "SSIB New Investigator Award" for her meritorious work on individual variability in leptin sensitivity, which allowed her to present her work at the SSIB meeting in Montréal, Canada. Kathy will defend her thesis on the 30th of October 2018.

Next to her academic career, Kathy also worked hard on her ballroom dancing during the past few years. Together with her partner, she became Dutch Champion in two categories in 2017 (NDO Medallist and Amateur B), Dutch Champion in a higher category in 2018 (WDC Dutch-AL open National Amateurs C), and won many other honorable prizes. Currently, she and her partner are standard finalists in the NDO Amateurs A and WDC Dutch-AL National Amateurs.

Let It Go - Frozen